

FIG. 1

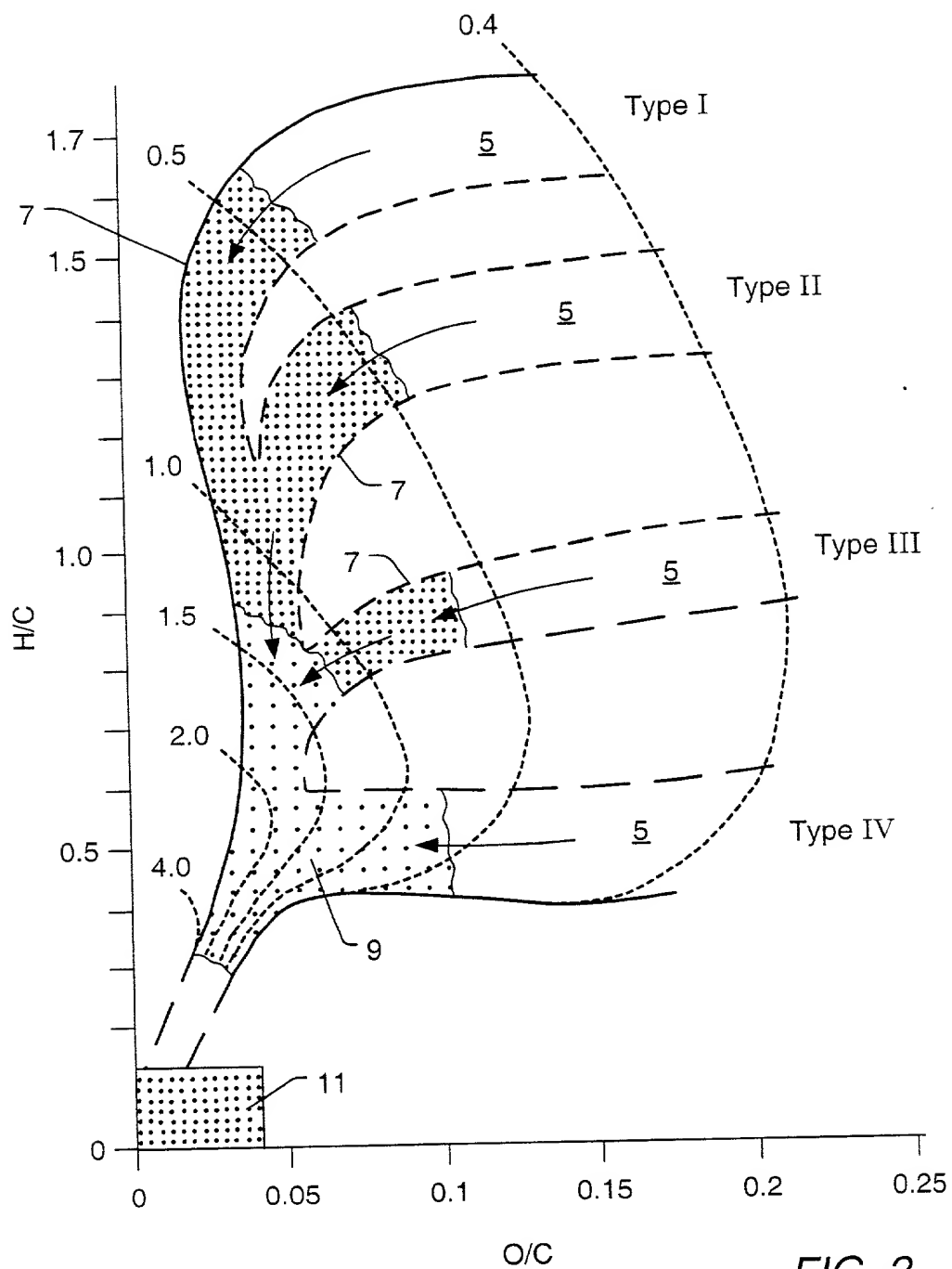


FIG. 2

FIG. 3 is a schematic diagram of a system 100 for providing a user with a personalized experience. The system 100 includes a user device 102, a server 104, and a database 106. The user device 102 is connected to the server 104, which is connected to the database 106. The server 104 is configured to receive data from the user device 102 and to provide data to the database 106. The database 106 is configured to store data received from the server 104 and to provide data to the server 104. The server 104 is configured to provide a personalized experience to the user based on the data received from the user device 102 and the data stored in the database 106.

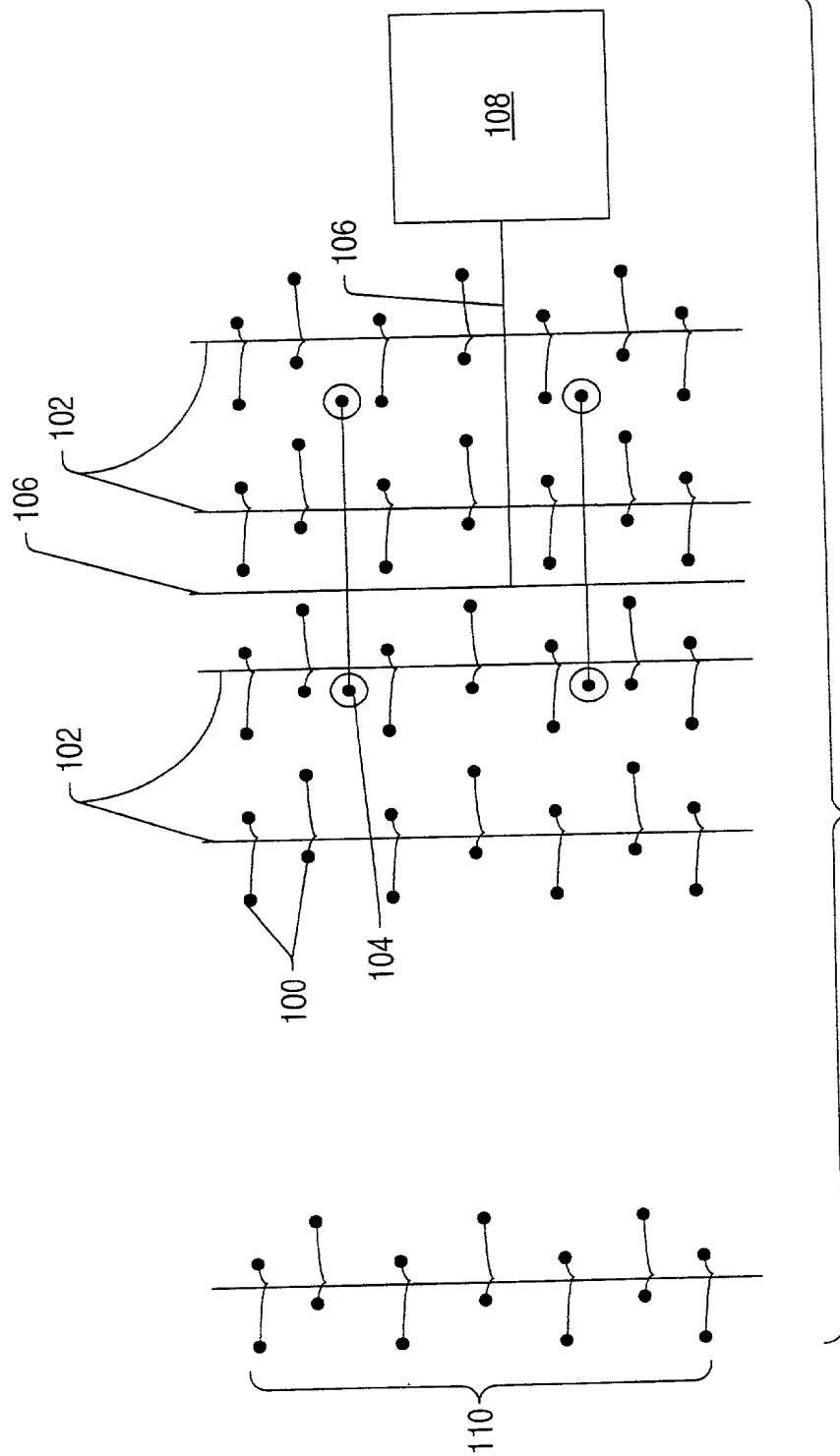


FIG. 3

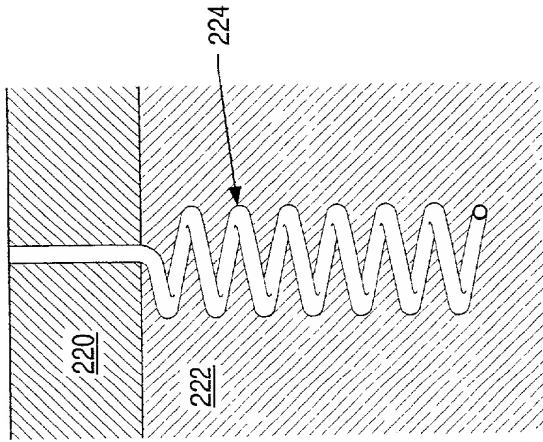


FIG. 3a

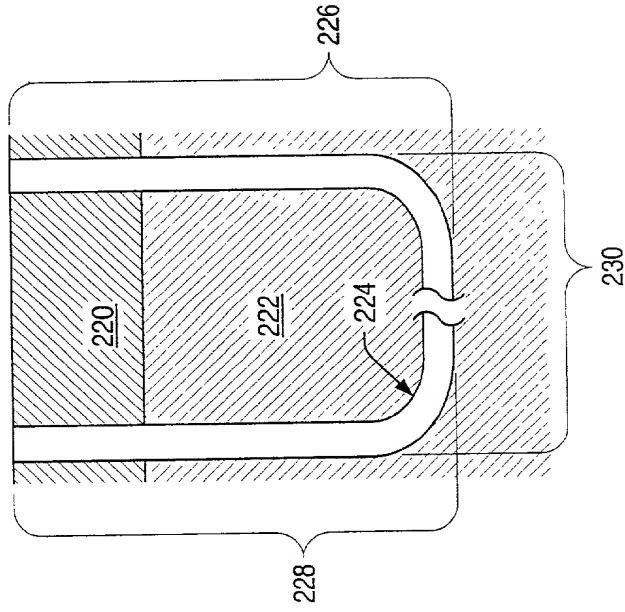


FIG. 3b

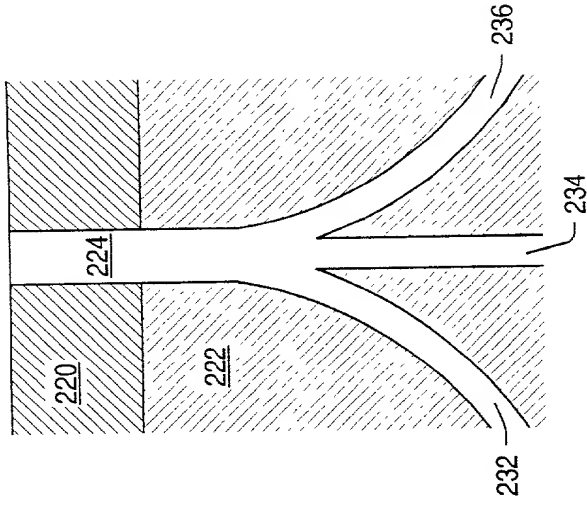


FIG. 3c

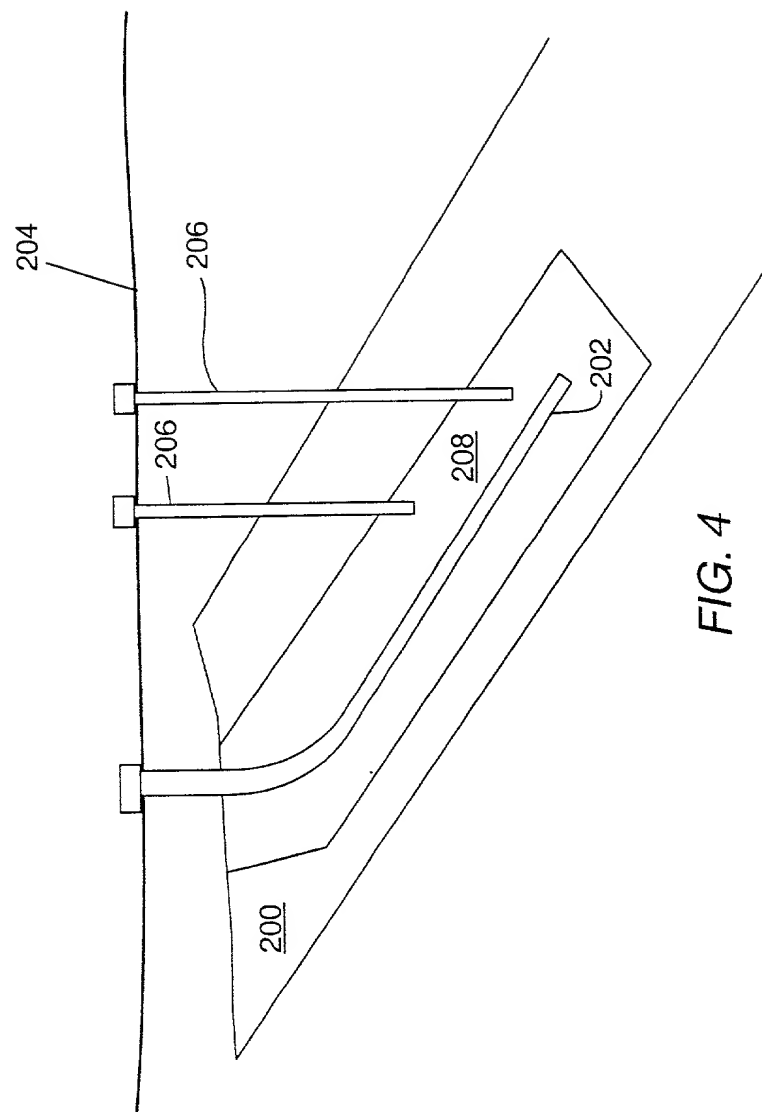
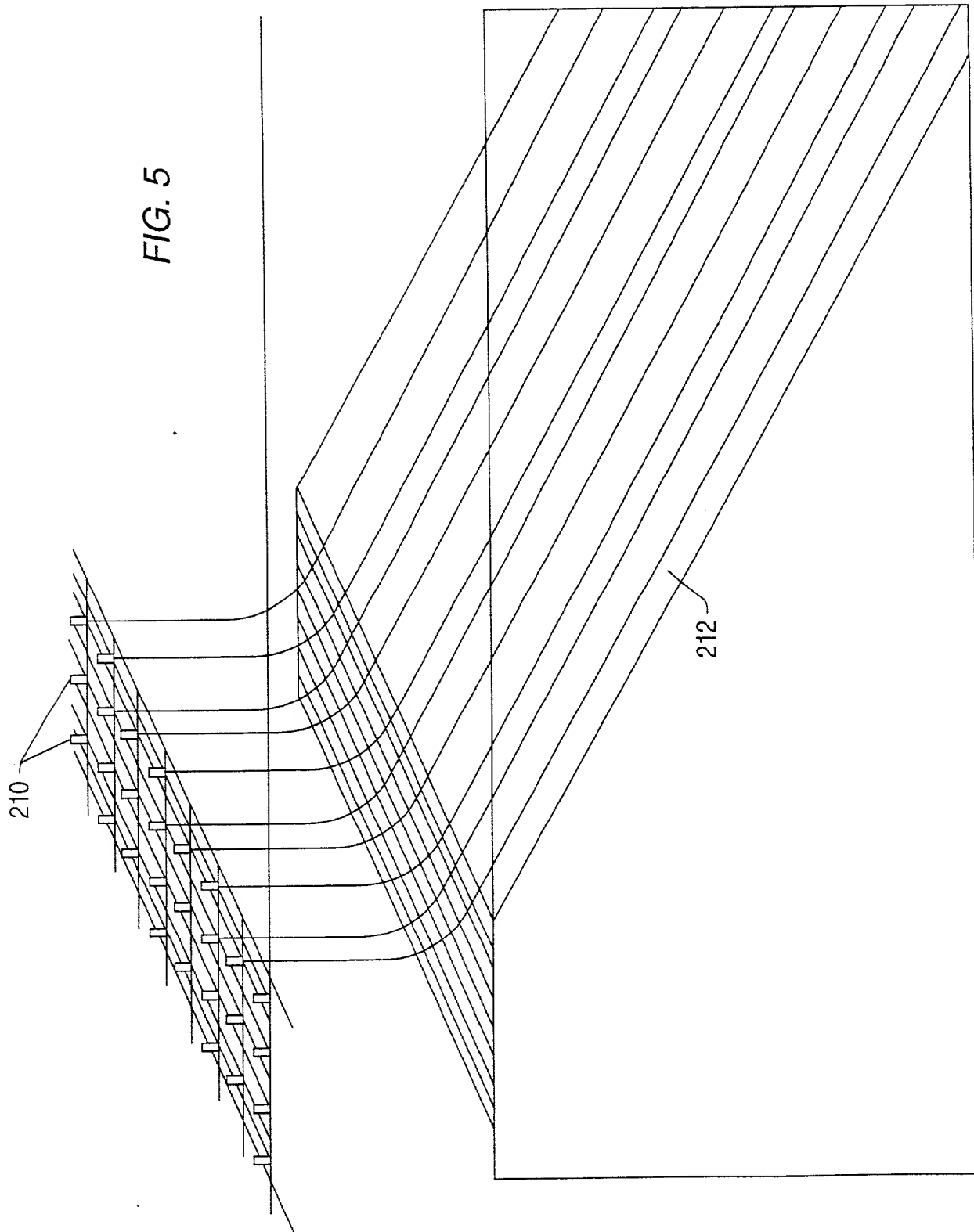


FIG. 4



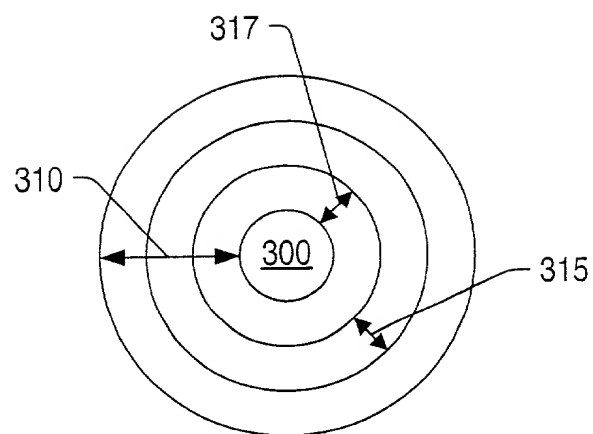


FIG. 6

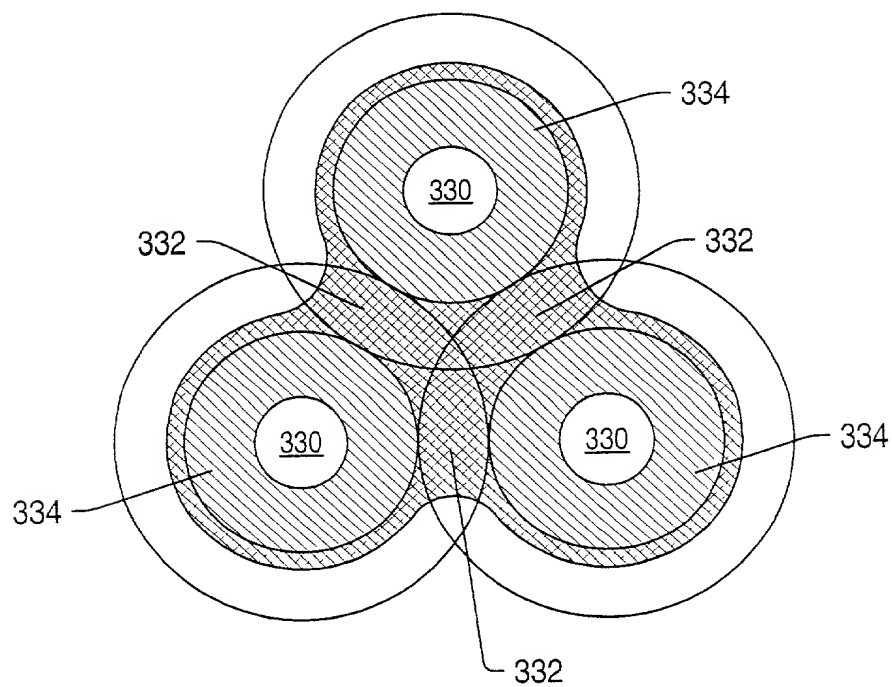


FIG. 7

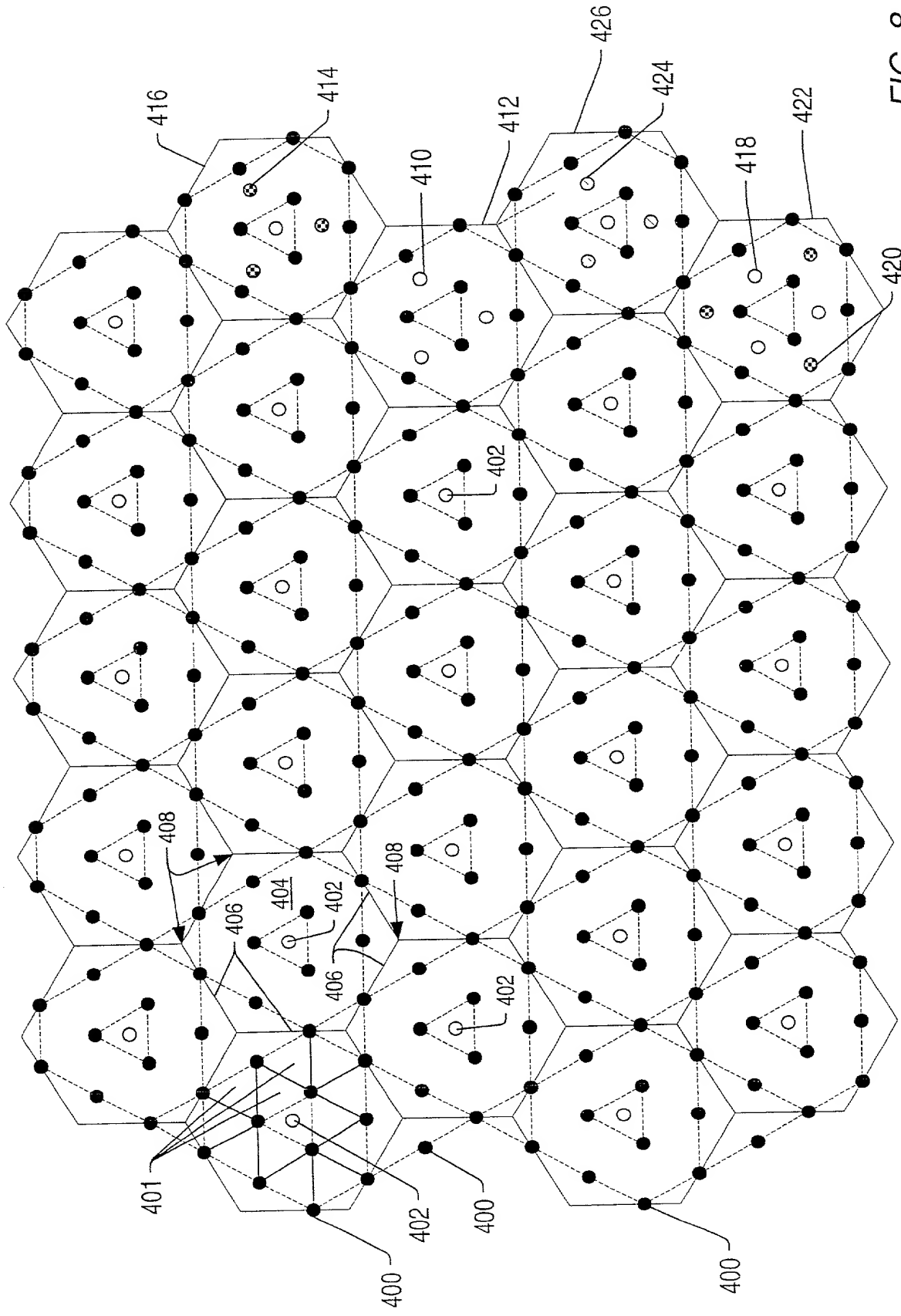


FIG. 8



FIG. 9 is a schematic diagram of a hexagonal lattice structure 400. The lattice is composed of a central hexagon 402 and six surrounding hexagons 404. The vertices of the central hexagon are labeled 400a and 400b. The vertices of the surrounding hexagons are labeled 400a and 400b. The lattice is shown in a perspective view.

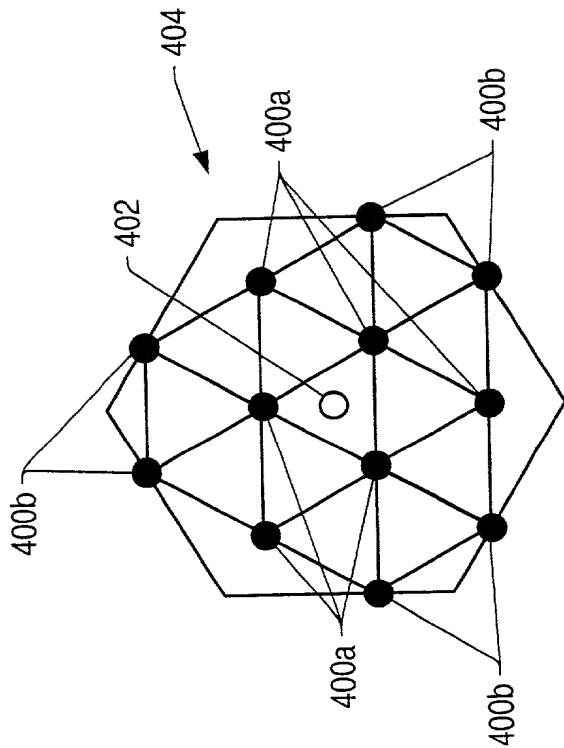


FIG. 9

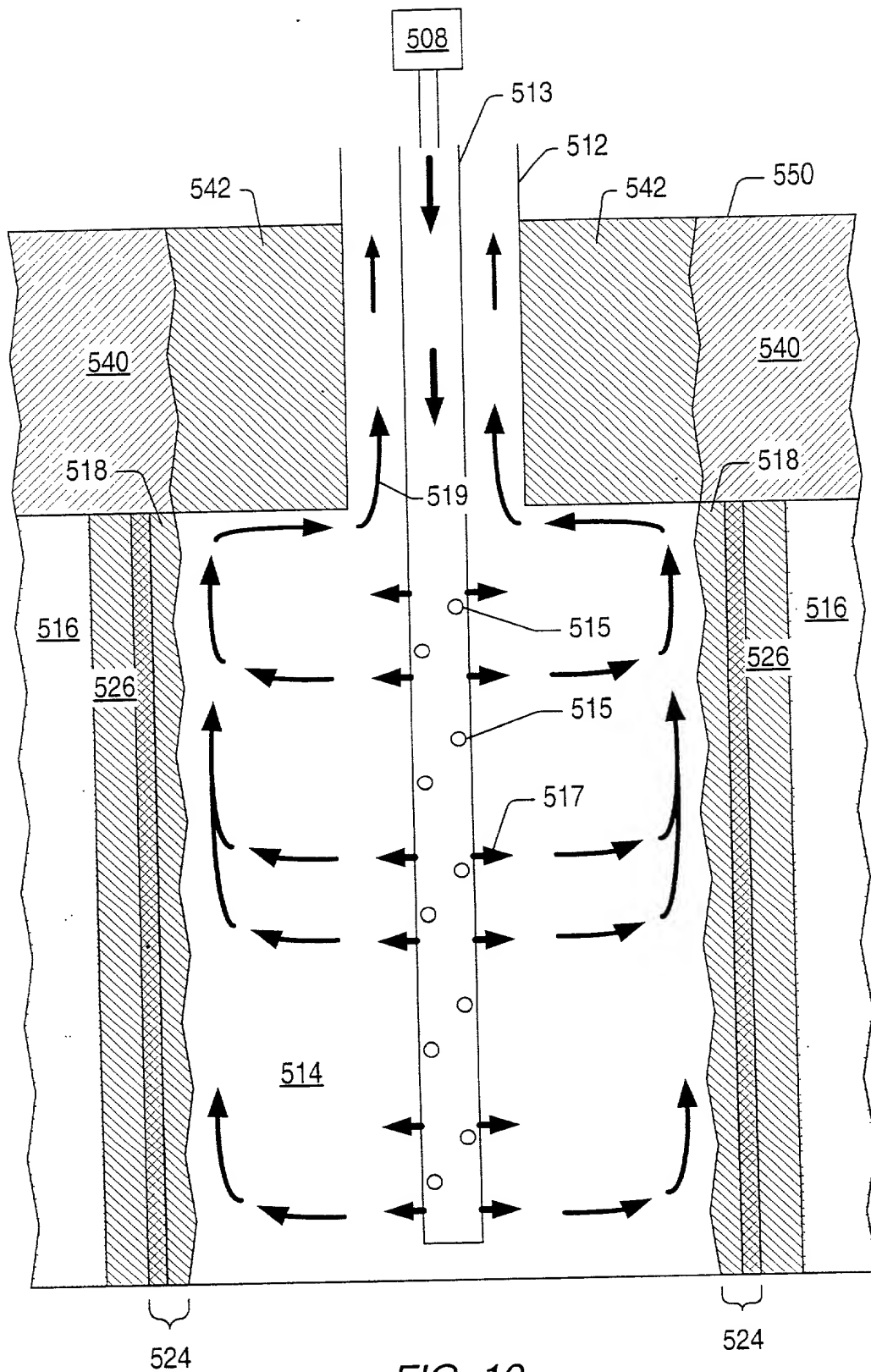


FIG. 10

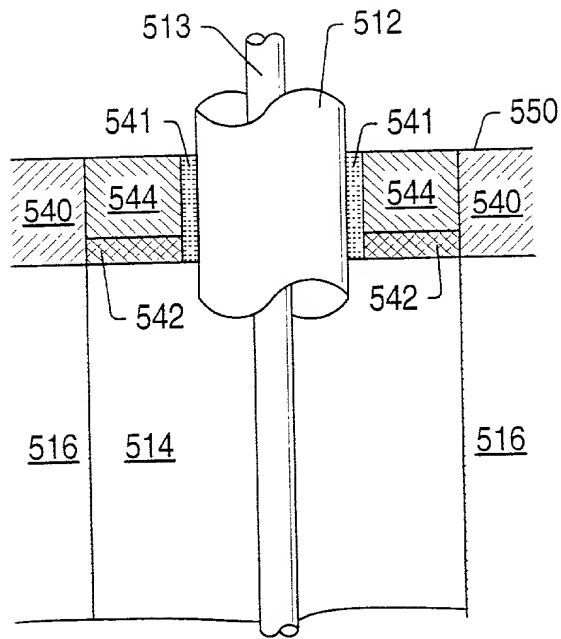


FIG. 11

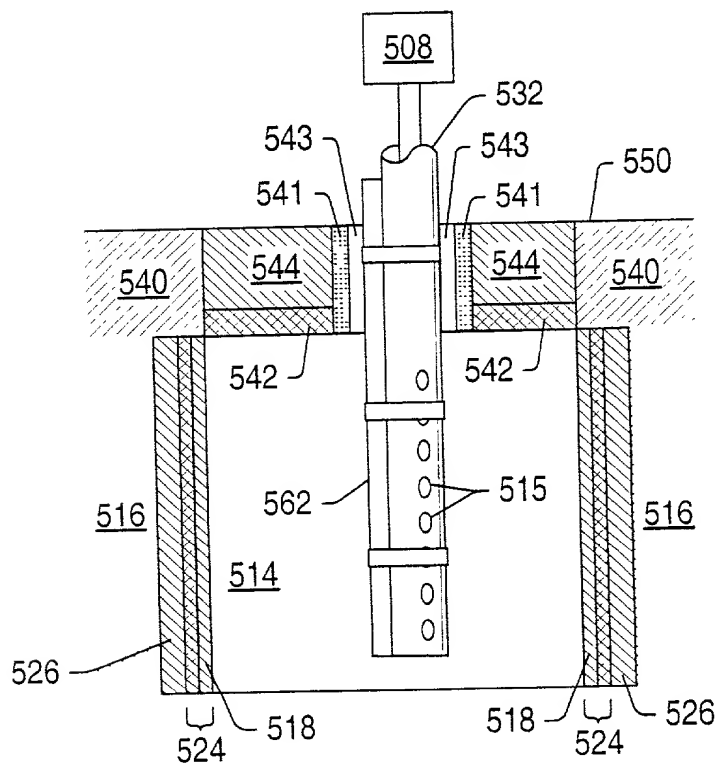


FIG. 12

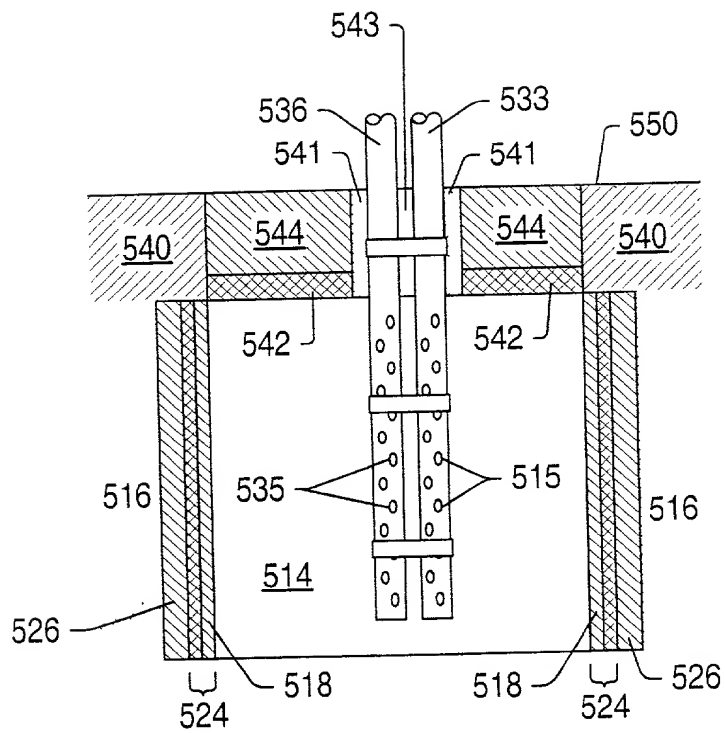


Fig. 13

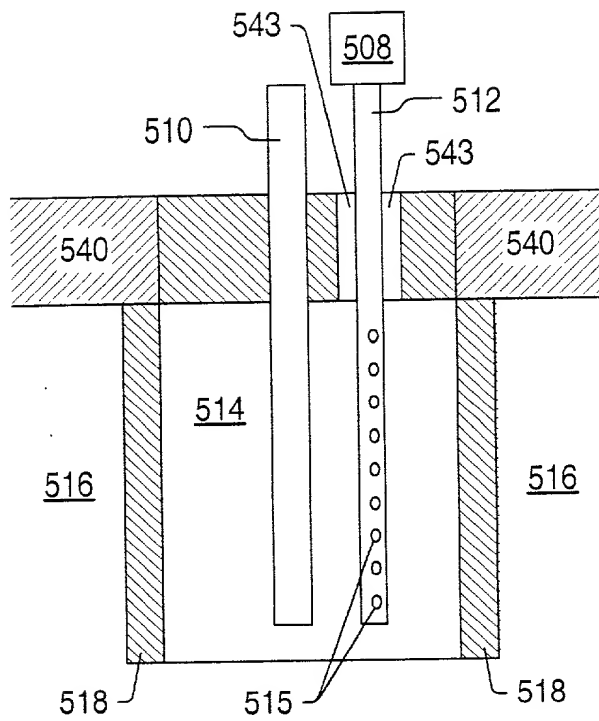


FIG. 14

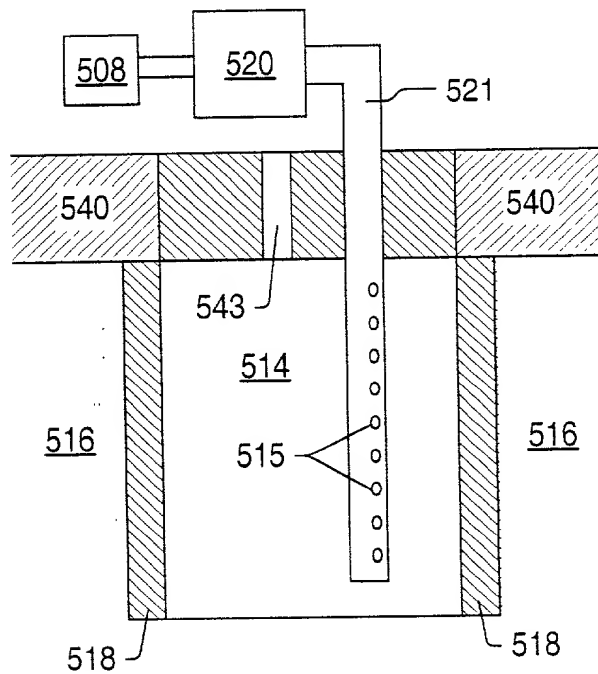


FIG. 15

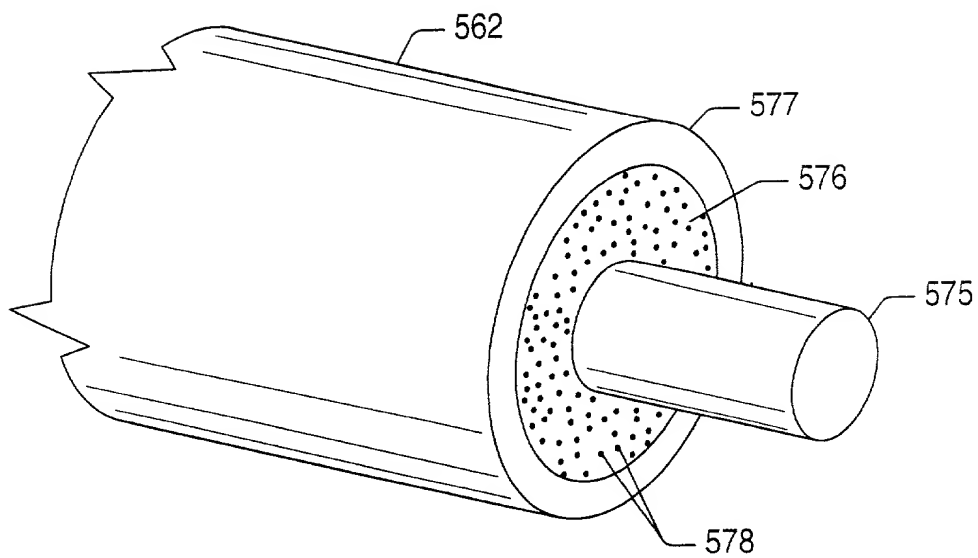


FIG. 16

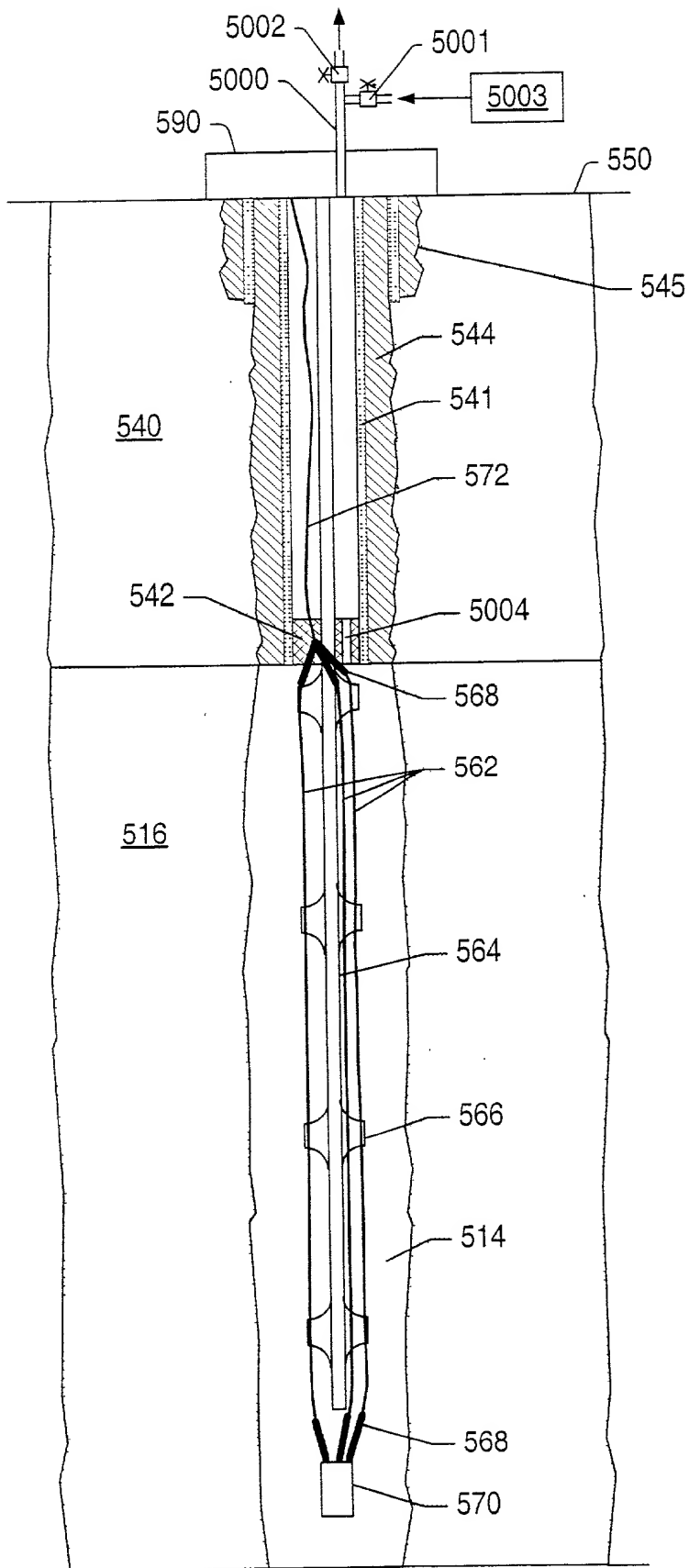


FIG. 17

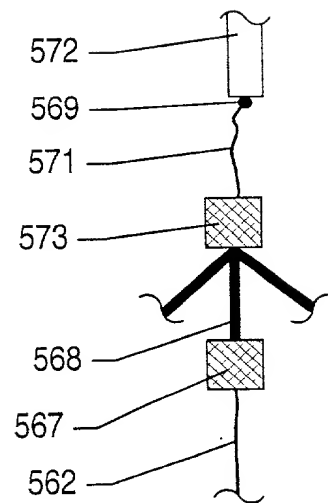


FIG. 17A

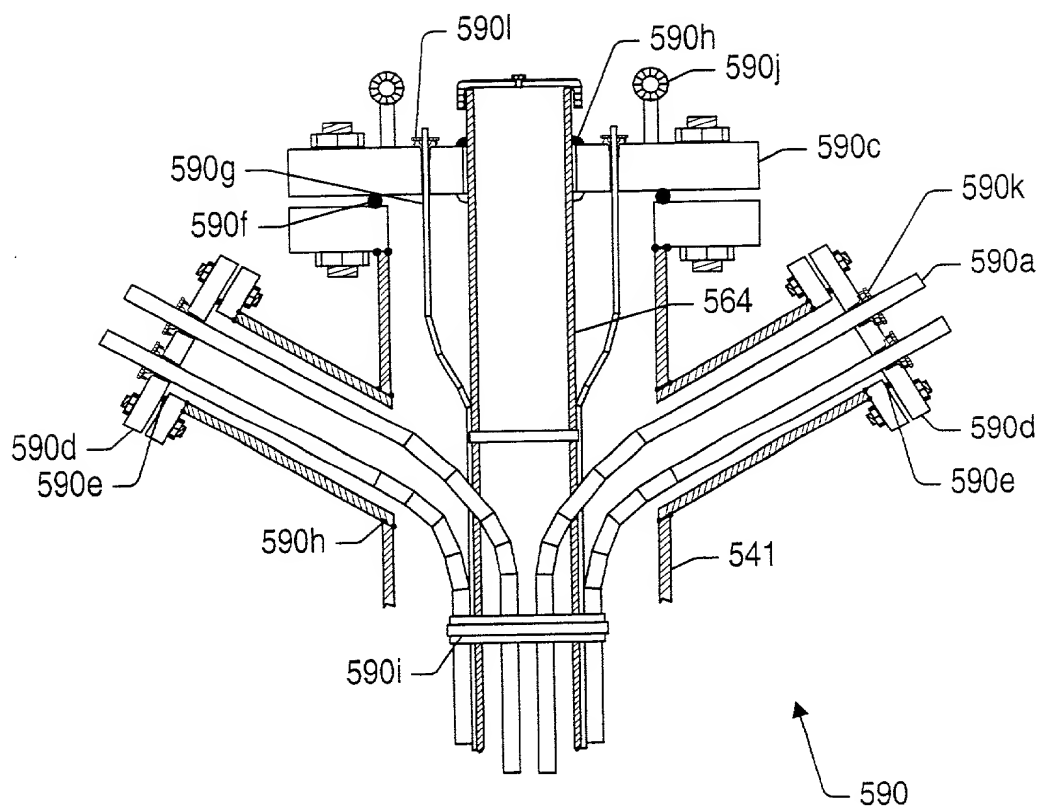


FIG. 18



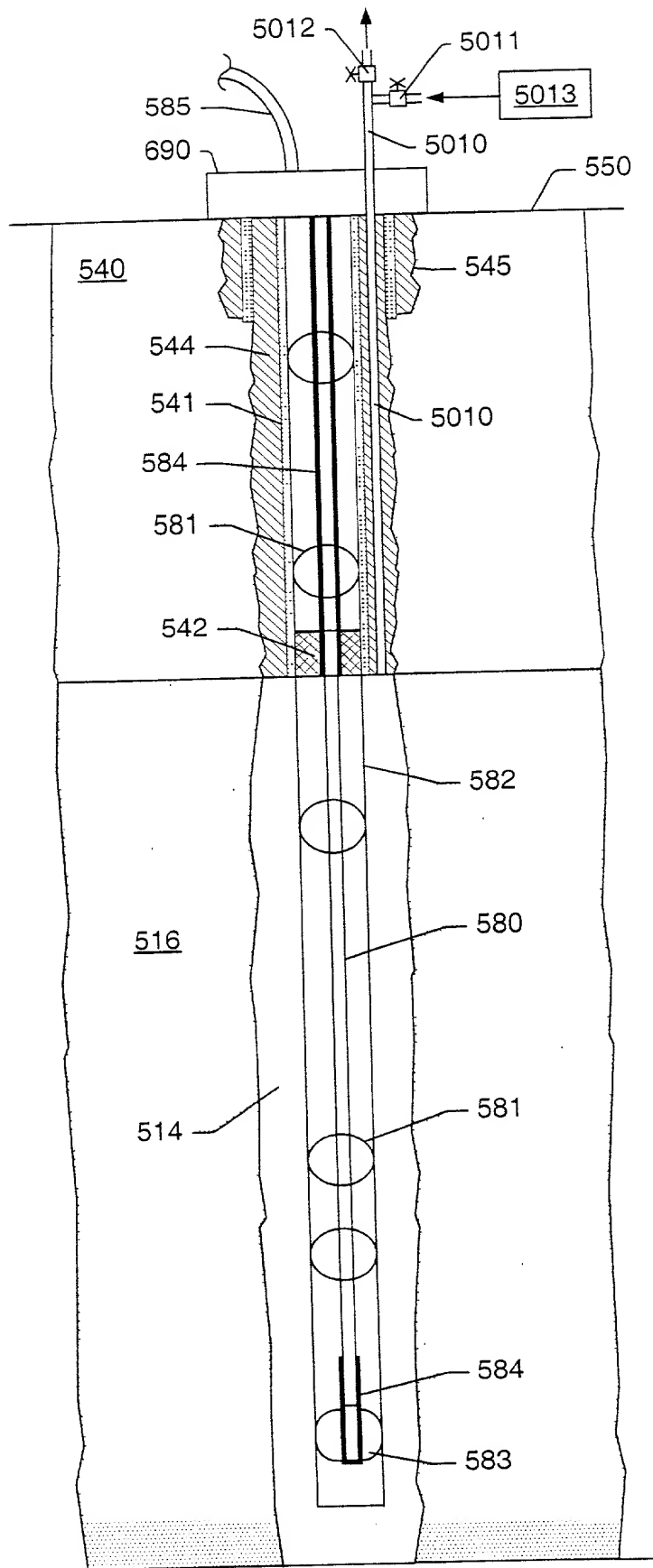


FIG. 19

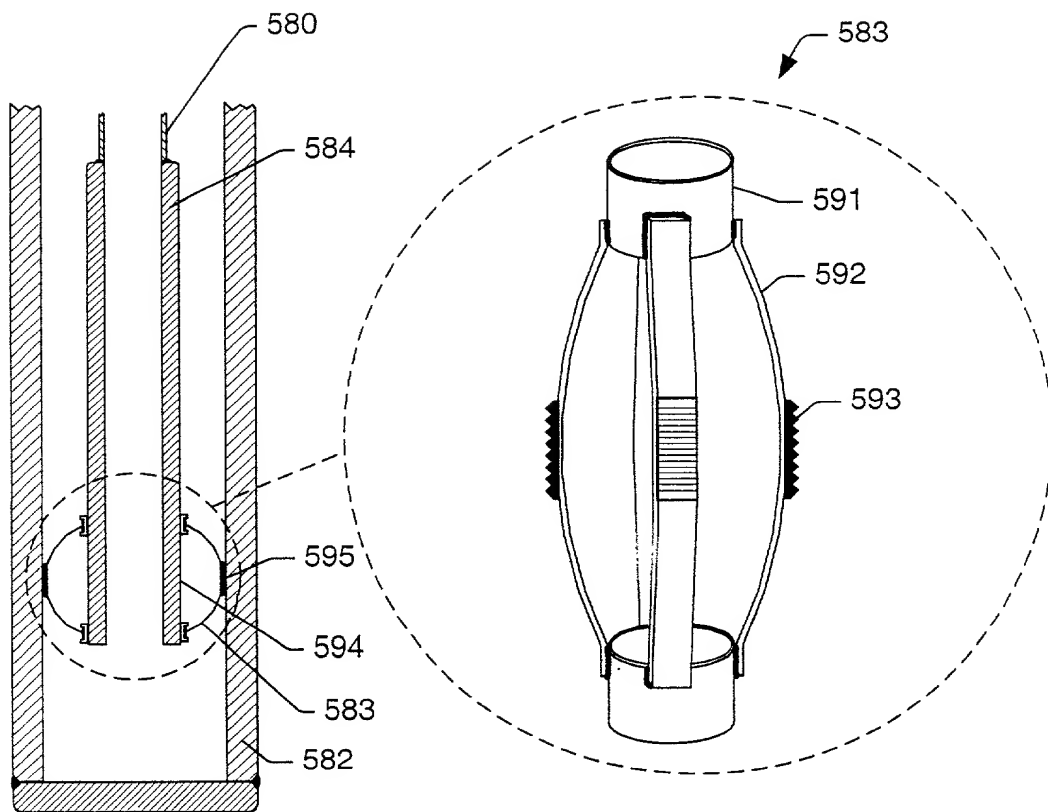


FIG. 20

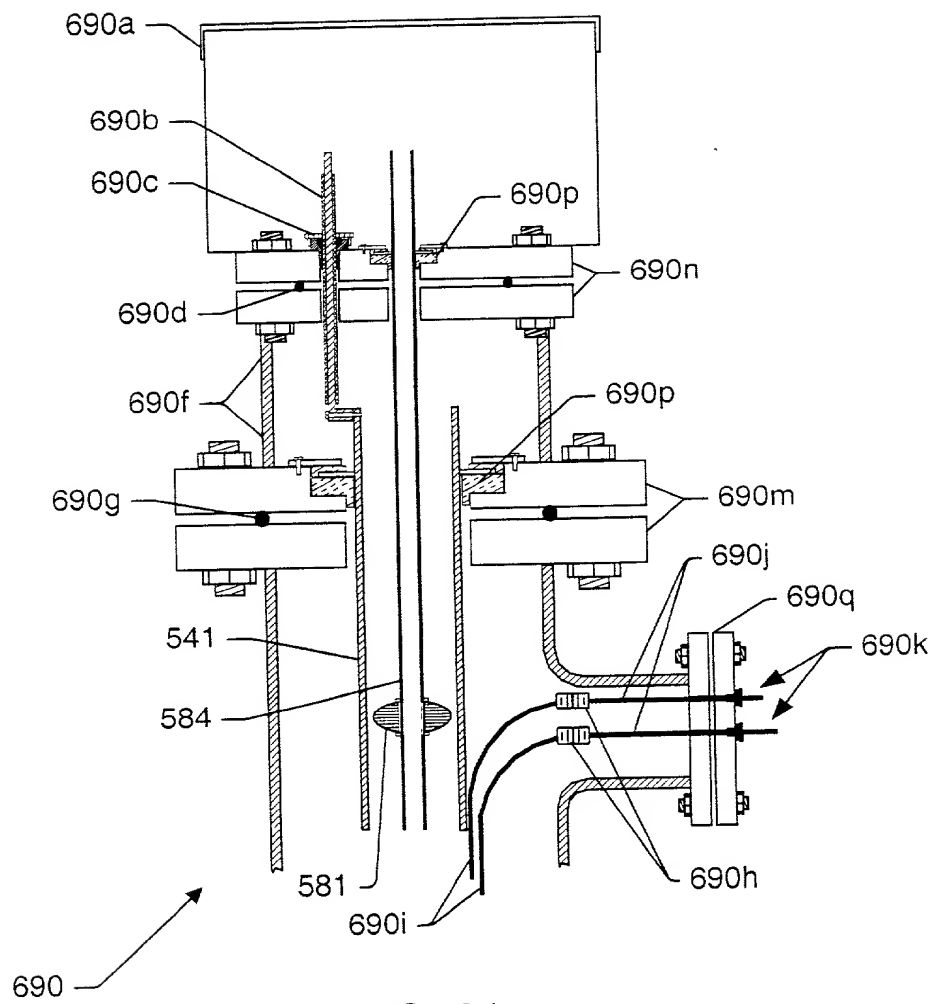


FIG. 21

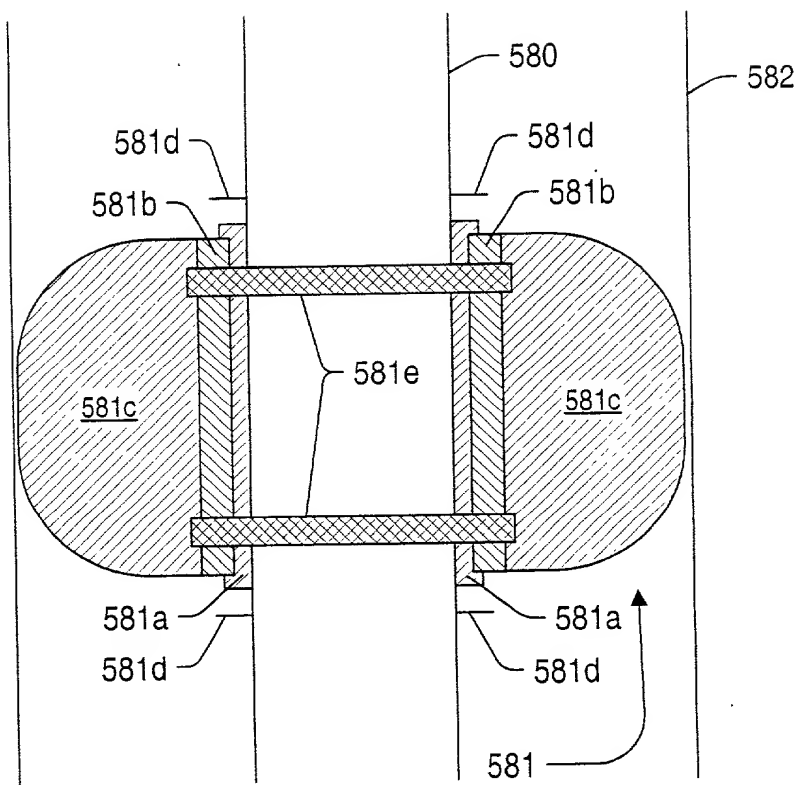


FIG. 22

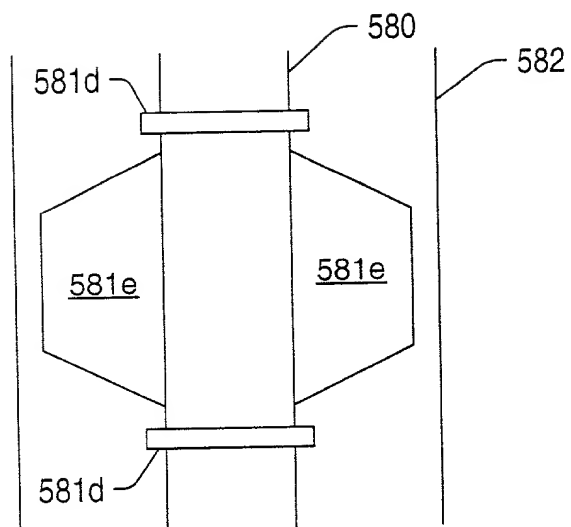


FIG. 23a

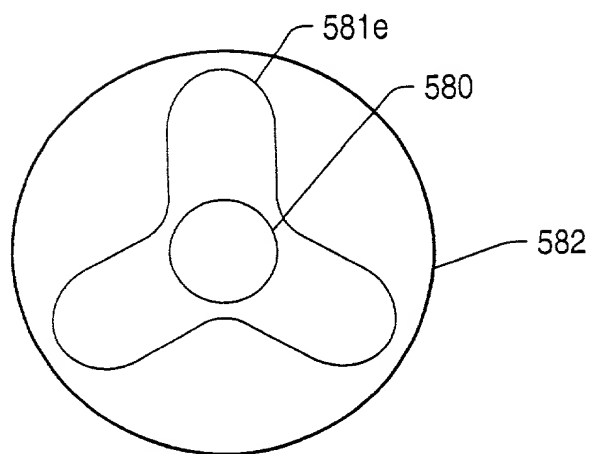


FIG. 23b

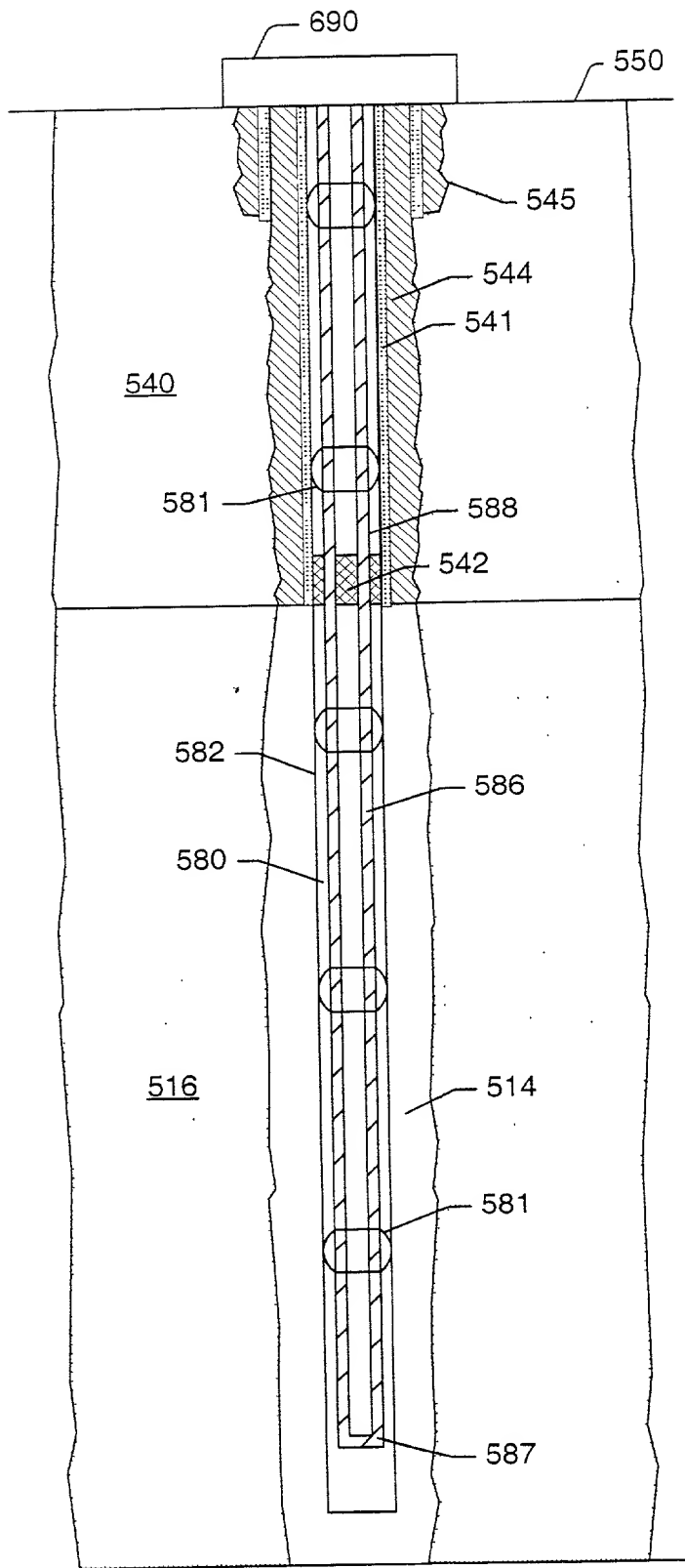


Fig. 24

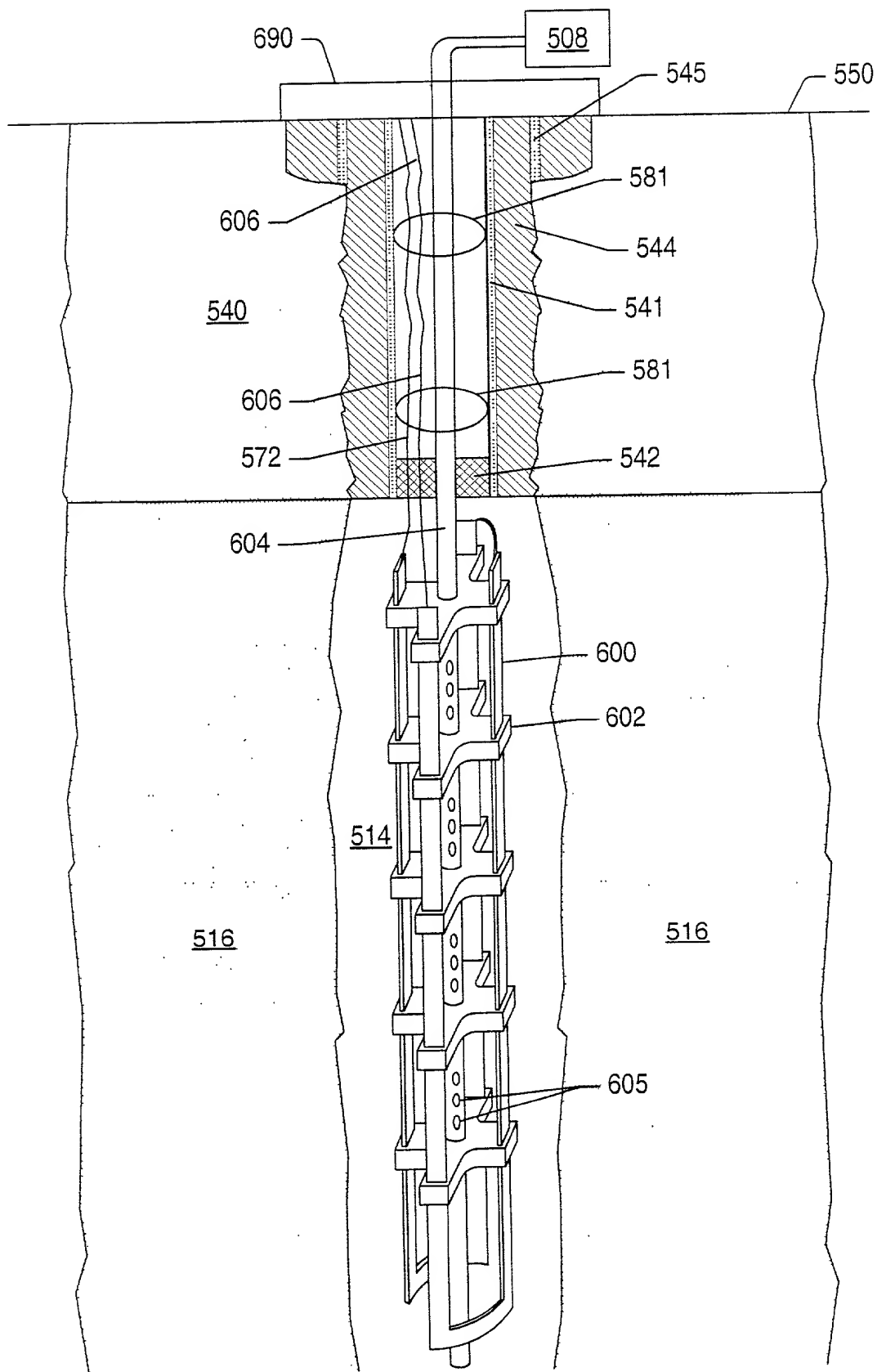


FIG. 25

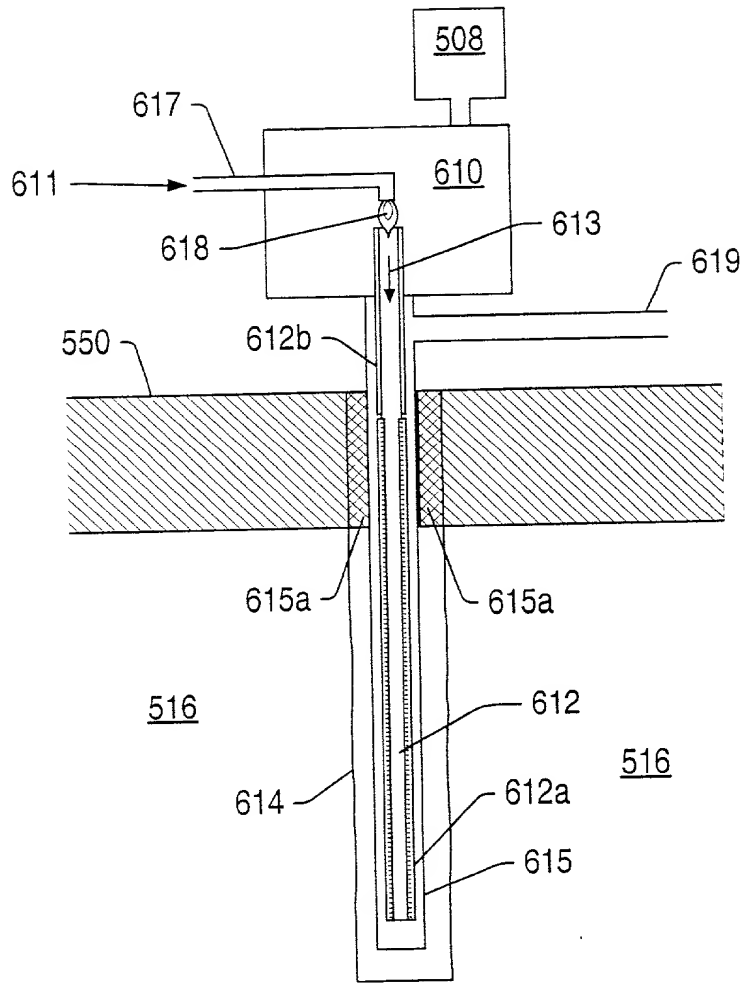


FIG. 26

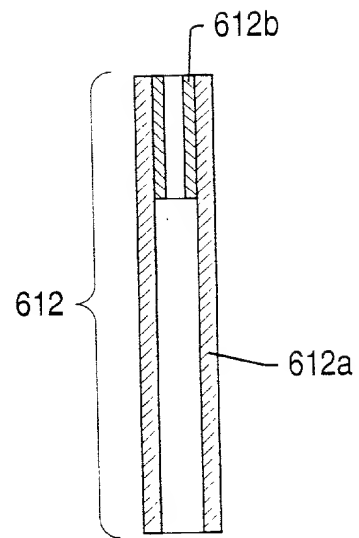


FIG. 27



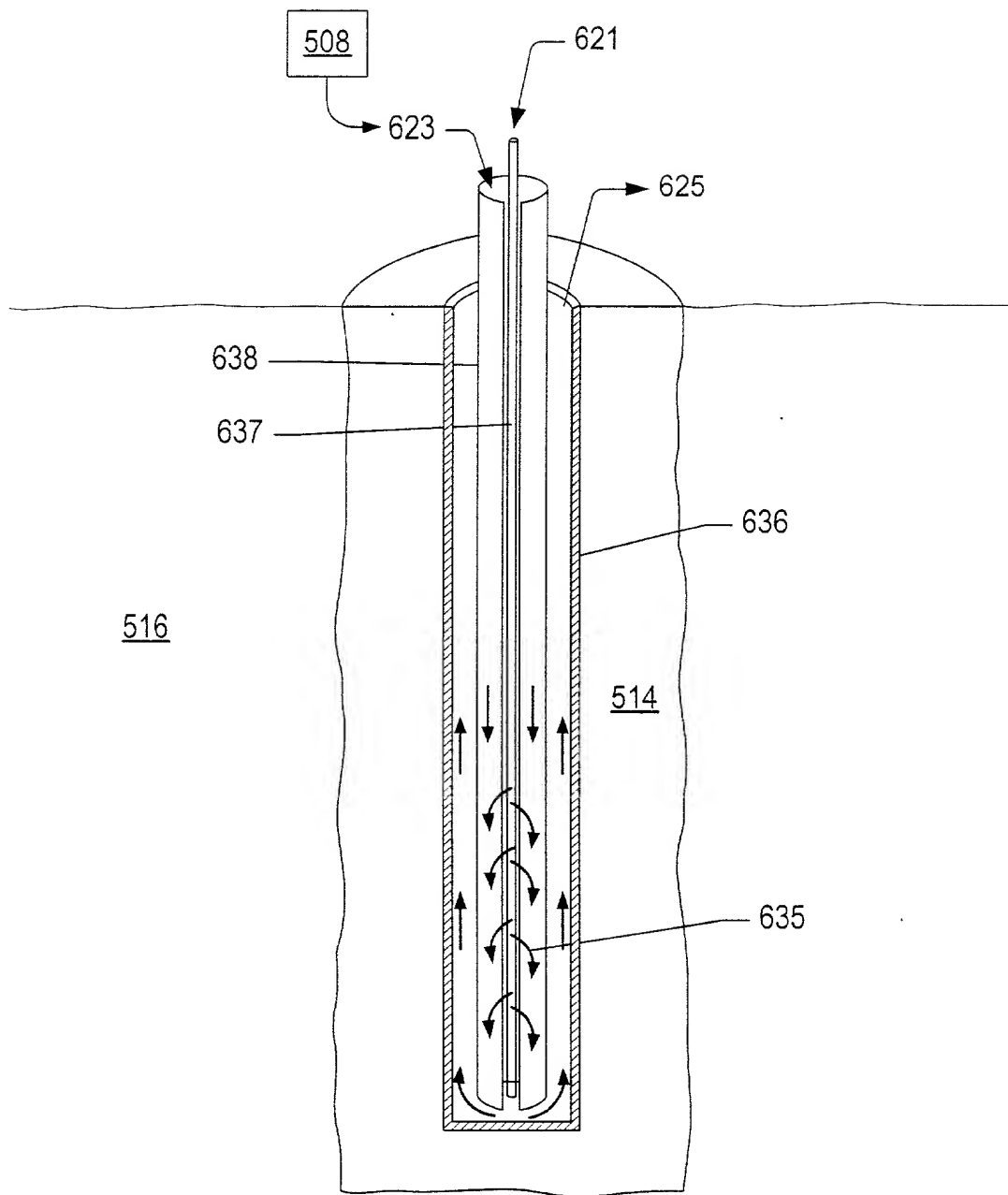


FIG. 28

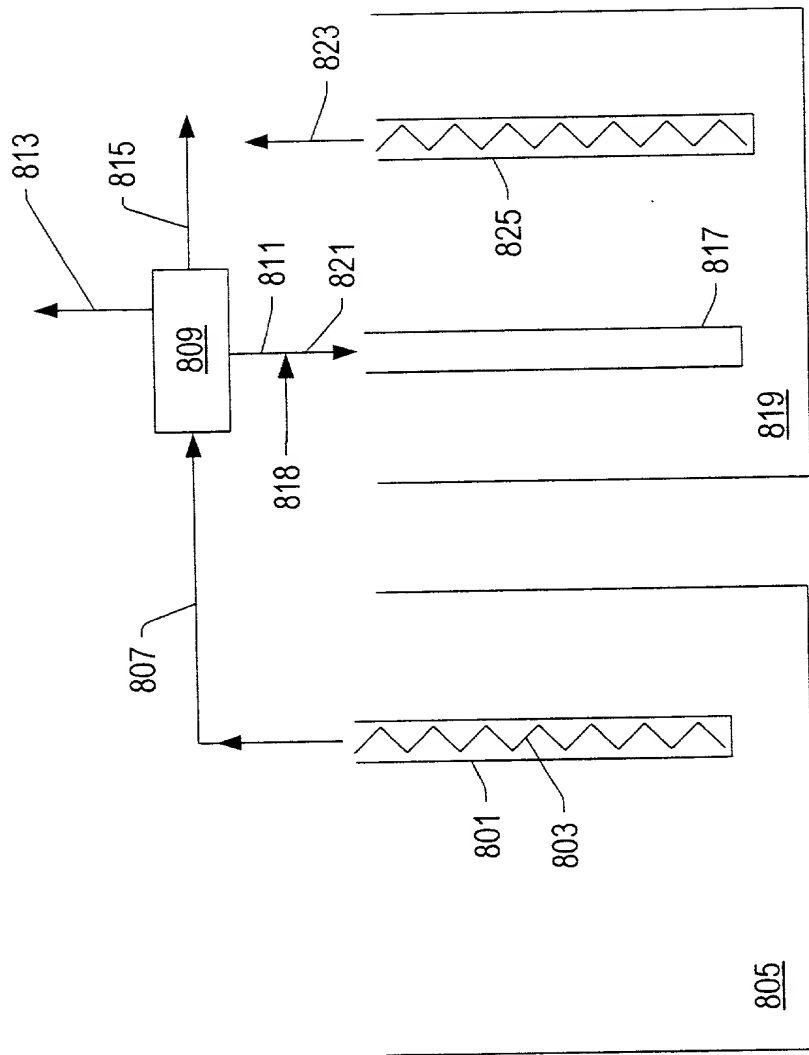


FIG. 29

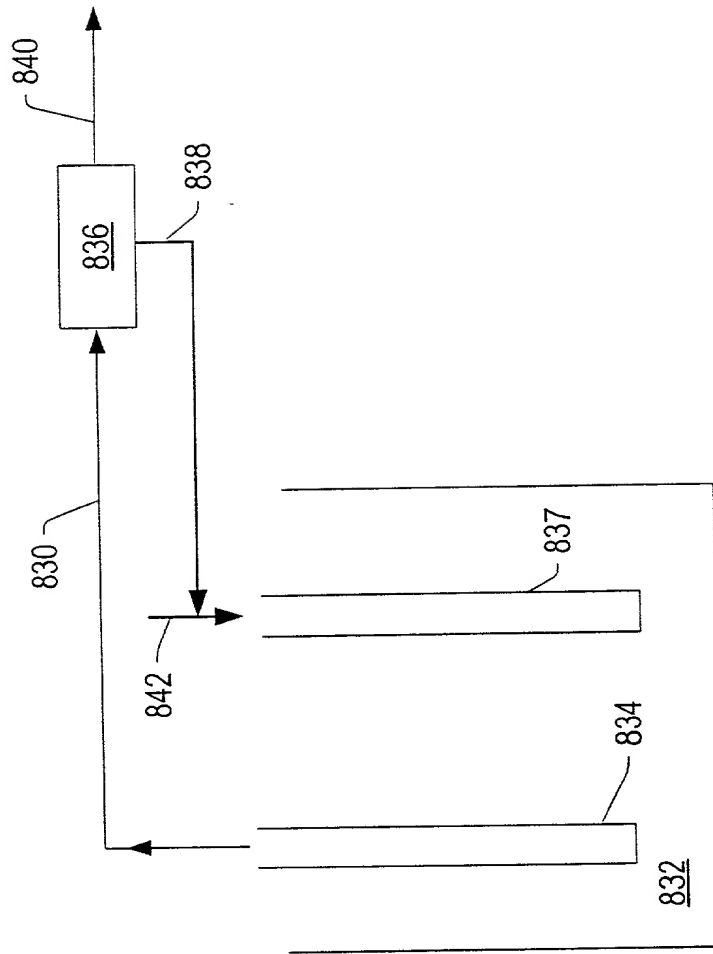


FIG. 30

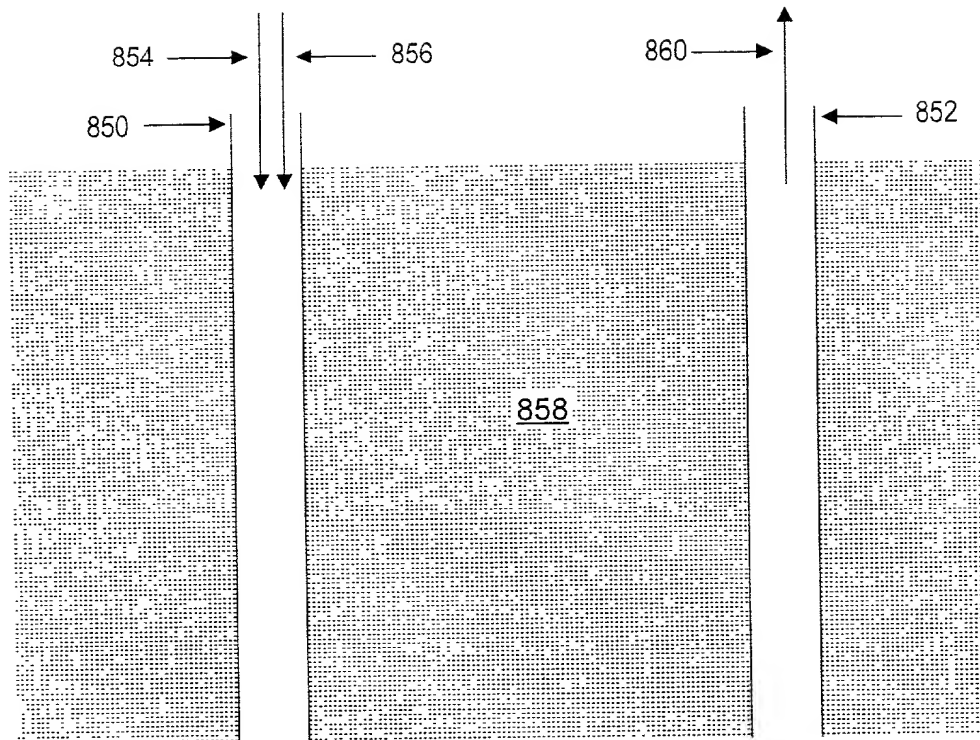


FIG. 31

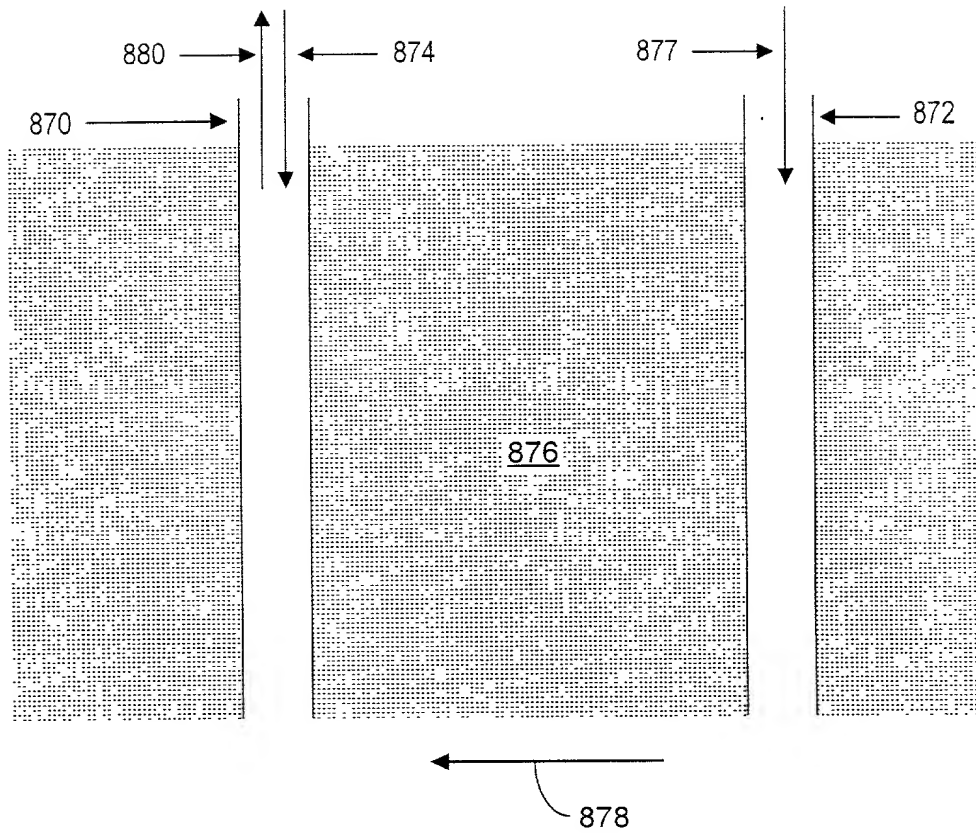


FIG. 32

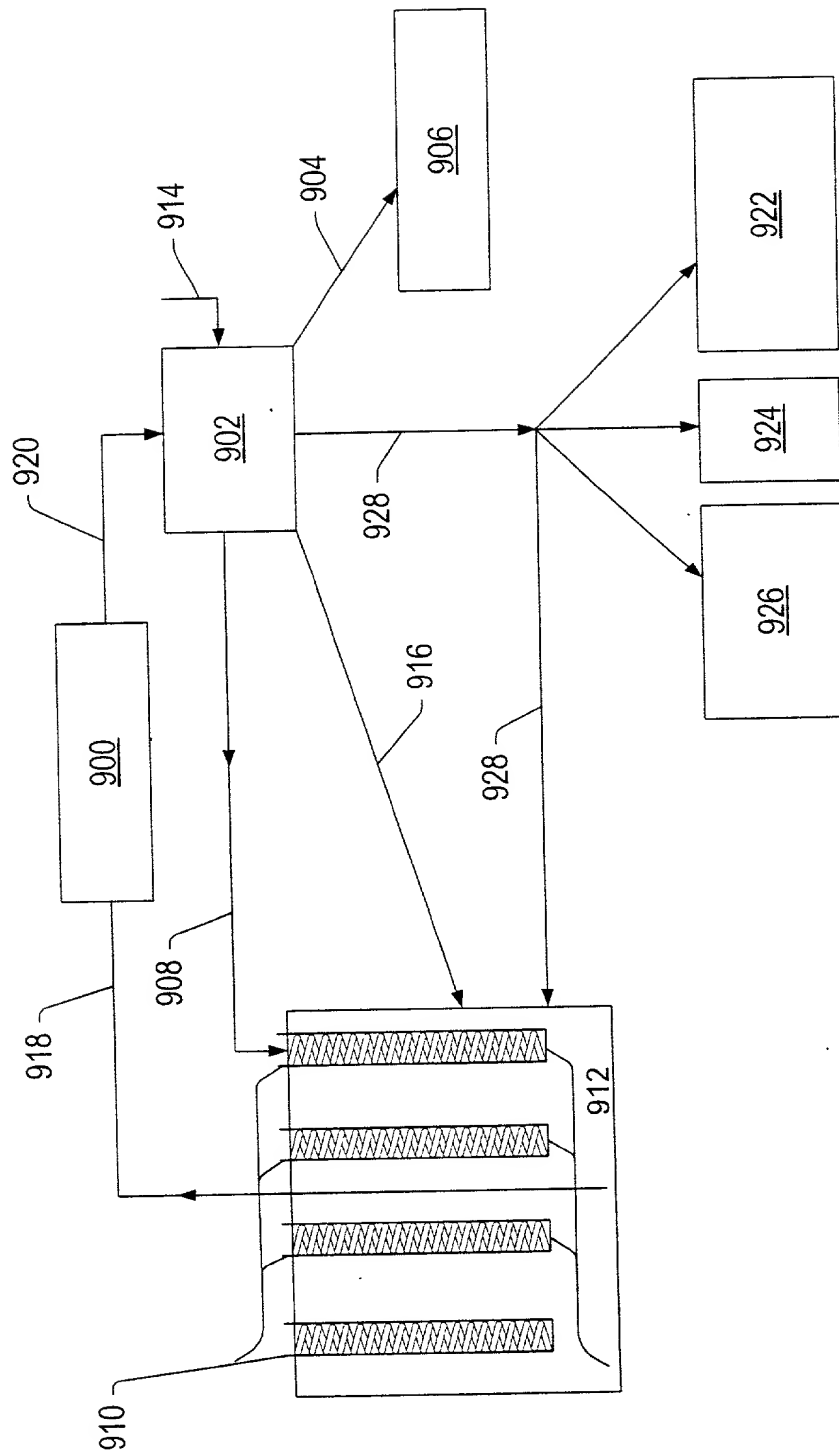


FIG. 33

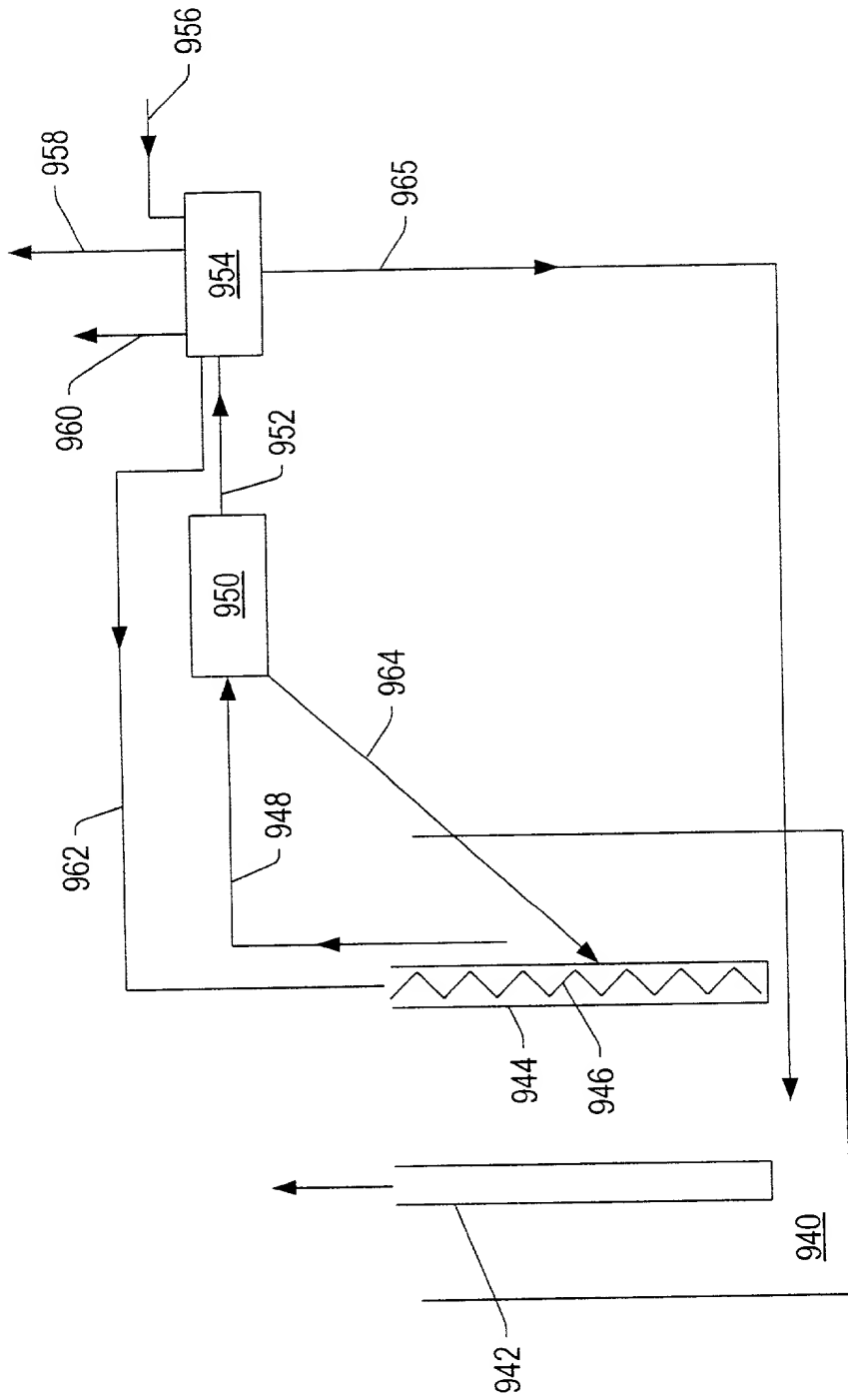


FIG. 34

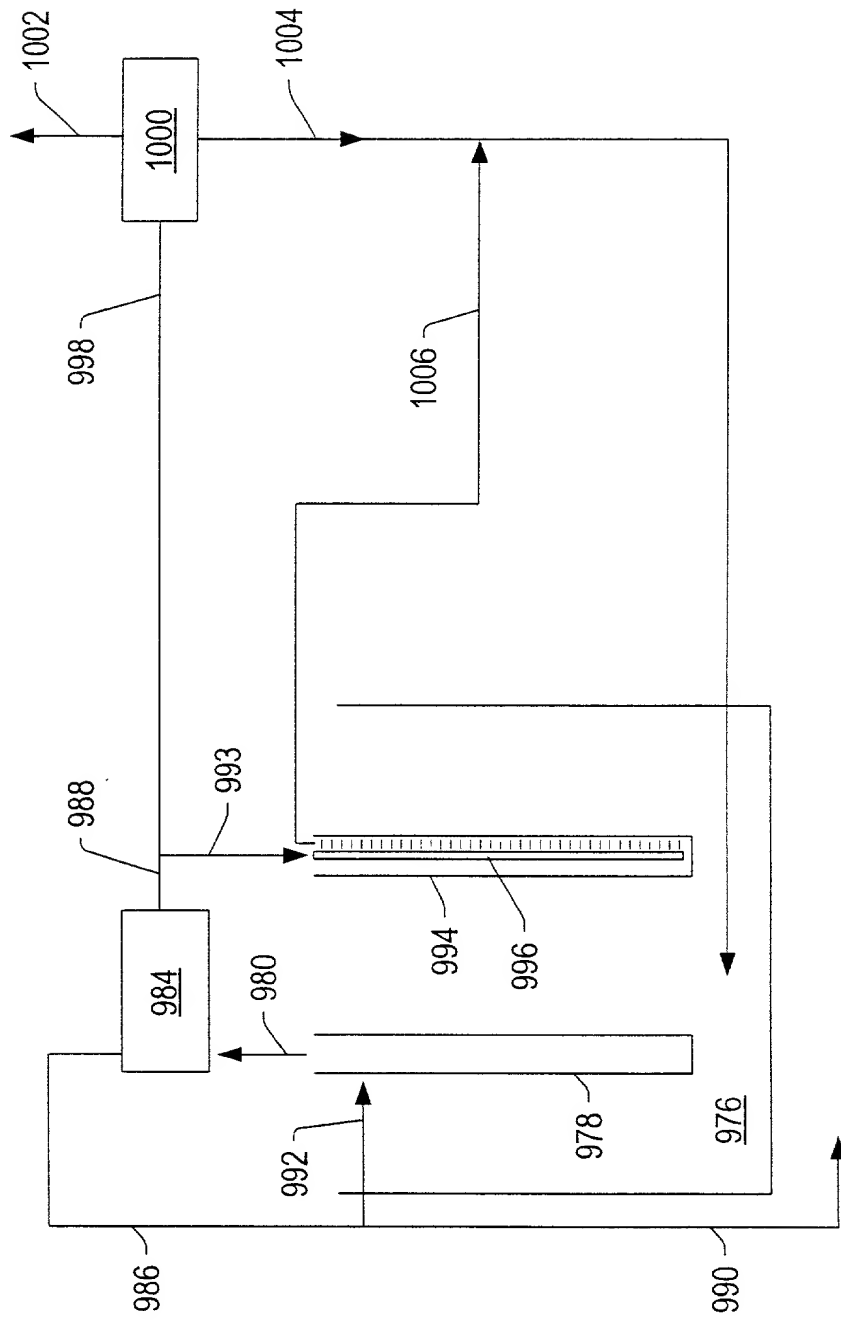


FIG. 35



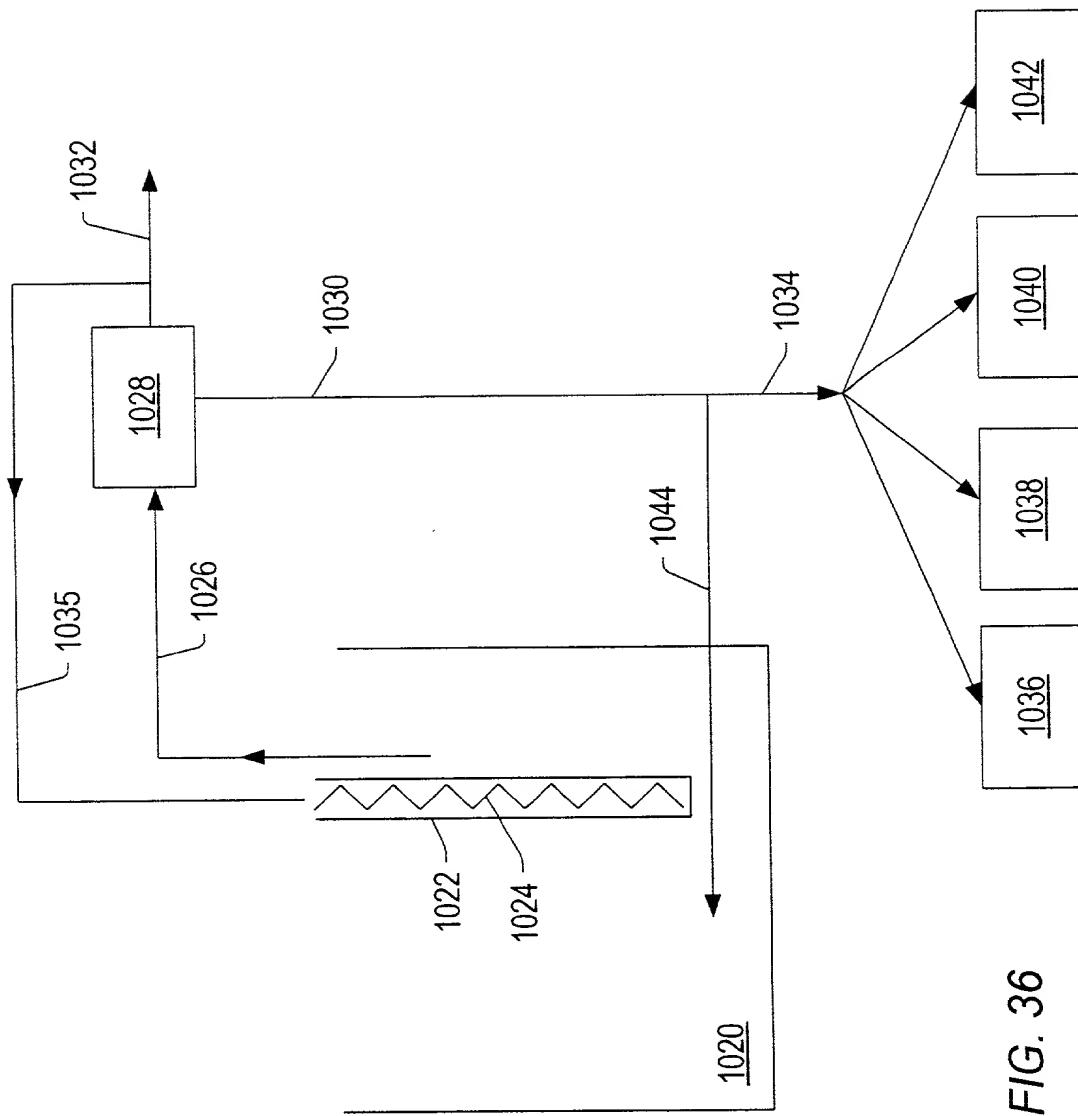


FIG. 36

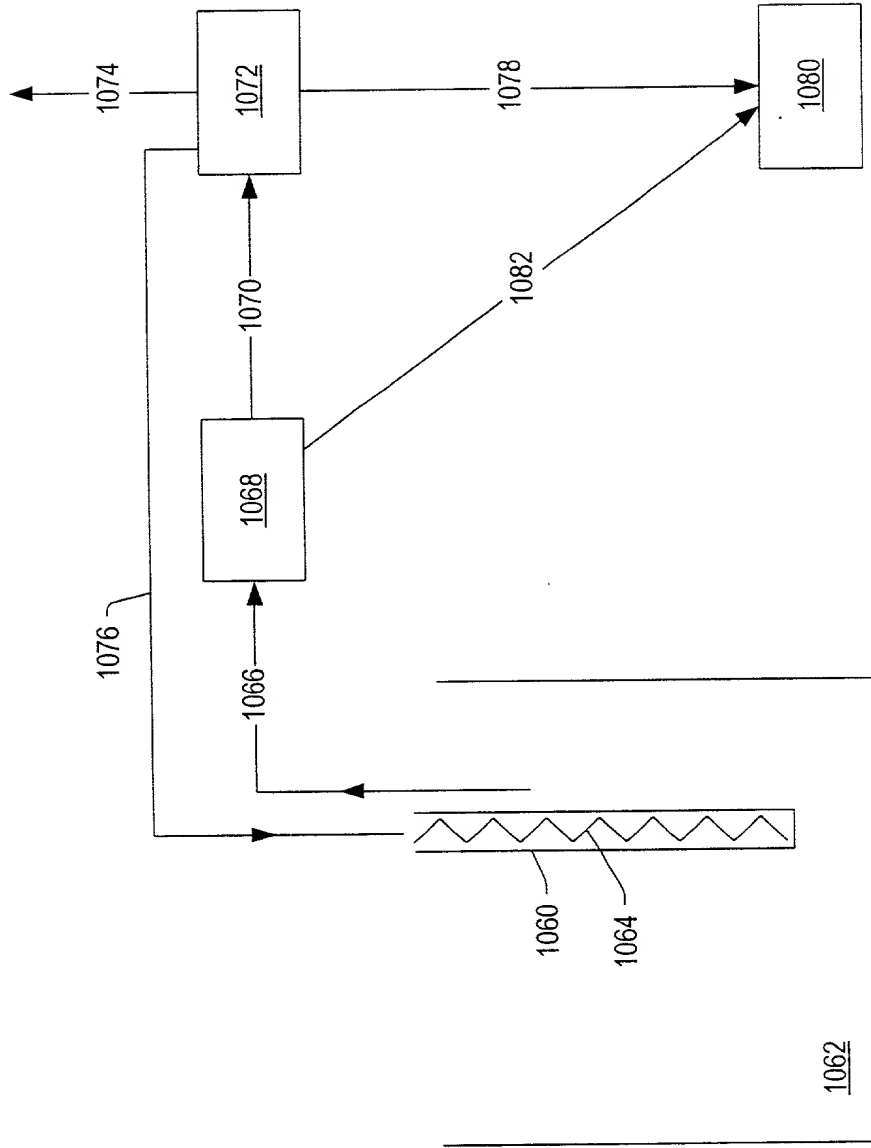


FIG. 37

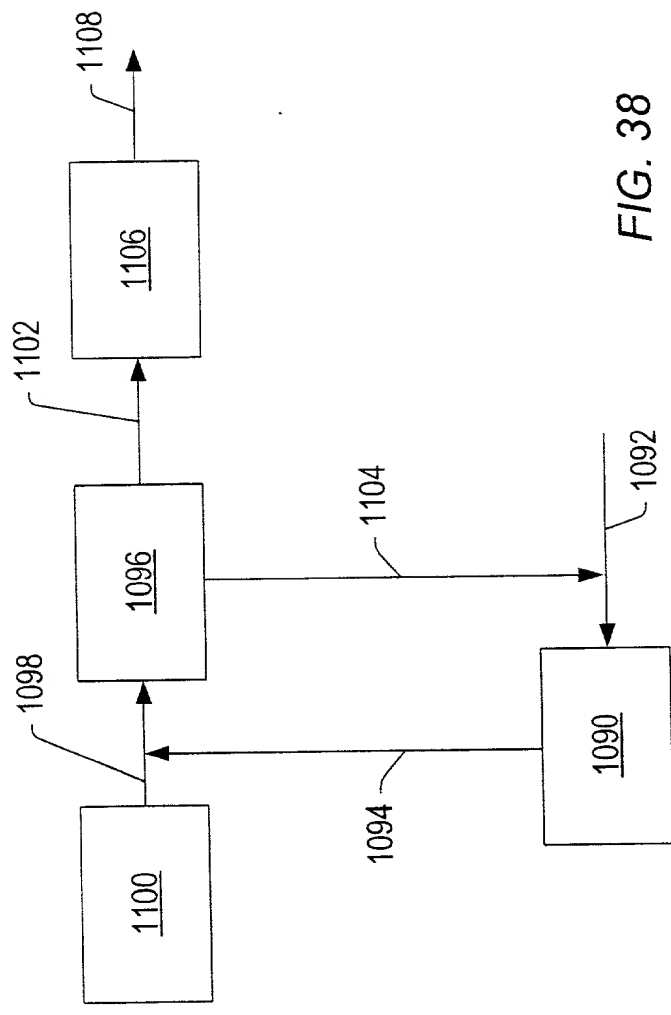


FIG. 38

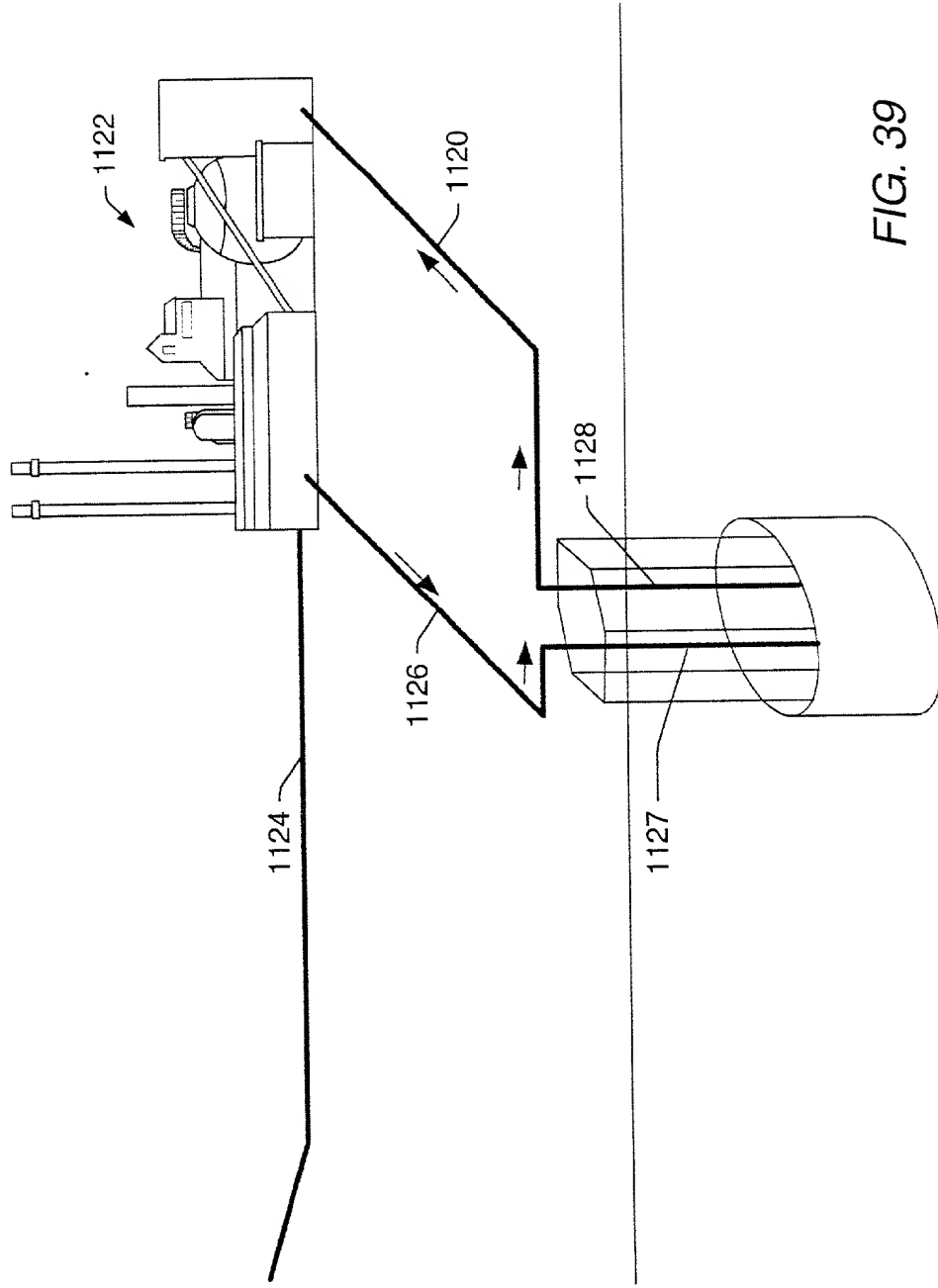


FIG. 39

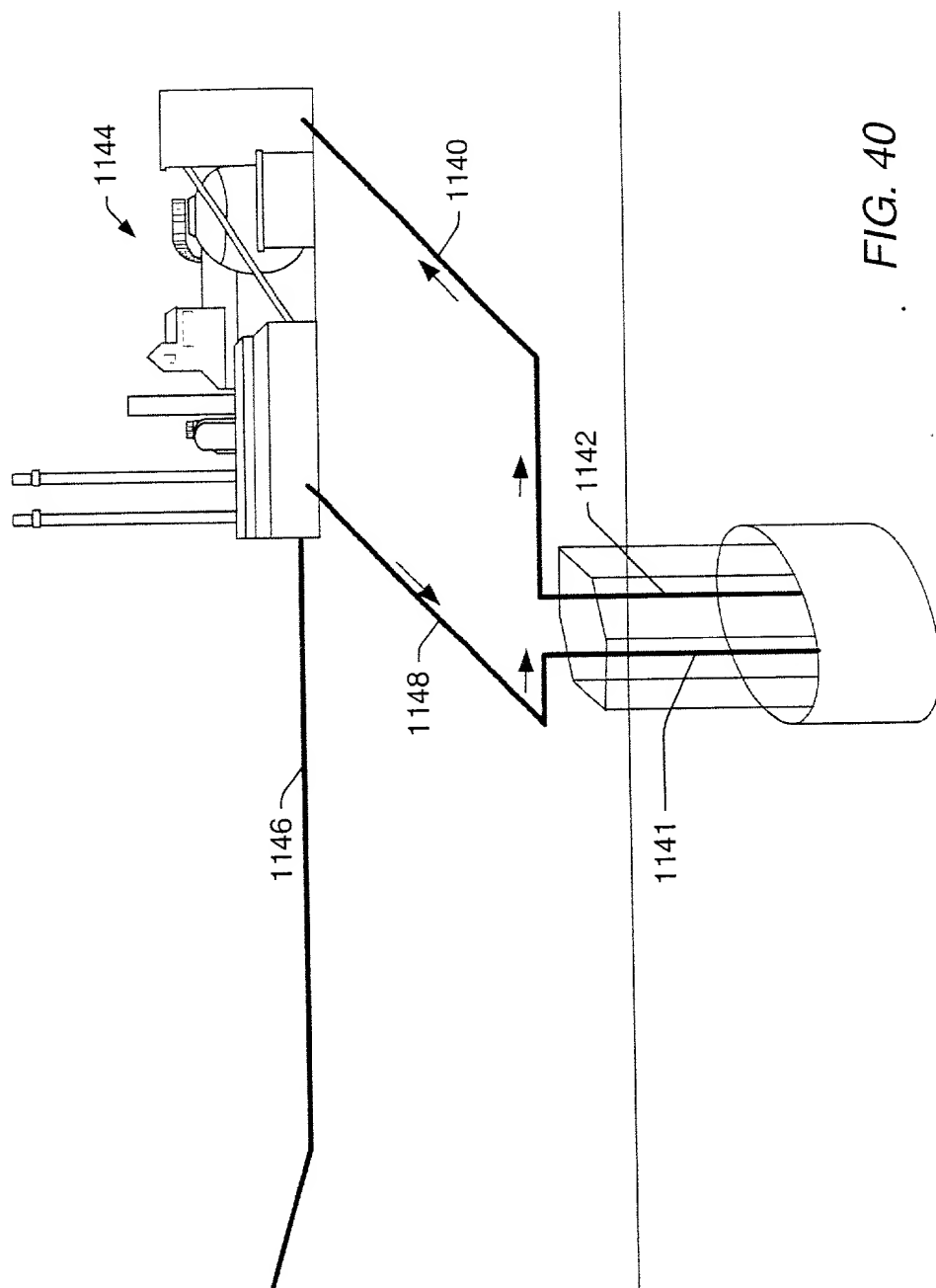


FIG. 40

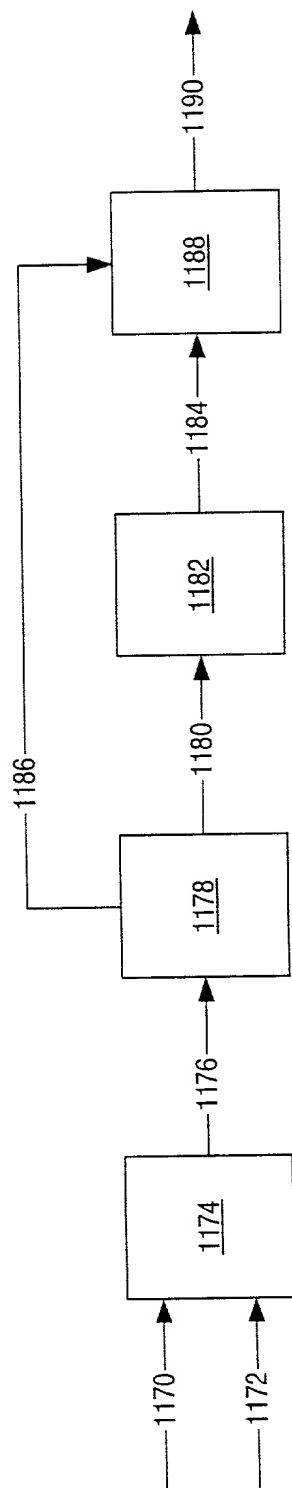


FIG. 41

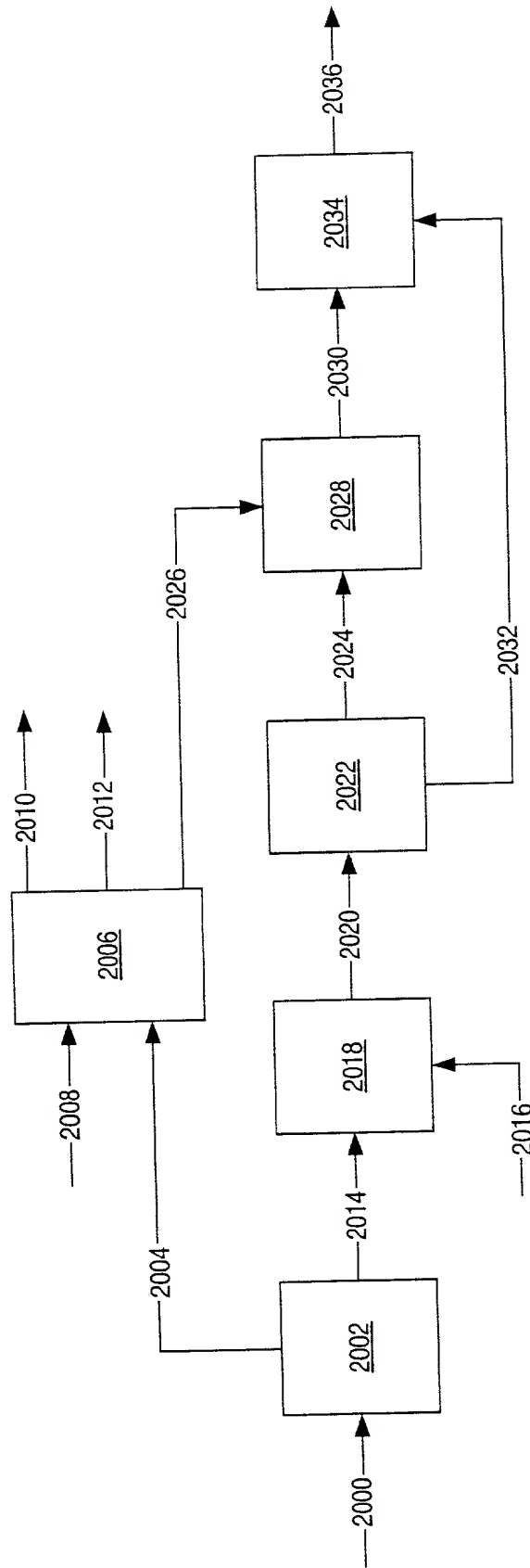


FIG. 42

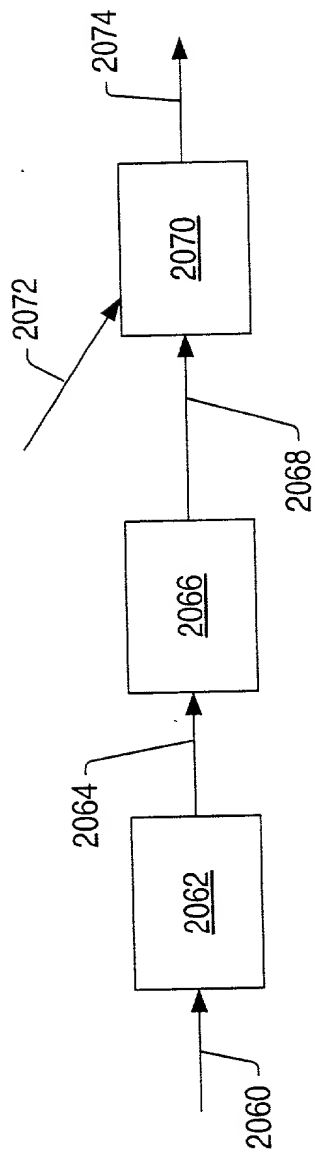


FIG. 43



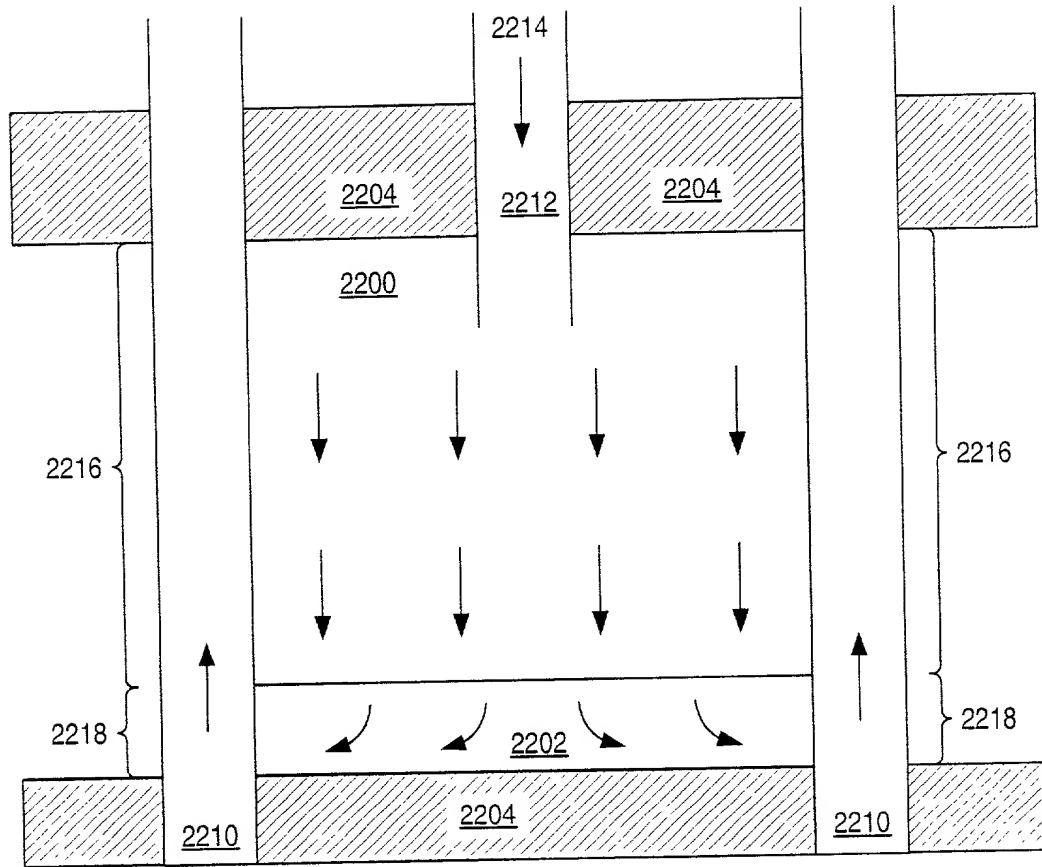


FIG. 44

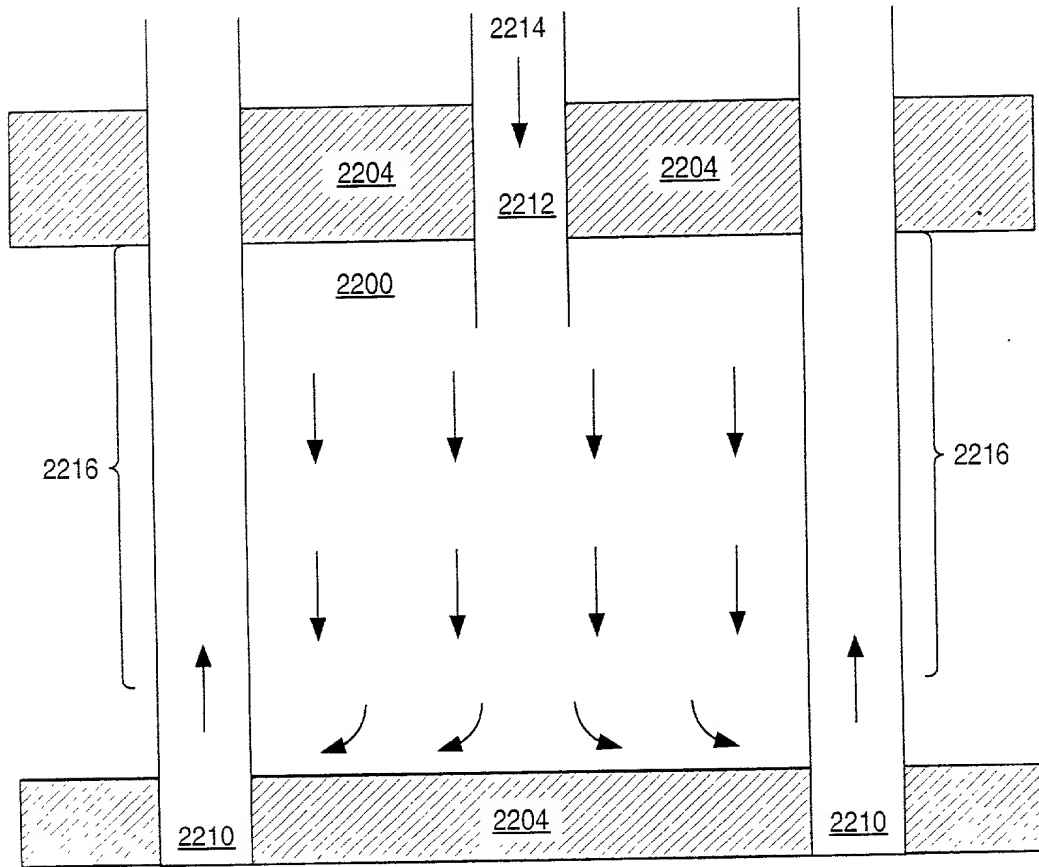


FIG. 45

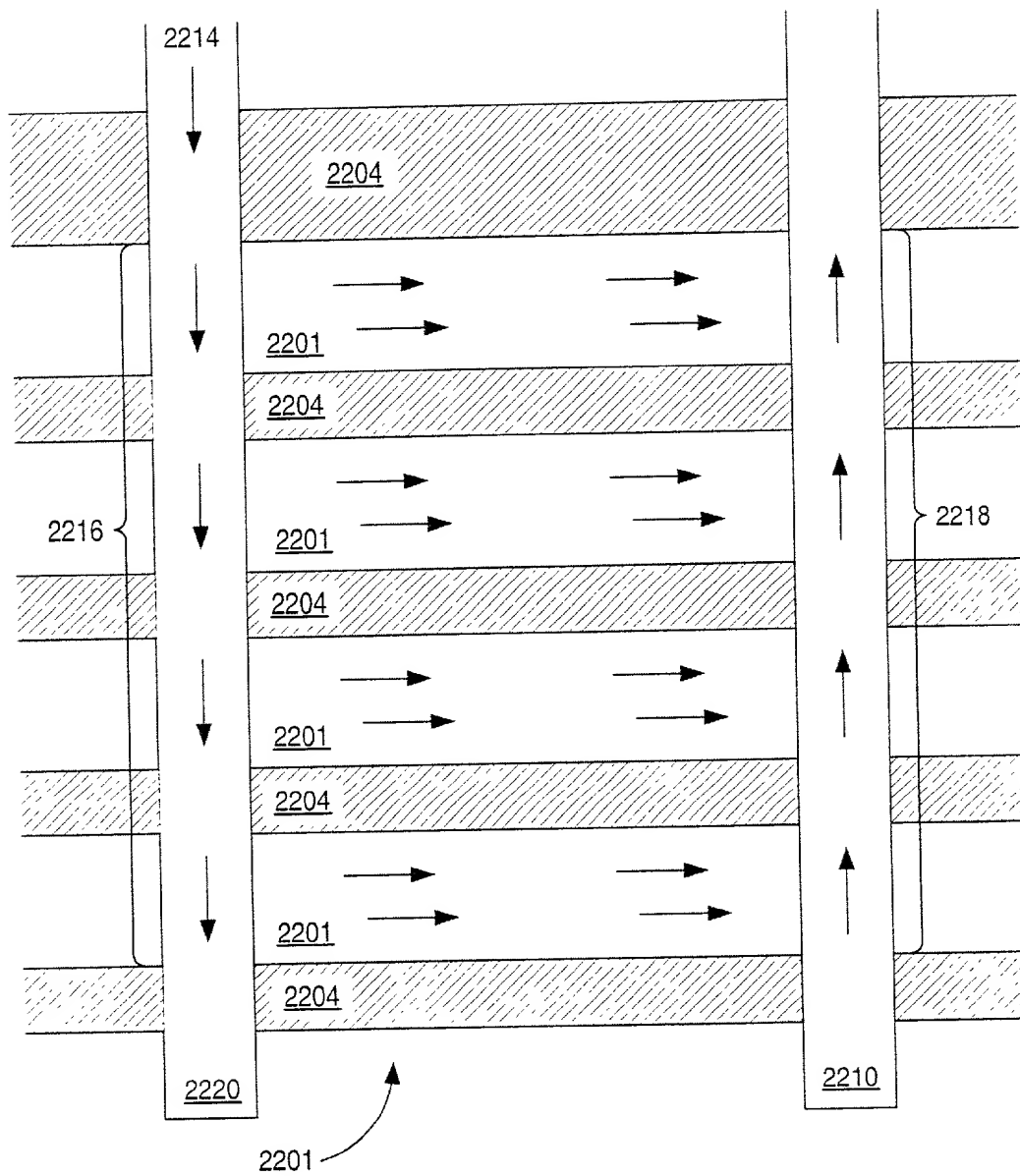


FIG. 46

FIG. 47 is a cross-sectional view of a device 2200, showing a substrate 2204 and a layer 2300.

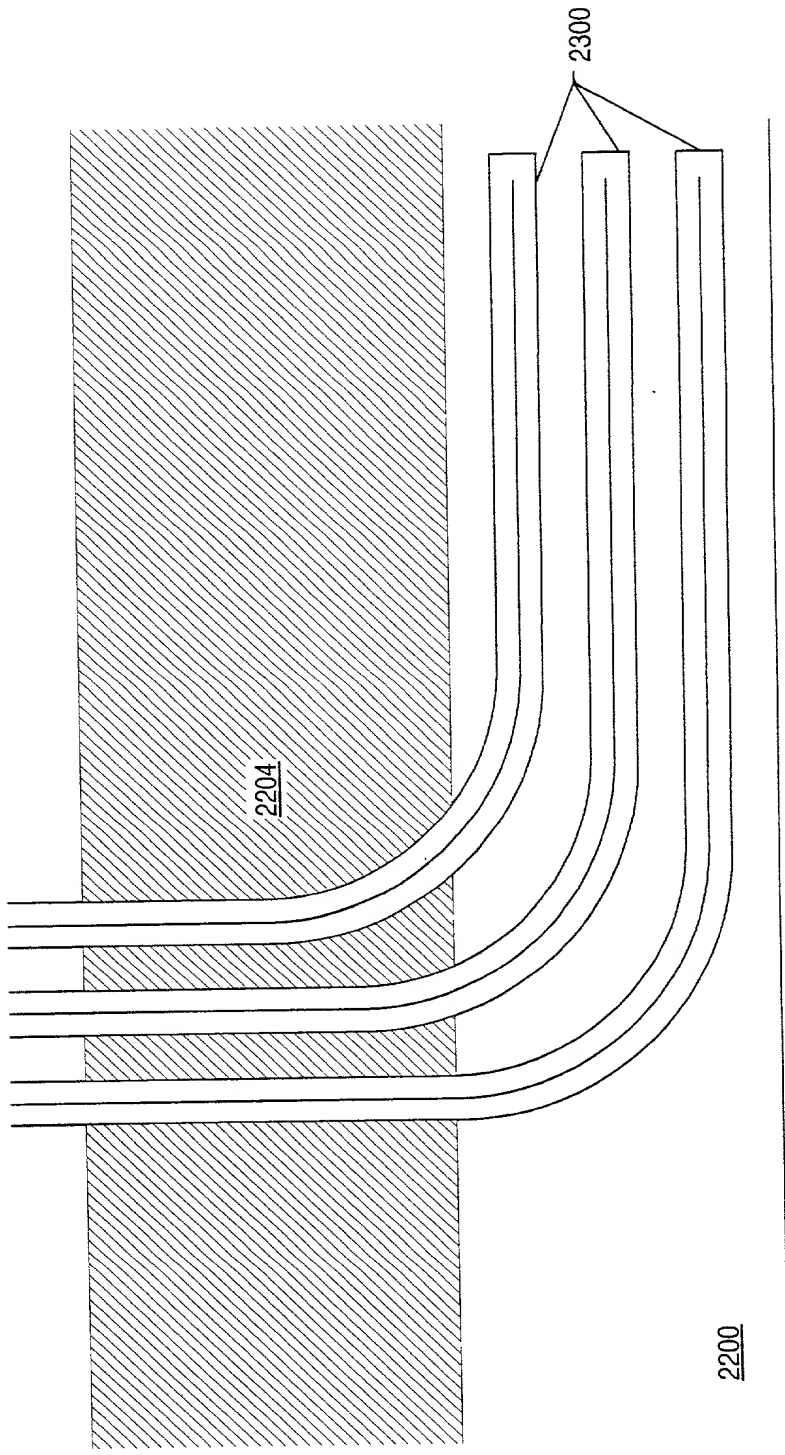


FIG. 47

Year	1970	1971	1972	1973	1974	1975	1976	1977	1978	1979	1980	1981	1982	1983	1984	1985	1986	1987	1988	1989	1990	1991	1992	1993	1994	1995	1996	1997	1998	1999	2000	2001	2002	2003	2004	2005	2006	2007	2008	2009	2010	2011	2012	2013	2014	2015	2016	2017	2018	2019	2020	2021	2022	2023	2024	2025	2026	2027	2028	2029	2030	2031	2032	2033	2034	2035	2036	2037	2038	2039	2040	2041	2042	2043	2044	2045	2046	2047	2048	2049	2050	2051	2052	2053	2054	2055	2056	2057	2058	2059	2060	2061	2062	2063	2064	2065	2066	2067	2068	2069	2070	2071	2072	2073	2074	2075	2076	2077	2078	2079	2080	2081	2082	2083	2084	2085	2086	2087	2088	2089	2090	2091	2092	2093	2094	2095	2096	2097	2098	2099	2100
1970	1971	1972	1973	1974	1975	1976	1977	1978	1979	1980	1981	1982	1983	1984	1985	1986	1987	1988	1989	1990	1991	1992	1993	1994	1995	1996	1997	1998	1999	2000	2001	2002	2003	2004	2005	2006	2007	2008	2009	2010	2011	2012	2013	2014	2015	2016	2017	2018	2019	2020	2021	2022	2023	2024	2025	2026	2027	2028	2029	2030	2031	2032	2033	2034	2035	2036	2037	2038	2039	2040	2041	2042	2043	2044	2045	2046	2047	2048	2049	2050	2051	2052	2053	2054	2055	2056	2057	2058	2059	2060	2061	2062	2063	2064	2065	2066	2067	2068	2069	2070	2071	2072	2073	2074	2075	2076	2077	2078	2079	2080	2081	2082	2083	2084	2085	2086	2087	2088	2089	2090	2091	2092	2093	2094	2095	2096	2097	2098	2099	2100	

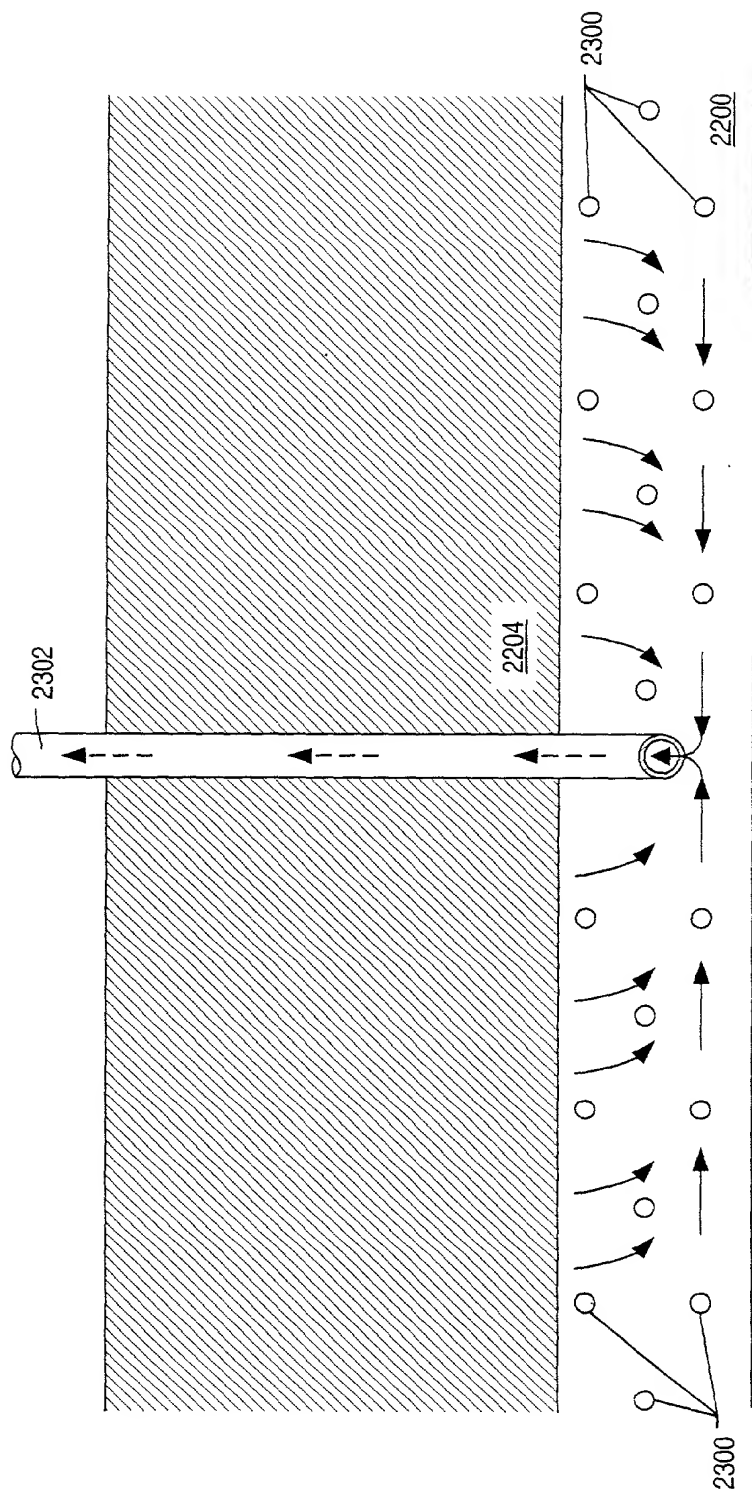


FIG. 48

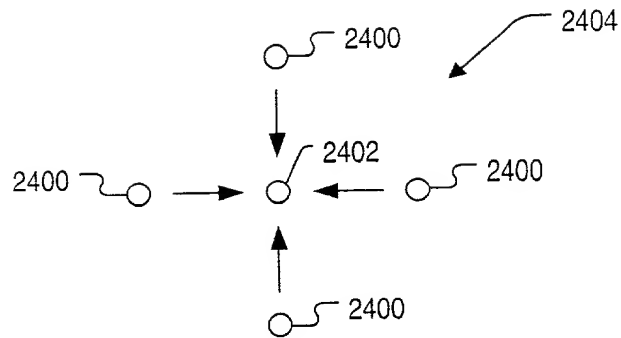


FIG. 49

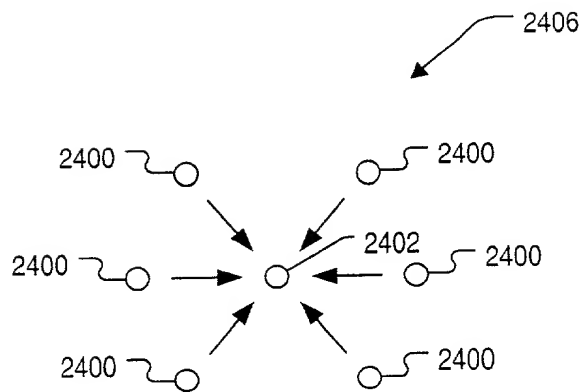


FIG. 50

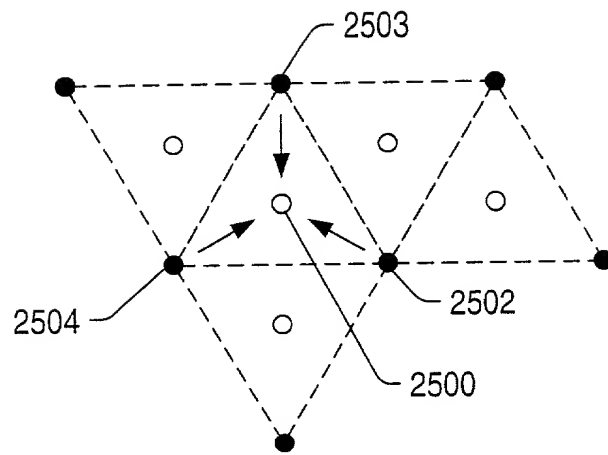


FIG. 51

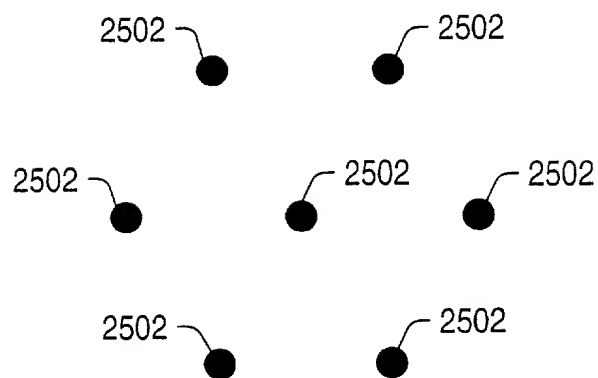


FIG. 52

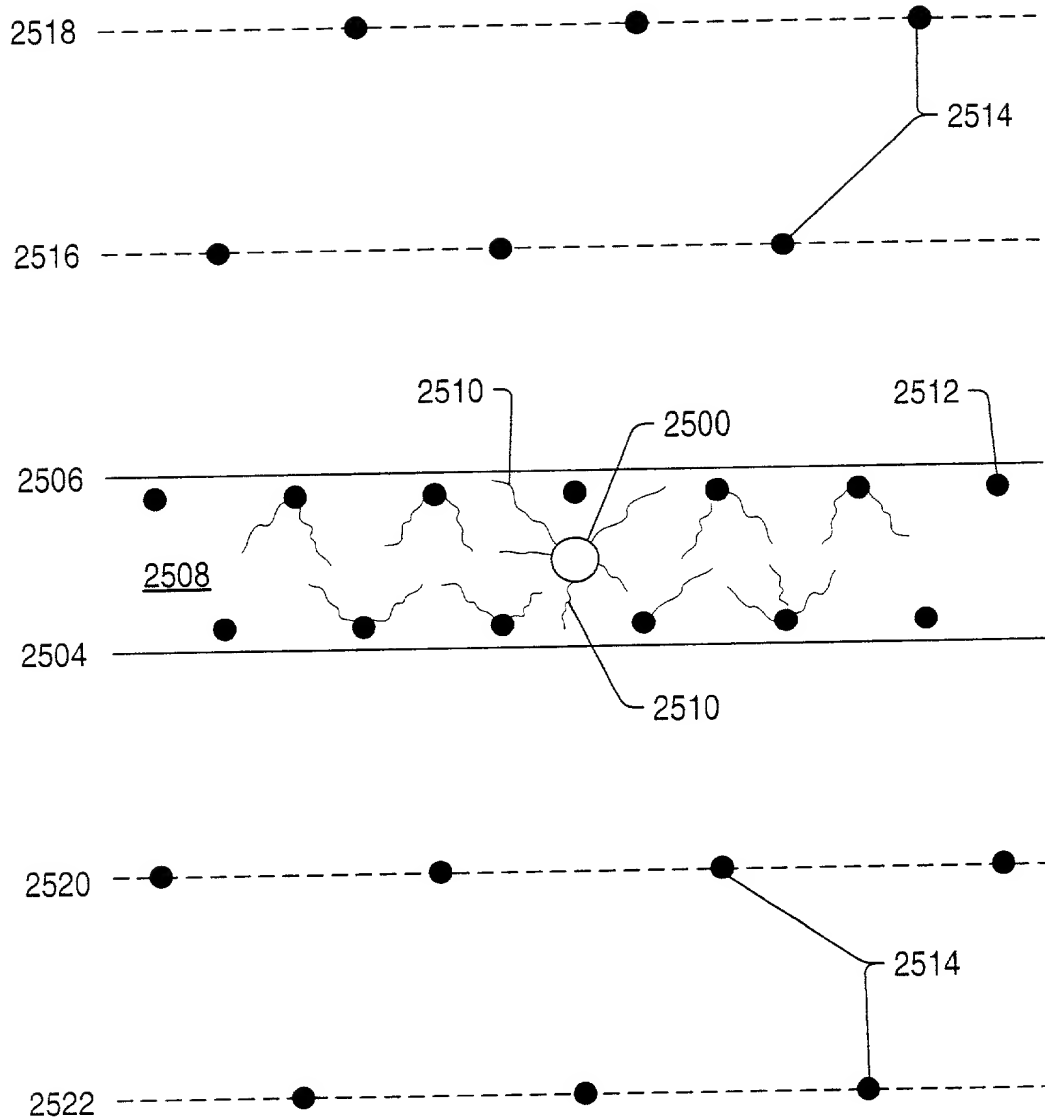


FIG. 53



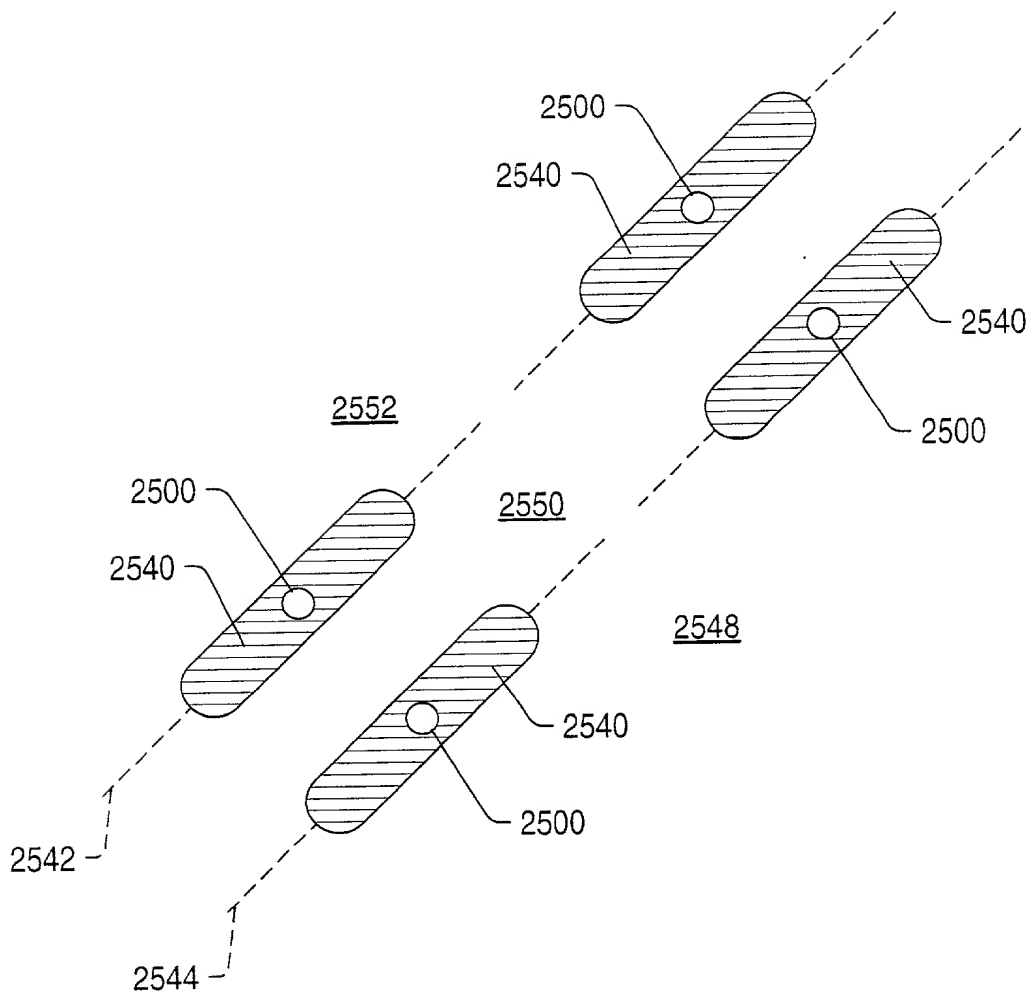


FIG. 54

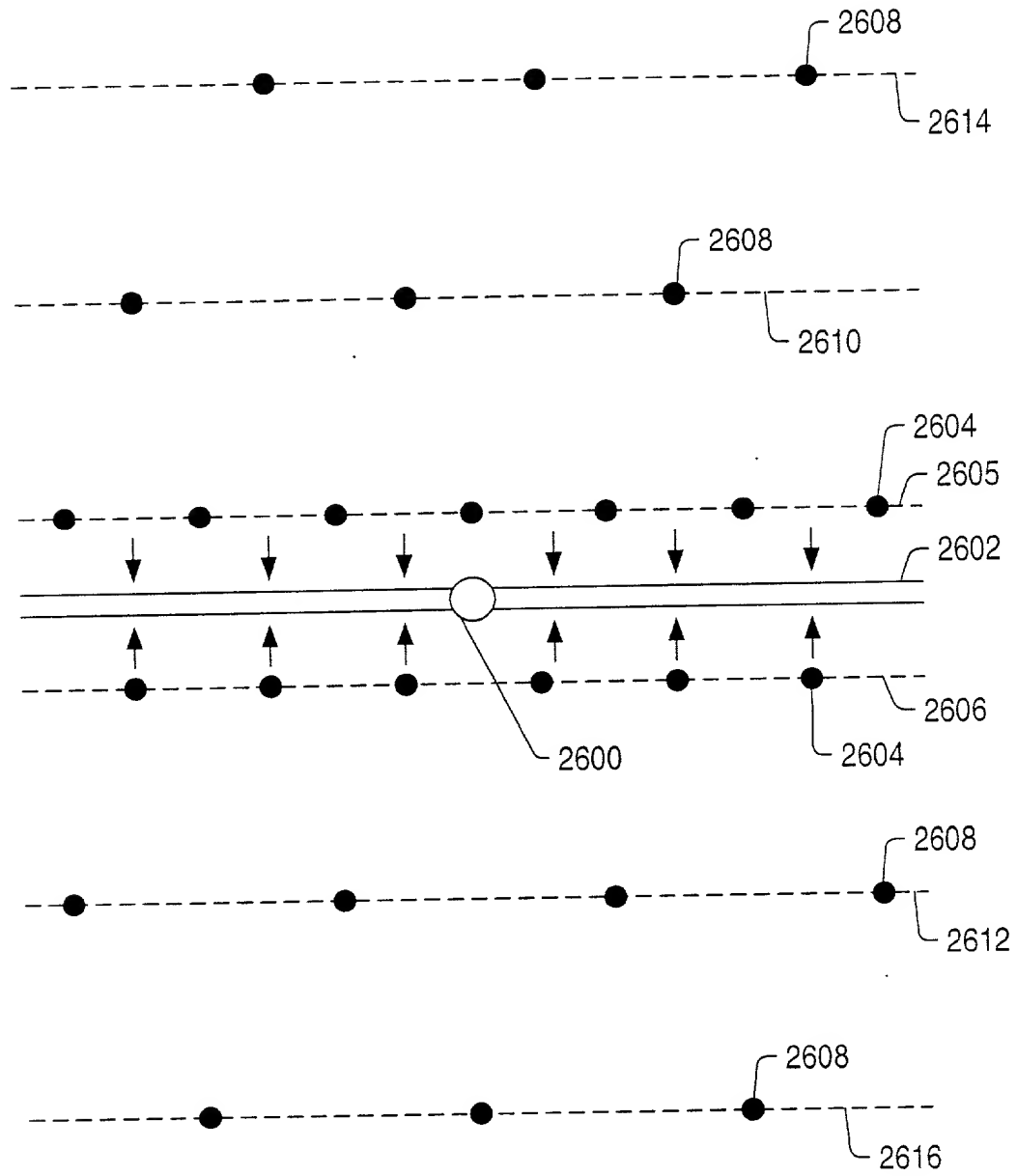


FIG. 55

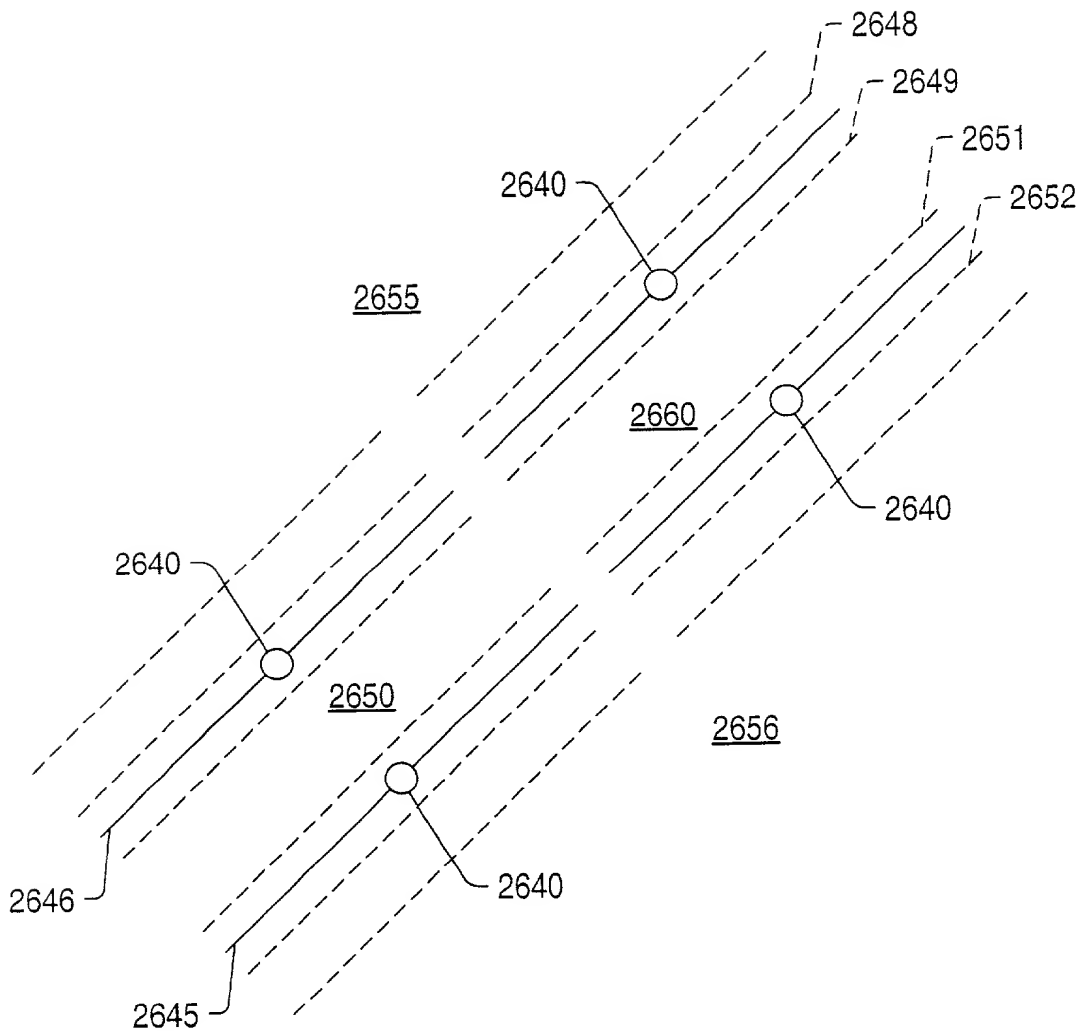


FIG. 56

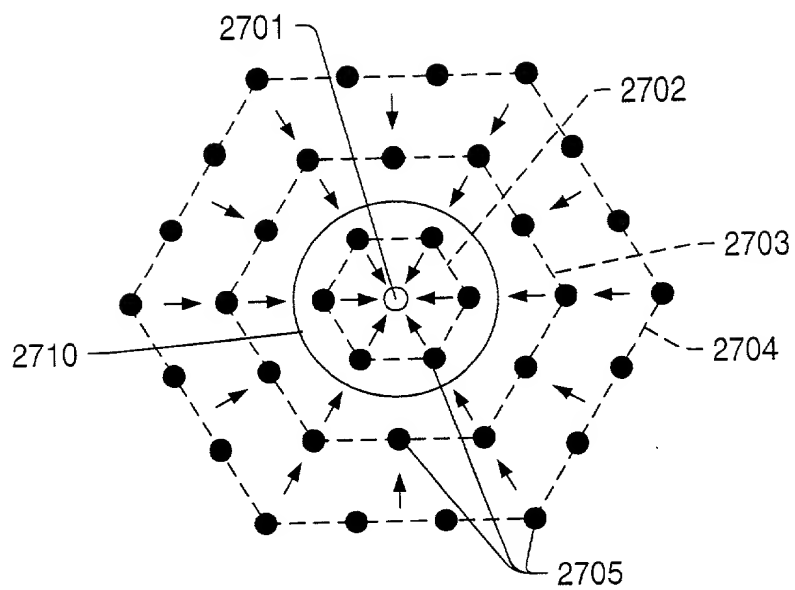


FIG. 57

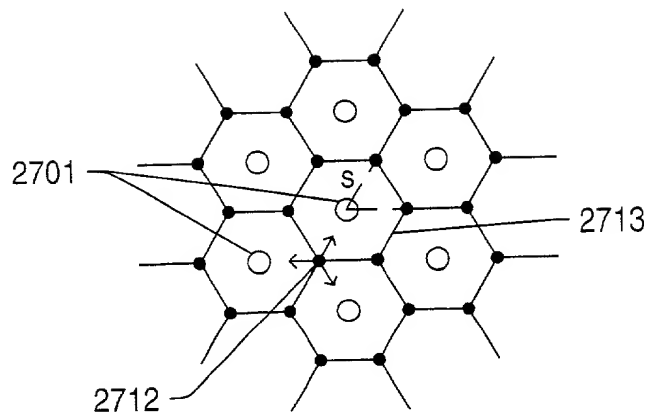


FIG. 58

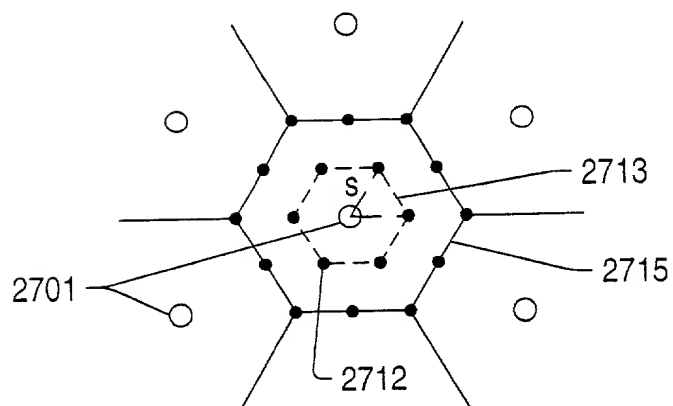


FIG. 59

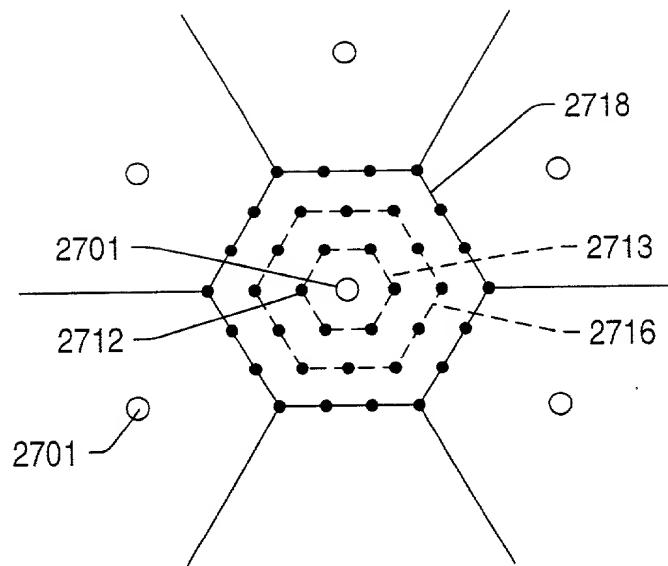


FIG. 60

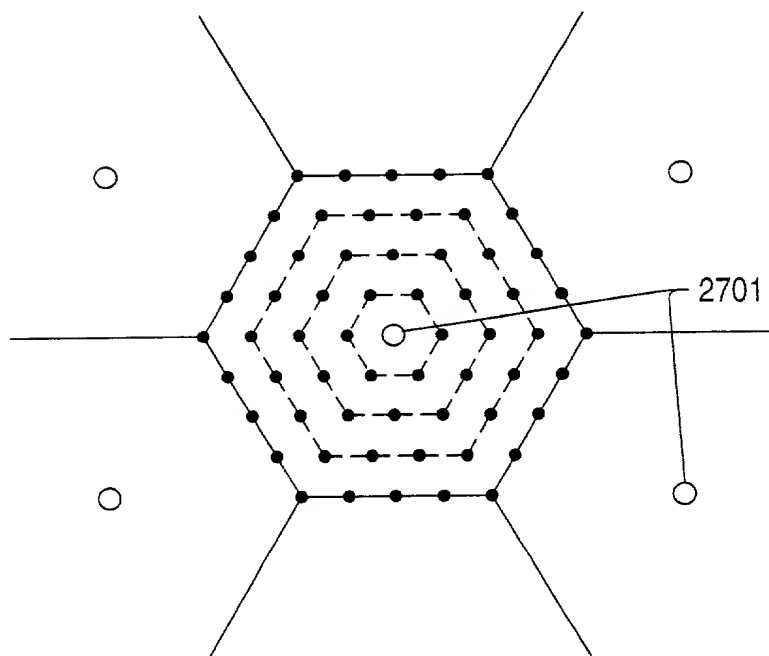


FIG. 61

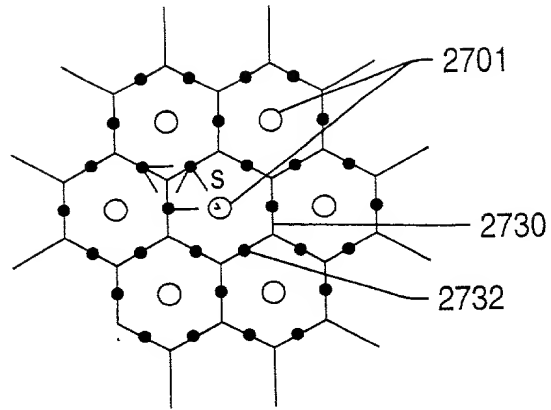


FIG. 62

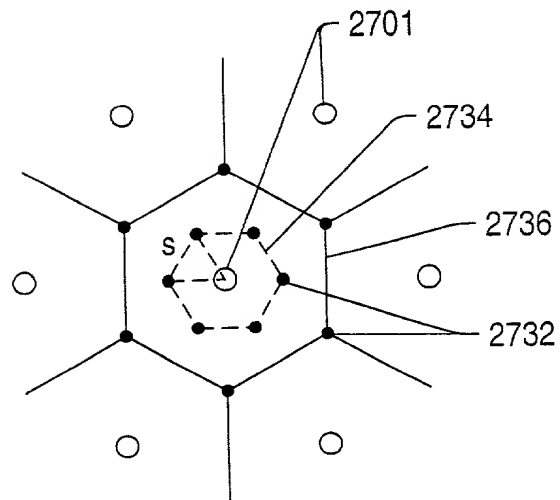


FIG. 63

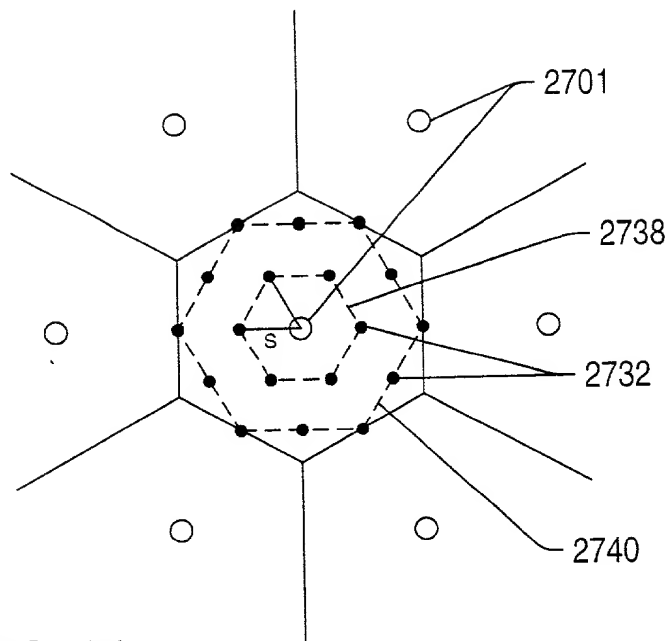


FIG. 64

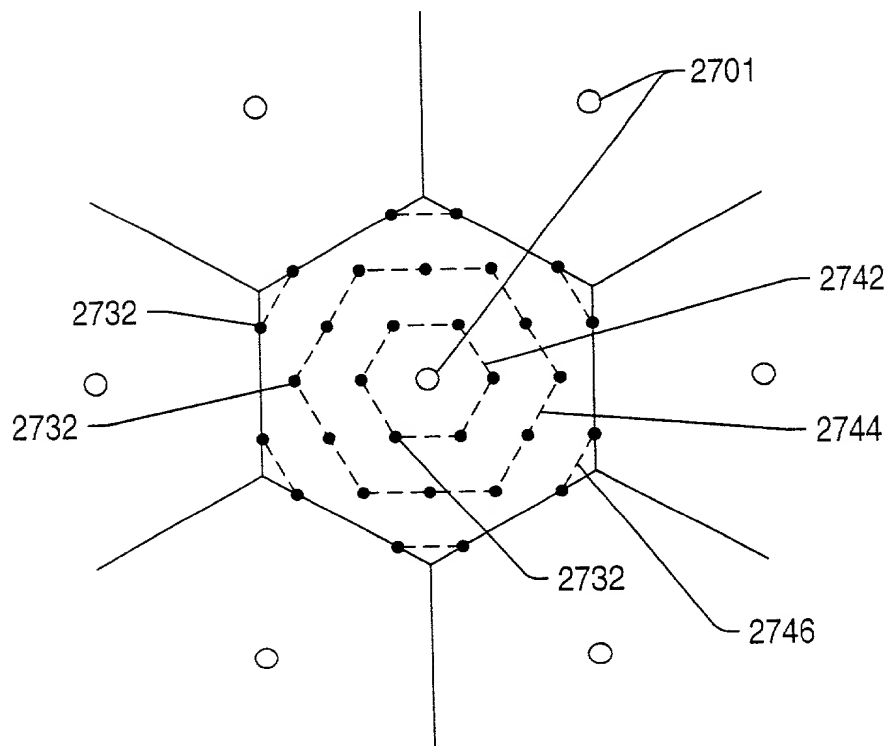


FIG. 65



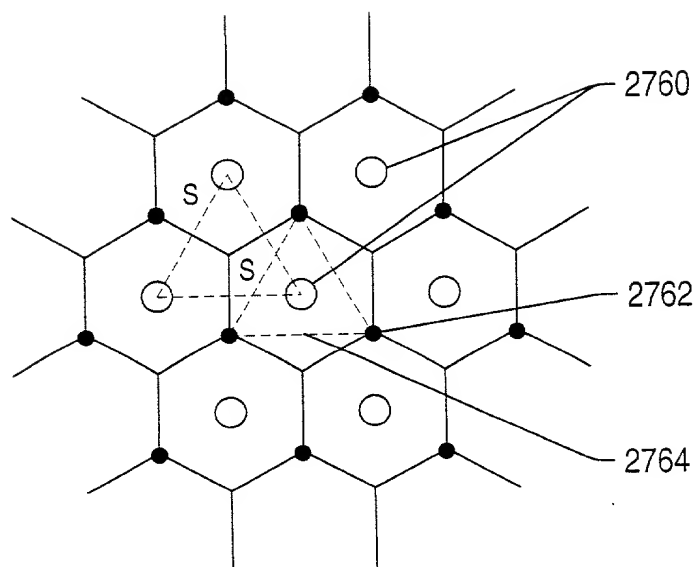


FIG. 66

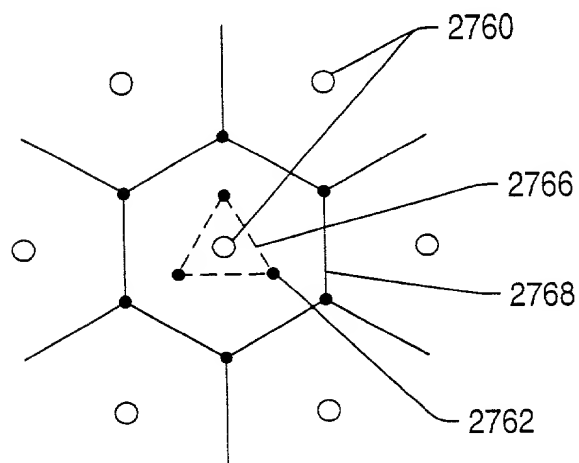


FIG. 67

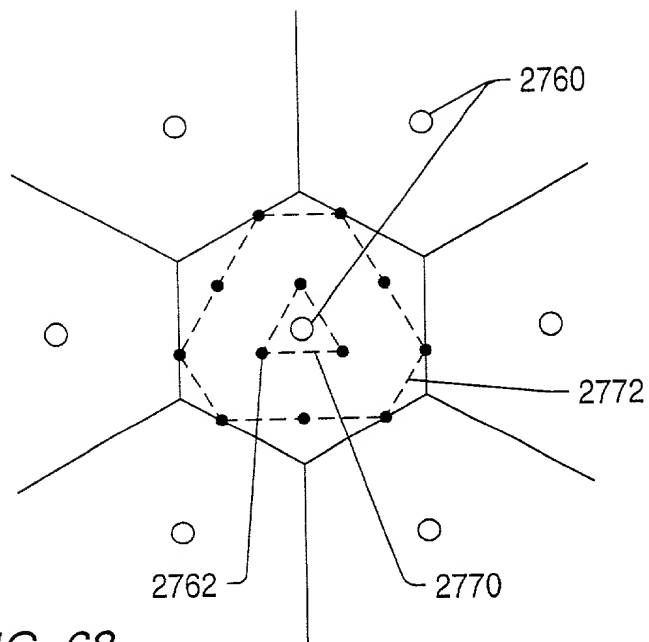


FIG. 68

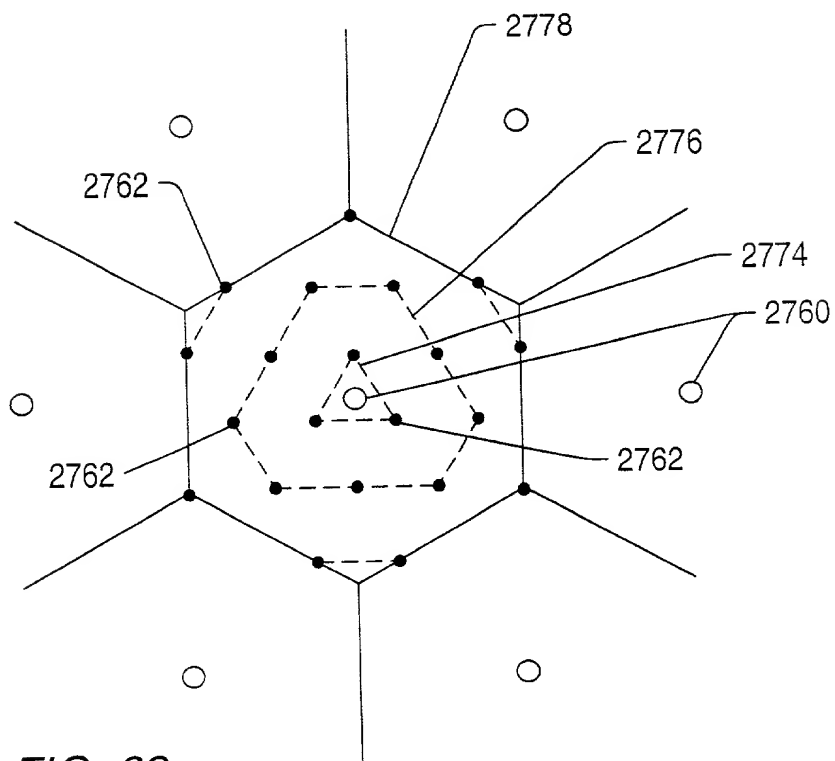


FIG. 69

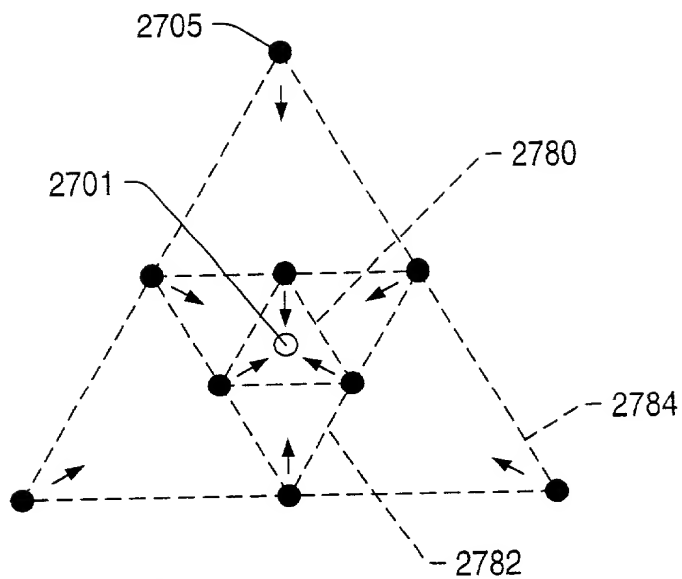


FIG. 70



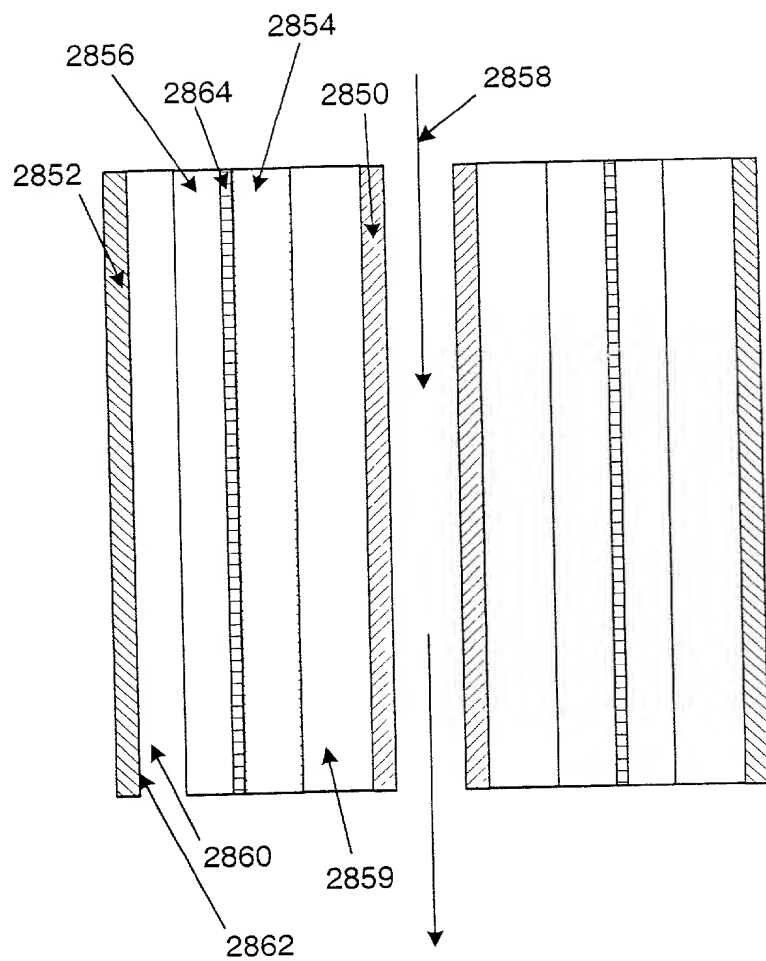


Fig. 72

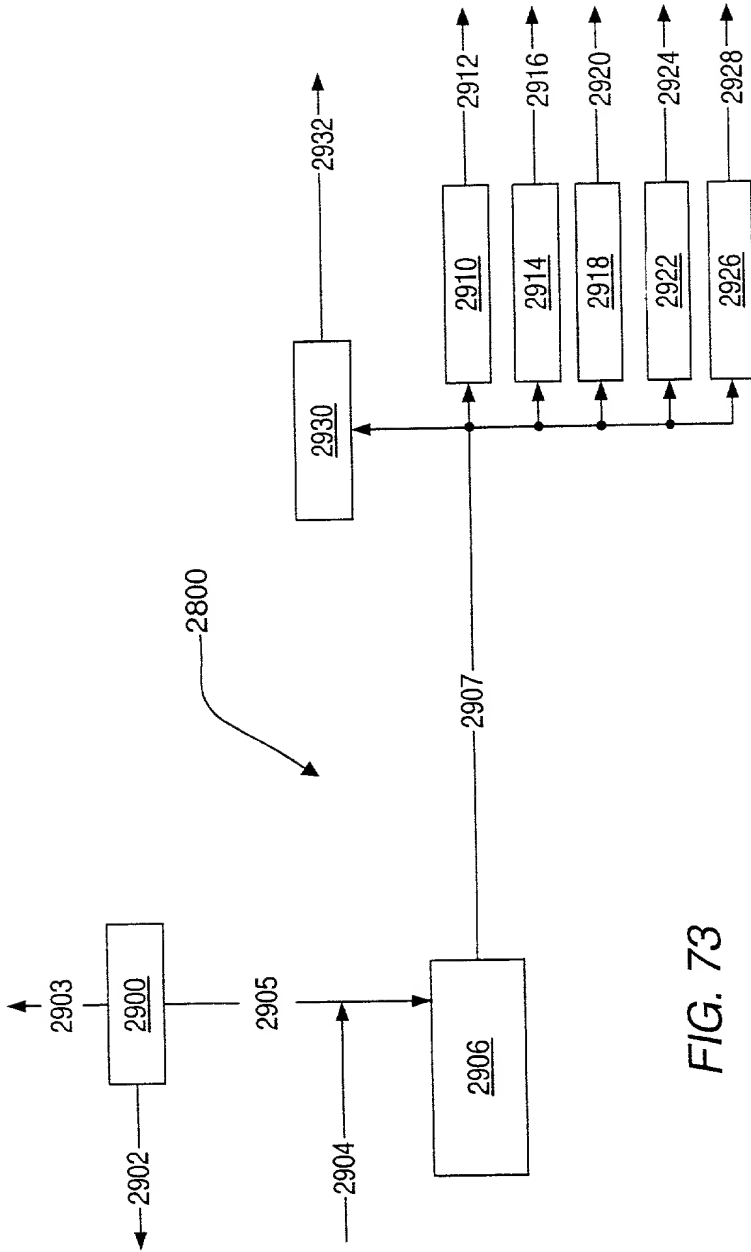


FIG. 73

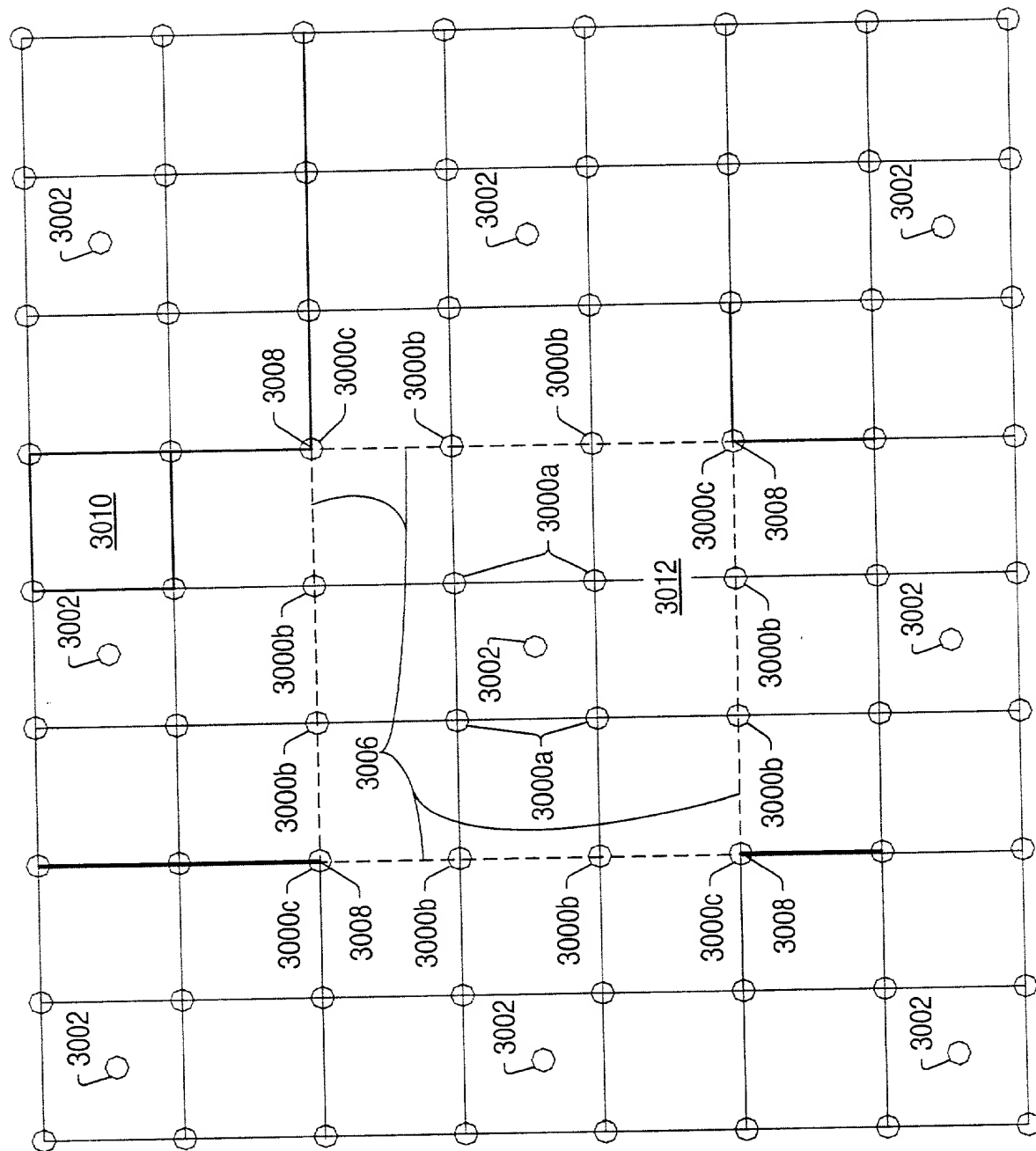


FIG. 74

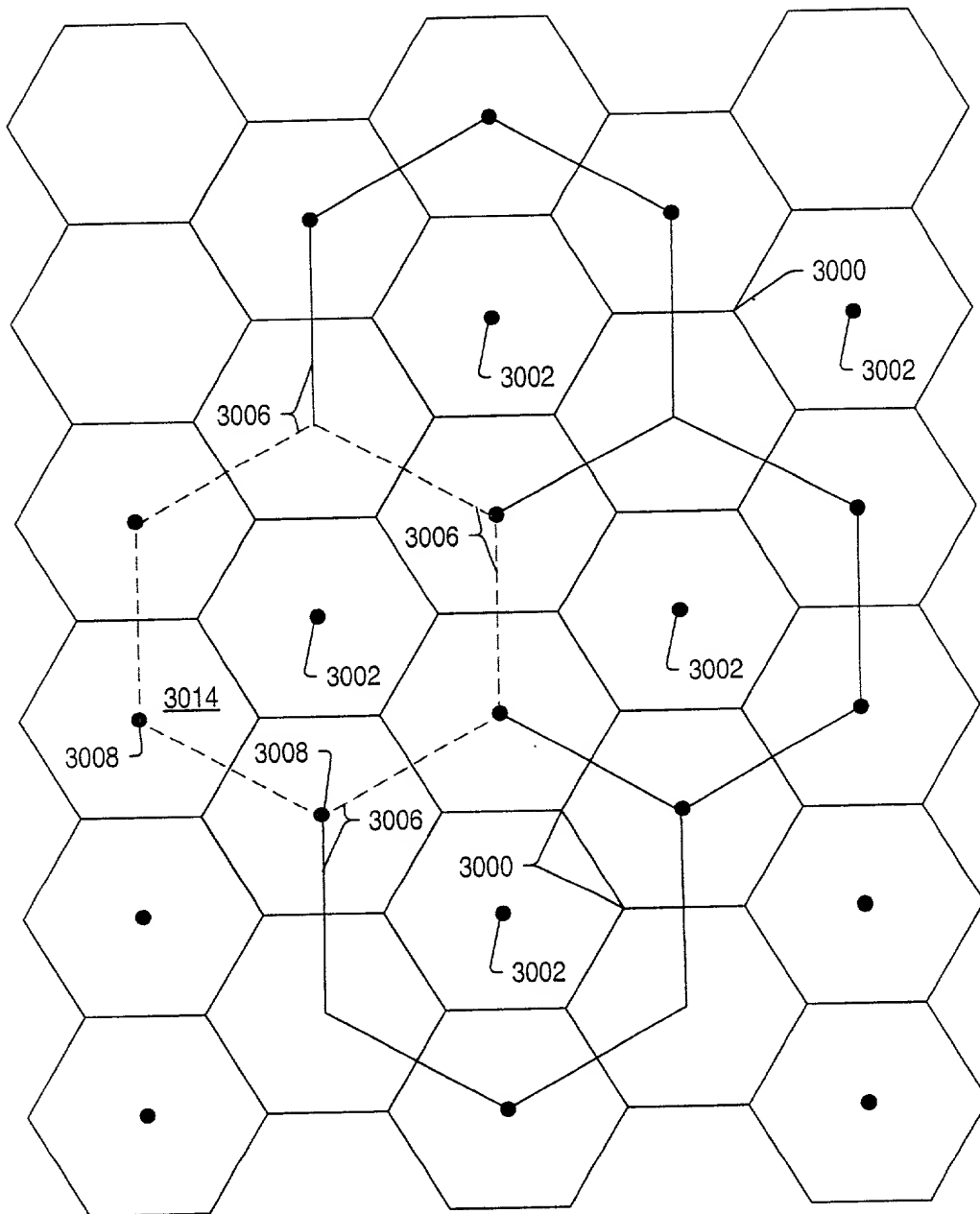


FIG. 75



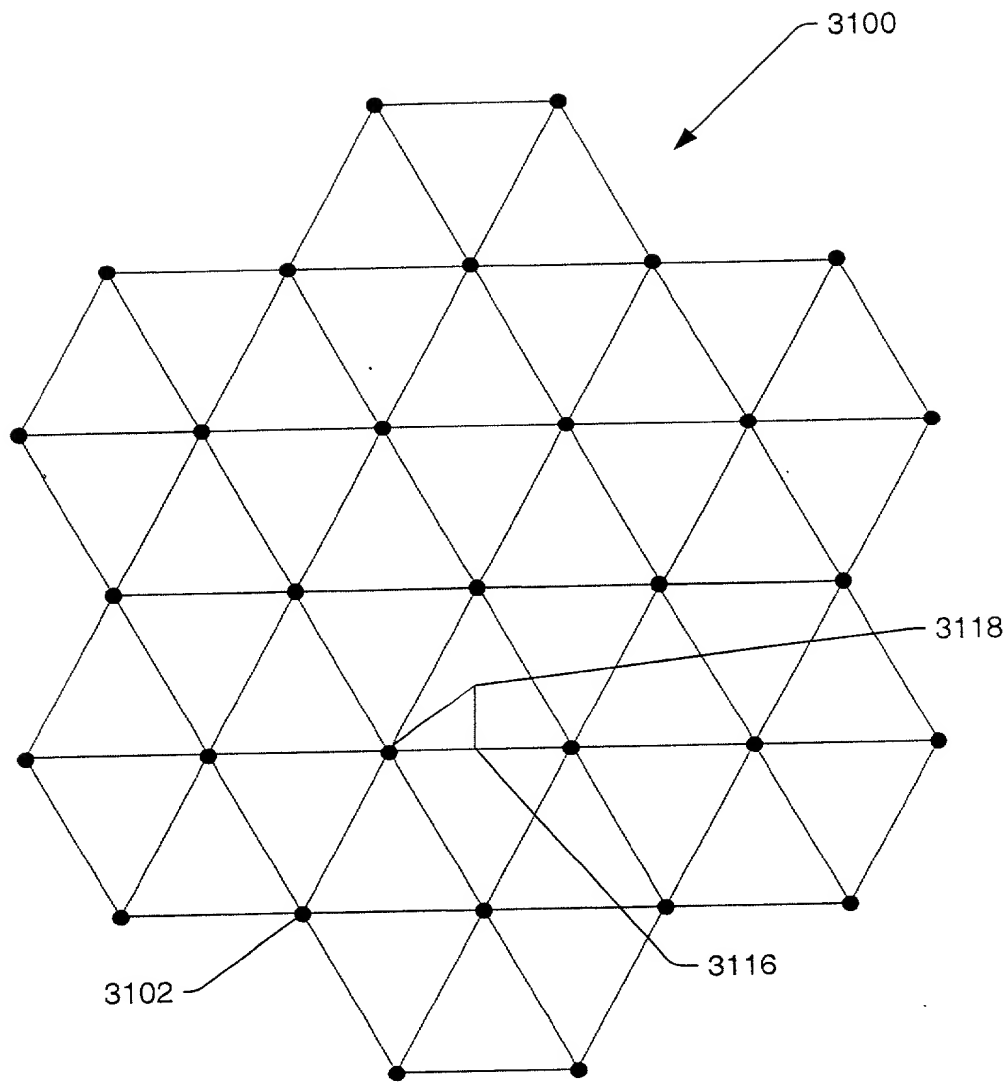


FIG. 76

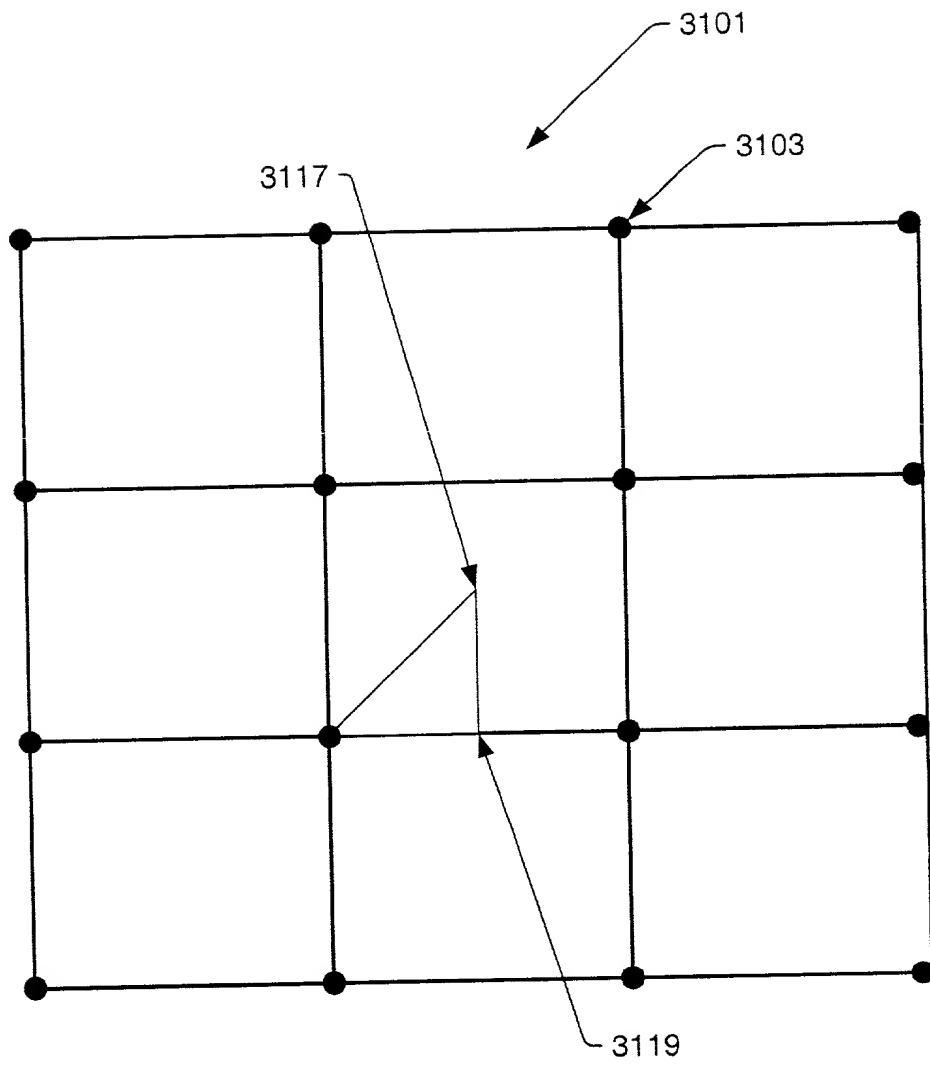


FIG. 76a

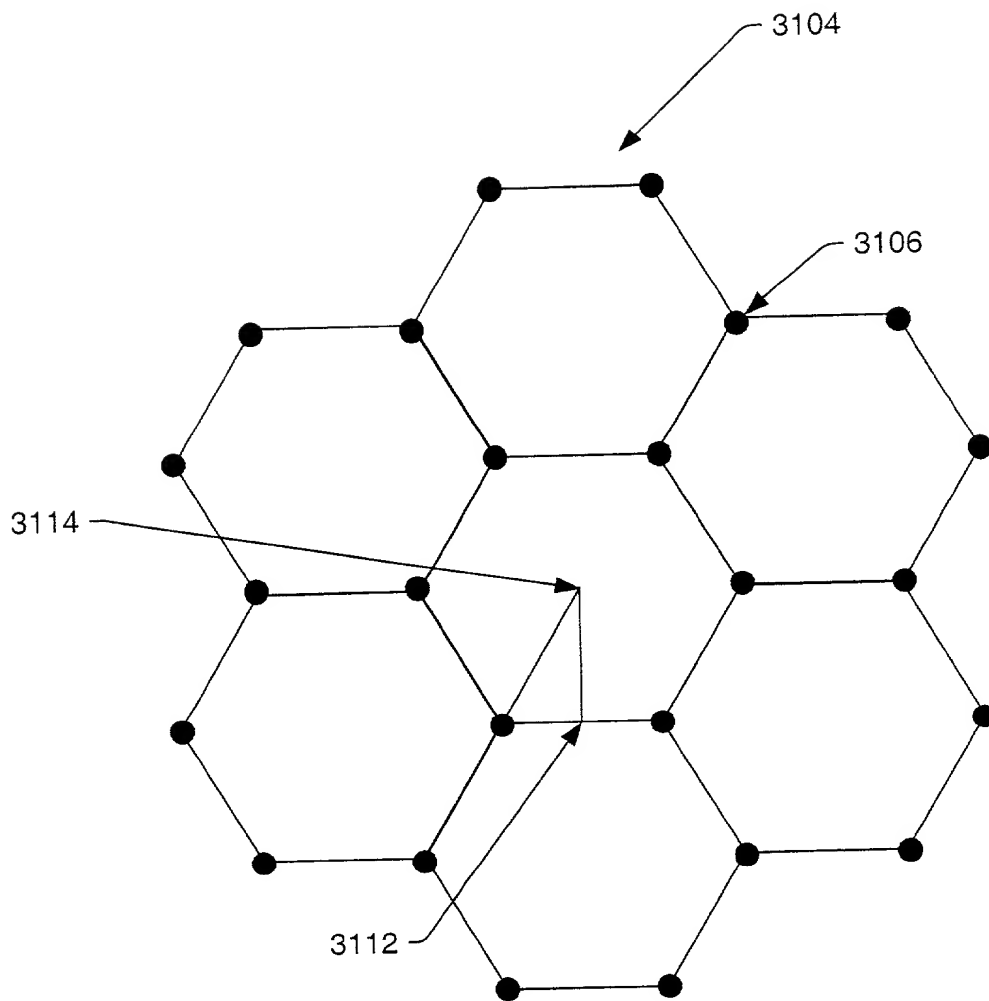


FIG. 77

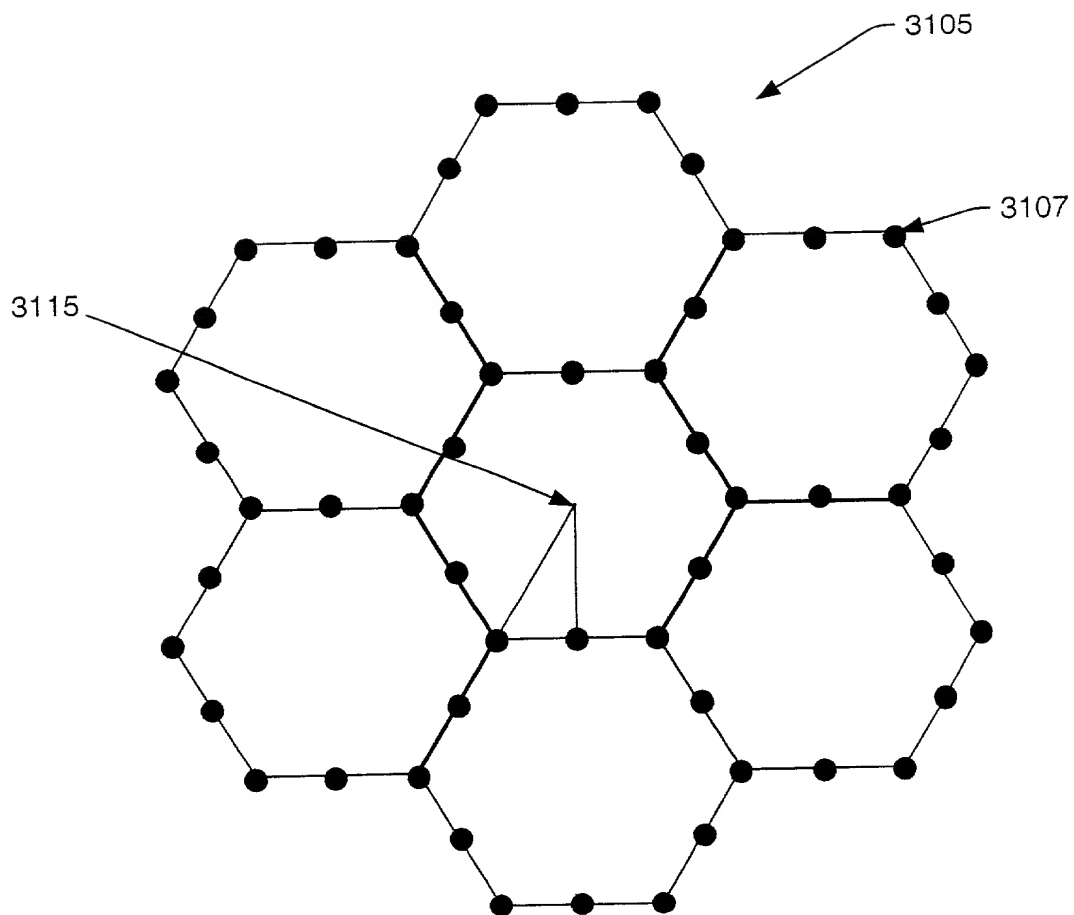


FIG. 77a

FIG. 78 is a 3D surface plot showing the temperature distribution T (°C) as a function of spatial coordinates x and y. The surface is characterized by several sharp peaks and valleys, indicating high spatial variations in temperature. The x and y axes range from -10 to 10, and the temperature T ranges from 500 to 600 °C.

3110

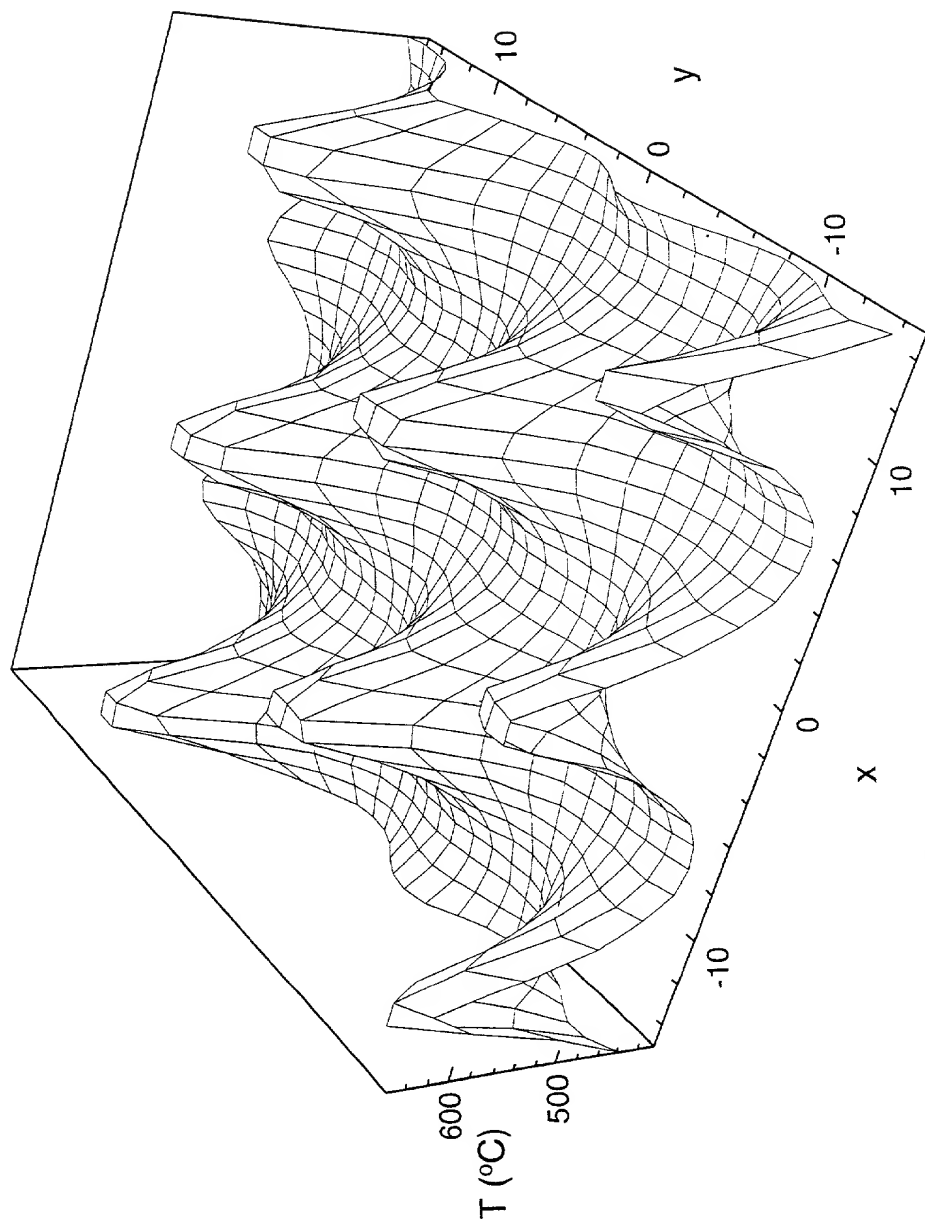


FIG. 78

FIG. 79 is a 3D surface plot showing the temperature distribution T (°C) as a function of position (x, y). The plot displays a complex, multi-peaked surface, indicating high temperature gradients. The x and y axes range from -10 to 10, and the temperature T ranges from 400 to 550 °C. The surface is characterized by several sharp peaks and valleys, suggesting localized heating or cooling regions.

3108

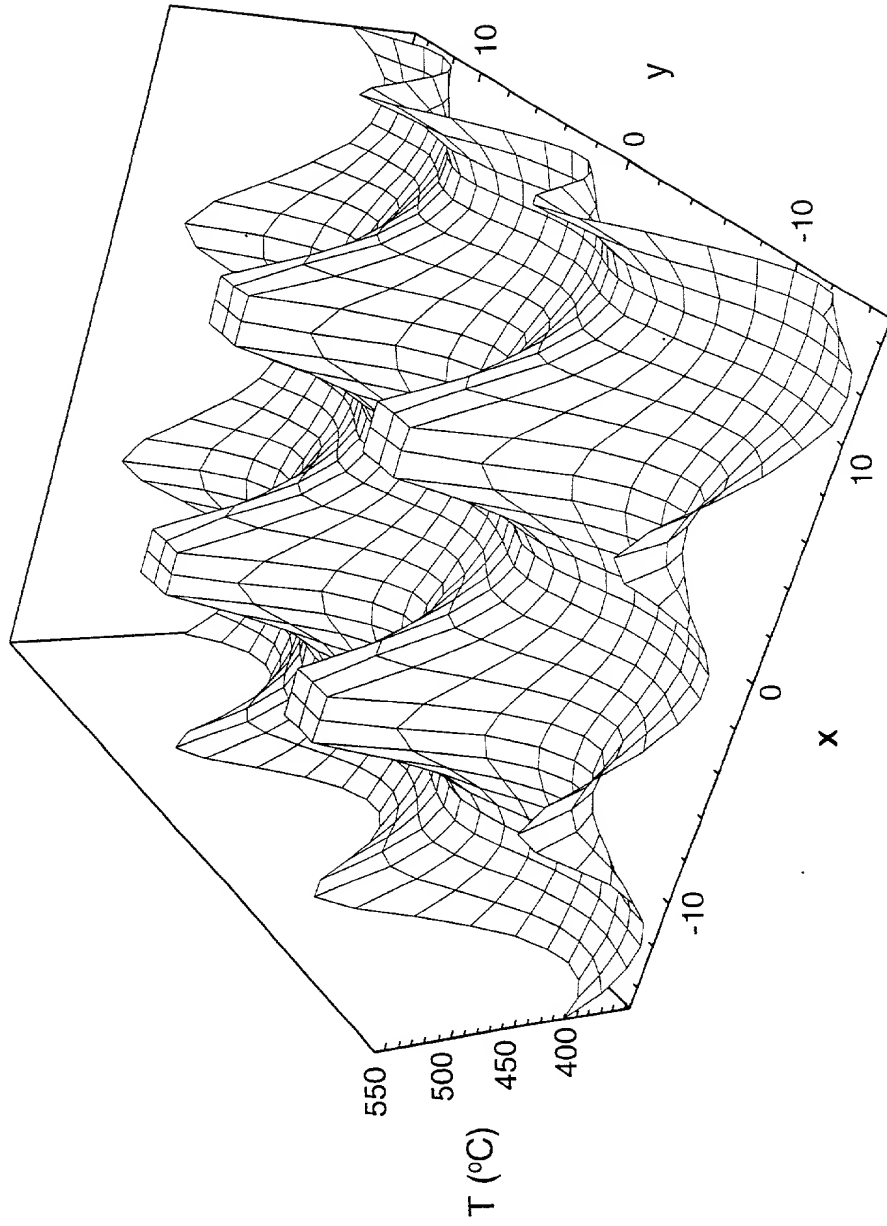


FIG. 79

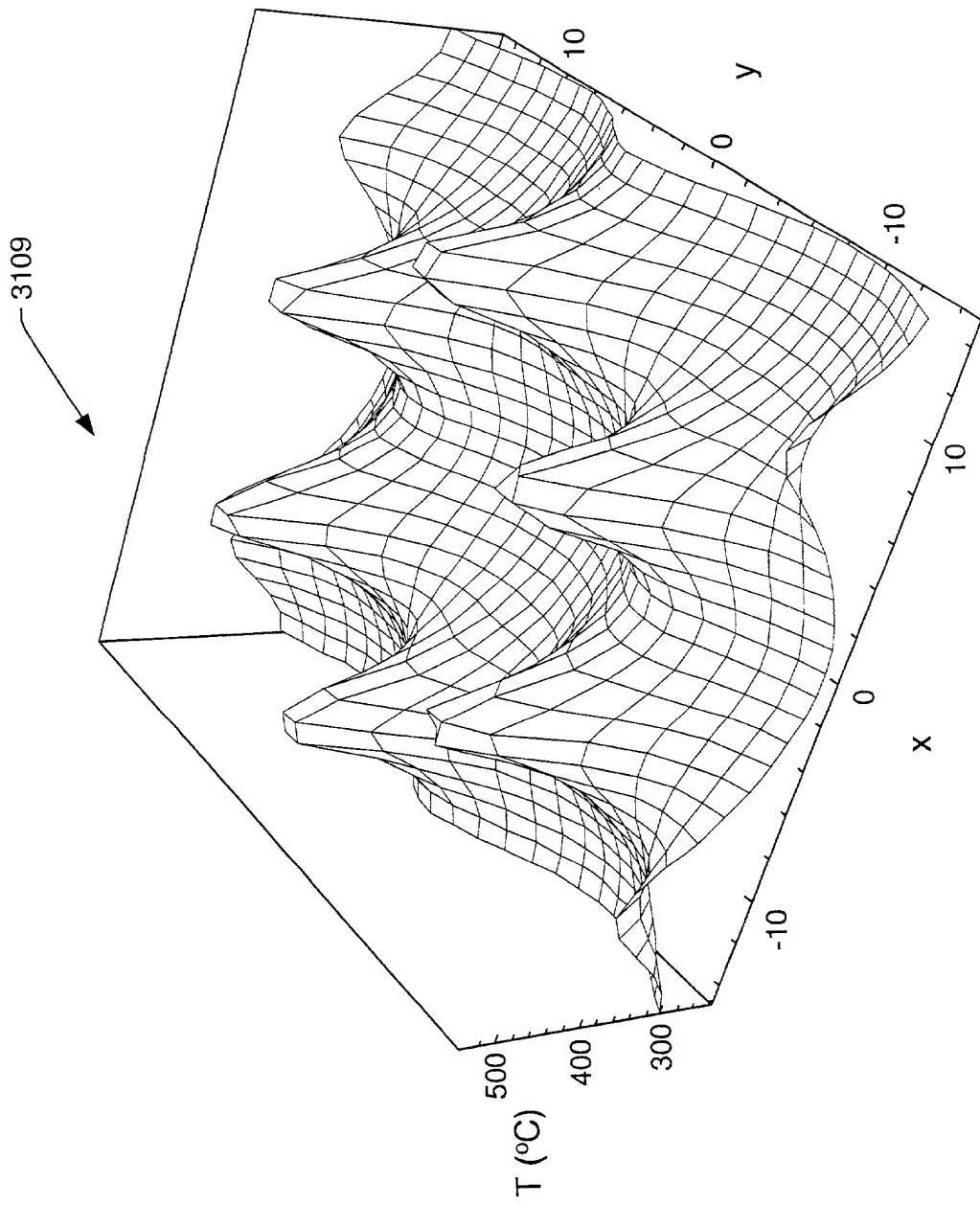


FIG. 79a

FIG. 80

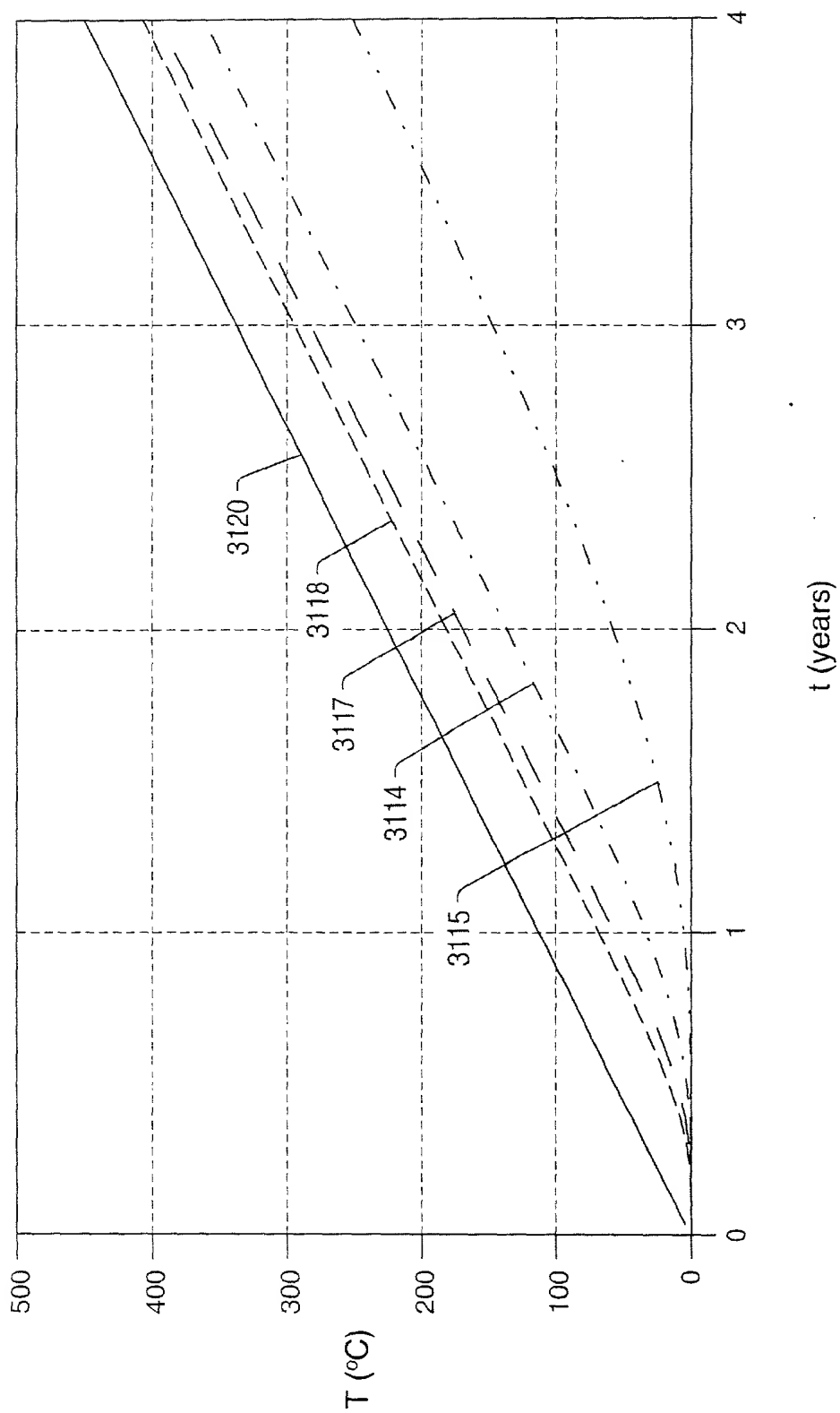


FIG. 80



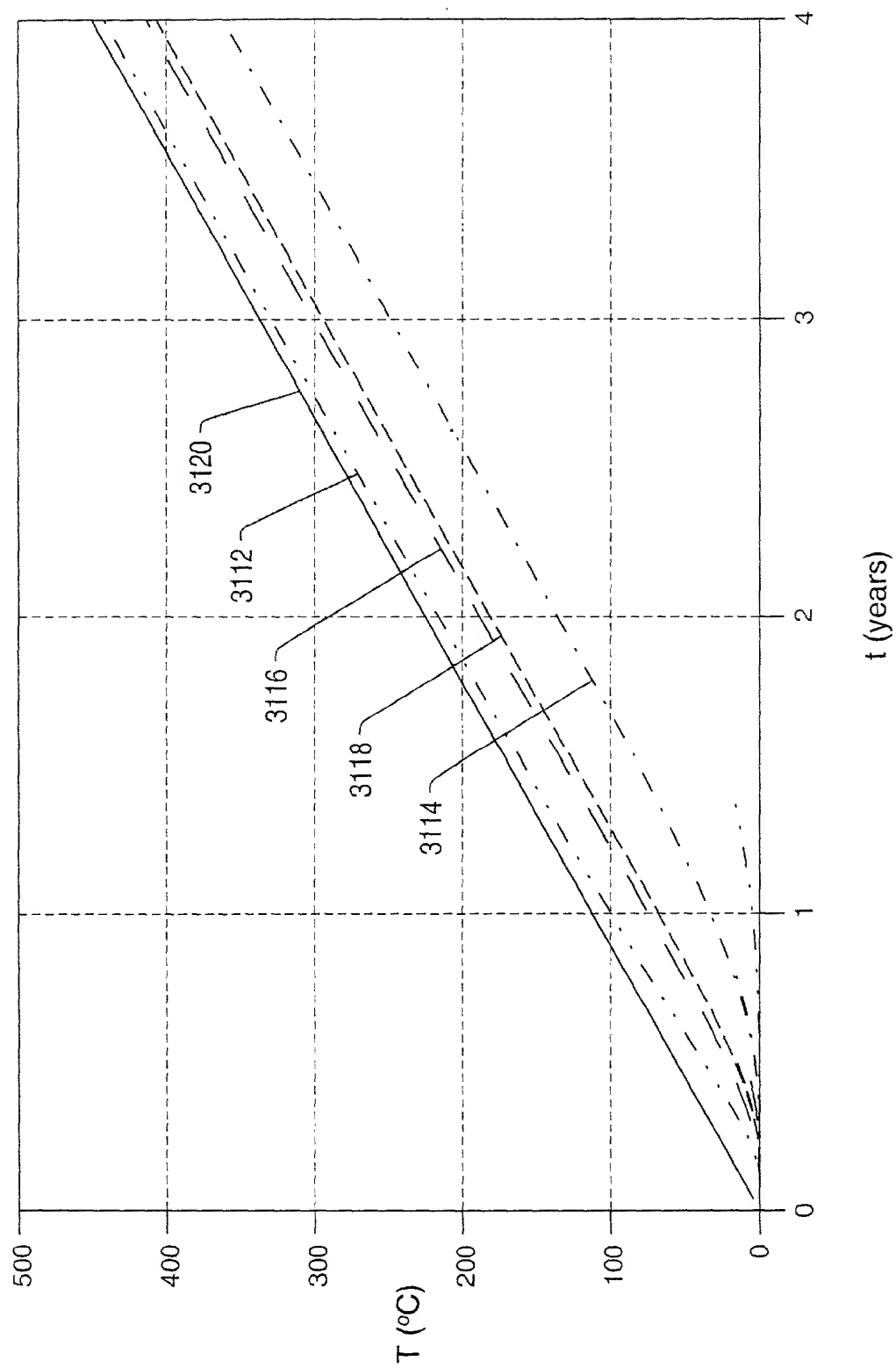


FIG. 81

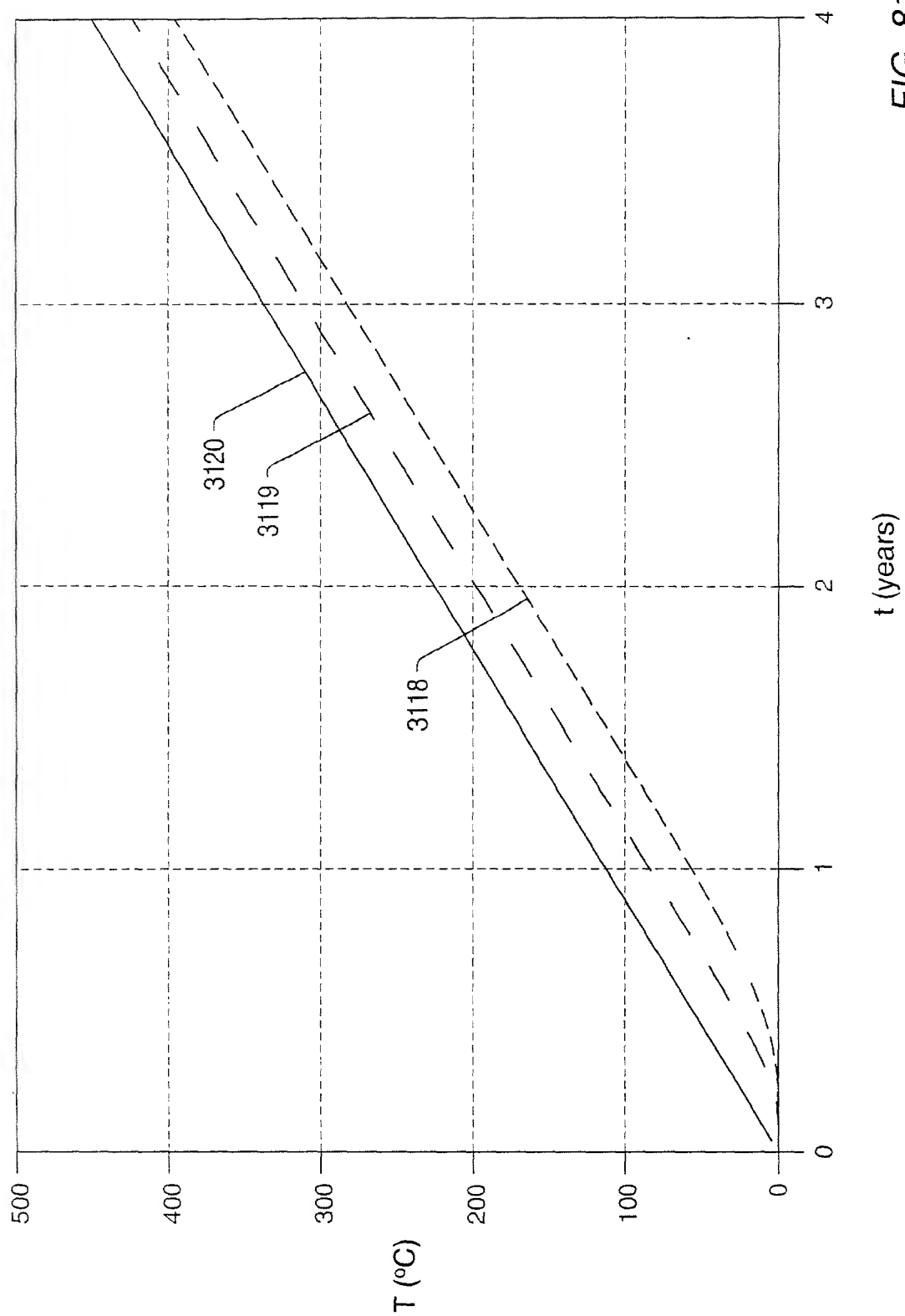


FIG. 81a

FIG. 81b

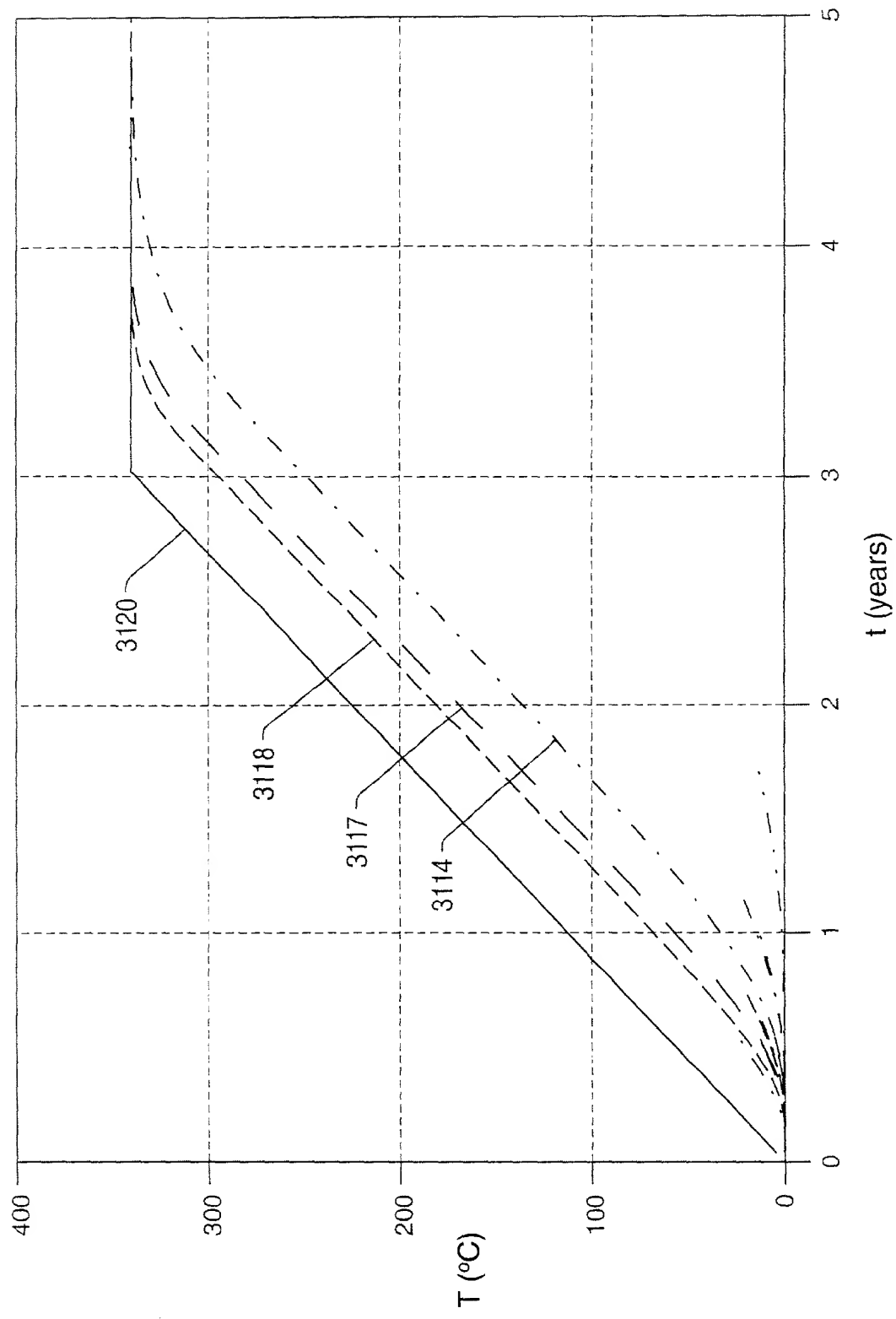


FIG. 81b



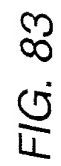


FIG. 83

$\frac{d(\ln \frac{P}{T})}{dT} = \frac{H_v}{RT^2}$

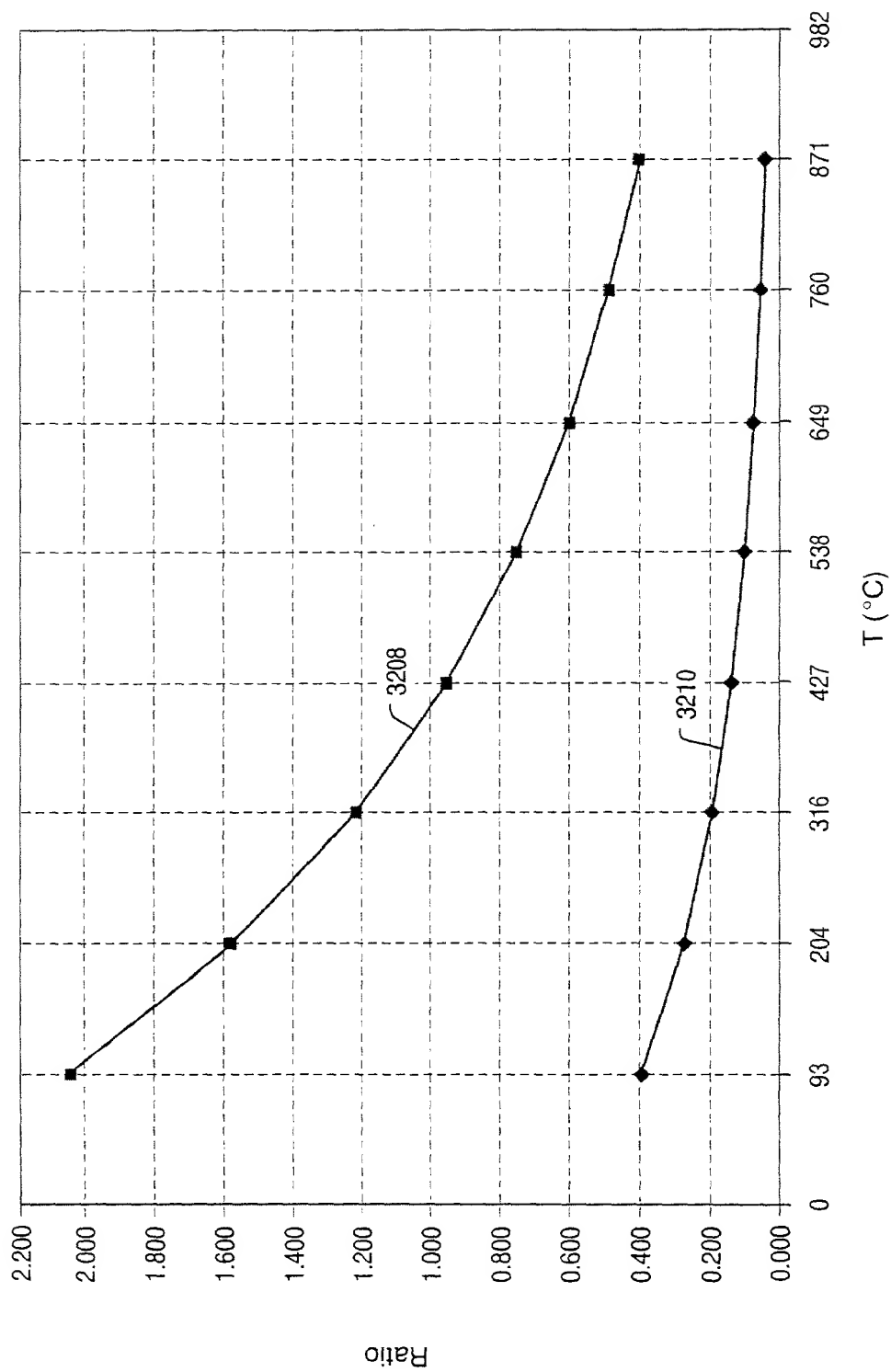


FIG. 84

FIG. 85

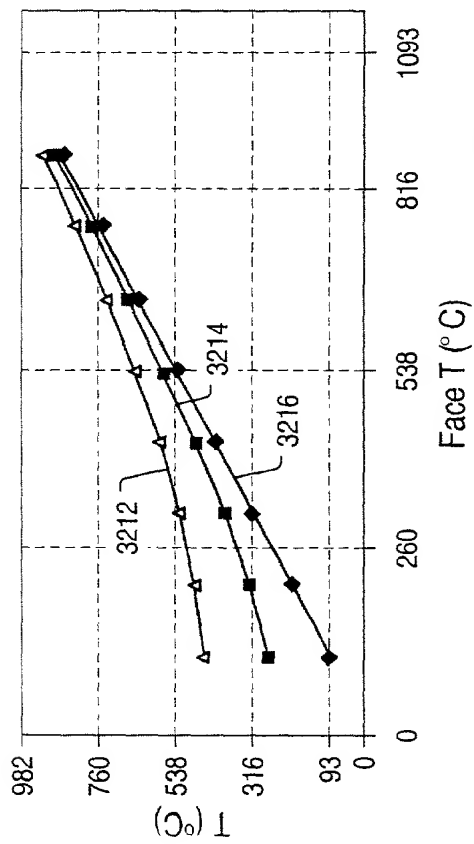


FIG. 85

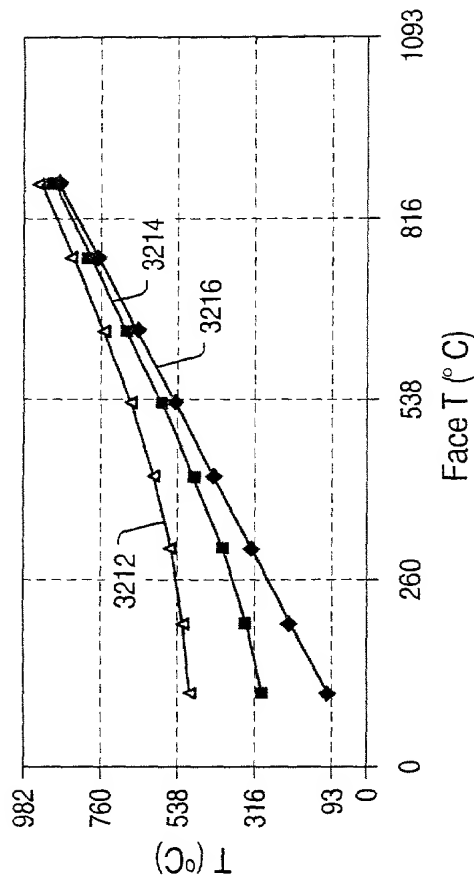


FIG. 86

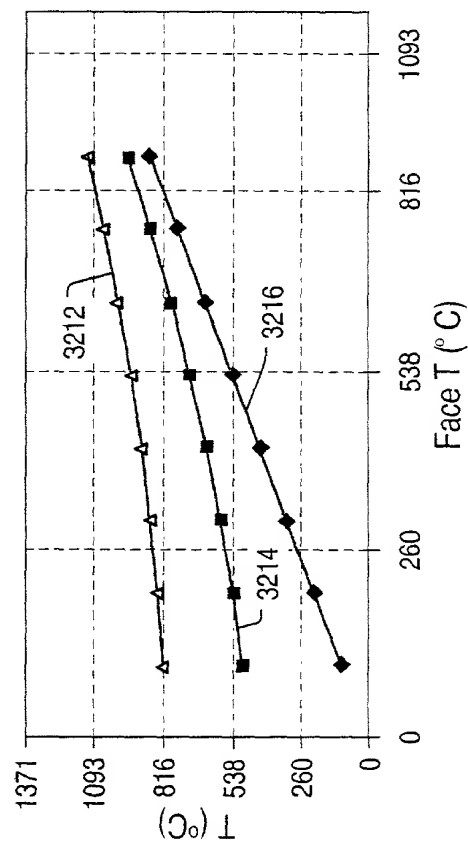


FIG. 87

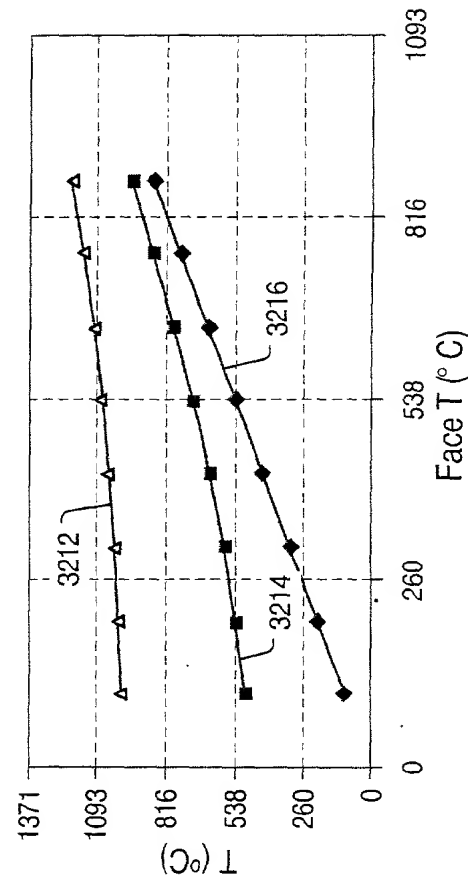


FIG. 88

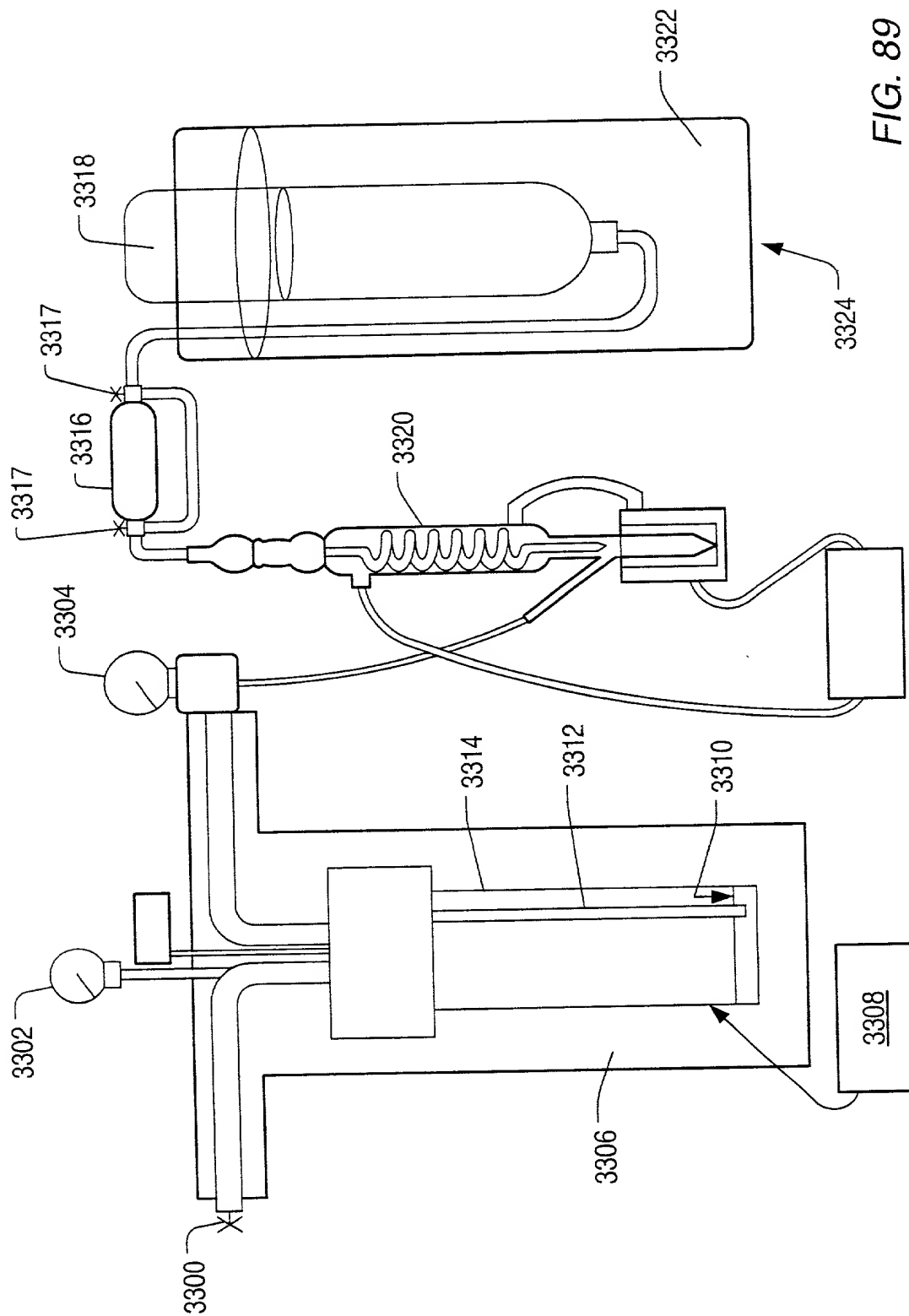


FIG. 89



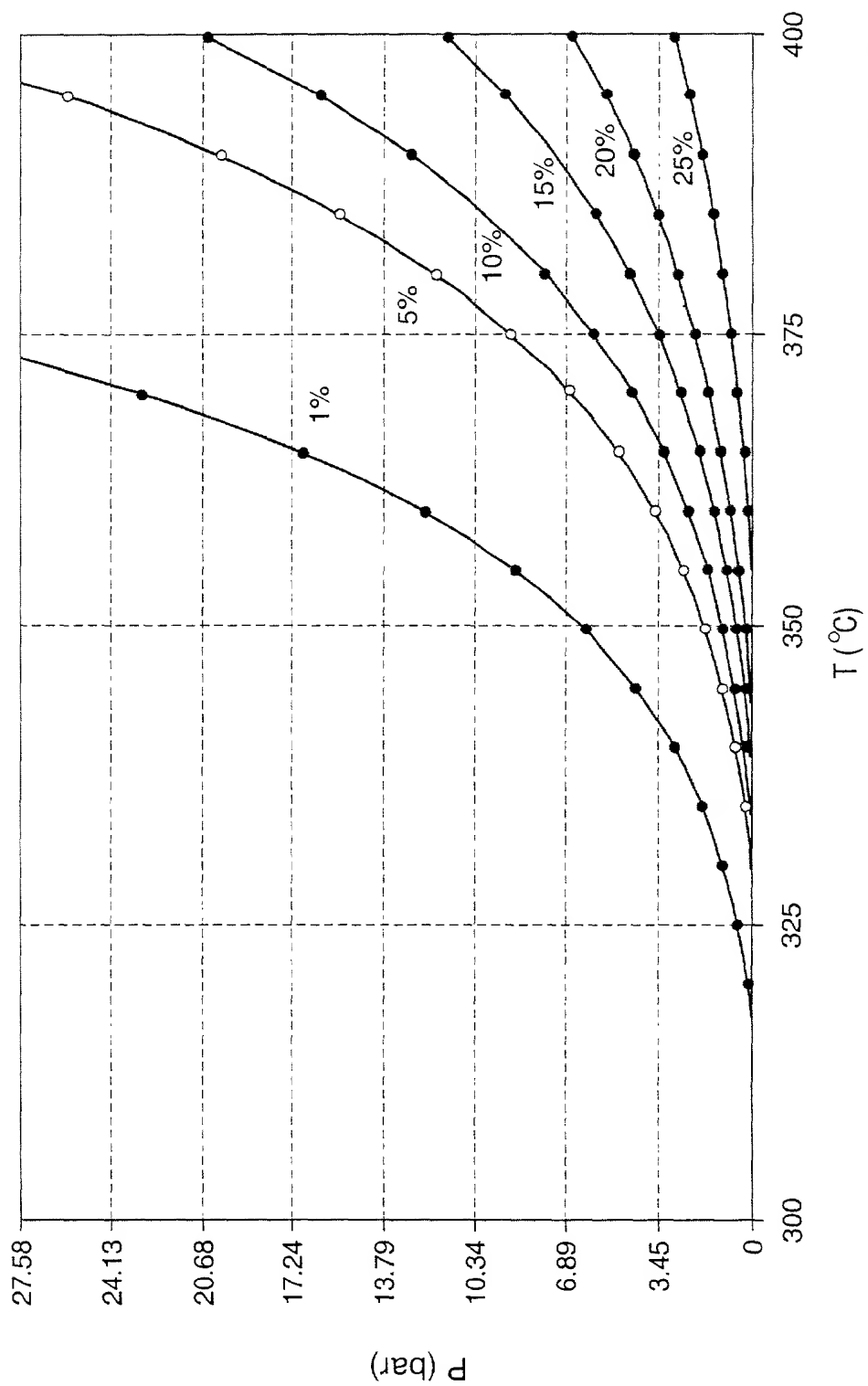


FIG. 90

$\frac{dP}{dT} = \frac{H_{vap} - H_{liq}}{T \Delta V}$   $\frac{dP}{dT} = \frac{H_{vap} - H_{liq}}{T \Delta V}$   $\frac{dP}{dT} = \frac{H_{vap} - H_{liq}}{T \Delta V}$   $\frac{dP}{dT} = \frac{H_{vap} - H_{liq}}{T \Delta V}$

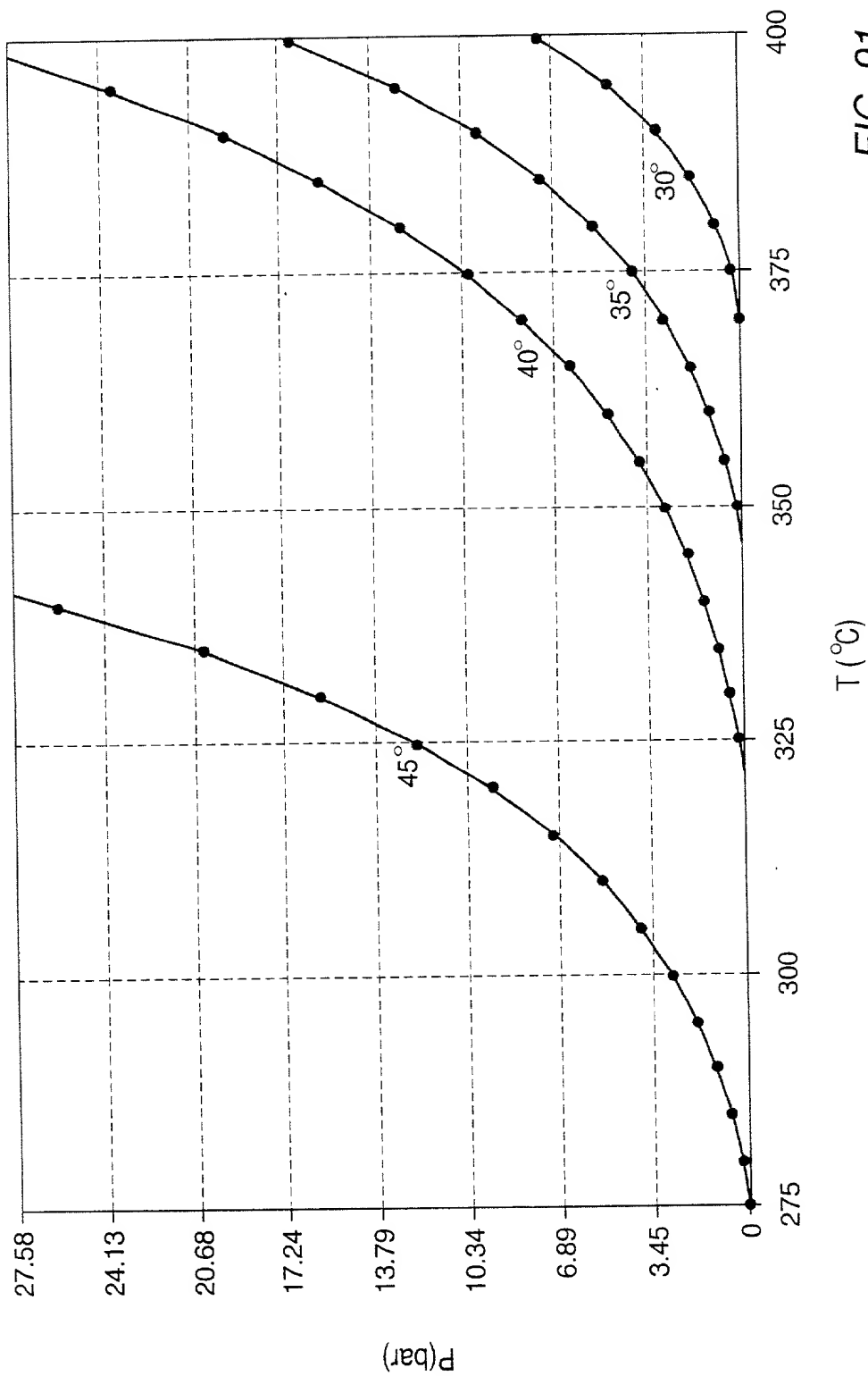


FIG. 91



1000 800 600 400 200 0  
10 20 30 40 50 60 70 80 90 100  
100 200 300 400 500 600 700 800 900 1000

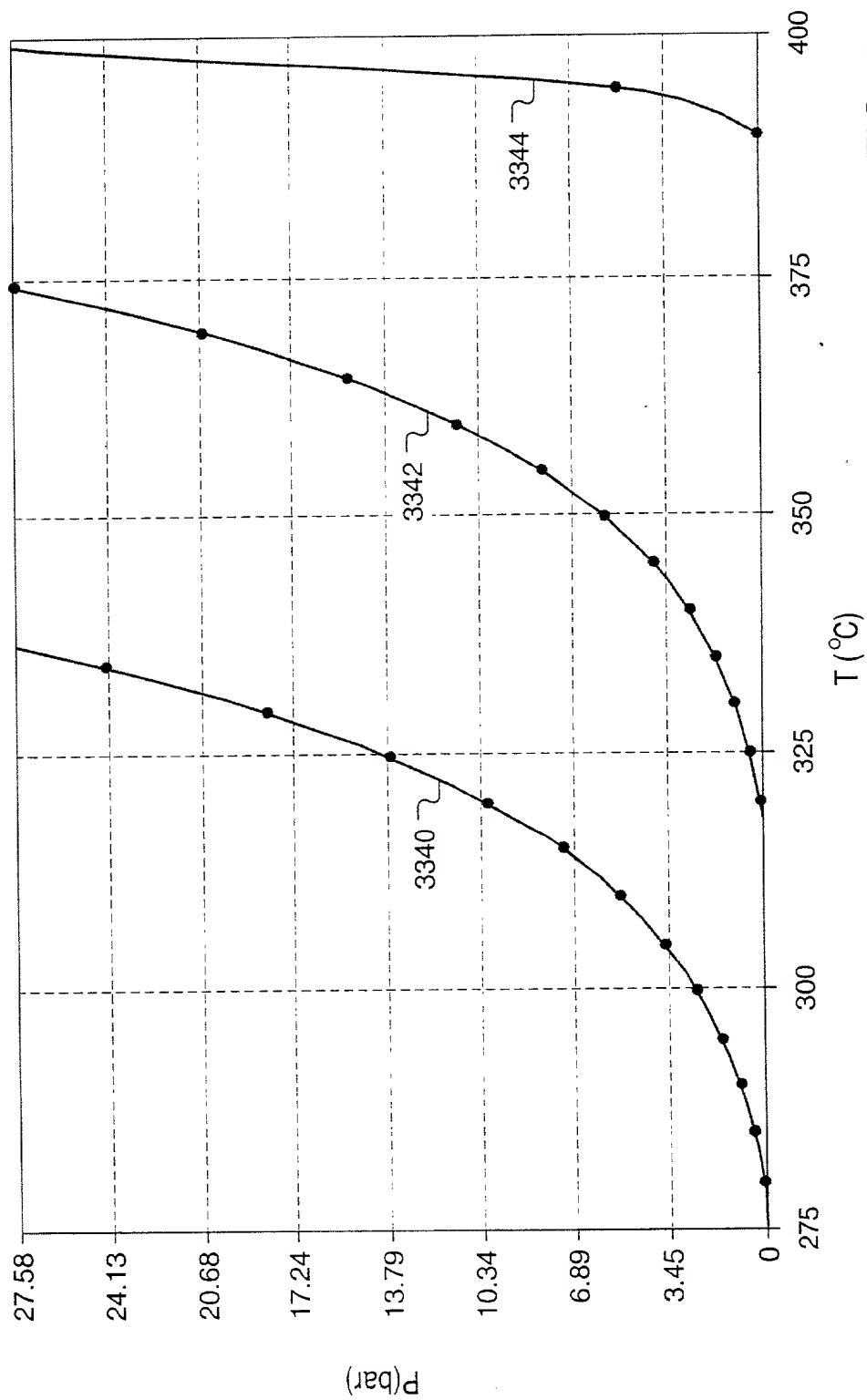


FIG. 93

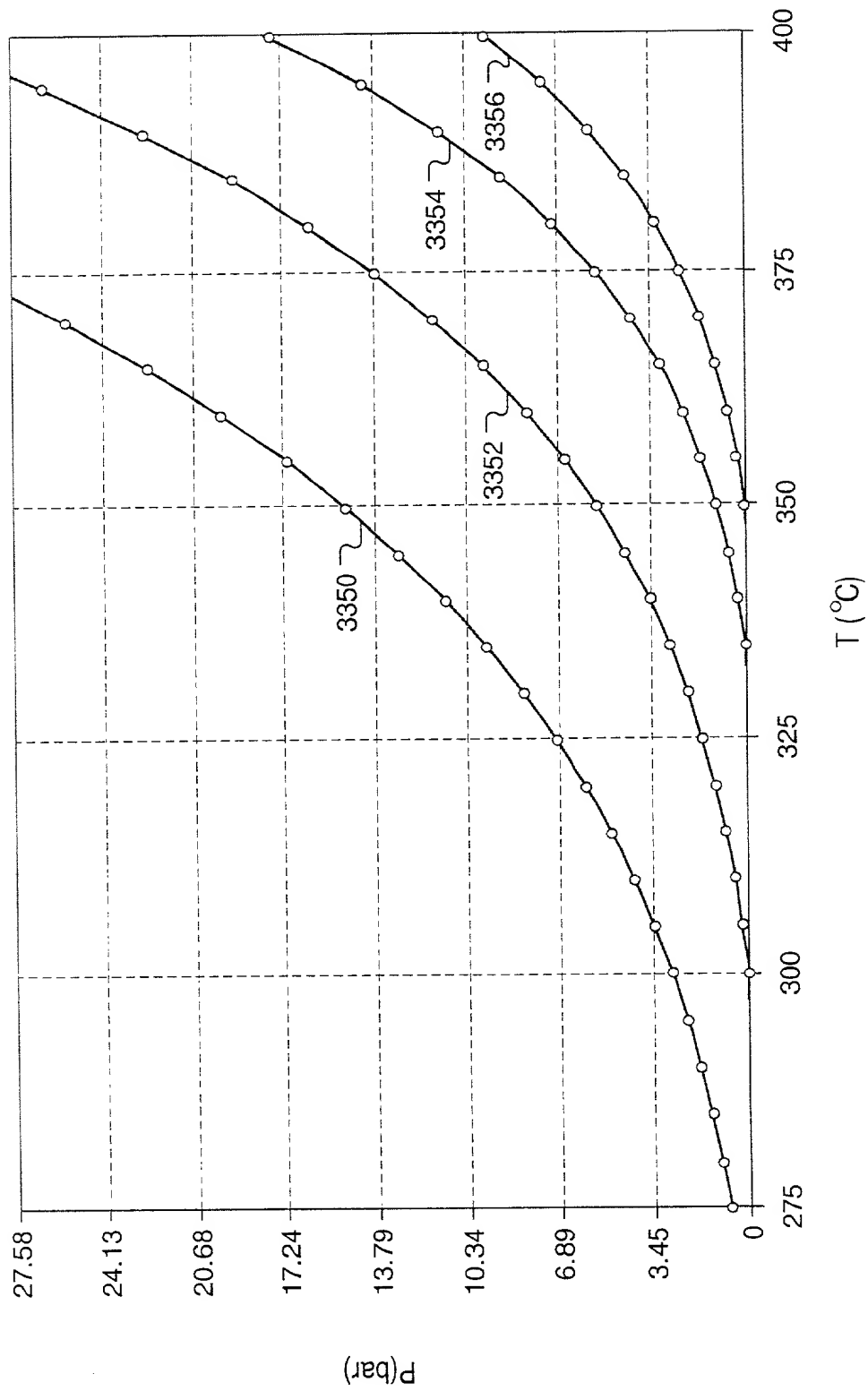


FIG. 94

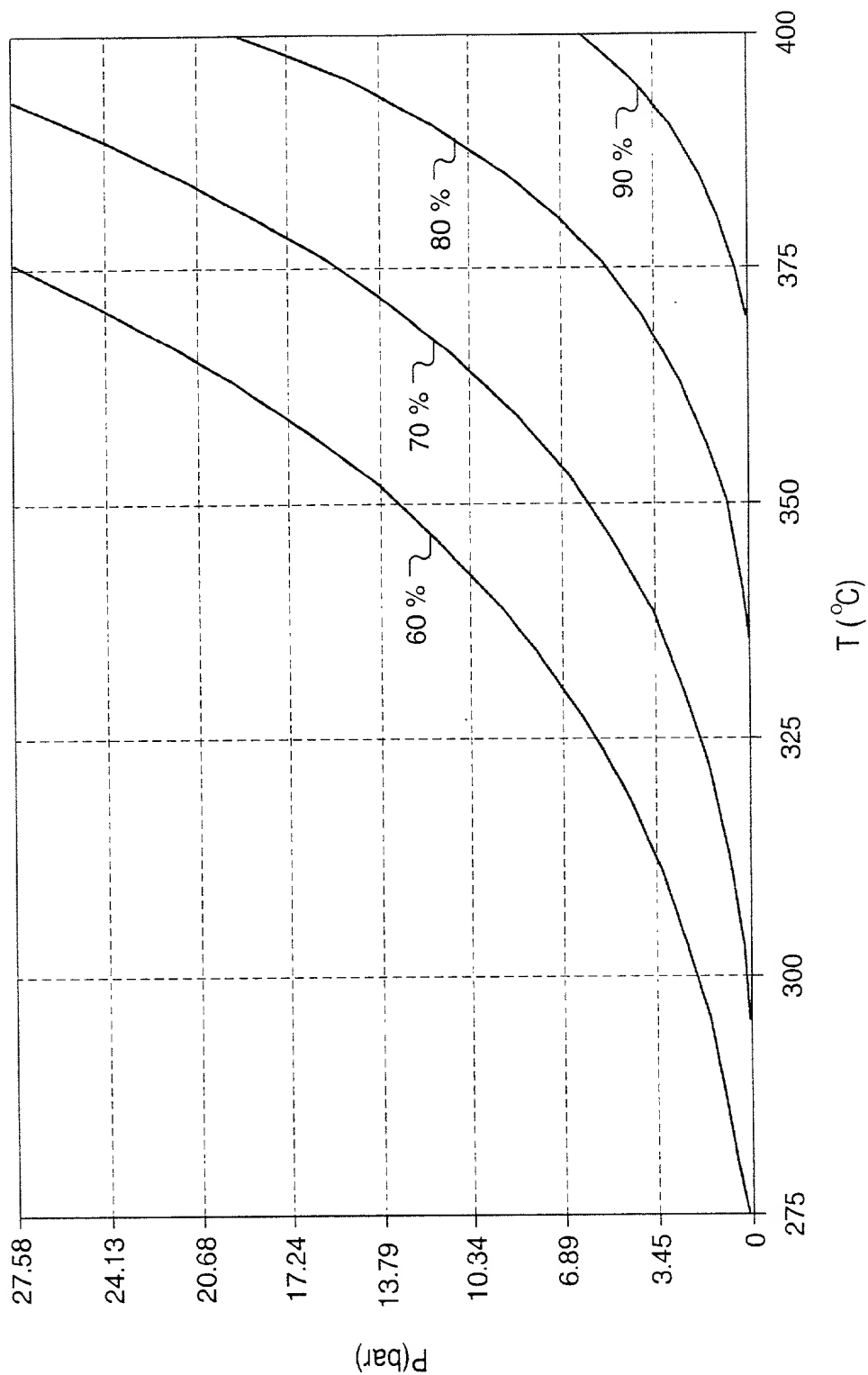
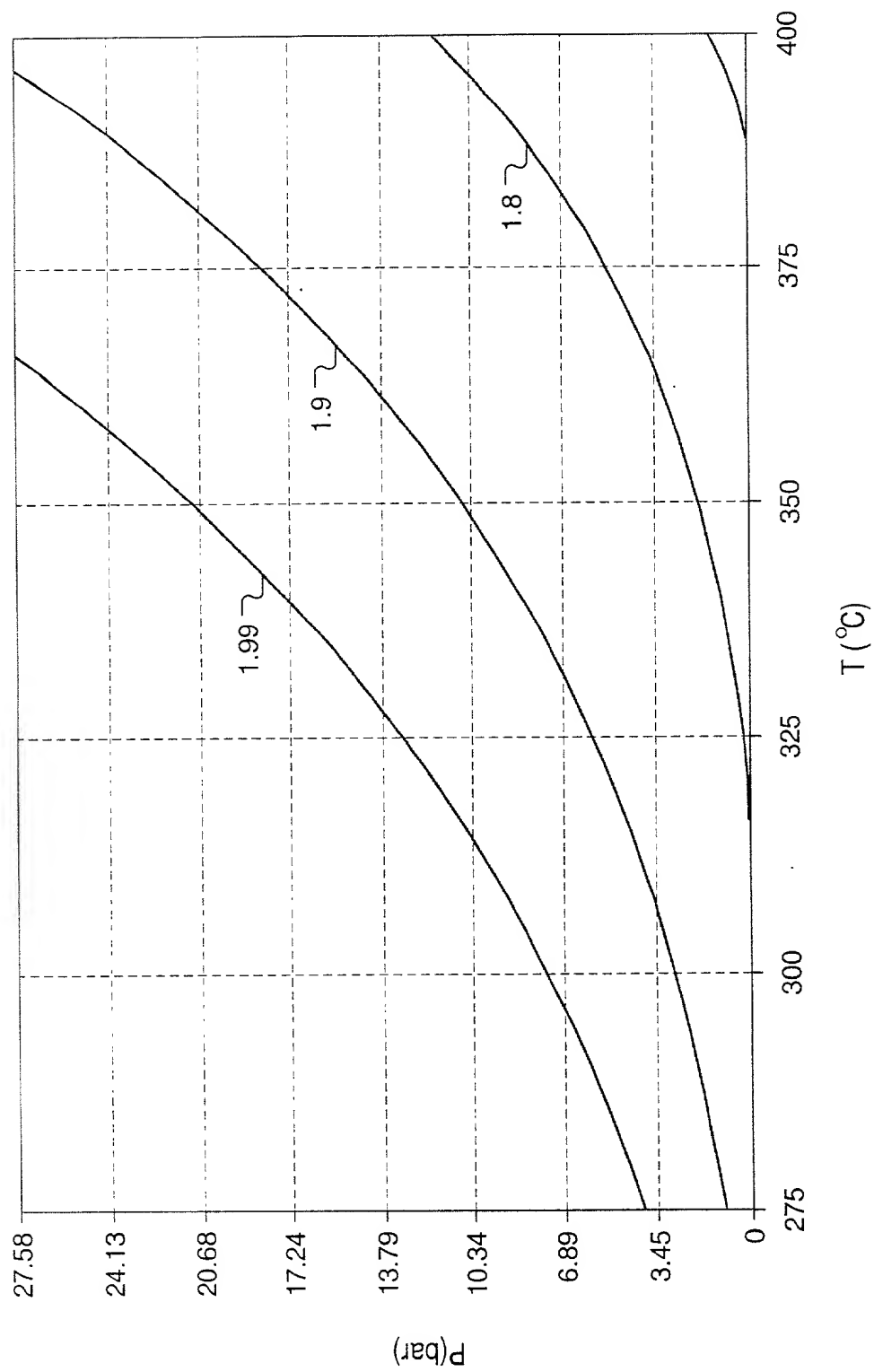


FIG. 95



**FIG. 96**

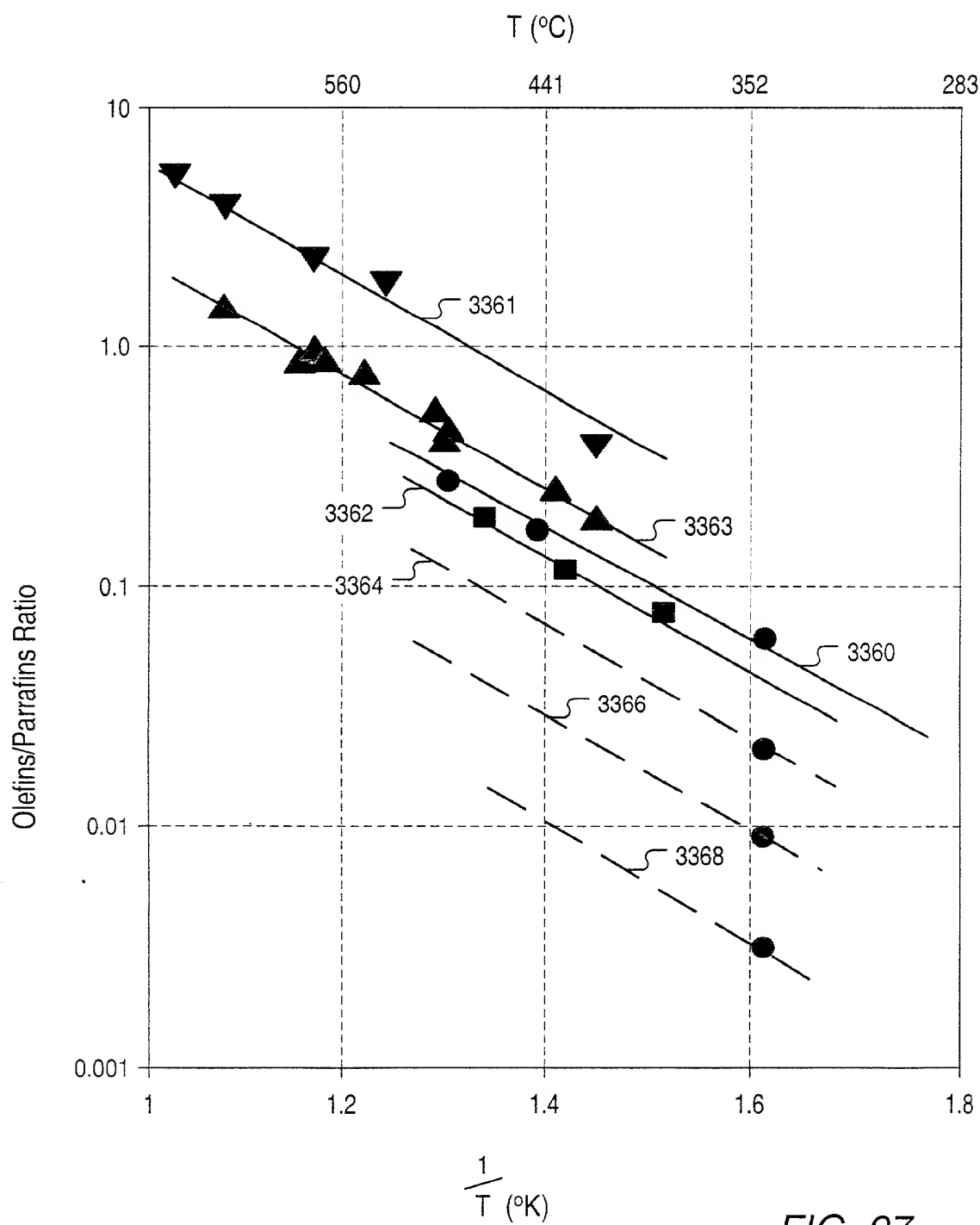


FIG. 97



API Gravity (°) vs. P<sub>H2</sub> (bar) for 325°C, 350°C, and 375°C

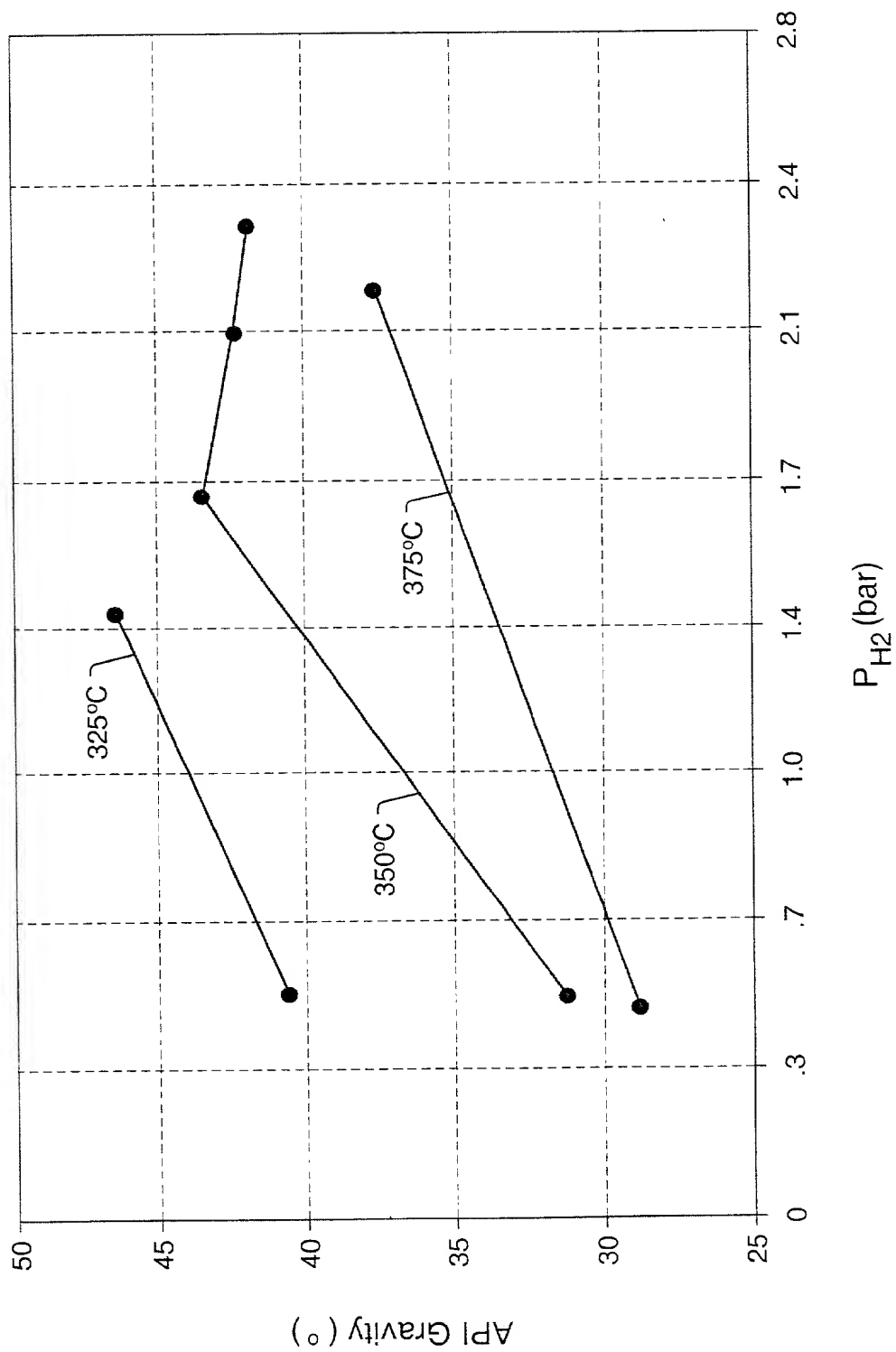


FIG. 98

Copyright © 1999 by John Wiley & Sons, Inc. All rights reserved. No part of this publication may be reproduced, stored in a retrieval system, or transmitted, in any form or by any means, electronic, mechanical, photocopying, recording, or by any information storage and retrieval system, without permission in writing from John Wiley & Sons, Inc.

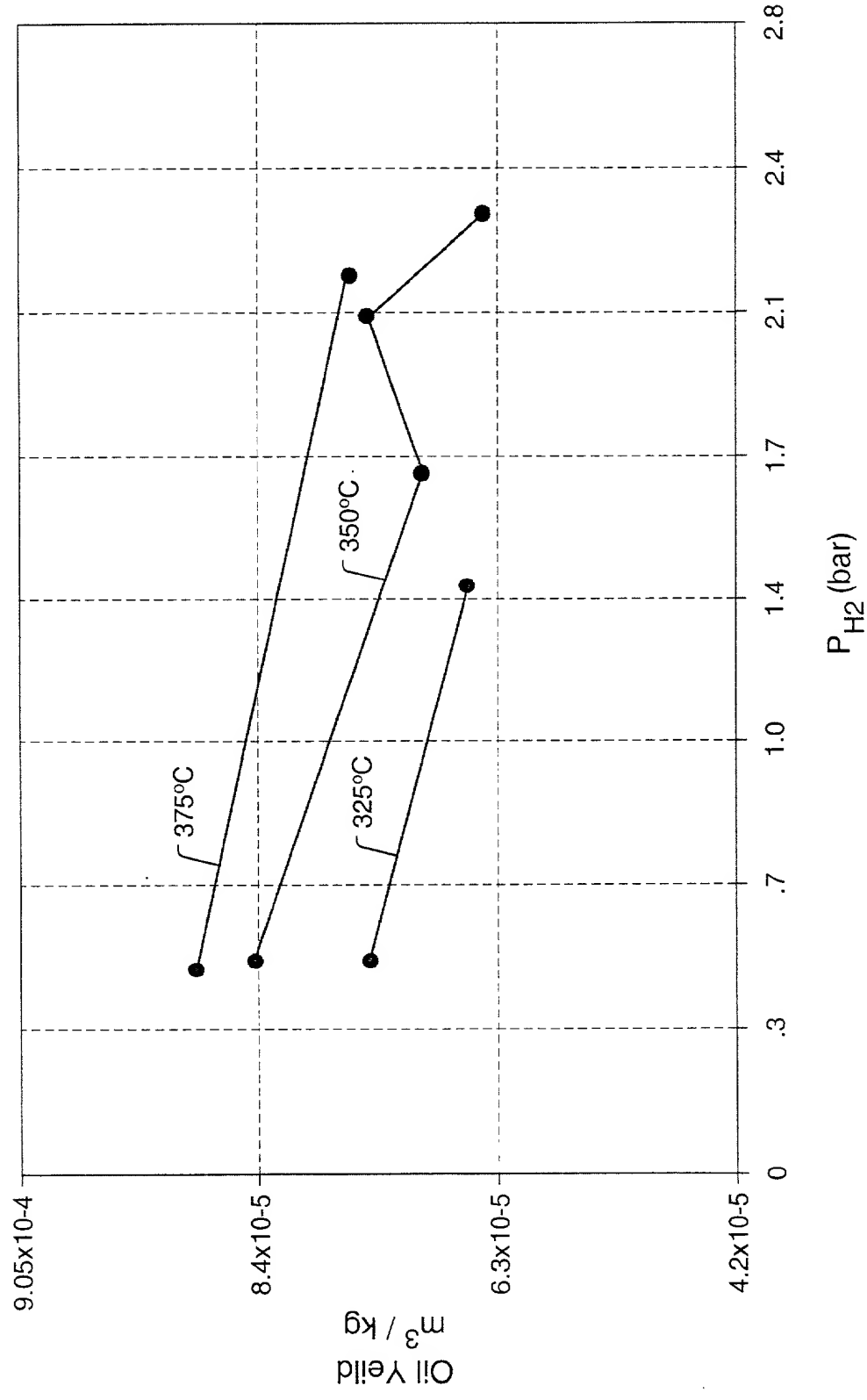


FIG. 99

FIG. 100

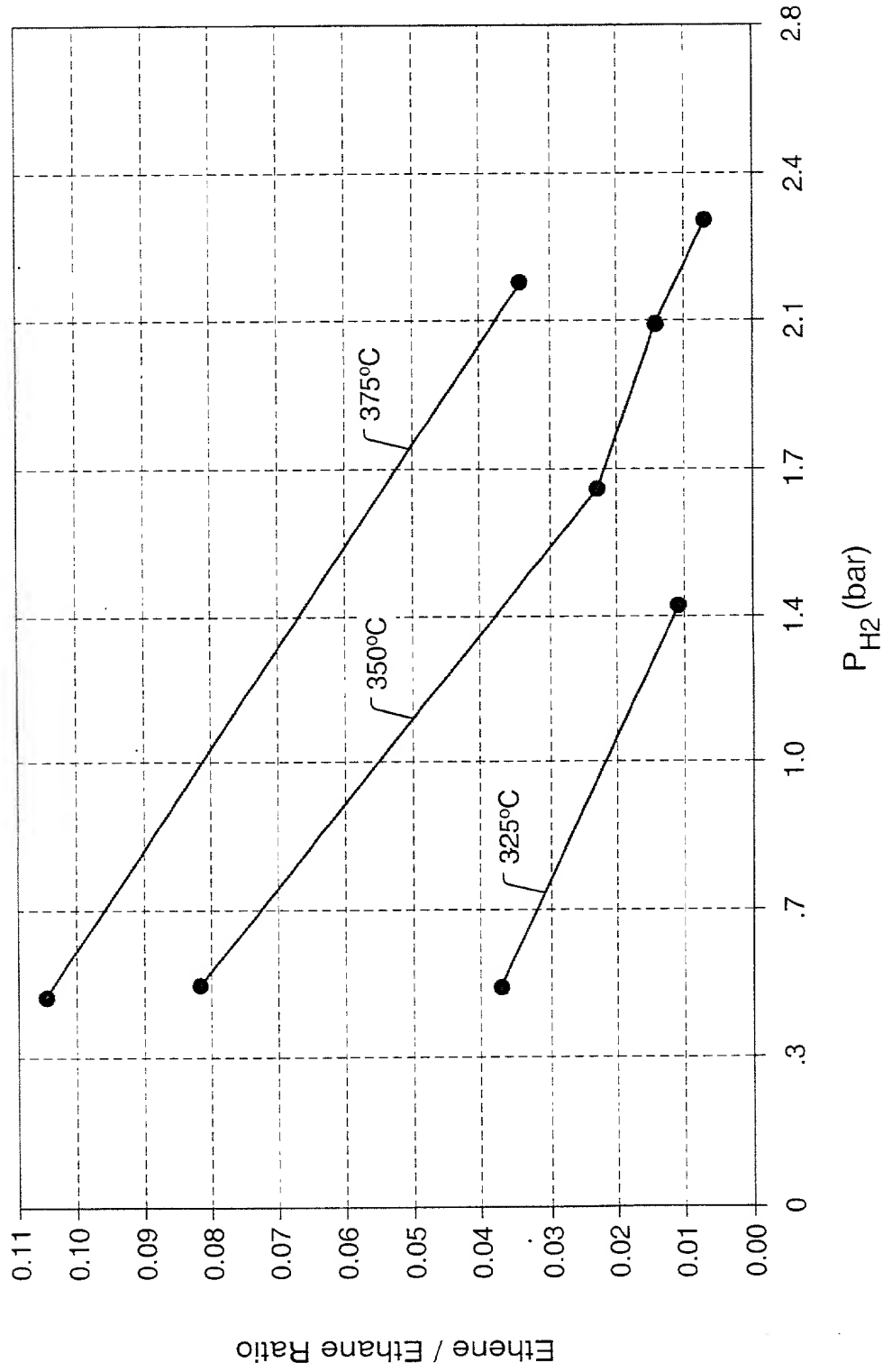


FIG. 100

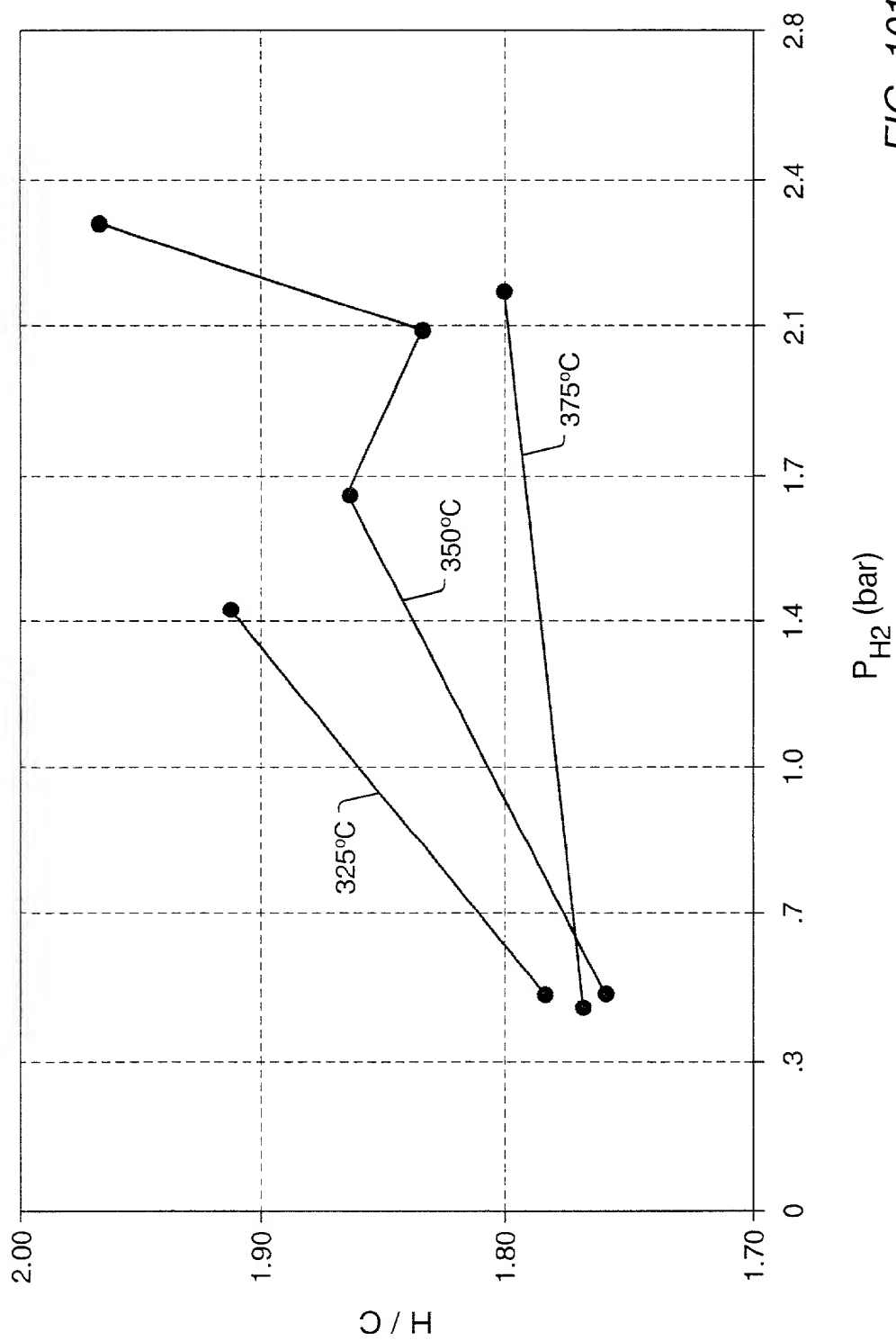


FIG. 101



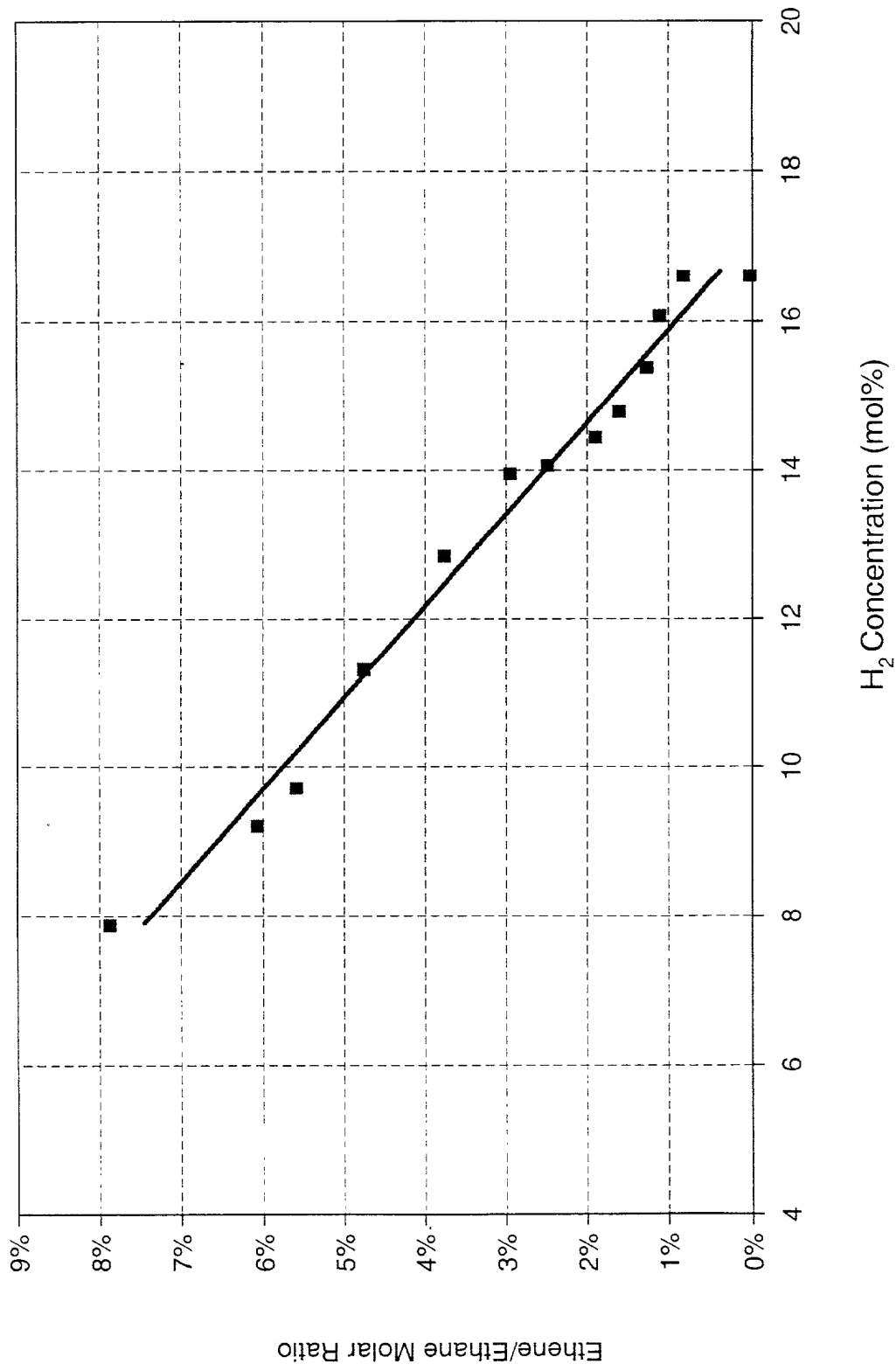
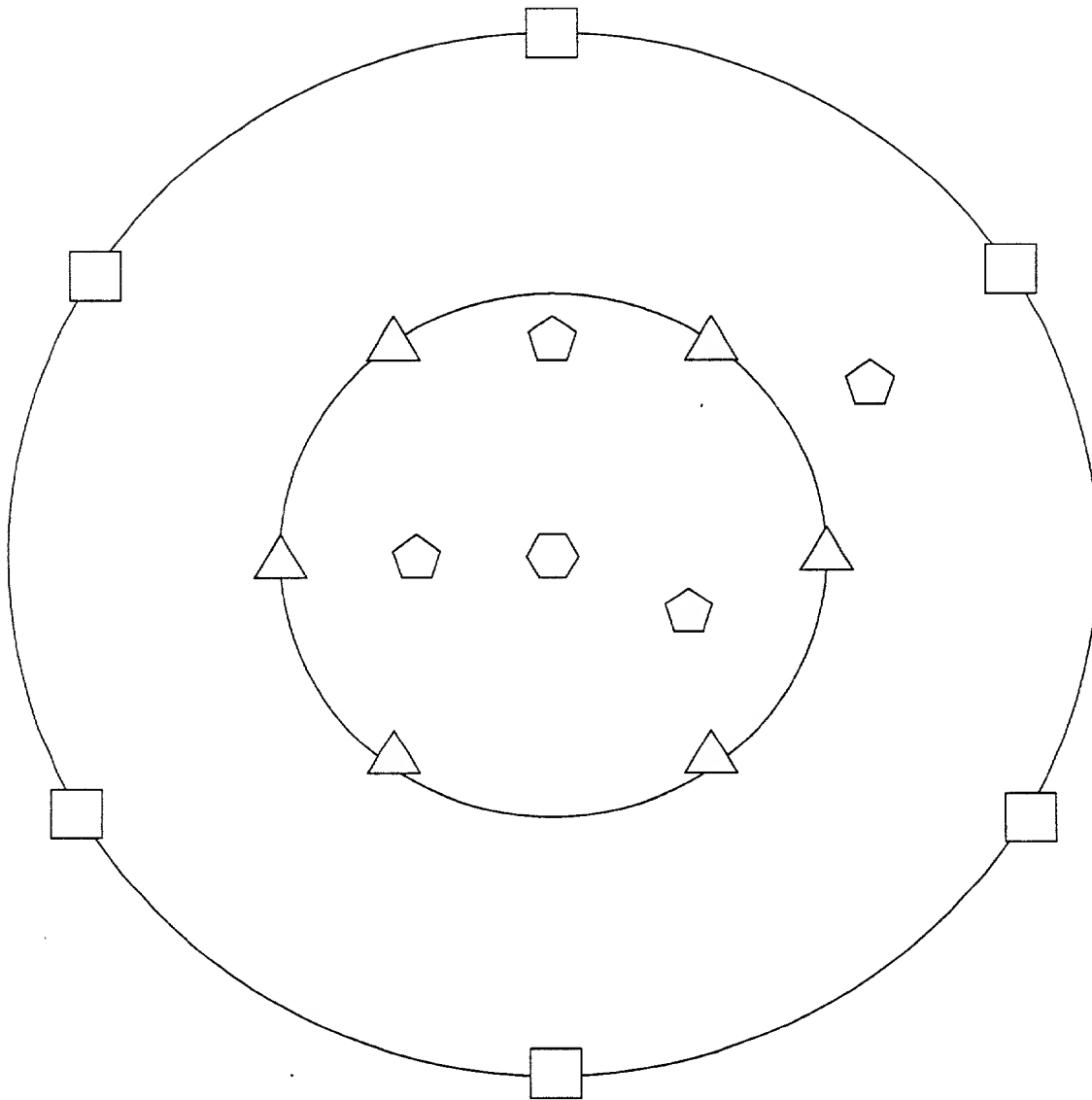


FIG. 103

FIG. 104 is a schematic diagram of a system 100 for providing a user with a visual representation of a system 100. The system 100 includes a user interface 102, a data source 104, and a data processing unit 106. The user interface 102 is configured to receive input from a user and to display output to the user. The data source 104 is configured to provide data to the data processing unit 106. The data processing unit 106 is configured to process the data received from the data source 104 and to provide output to the user interface 102. The system 100 is configured to provide a user with a visual representation of a system 100.



△ - 3600

⬠ - 3603

□ - 3604

⬡ - 3602

FIG. 104





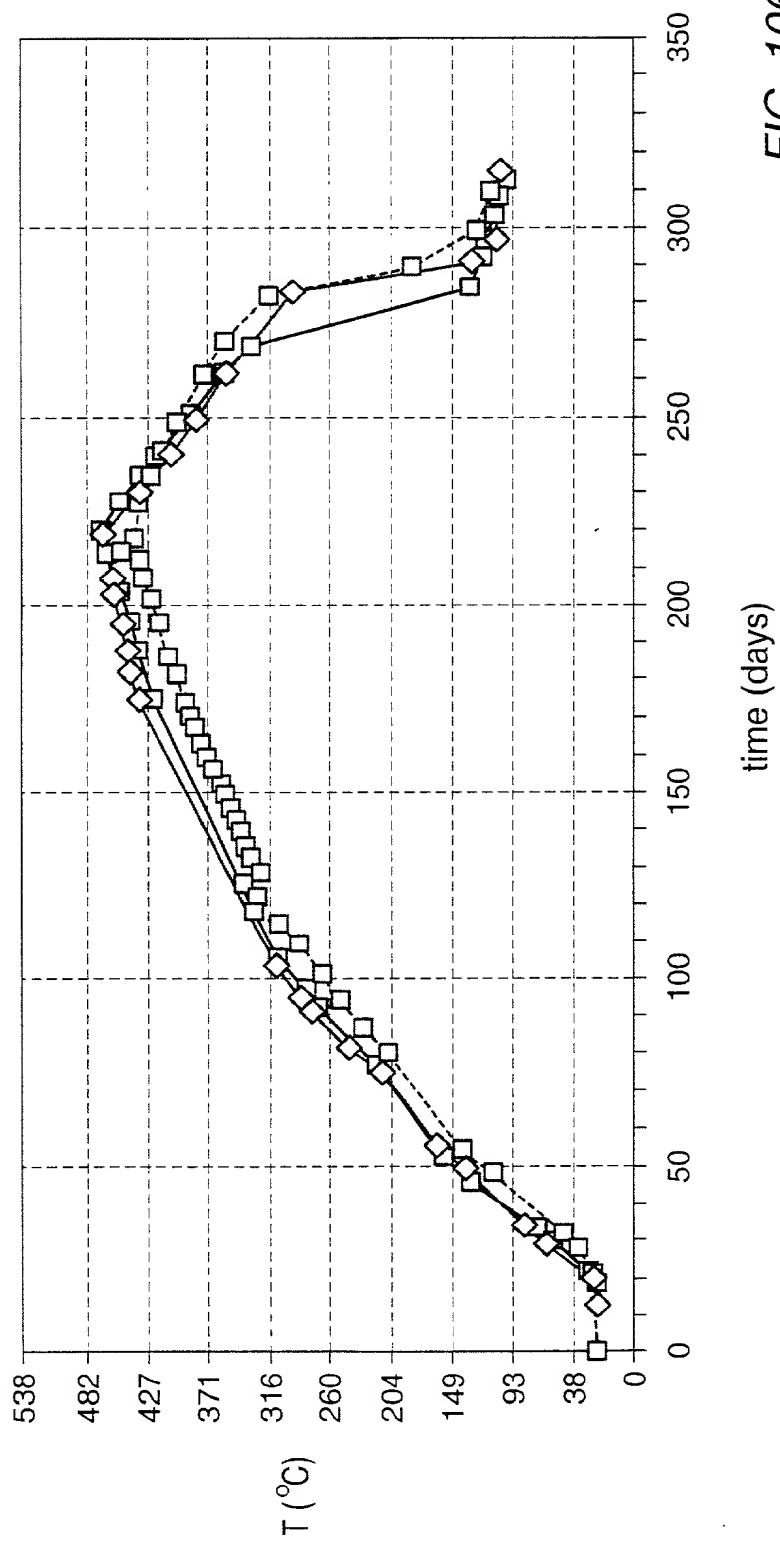


FIG. 106



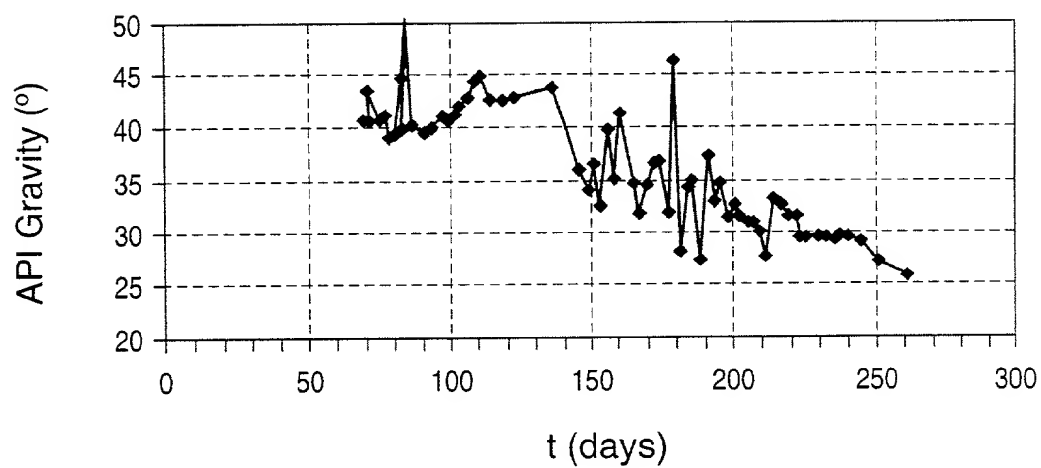


FIG. 108

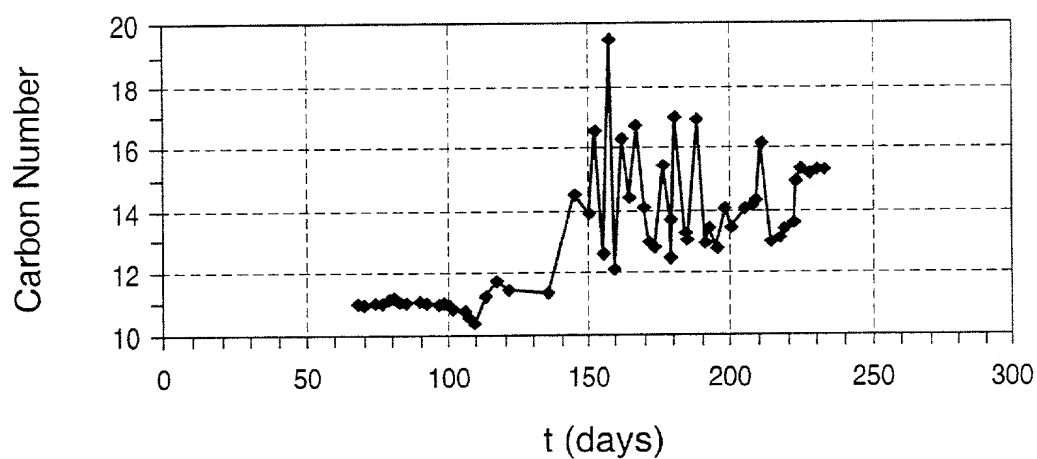


FIG. 109

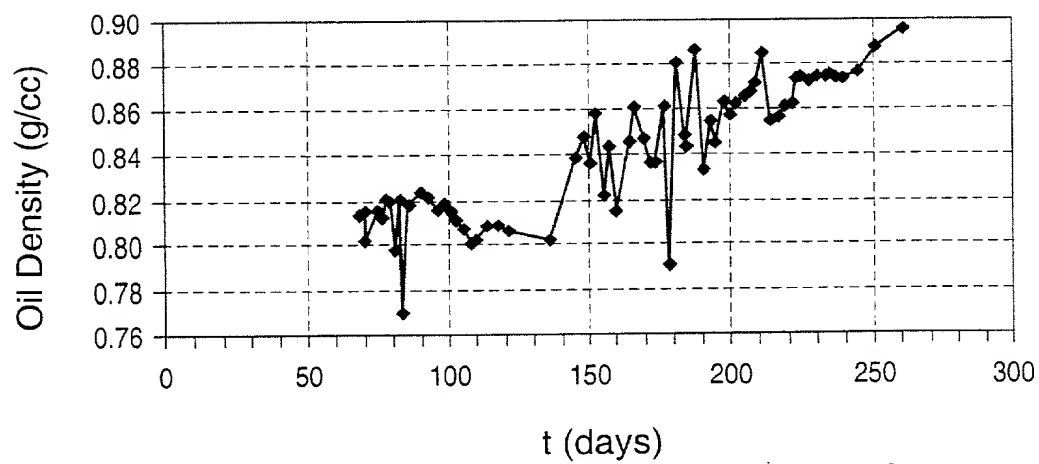


FIG. 110

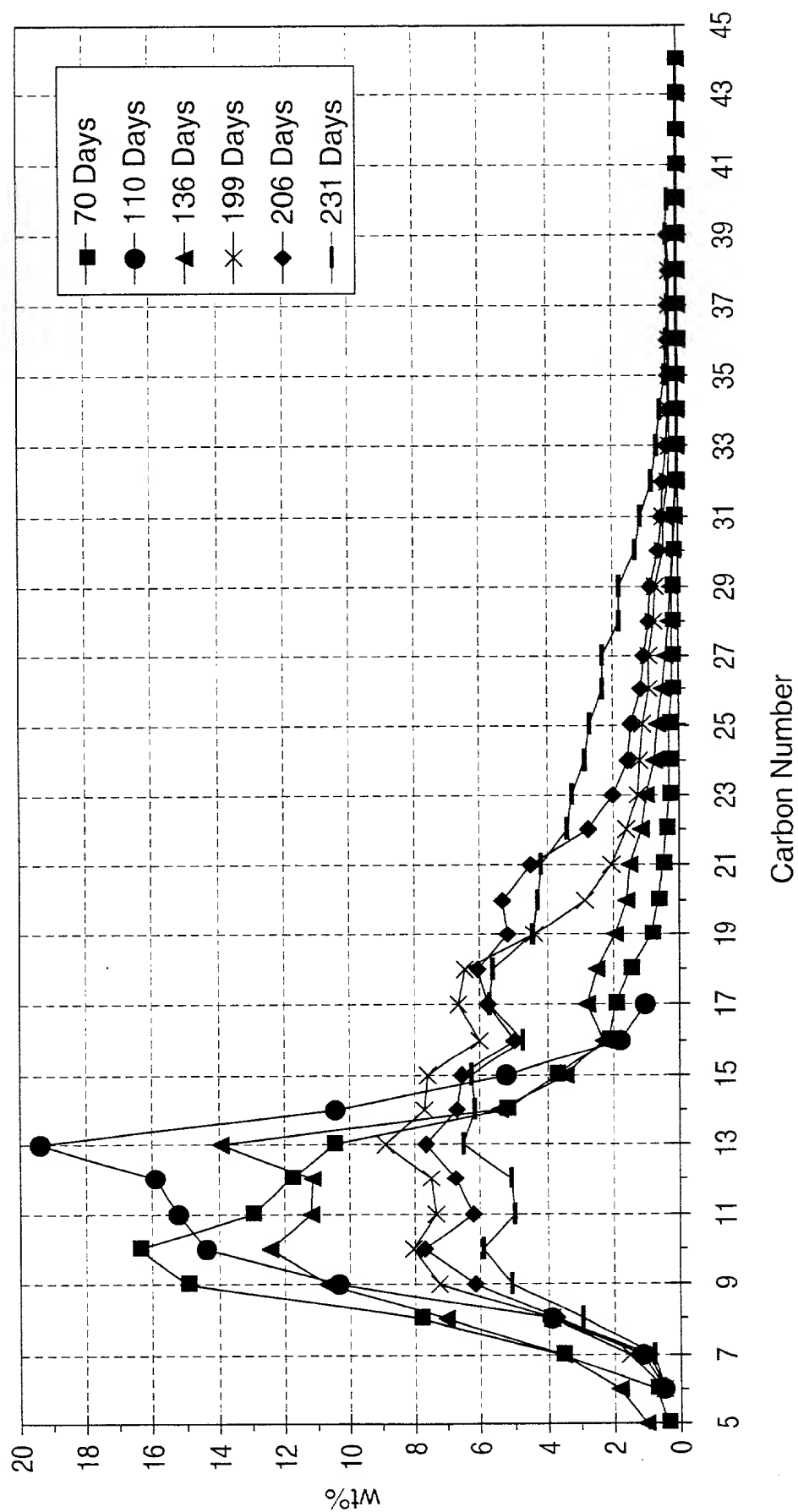
[illegible]

Figure 112 is a graph showing the weight percentage of the various components of the polymer as a function of the carbon number (C#) of the component. The weight percentage is plotted on the y-axis (0 to 10) and the carbon number is plotted on the x-axis (5 to 43). The graph shows two curves: one with open circles and one with solid squares. The curve with open circles shows a peak at C# 19 (3620) and a smaller peak at C# 21 (3622). The curve with solid squares shows a peak at C# 21 (3620) and a smaller peak at C# 23 (3622).

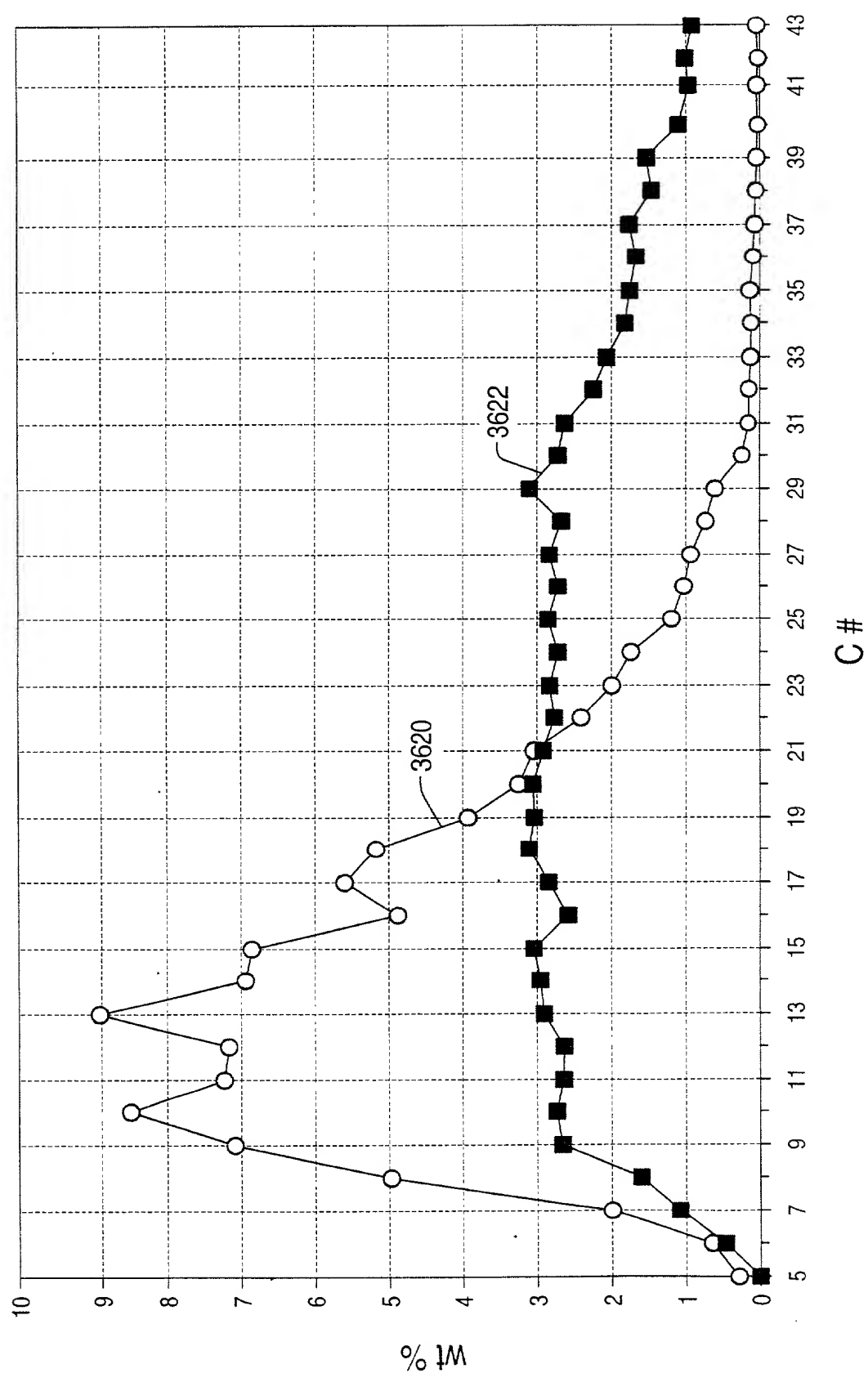


FIG. 112

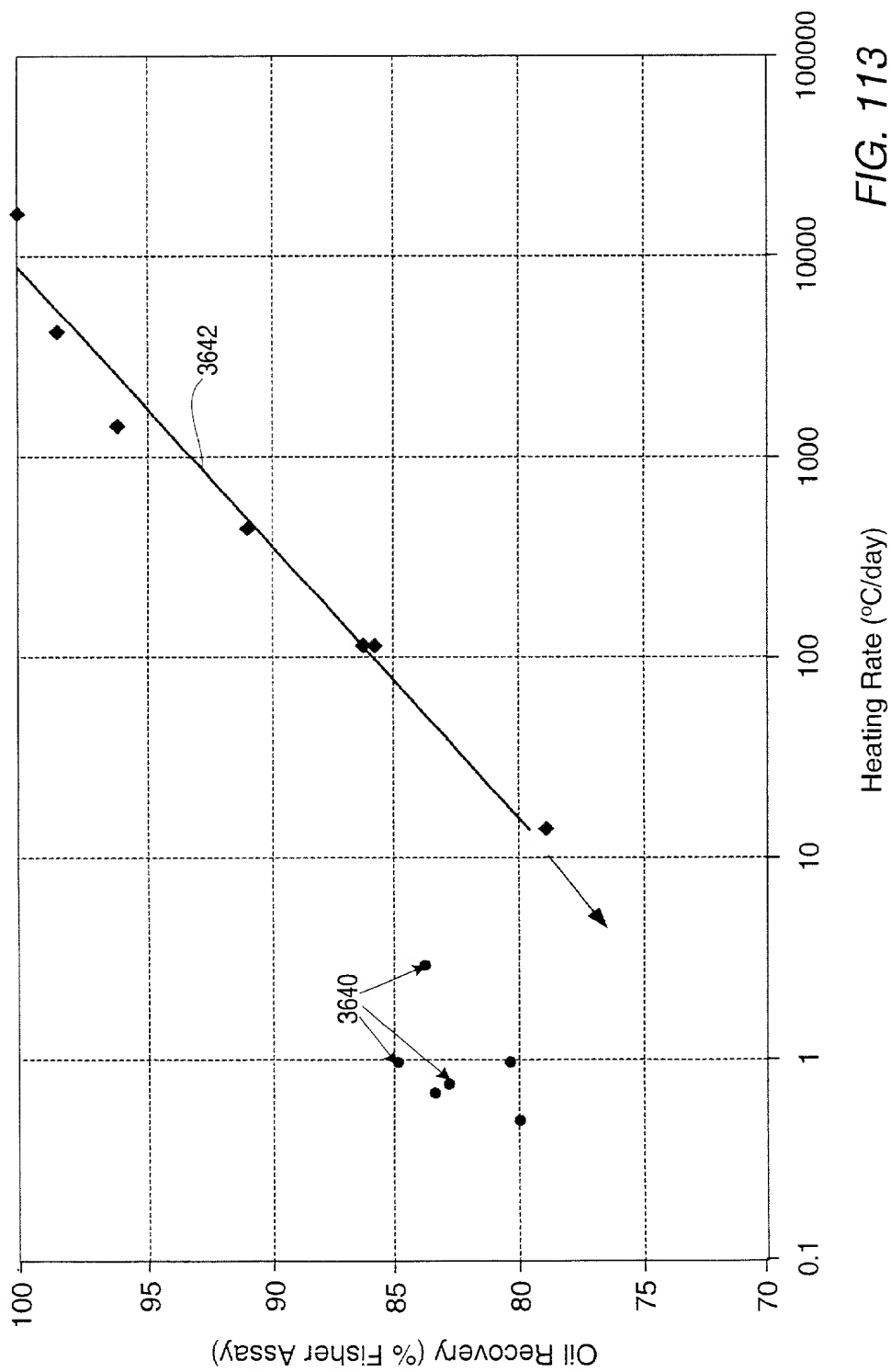


FIG. 113

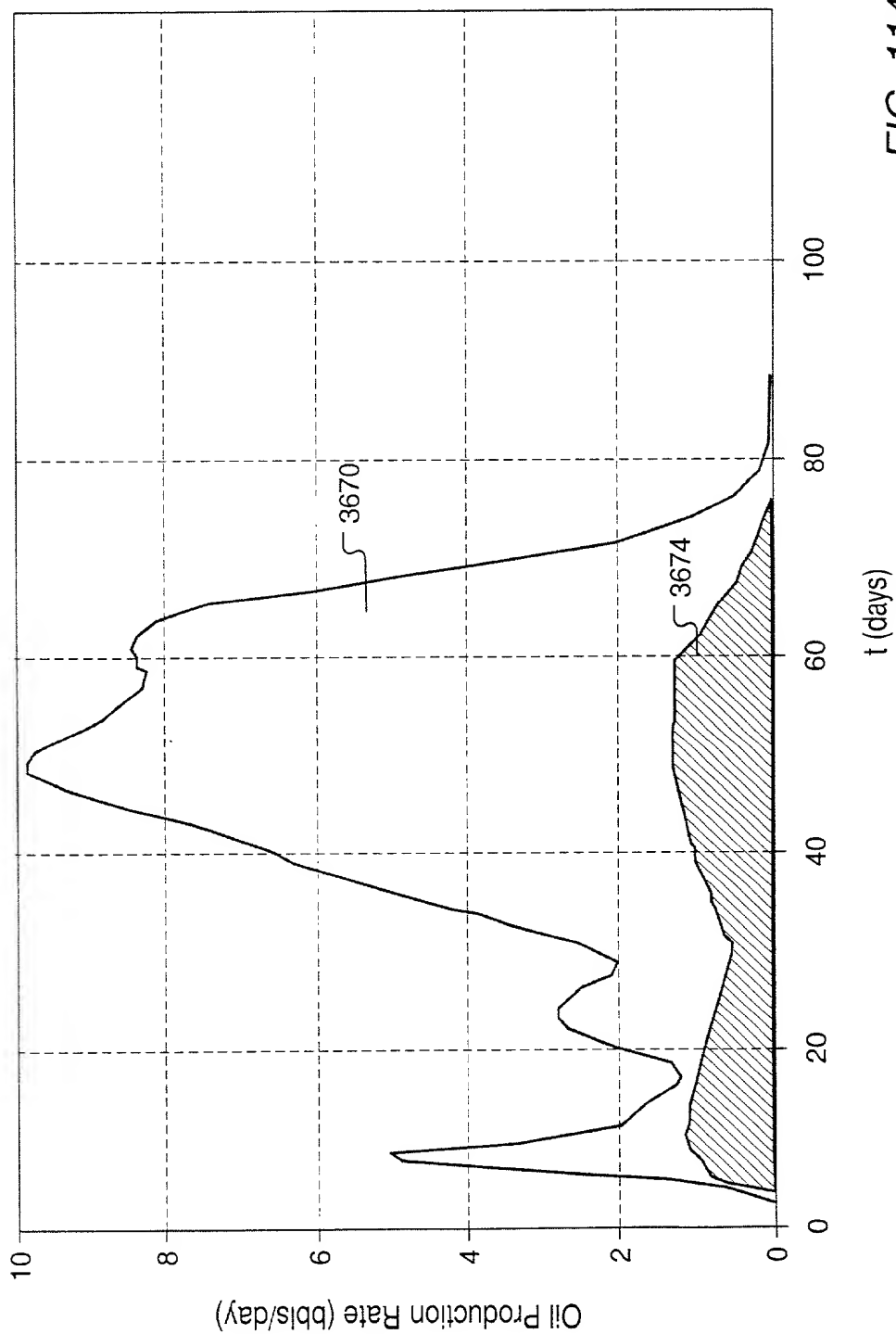


FIG. 114





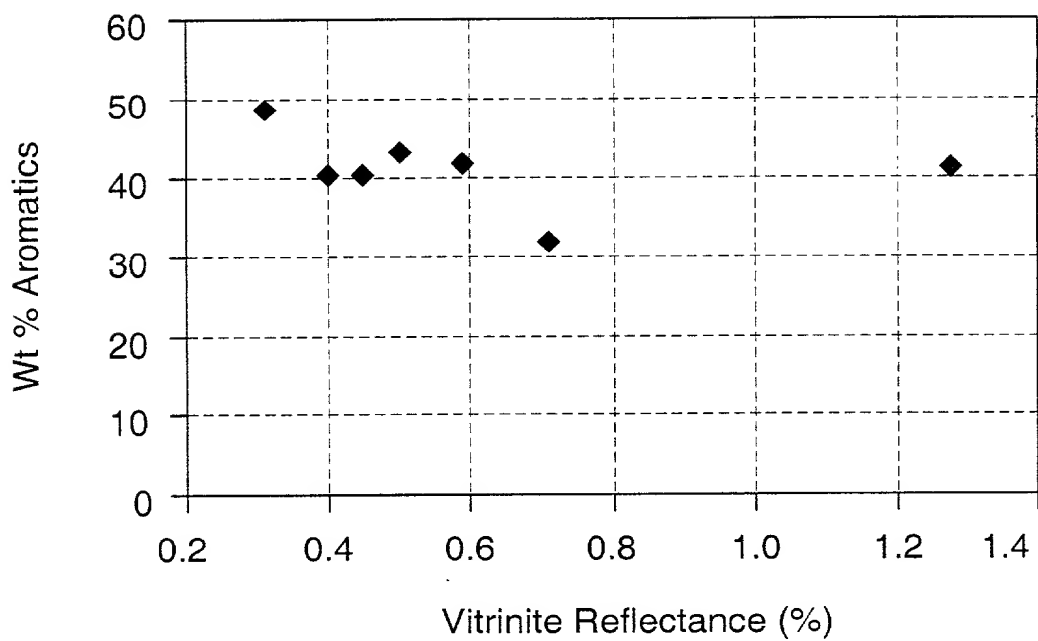


FIG. 119

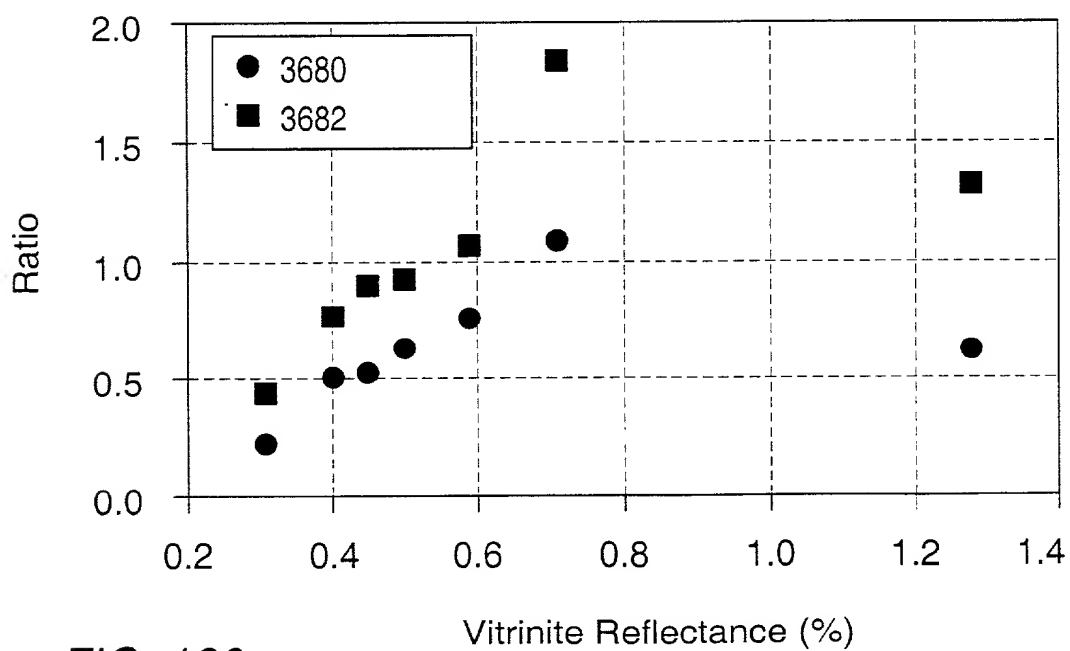


FIG. 120

Figure 121, 122, 123, and 124 are scatter plots showing the relationship between Vitritite Reflectance (%) and  $m^3/kg$  for different samples. The data points are plotted on a grid with Vitritite Reflectance (%) on the x-axis (0.2 to 1.4) and  $m^3/kg$  on the y-axis (0 to  $4.2 \times 10^{-5}$ ).

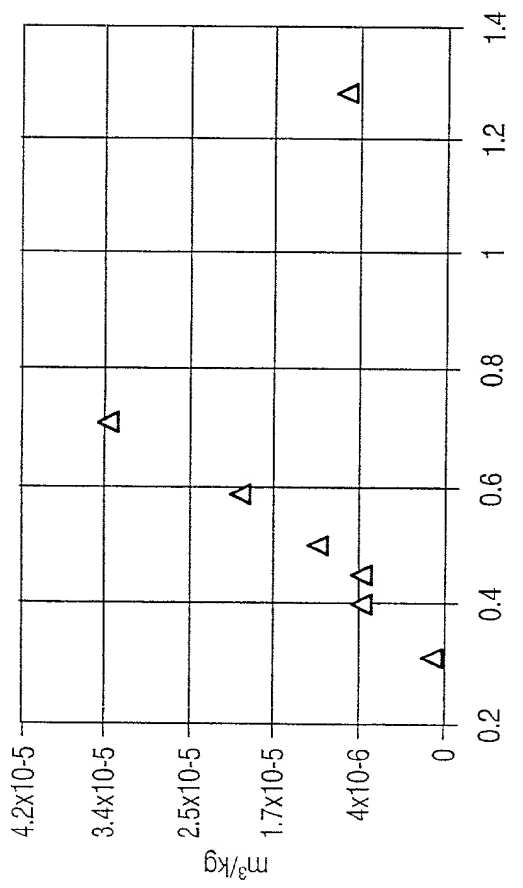


FIG. 121

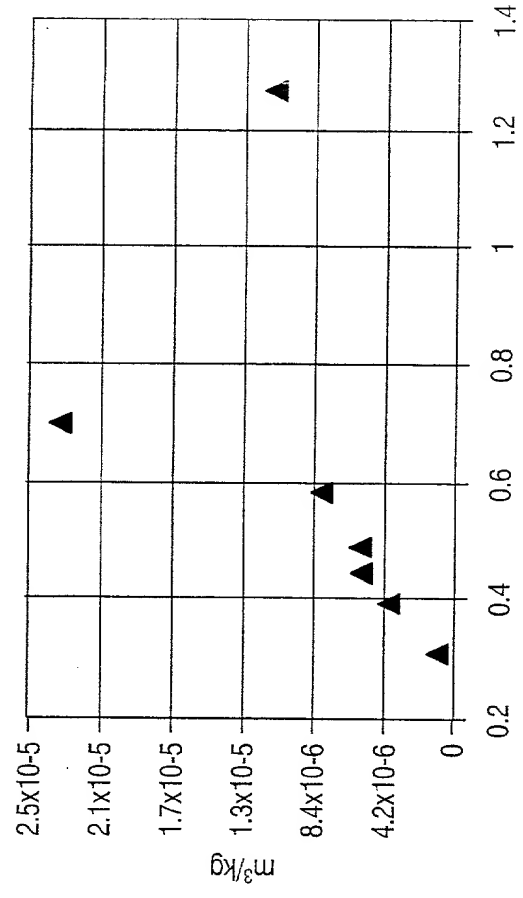


FIG. 122

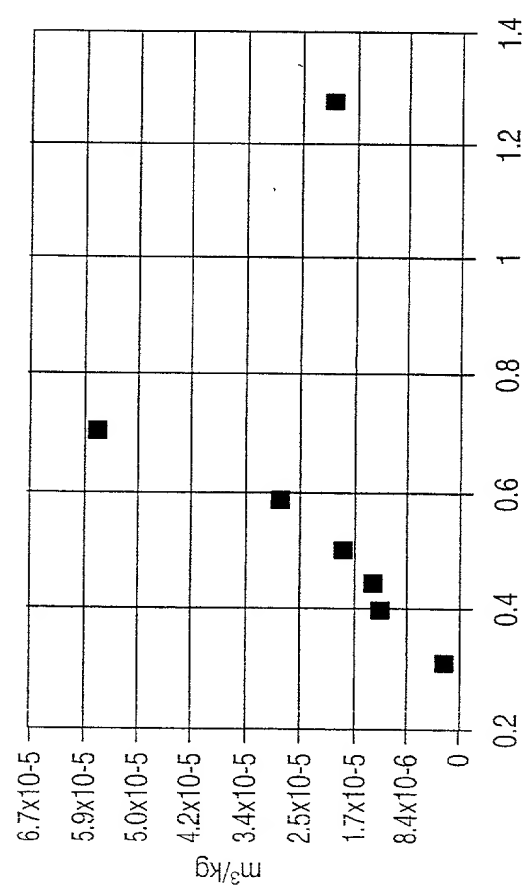


FIG. 123

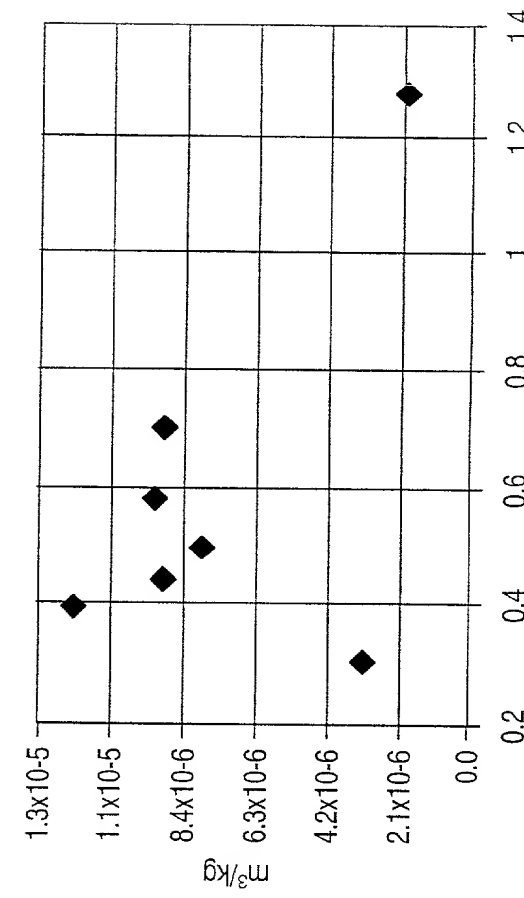


FIG. 124

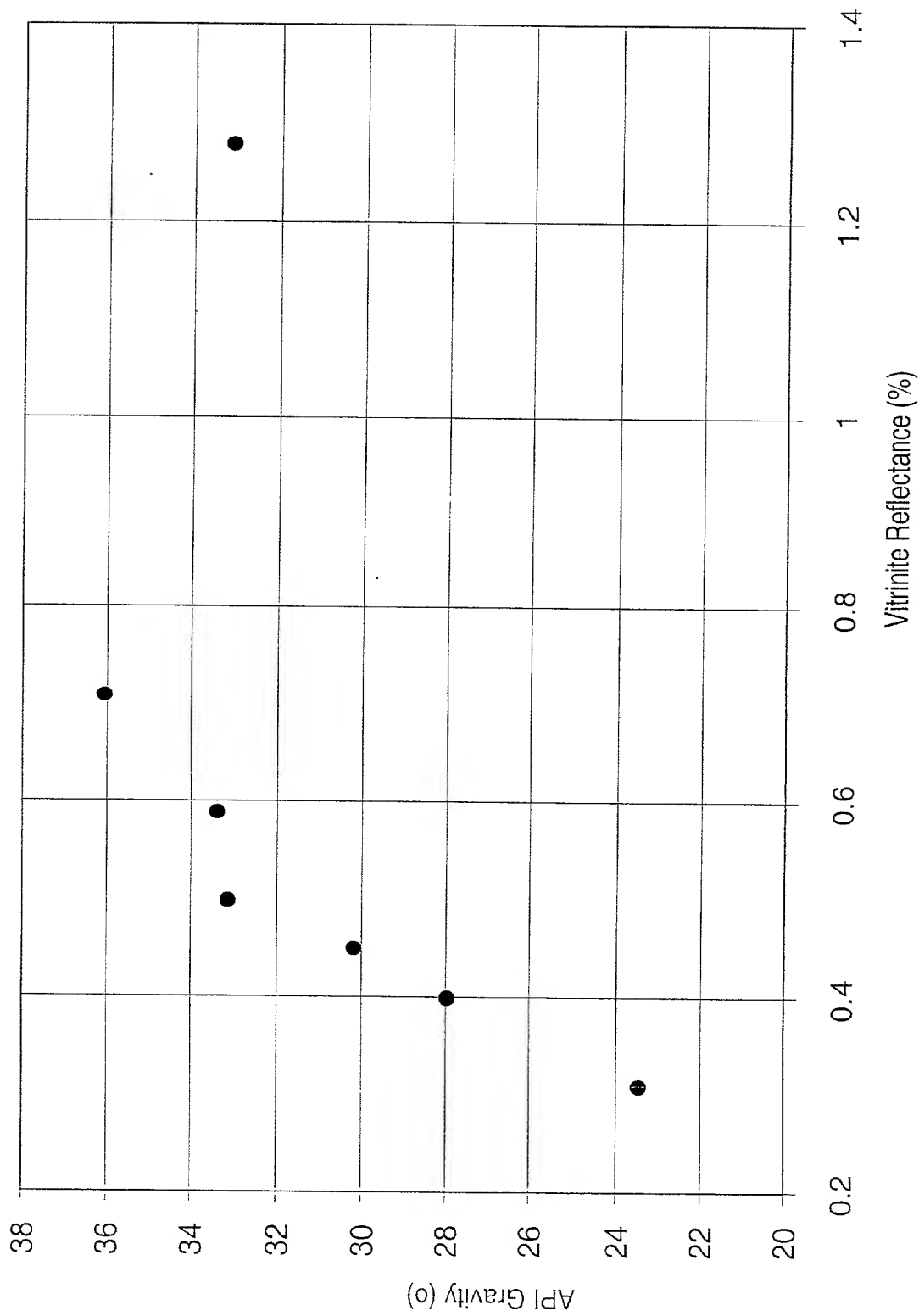
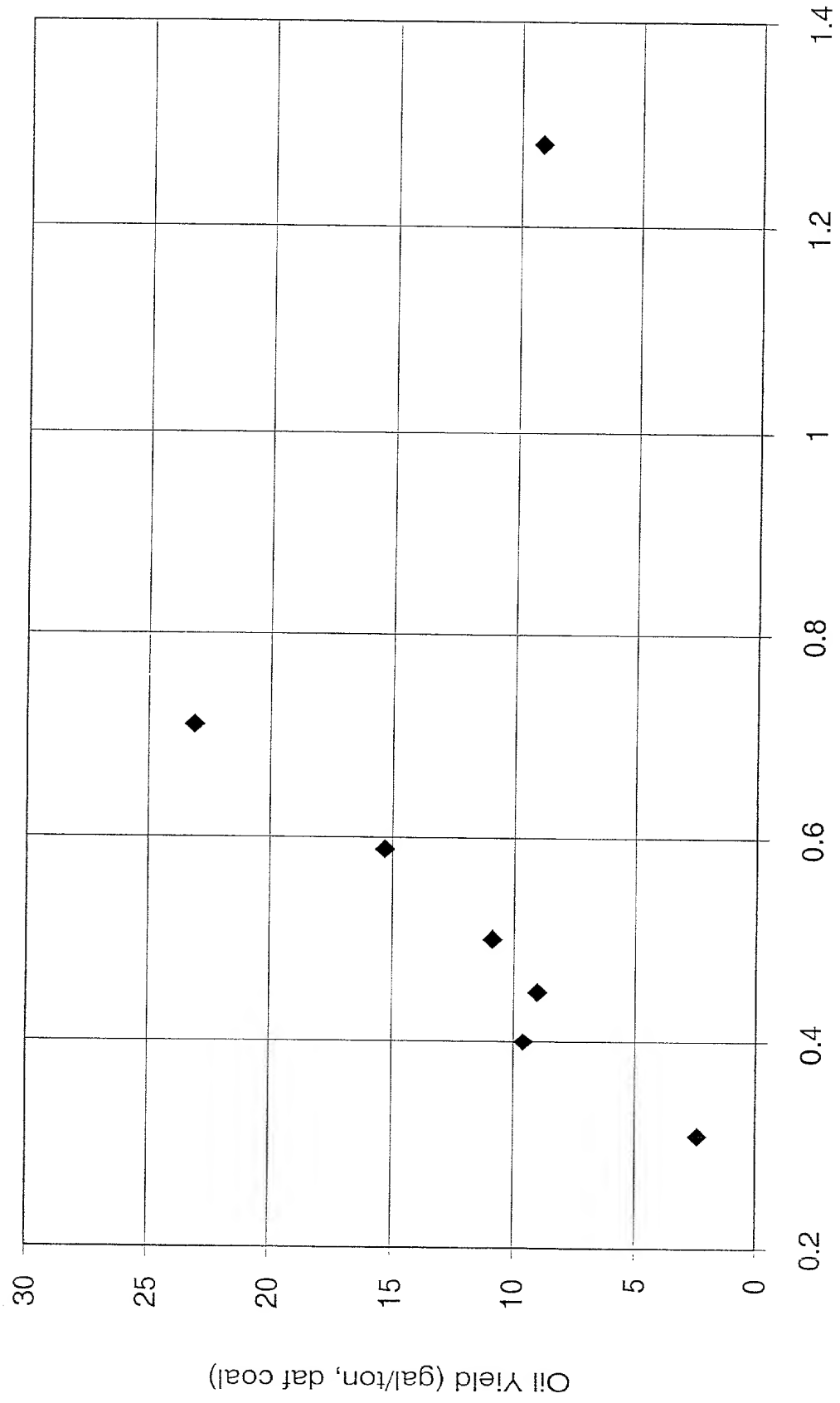


FIG. 125

Figure 126 is a scatter plot showing the relationship between Oil Yield (gal/ton, daf coal) on the Y-axis and Vitrinite Reflectance (%) on the X-axis. The Y-axis ranges from 0 to 30 in increments of 5. The X-axis ranges from 0.2 to 1.4 in increments of 0.2. There are seven data points plotted as solid diamonds.



Vitrinite Reflectance (%)

Oil Yield (gal/ton, daf coal)

FIG. 126



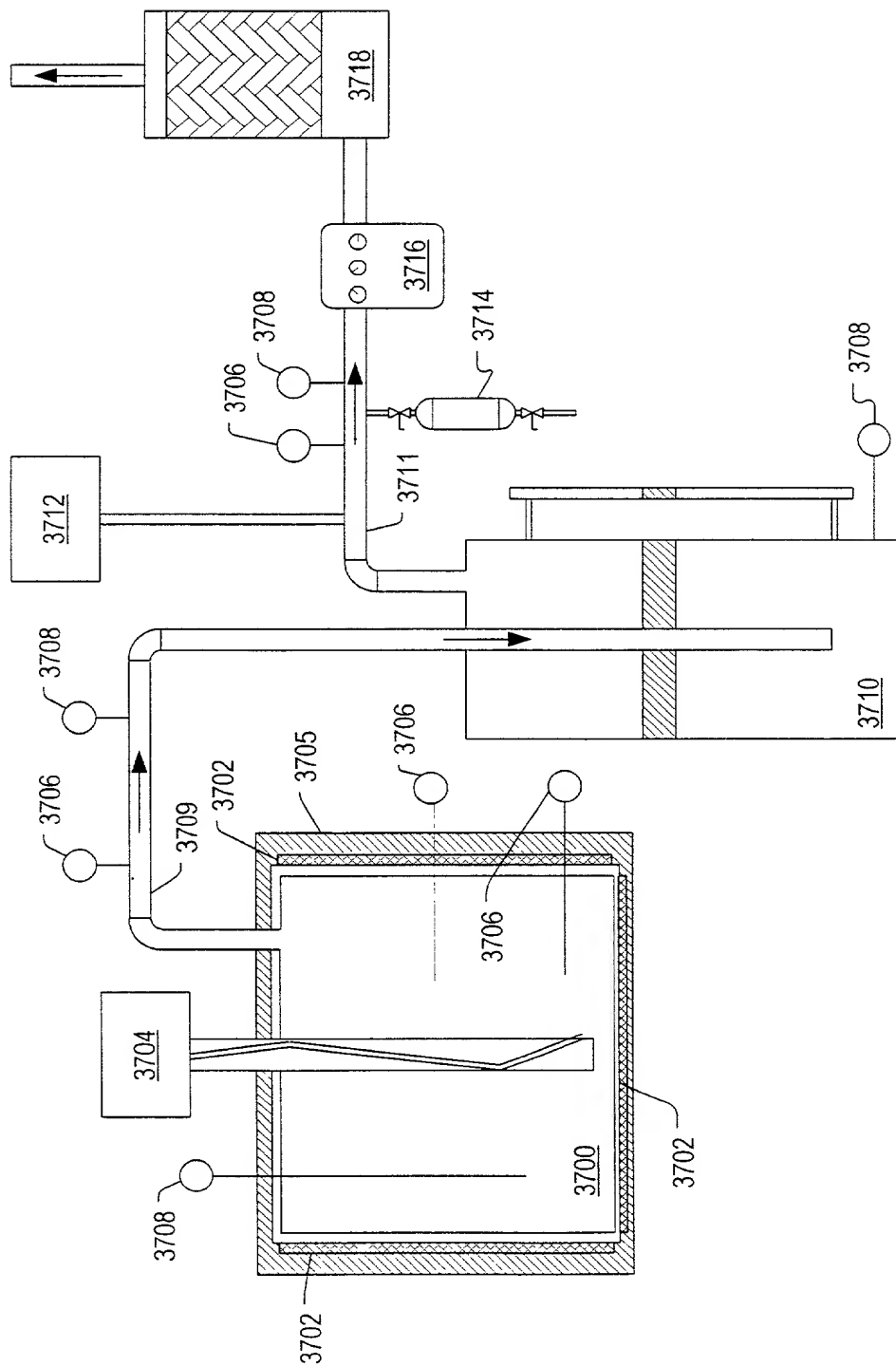


FIG. 129



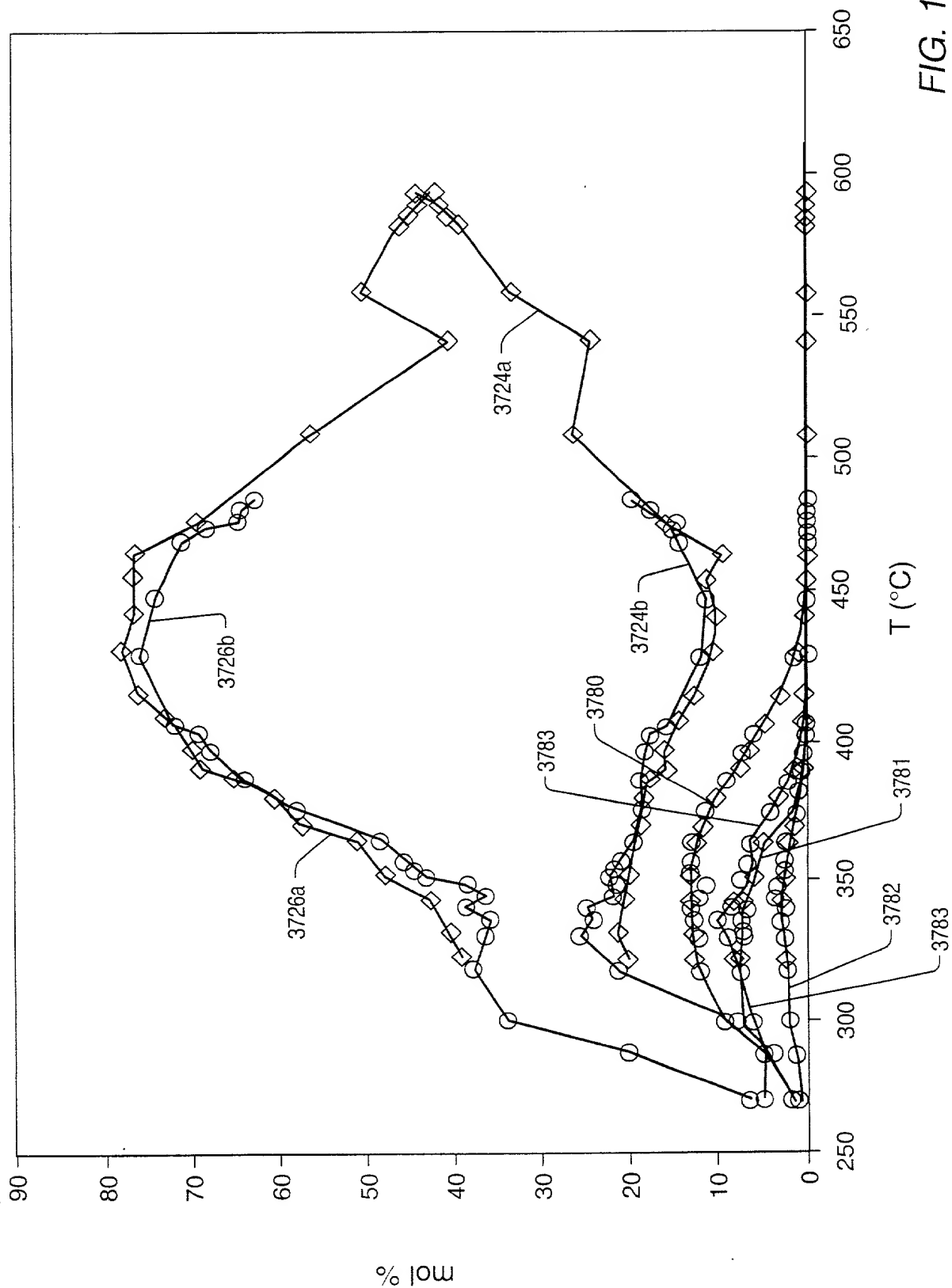


FIG. 131





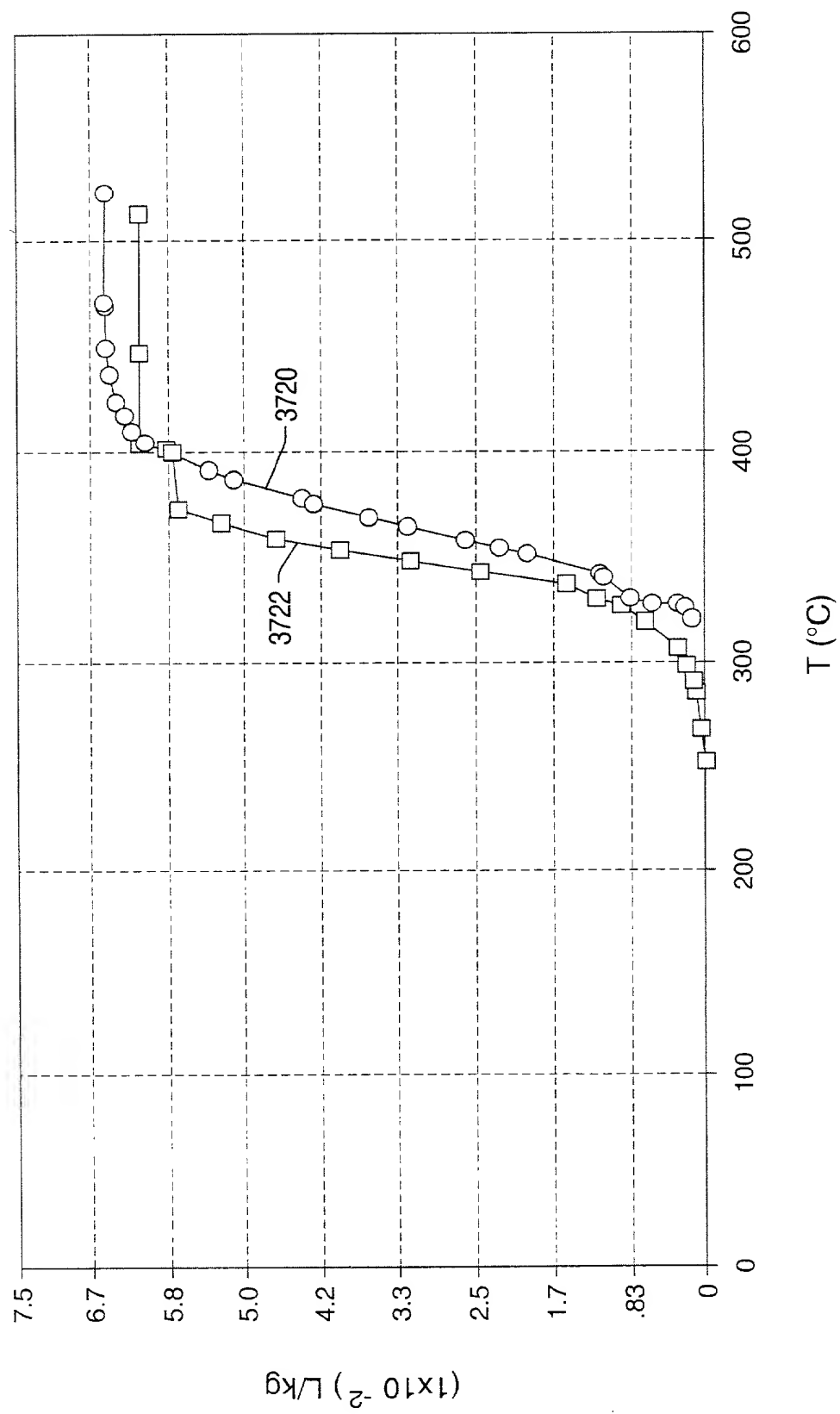


FIG. 133

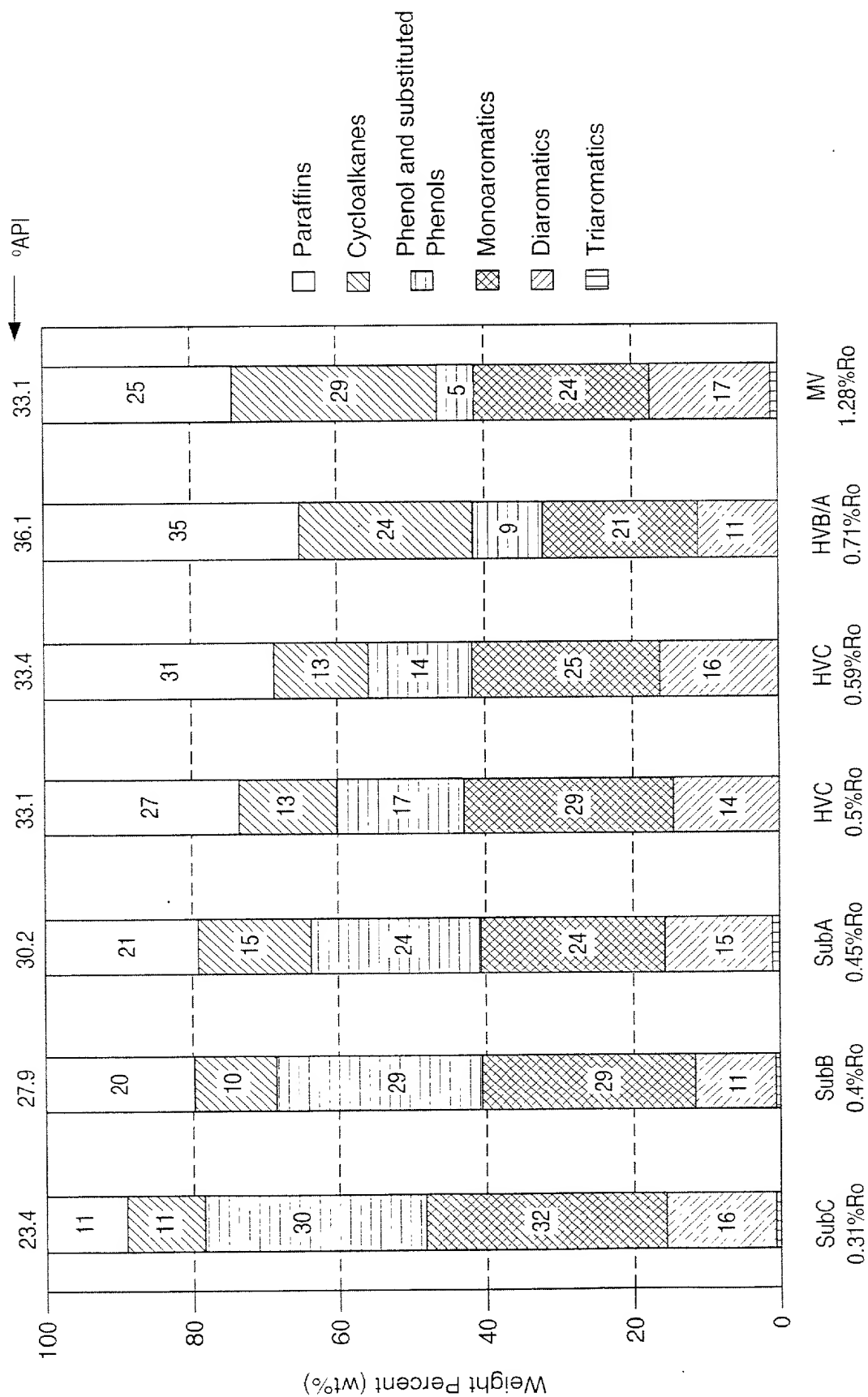


FIG. 134

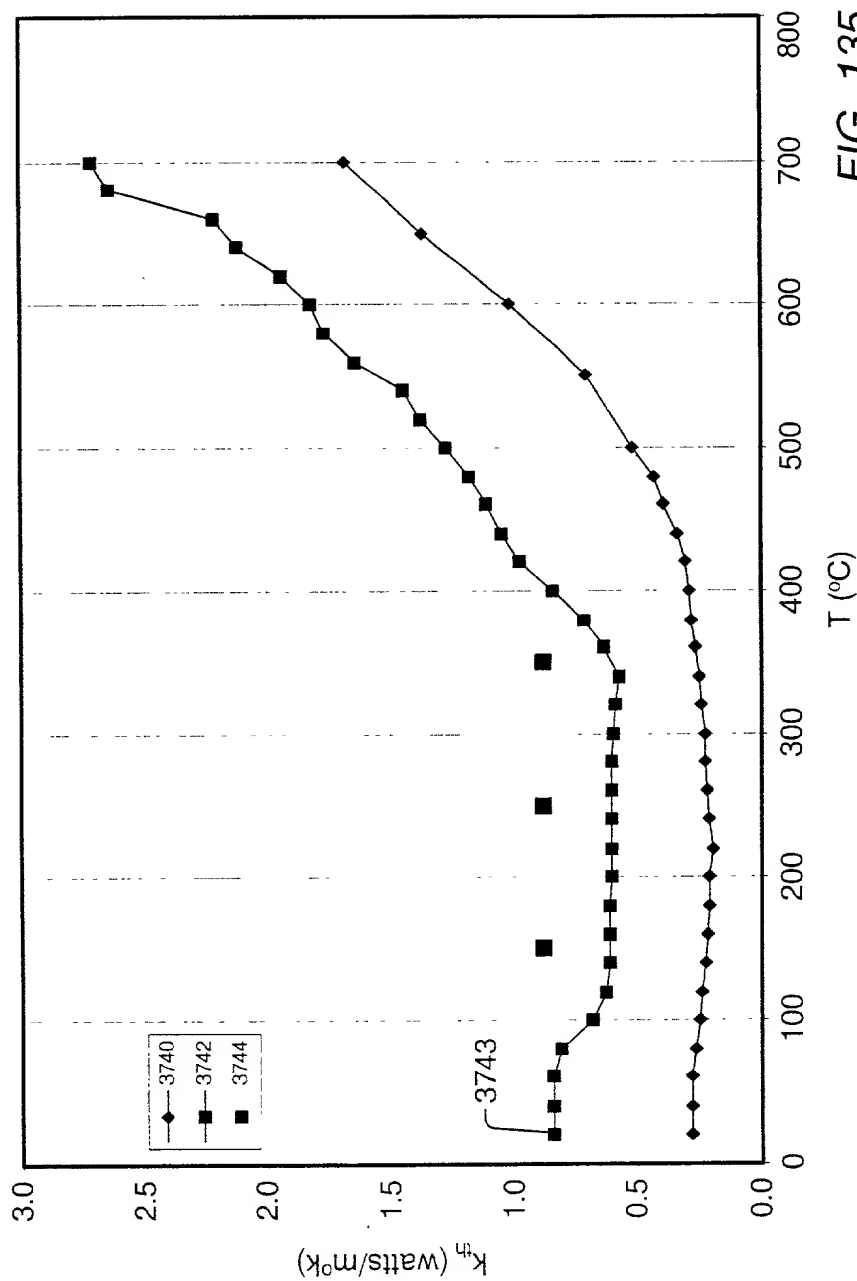


FIG. 135

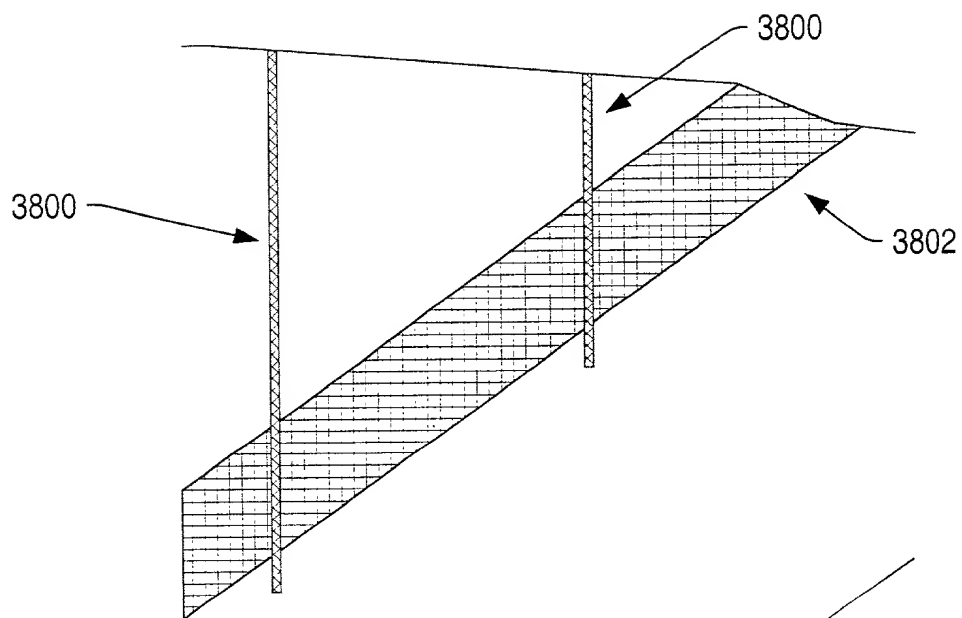


FIG. 136

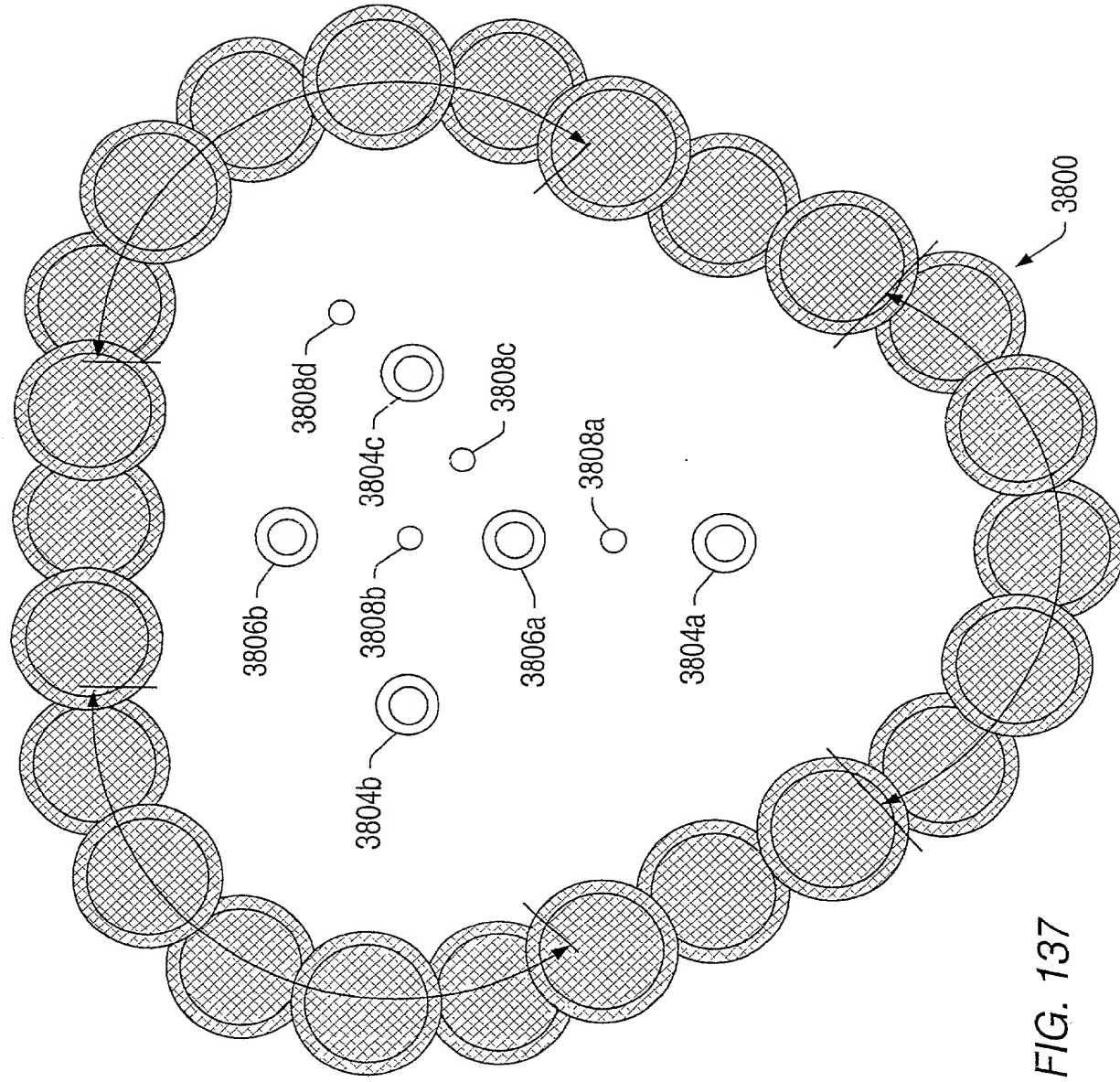
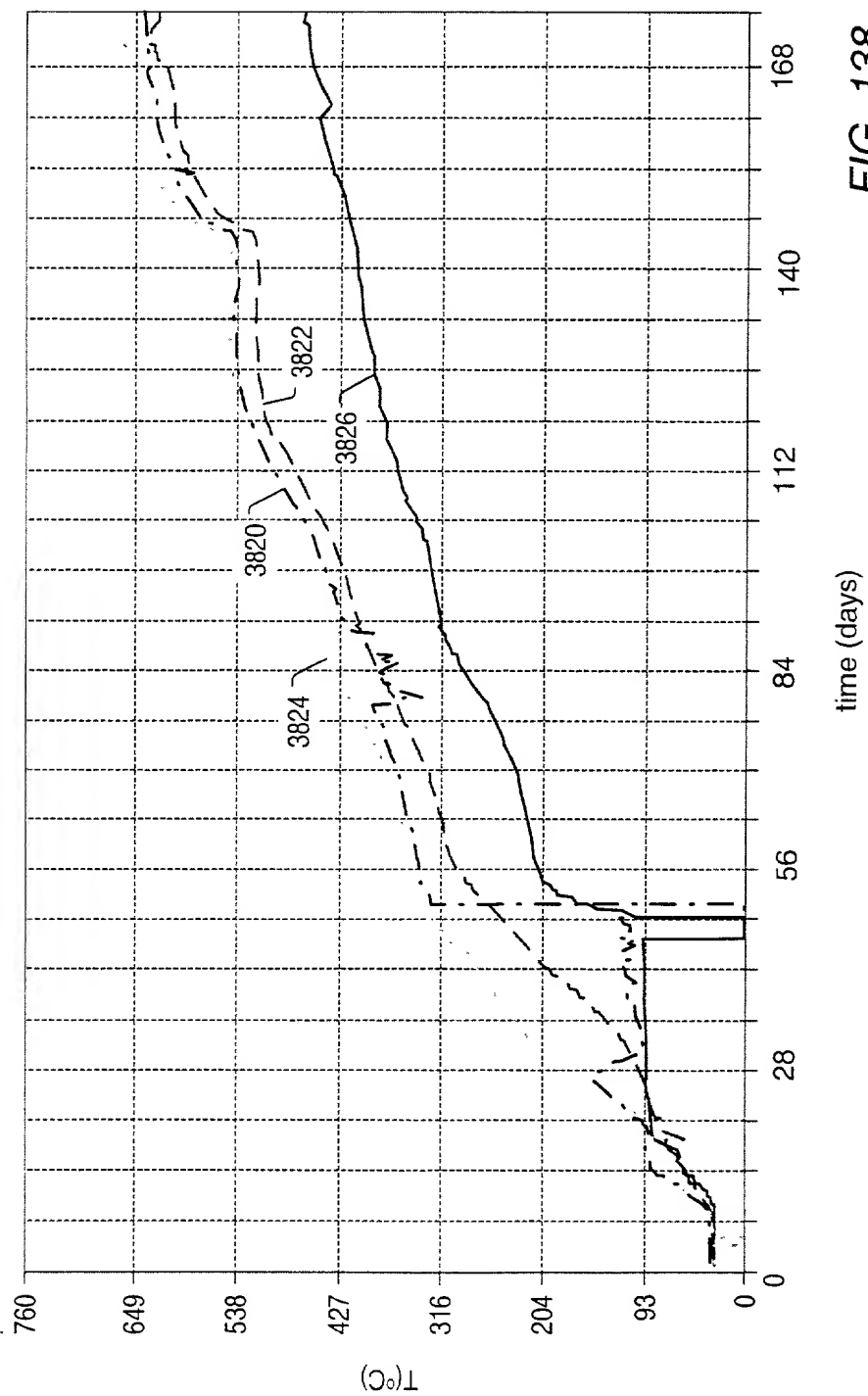


FIG. 137



Copyright © 2000 by the American Chemical Society  
Published by the American Chemical Society

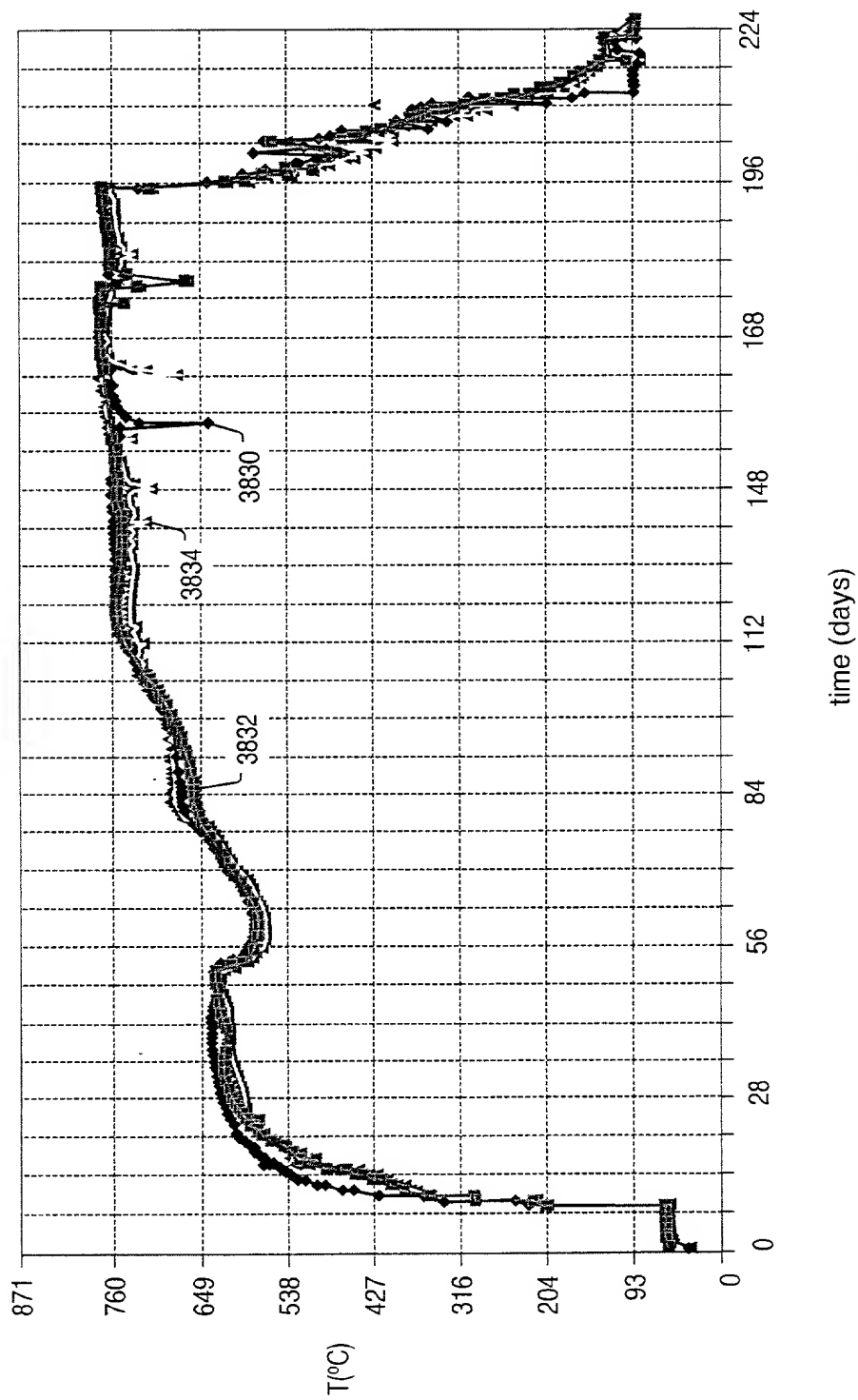


FIG. 139



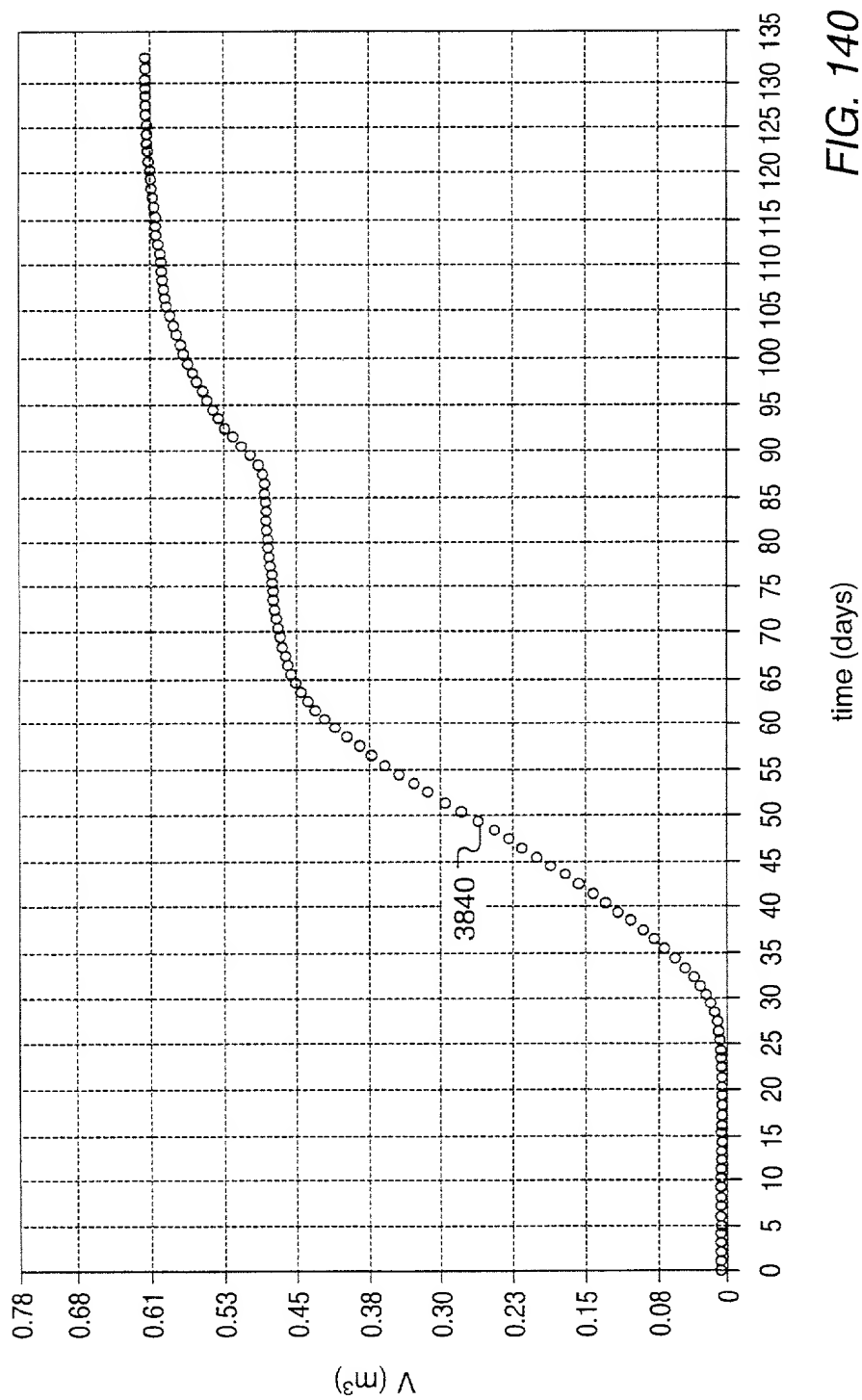




Figure 142 shows the weight percentage of carbon in the residue as a function of carbon number for the two samples. The heating rate was 10°C/day.

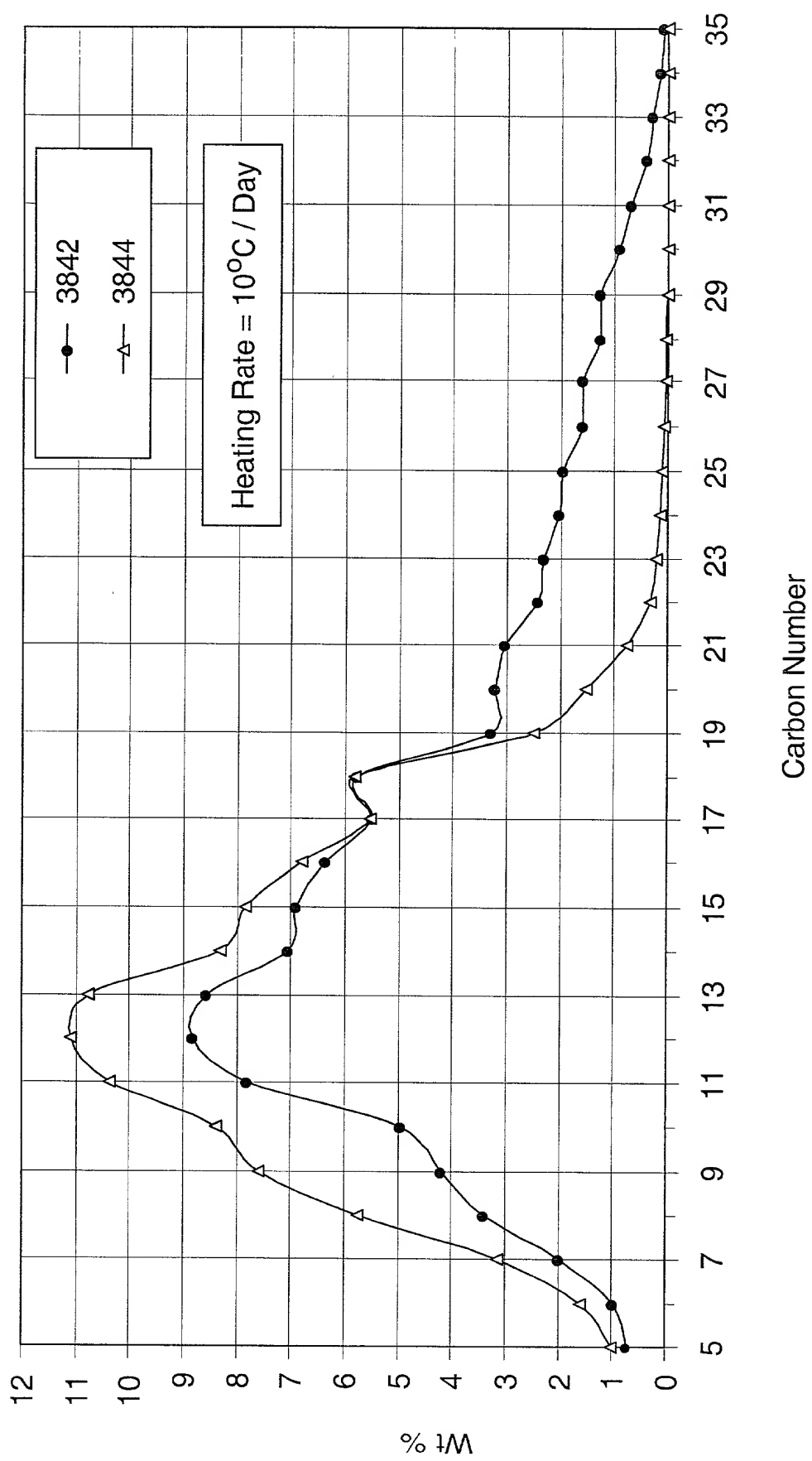


FIG. 142

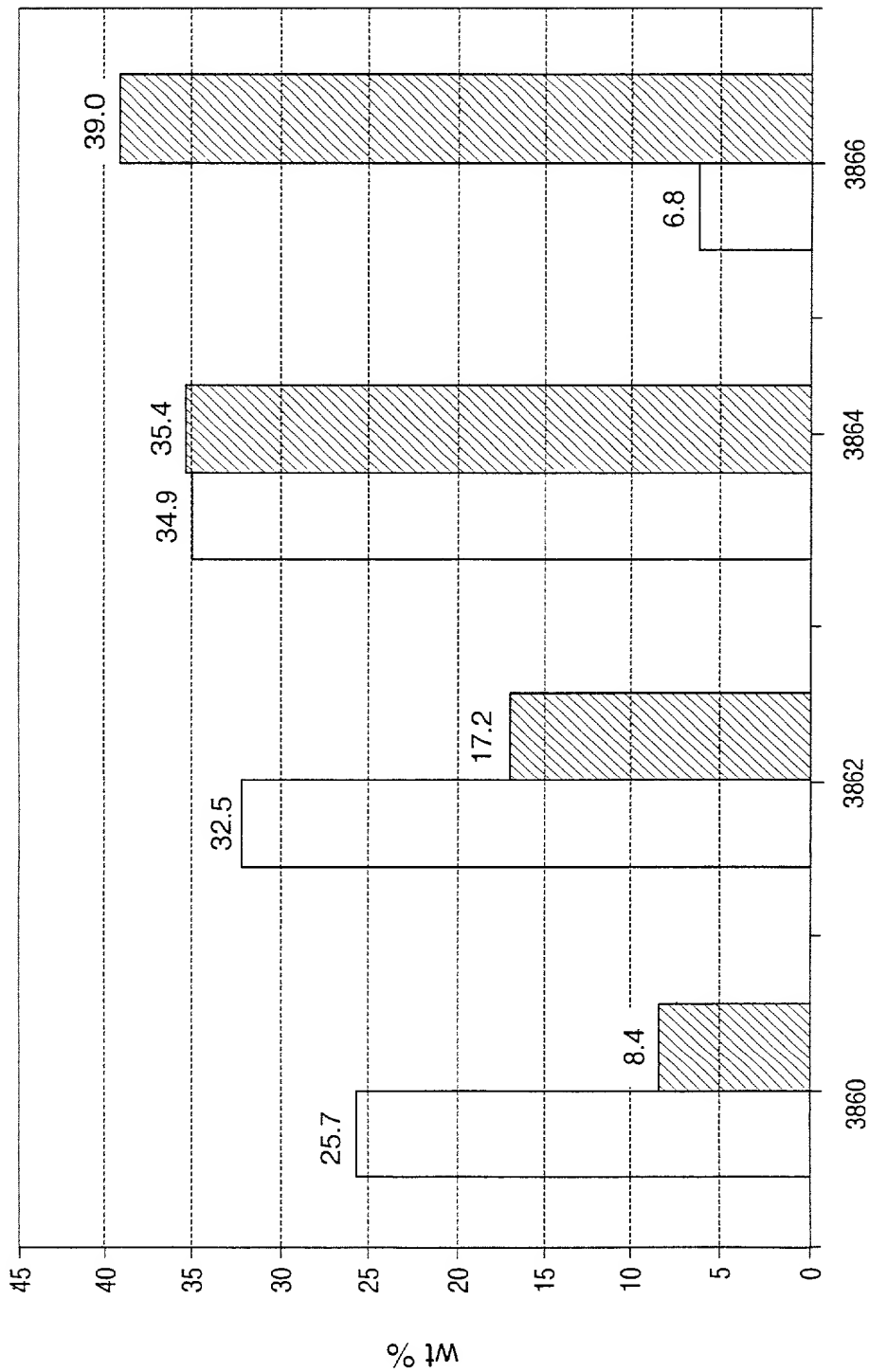


FIG. 143

Figure 144 is a graph showing the Ethene/Ethane Ratio versus the Heating Rate in °C/day. The graph shows a sharp increase in the Ethene/Ethane Ratio as the Heating Rate increases, particularly above 1000 °C/day.

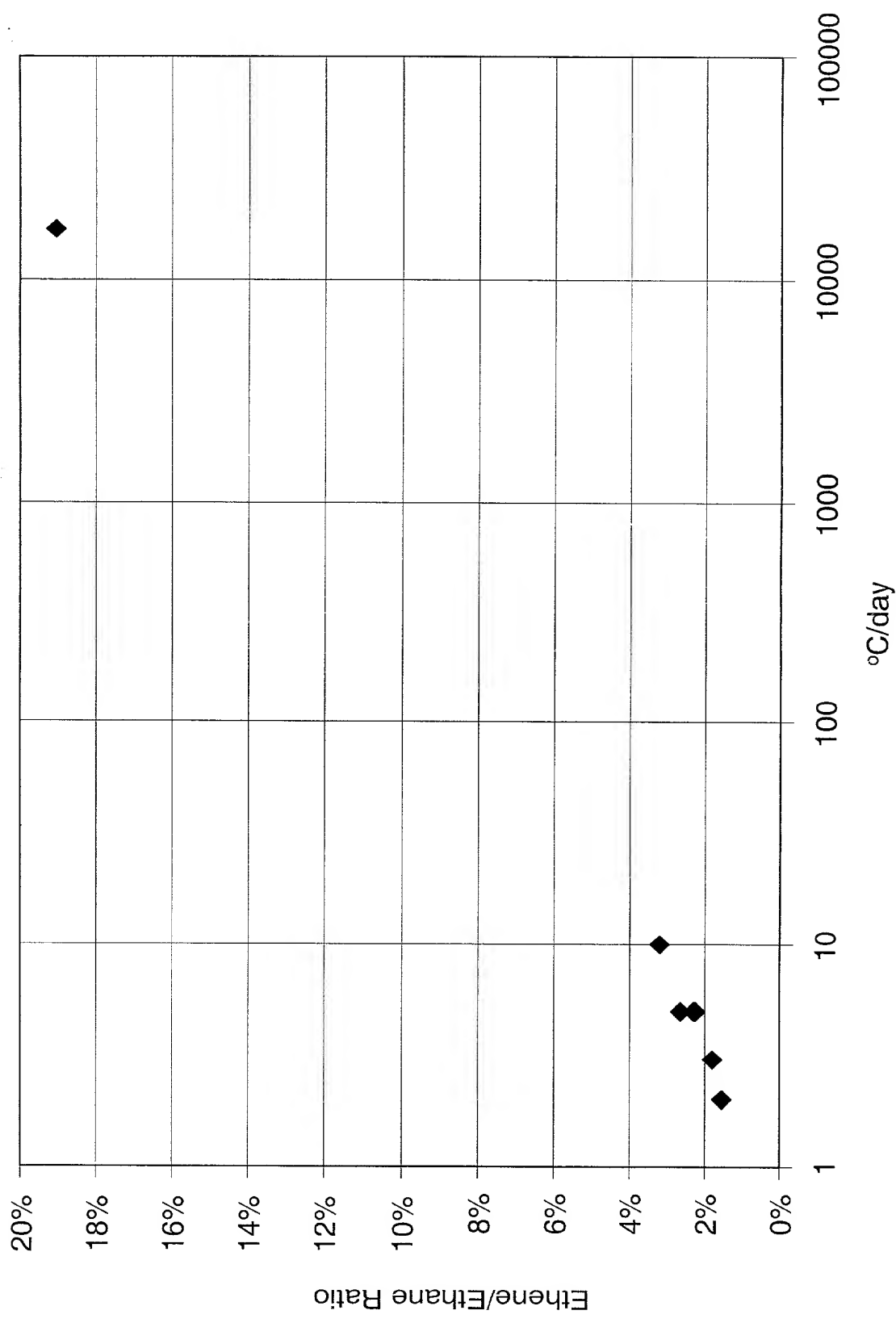


FIG. 144

Copyright © 2000 by American Petroleum Institute

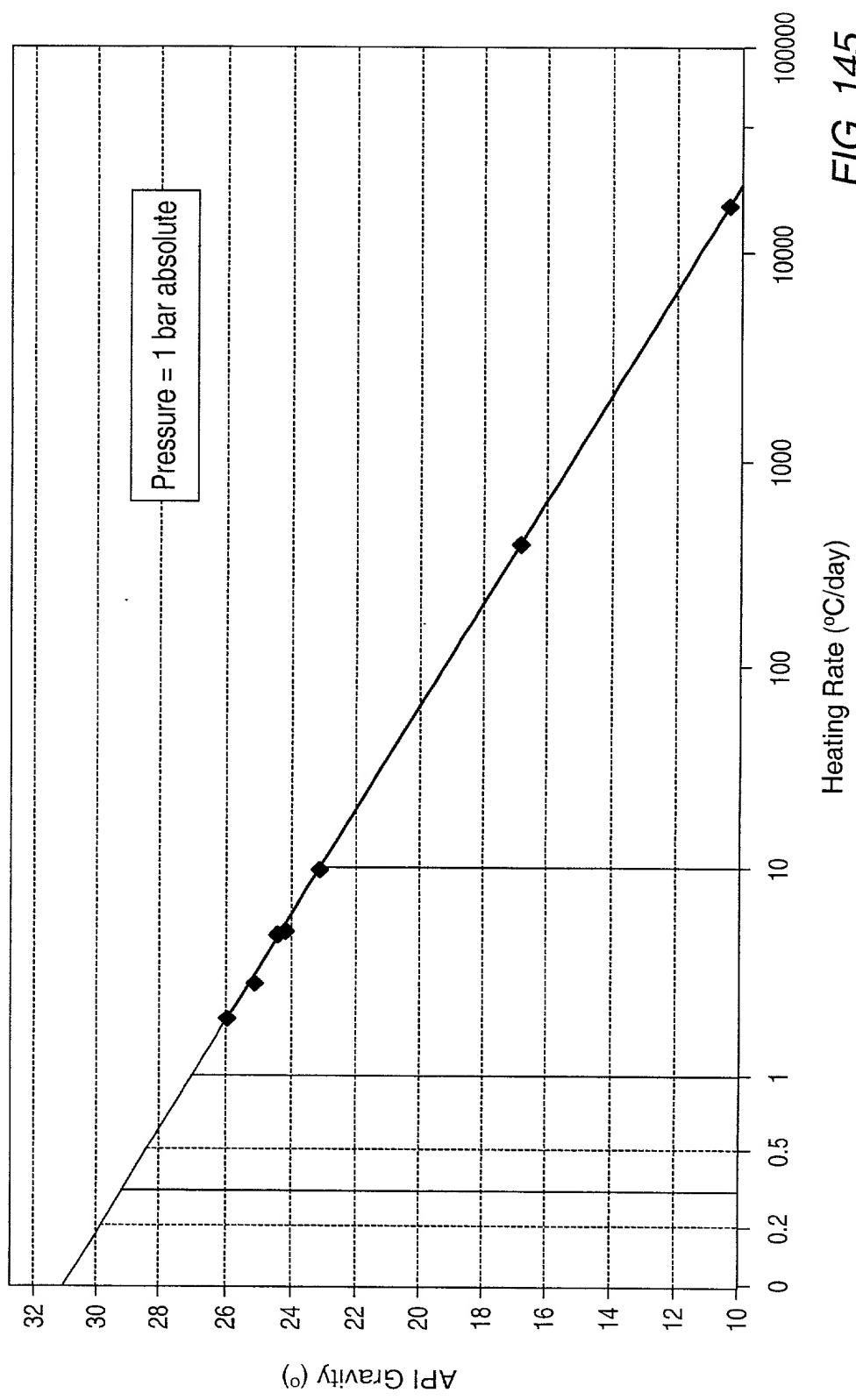


FIG. 145

Figure 146 shows the weight percentage of the various components in the various samples. The weight percentage of the various components is plotted against the sample number. The weight percentage of the various components is plotted against the sample number.

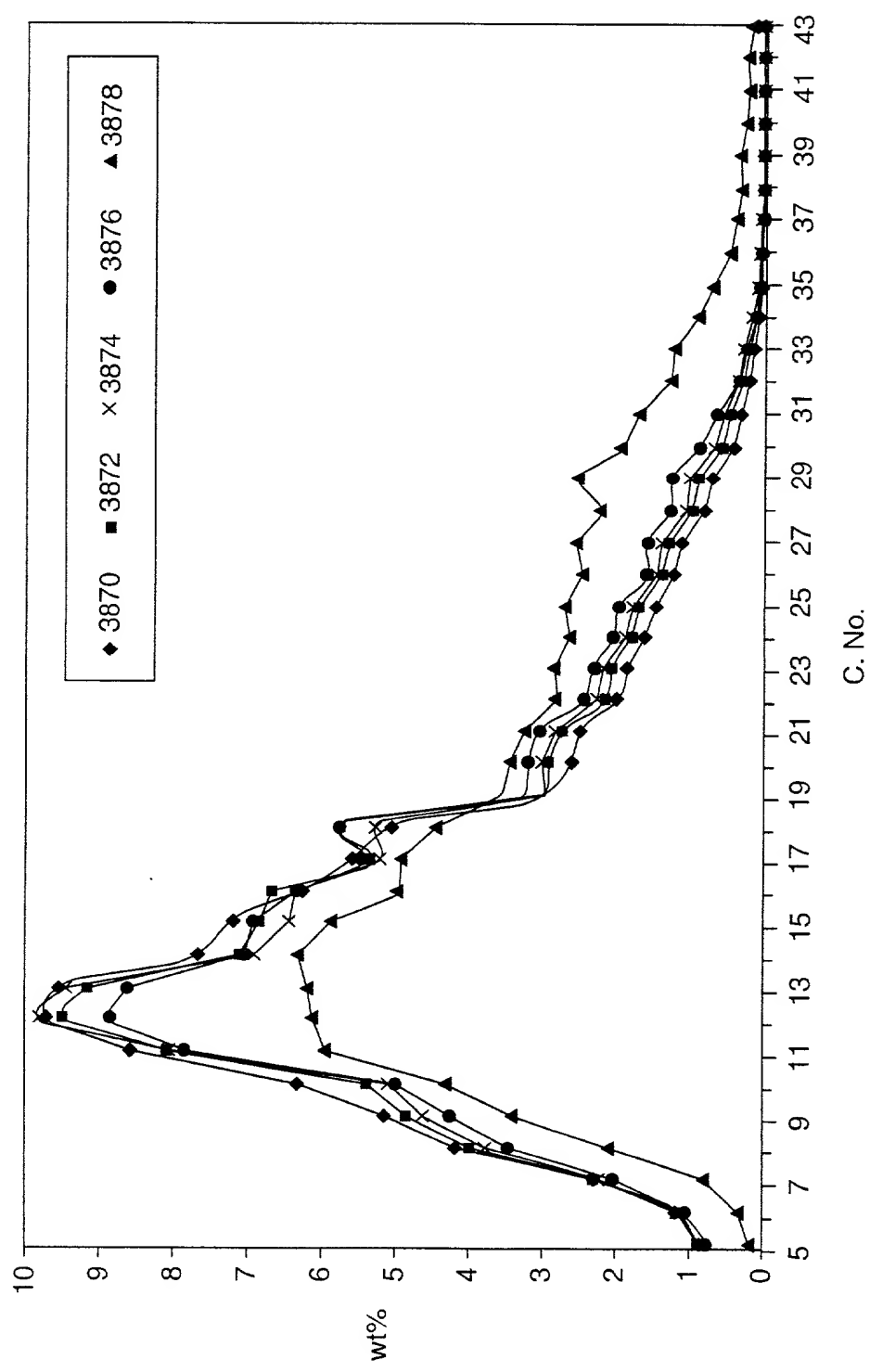


FIG. 146

Figure 147 is a graph showing the variation of the concentration of  $\text{CO}_2$  in the gas phase,  $C_{\text{CO}_2}$ , as a function of time,  $t$ , for the reaction of  $\text{CaCO}_3$  with  $\text{HCl}$  in a closed system. The concentration of  $\text{CO}_2$  is plotted on the y-axis (ranging from 20 to 40) and time is plotted on the x-axis (ranging from 0 to 140 minutes). The data points are represented by open diamonds. The curve shows a rapid initial increase in  $\text{CO}_2$  concentration, reaching a maximum of approximately 35% at about 20 minutes, followed by a gradual decrease to about 28% at 140 minutes. The curve is labeled with 3904, 3902, and 3900.

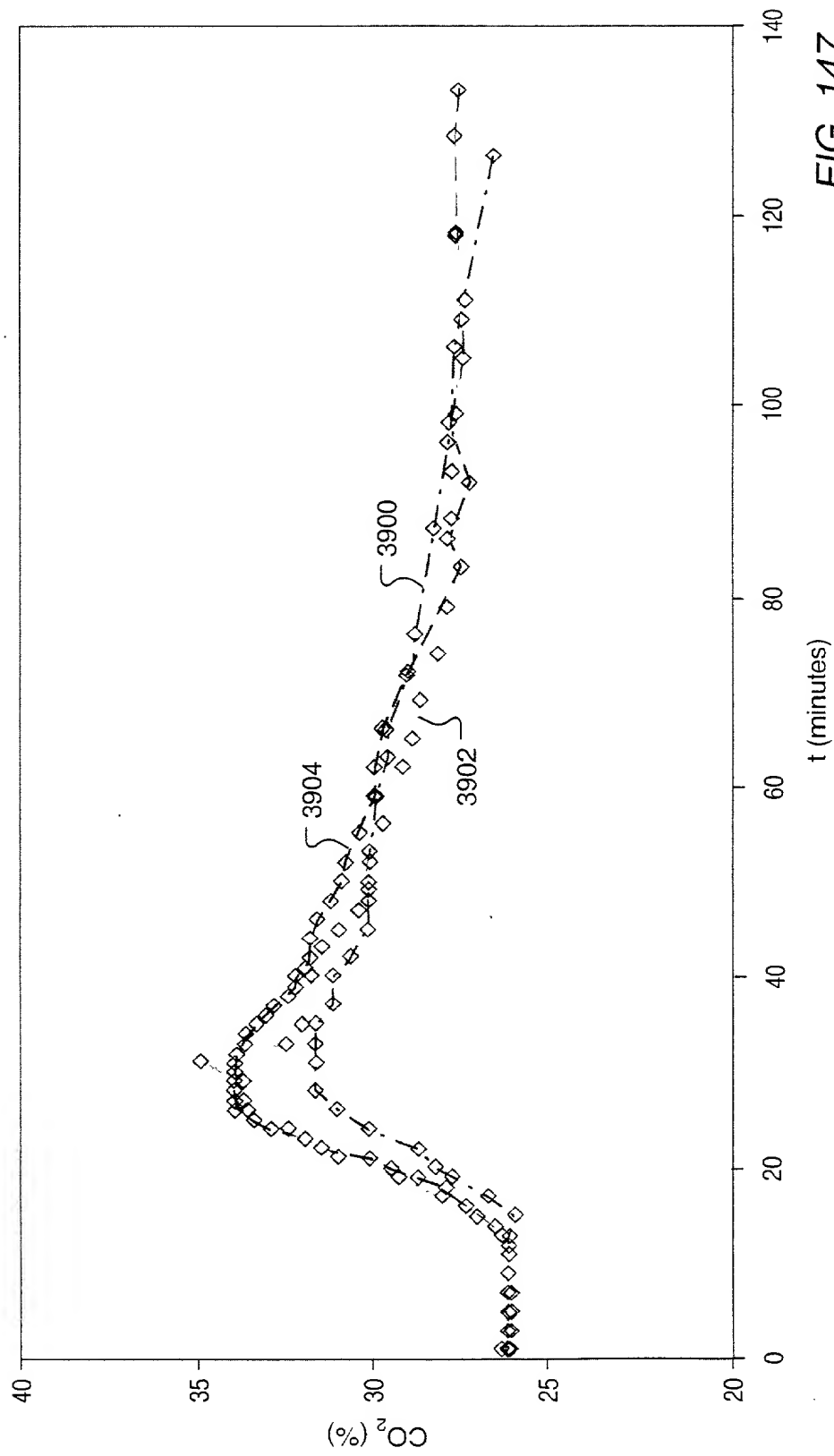


FIG. 147



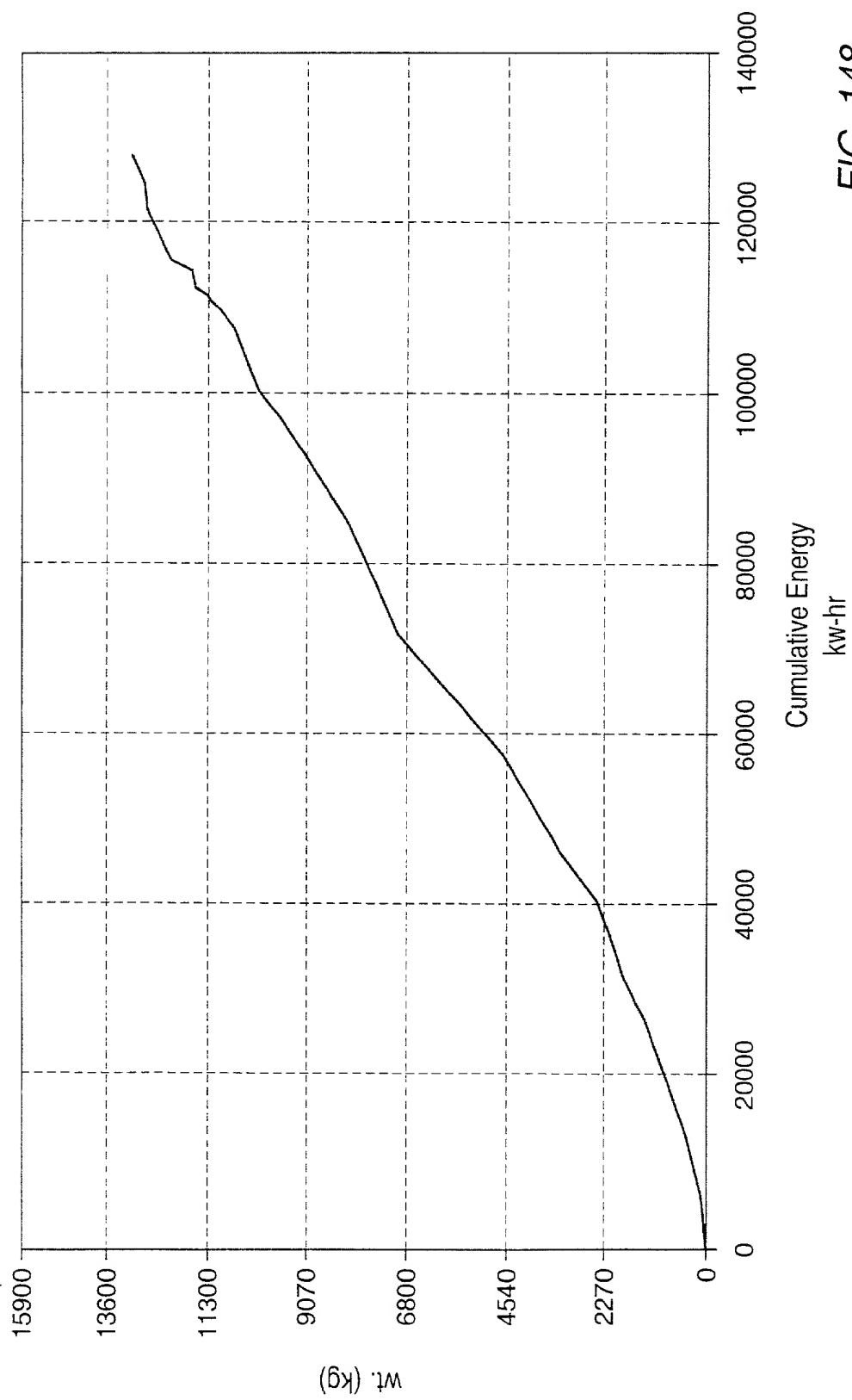


FIG. 148

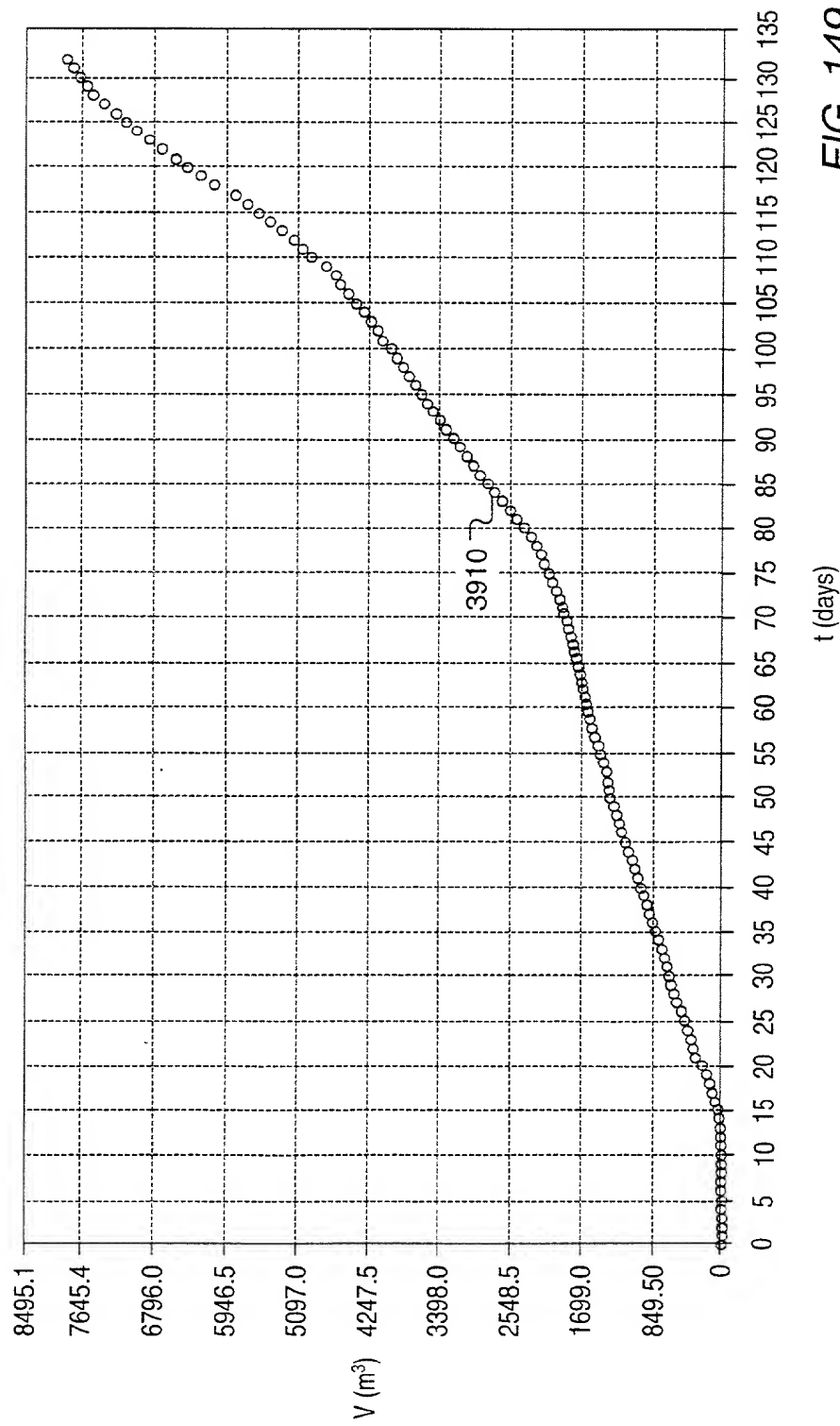


FIG. 149

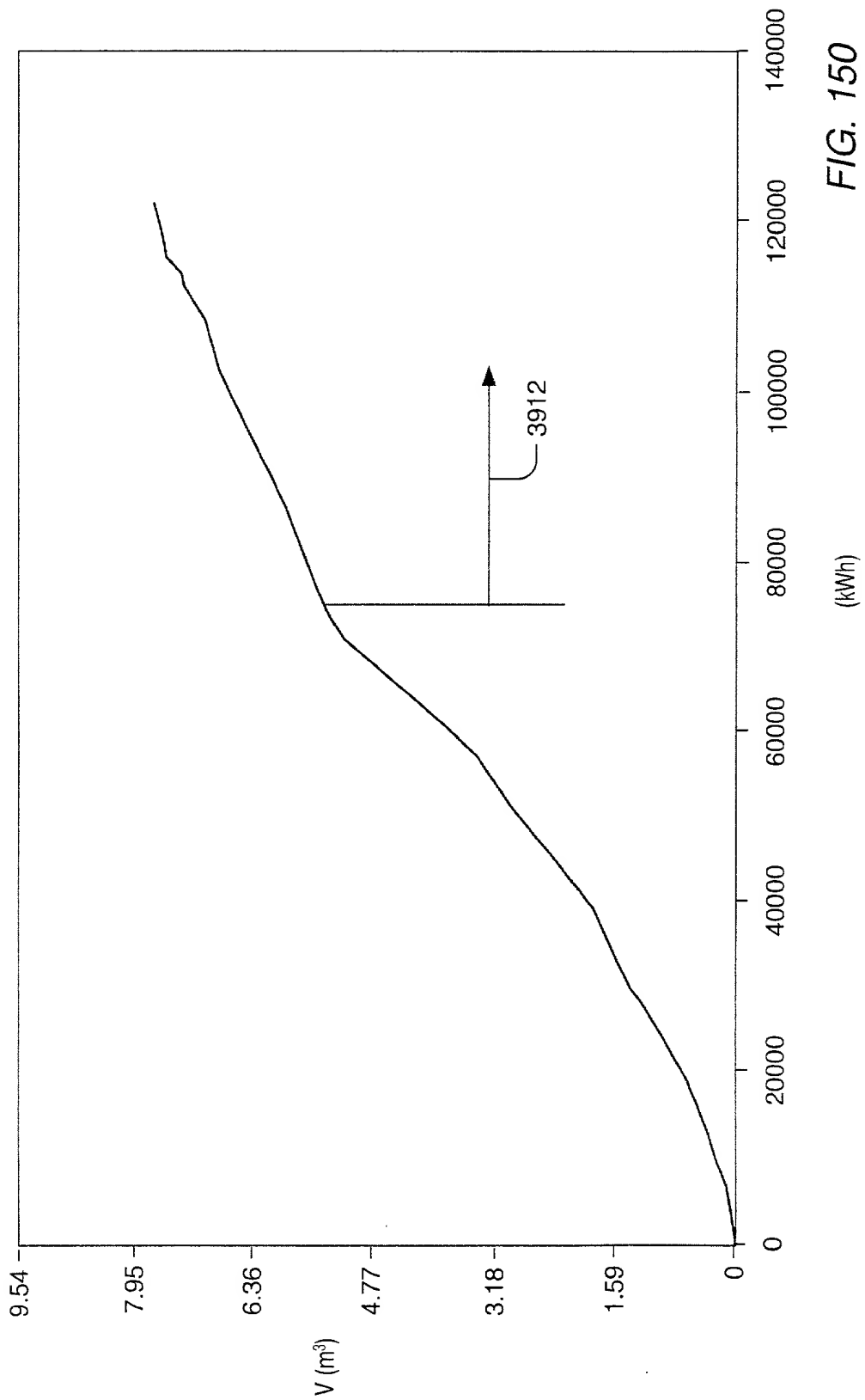


FIG. 150

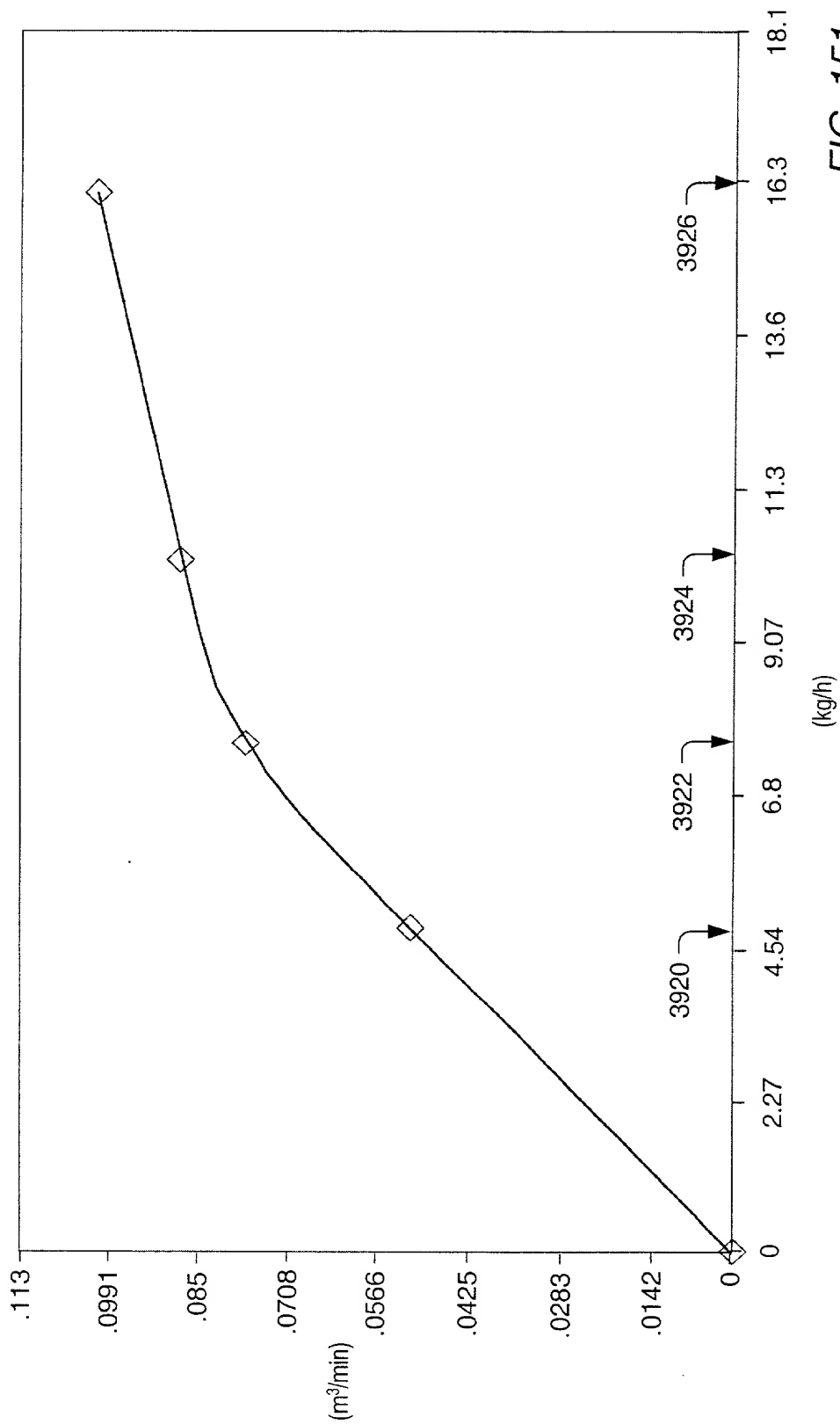
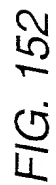


FIG. 151



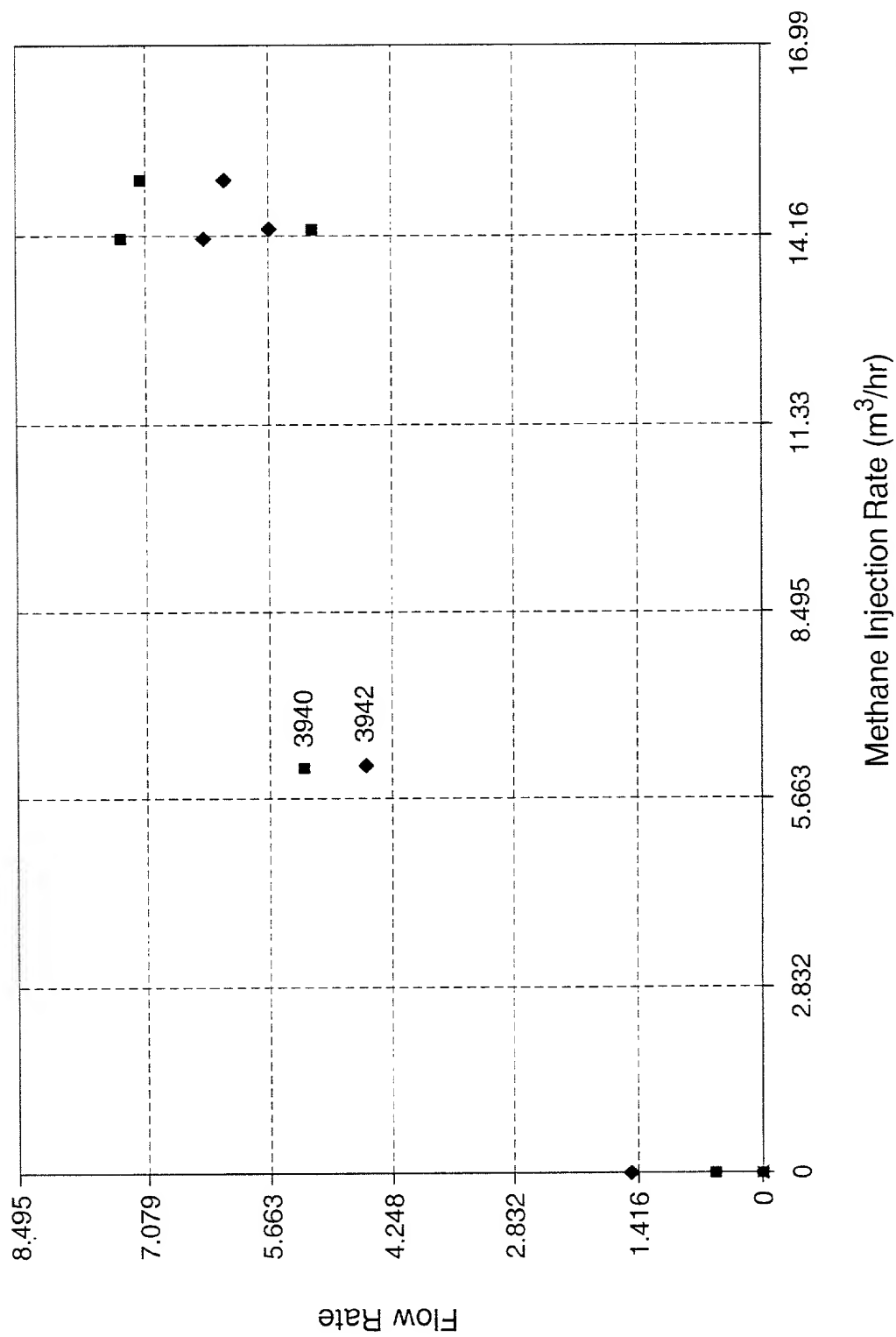


FIG. 153

$\frac{Q_{\text{gas}}}{Q_{\text{total}}} = \frac{Q_{\text{gas}}}{Q_{\text{gas}} + Q_{\text{liquid}}} = \frac{Q_{\text{gas}}}{Q_{\text{total}}}$

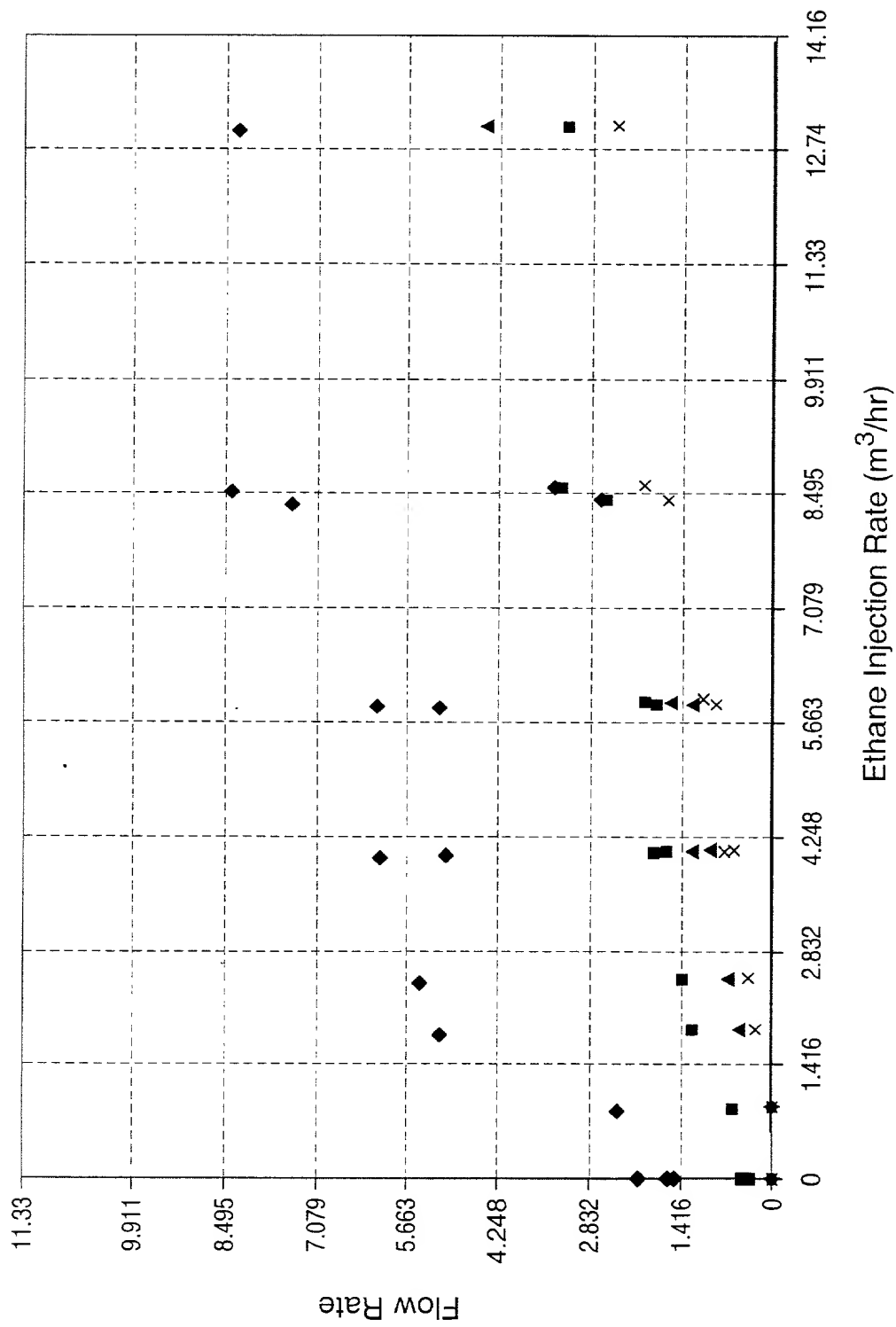
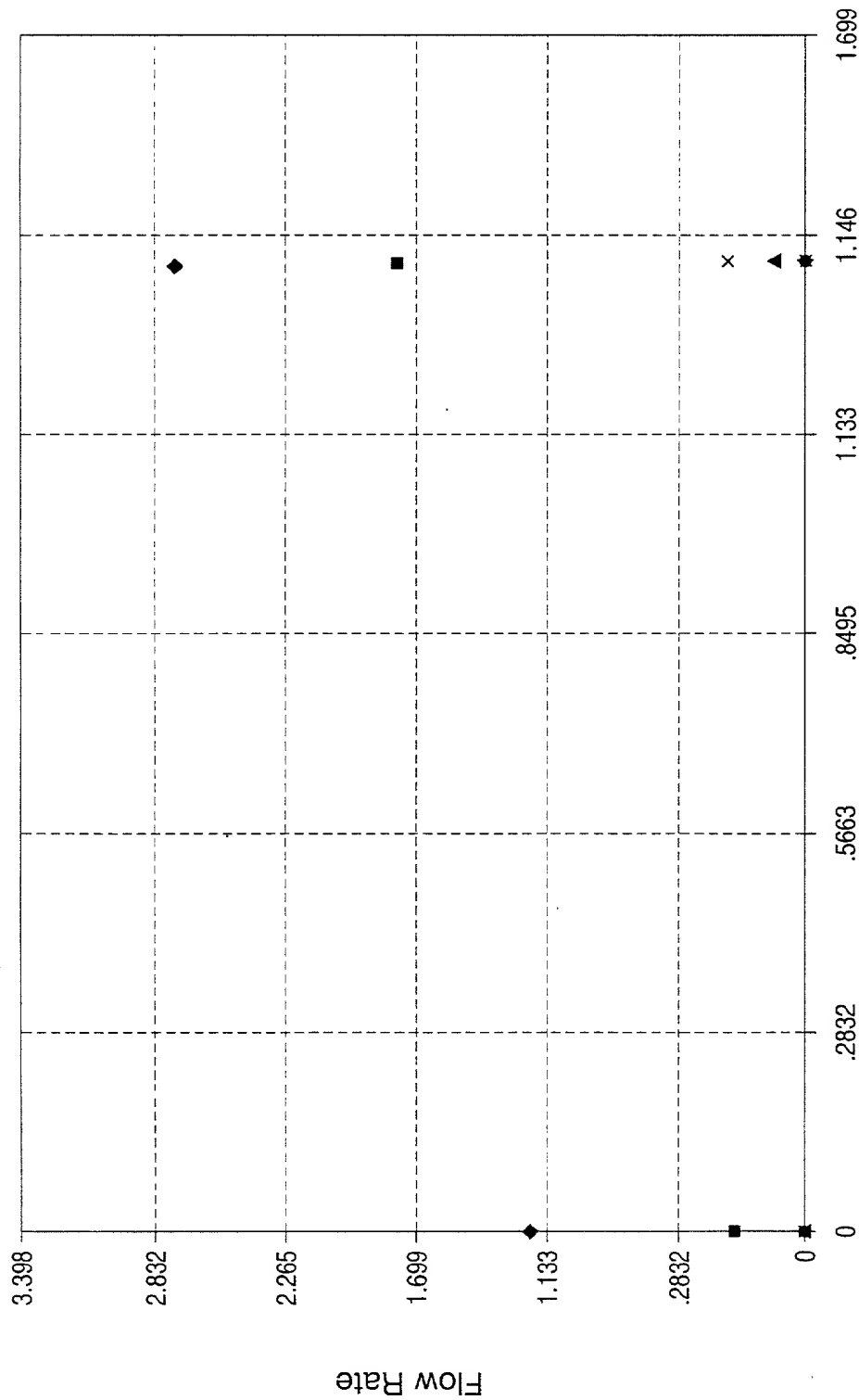


FIG. 154







Butane Injection Rate (m³/hr)

■ 3970 ▲ 3972 ◆ 3974 × 3976 \* 3978 ● 3979

FIG. 156

Figure 157 is a line graph showing the mole percentage of various components over time (t in days). The y-axis represents Mole % (0 to 90) and the x-axis represents t (days) (0 to 300). The graph displays several peaks labeled with their corresponding mole percentages: 3980, 3982, 3984, 3986, and 3988.

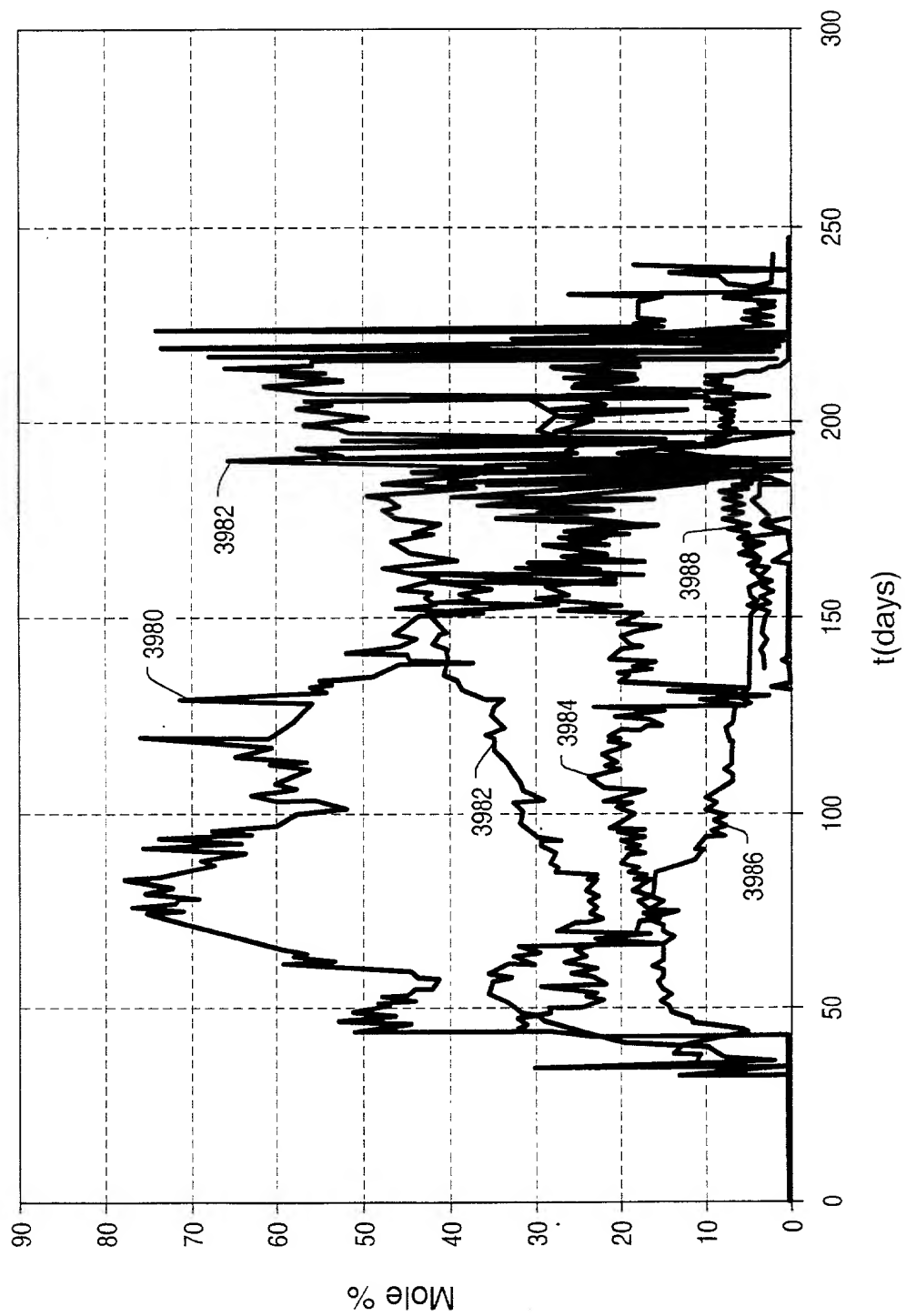


FIG. 157

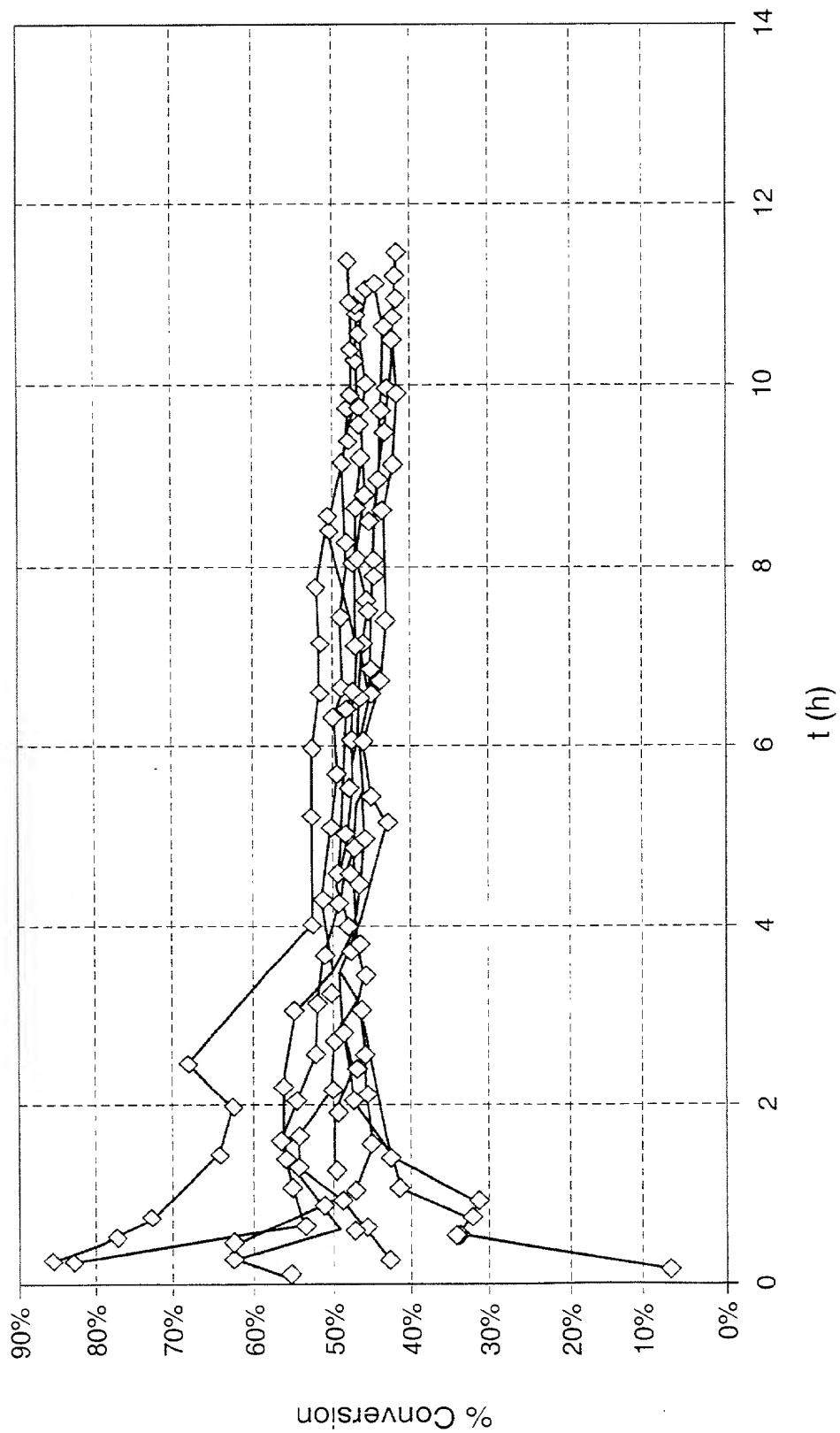


FIG. 158

Figure 159 shows the variation of the dry mole fraction of the gas phase with temperature for the system  $\text{H}_2\text{O}-\text{H}_2\text{SO}_4$  at 100 mm Hg. The curves are labeled 4000, 4002, and 4004.

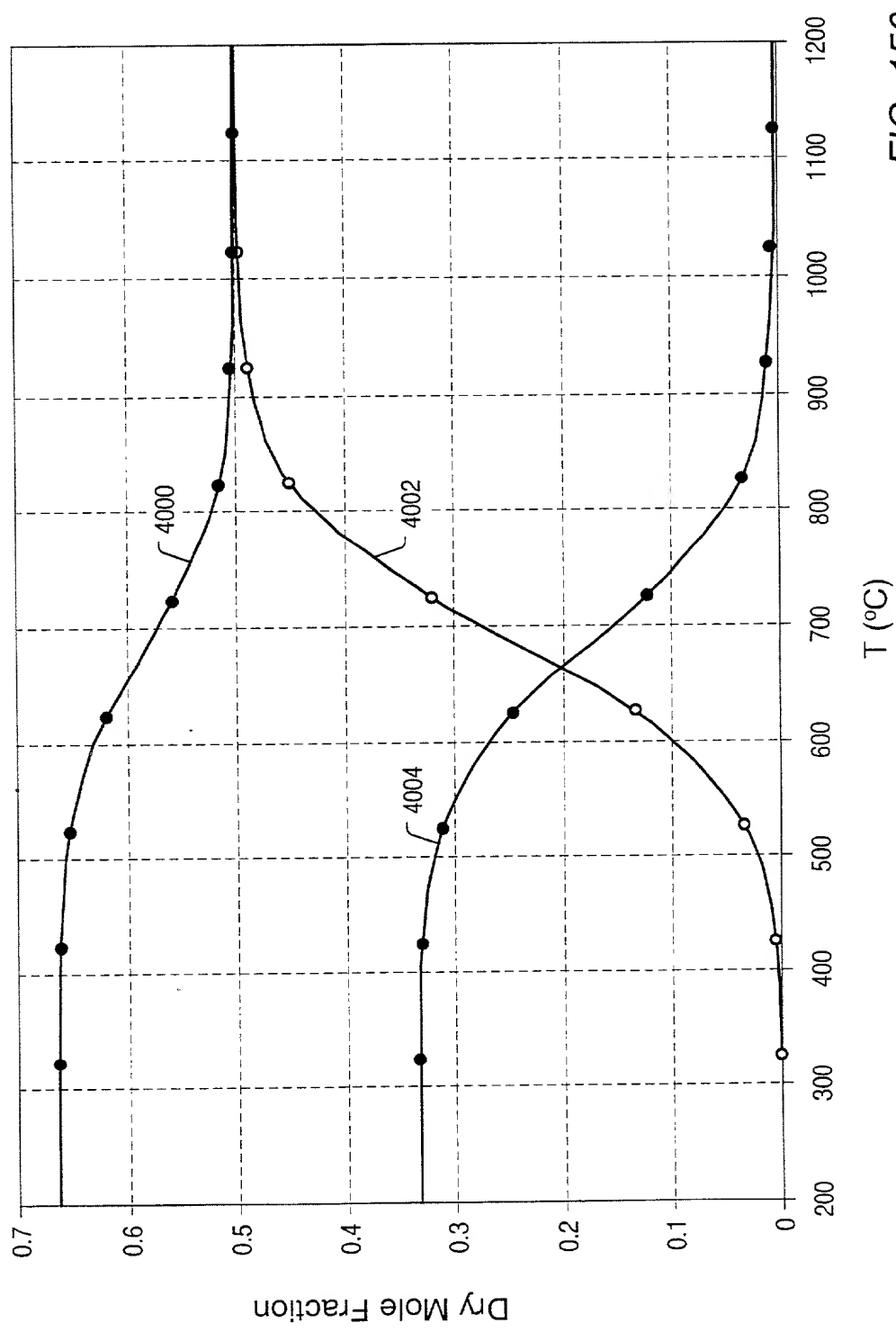


FIG. 159

4006, 4008, 4010, 4012, 4014, 4016, 4018, 4020, 4022, 4024, 4026, 4028, 4030, 4032, 4034, 4036, 4038, 4040, 4042, 4044, 4046, 4048, 4050, 4052, 4054, 4056, 4058, 4060, 4062, 4064, 4066, 4068, 4070, 4072, 4074, 4076, 4078, 4080, 4082, 4084, 4086, 4088, 4090, 4092, 4094, 4096, 4098, 4100, 4102, 4104, 4106, 4108, 4110, 4112, 4114, 4116, 4118, 4120, 4122, 4124, 4126, 4128, 4130, 4132, 4134, 4136, 4138, 4140, 4142, 4144, 4146, 4148, 4150, 4152, 4154, 4156, 4158, 4160, 4162, 4164, 4166, 4168, 4170, 4172, 4174, 4176, 4178, 4180, 4182, 4184, 4186, 4188, 4190, 4192, 4194, 4196, 4198, 4200, 4202, 4204, 4206, 4208, 4210, 4212, 4214, 4216, 4218, 4220, 4222, 4224, 4226, 4228, 4230, 4232, 4234, 4236, 4238, 4240, 4242, 4244, 4246, 4248, 4250, 4252, 4254, 4256, 4258, 4260, 4262, 4264, 4266, 4268, 4270, 4272, 4274, 4276, 4278, 4280, 4282, 4284, 4286, 4288, 4290, 4292, 4294, 4296, 4298, 4300, 4302, 4304, 4306, 4308, 4310, 4312, 4314, 4316, 4318, 4320, 4322, 4324, 4326, 4328, 4330, 4332, 4334, 4336, 4338, 4340, 4342, 4344, 4346, 4348, 4350, 4352, 4354, 4356, 4358, 4360, 4362, 4364, 4366, 4368, 4370, 4372, 4374, 4376, 4378, 4380, 4382, 4384, 4386, 4388, 4390, 4392, 4394, 4396, 4398, 4400, 4402, 4404, 4406, 4408, 4410, 4412, 4414, 4416, 4418, 4420, 4422, 4424, 4426, 4428, 4430, 4432, 4434, 4436, 4438, 4440, 4442, 4444, 4446, 4448, 4450, 4452, 4454, 4456, 4458, 4460, 4462, 4464, 4466, 4468, 4470, 4472, 4474, 4476, 4478, 4480, 4482, 4484, 4486, 4488, 4490, 4492, 4494, 4496, 4498, 4500, 4502, 4504, 4506, 4508, 4510, 4512, 4514, 4516, 4518, 4520, 4522, 4524, 4526, 4528, 4530, 4532, 4534, 4536, 4538, 4540, 4542, 4544, 4546, 4548, 4550, 4552, 4554, 4556, 4558, 4560, 4562, 4564, 4566, 4568, 4570, 4572, 4574, 4576, 4578, 4580, 4582, 4584, 4586, 4588, 4590, 4592, 4594, 4596, 4598, 4600, 4602, 4604, 4606, 4608, 4610, 4612, 4614, 4616, 4618, 4620, 4622, 4624, 4626, 4628, 4630, 4632, 4634, 4636, 4638, 4640, 4642, 4644, 4646, 4648, 4650, 4652, 4654, 4656, 4658, 4660, 4662, 4664, 4666, 4668, 4670, 4672, 4674, 4676, 4678, 4680, 4682, 4684, 4686, 4688, 4690, 4692, 4694, 4696, 4698, 4700, 4702, 4704, 4706, 4708, 4710, 4712, 4714, 4716, 4718, 4720, 4722, 4724, 4726, 4728, 4730, 4732, 4734, 4736, 4738, 4740, 4742, 4744, 4746, 4748, 4750, 4752, 4754, 4756, 4758, 4760, 4762, 4764, 4766, 4768, 4770, 4772, 4774, 4776, 4778, 4780, 4782, 4784, 4786, 4788, 4790, 4792, 4794, 4796, 4798, 4800, 4802, 4804, 4806, 4808, 4810, 4812, 4814, 4816, 4818, 4820, 4822, 4824, 4826, 4828, 4830, 4832, 4834, 4836, 4838, 4840, 4842, 4844, 4846, 4848, 4850, 4852, 4854, 4856, 4858, 4860, 4862, 4864, 4866, 4868, 4870, 4872, 4874, 4876, 4878, 4880, 4882, 4884, 4886, 4888, 4890, 4892, 4894, 4896, 4898, 4900, 4902, 4904, 4906, 4908, 4910, 4912, 4914, 4916, 4918, 4920, 4922, 4924, 4926, 4928, 4930, 4932, 4934, 4936, 4938, 4940, 4942, 4944, 4946, 4948, 4950, 4952, 4954, 4956, 4958, 4960, 4962, 4964, 4966, 4968, 4970, 4972, 4974, 4976, 4978, 4980, 4982, 4984, 4986, 4988, 4990, 4992, 4994, 4996, 4998, 4999

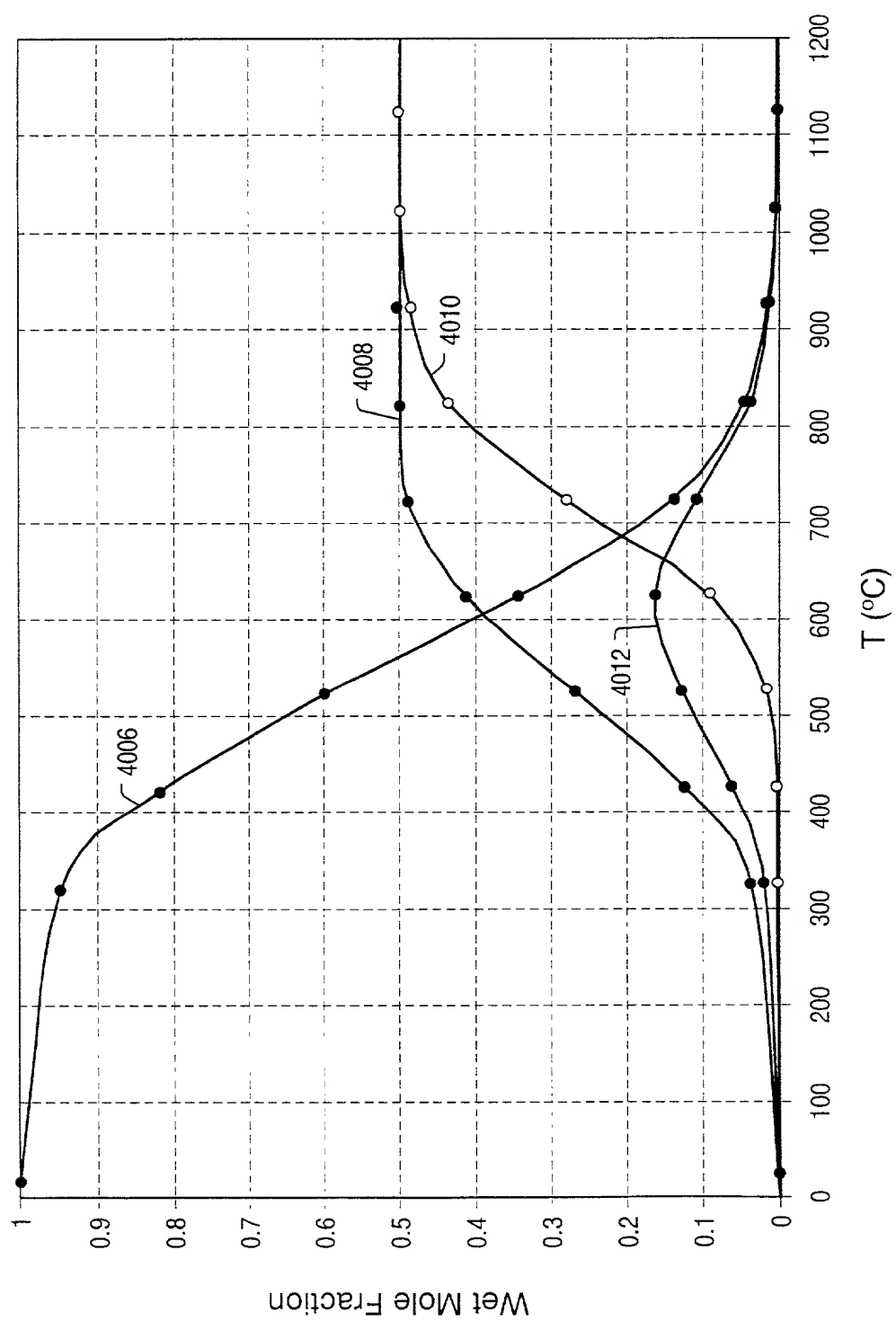


FIG. 160

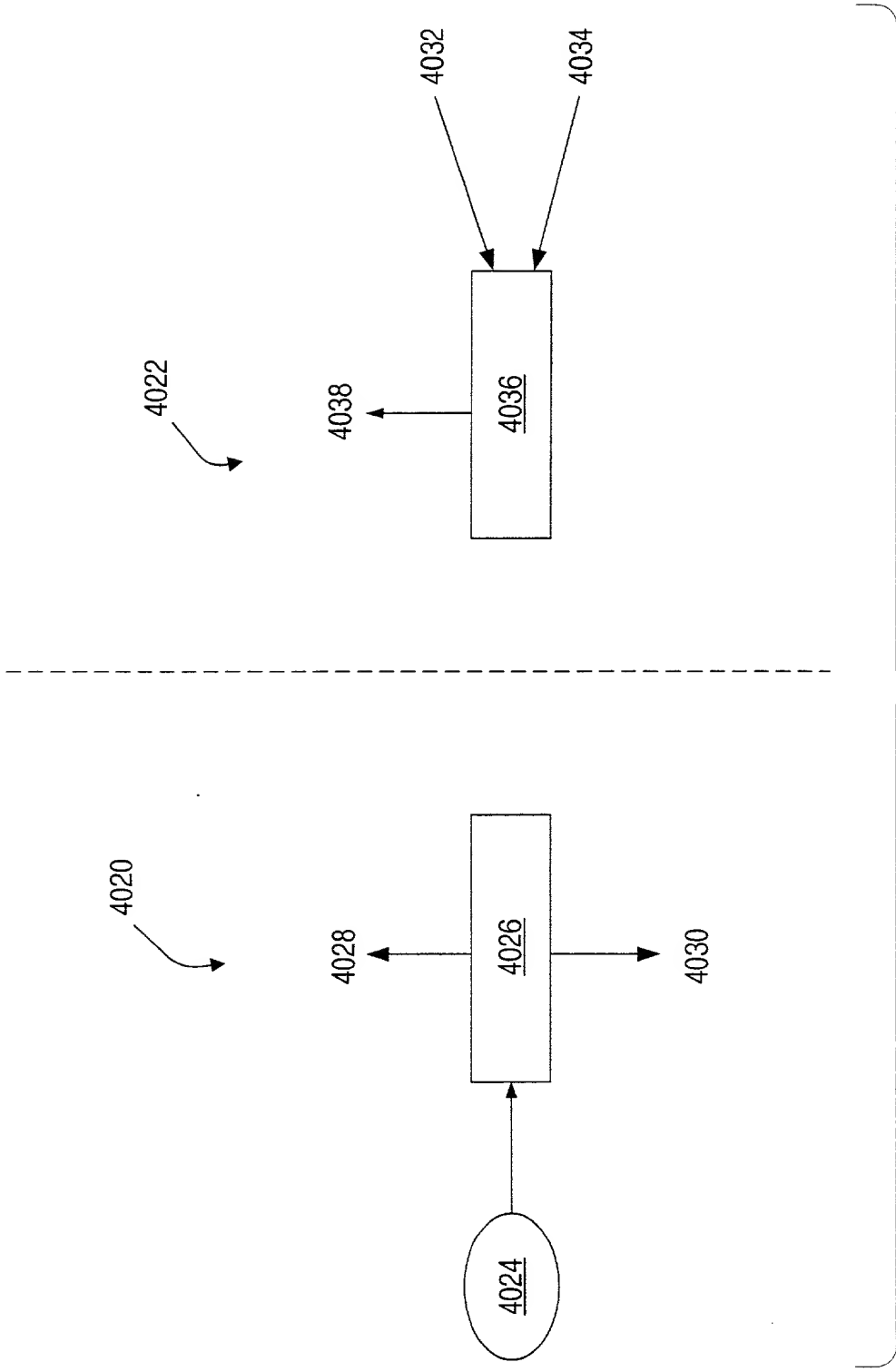


FIG. 161

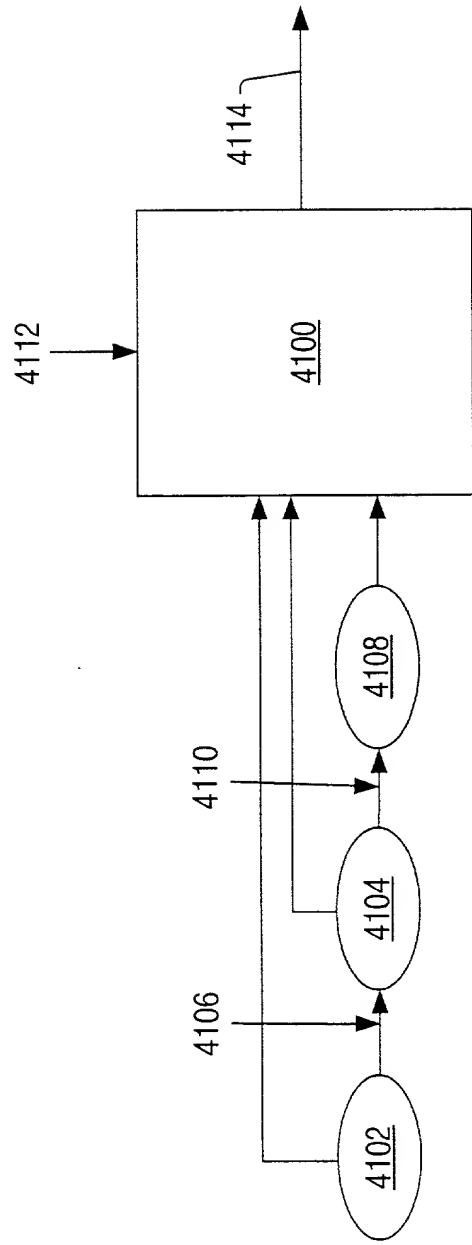


FIG. 162

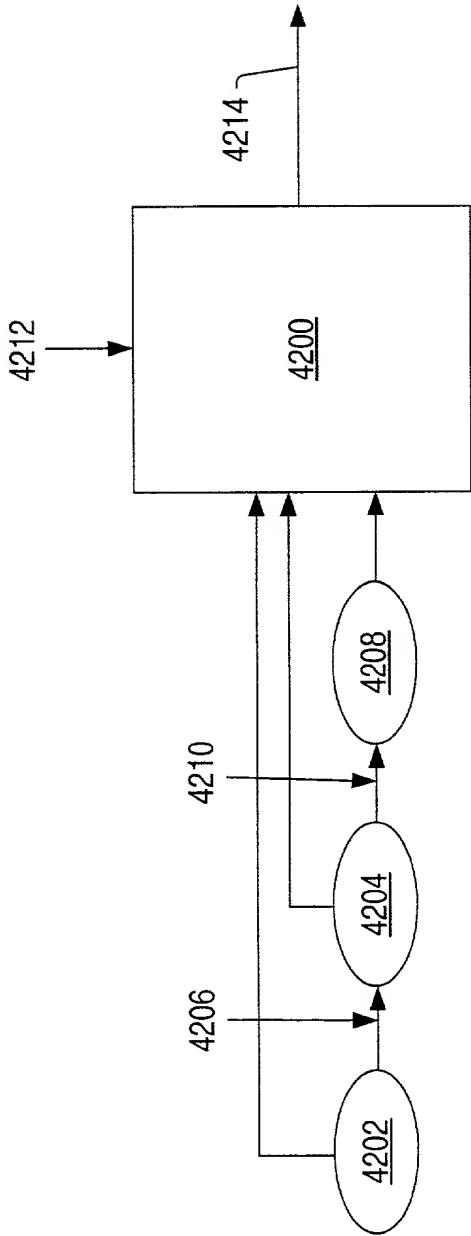


FIG. 163



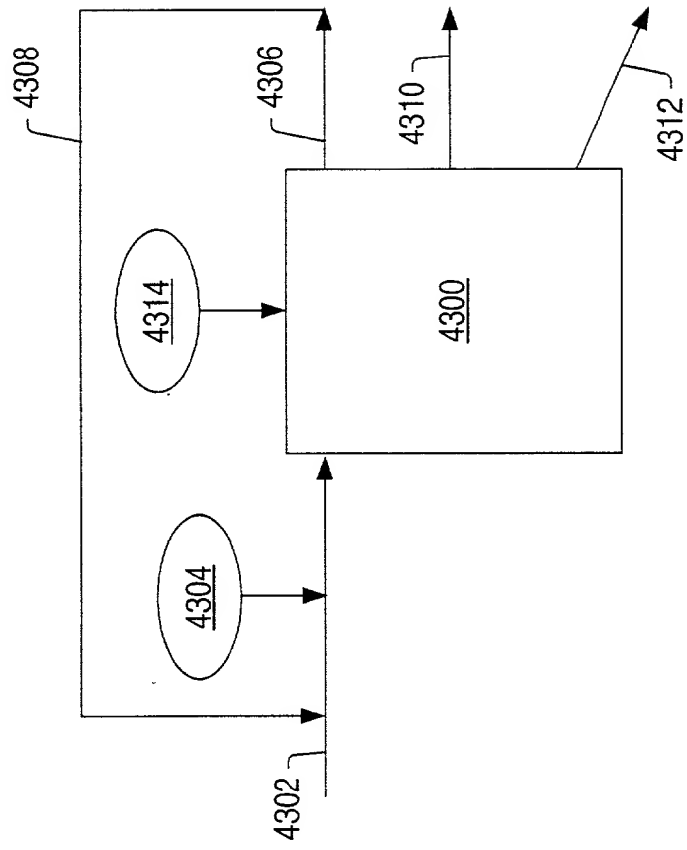


FIG. 164

184.33  
 163.85  
 143.37  
 122.89  
 102.41  
 81.92  
 61.44  
 40.96  
 20.48  
 0.000

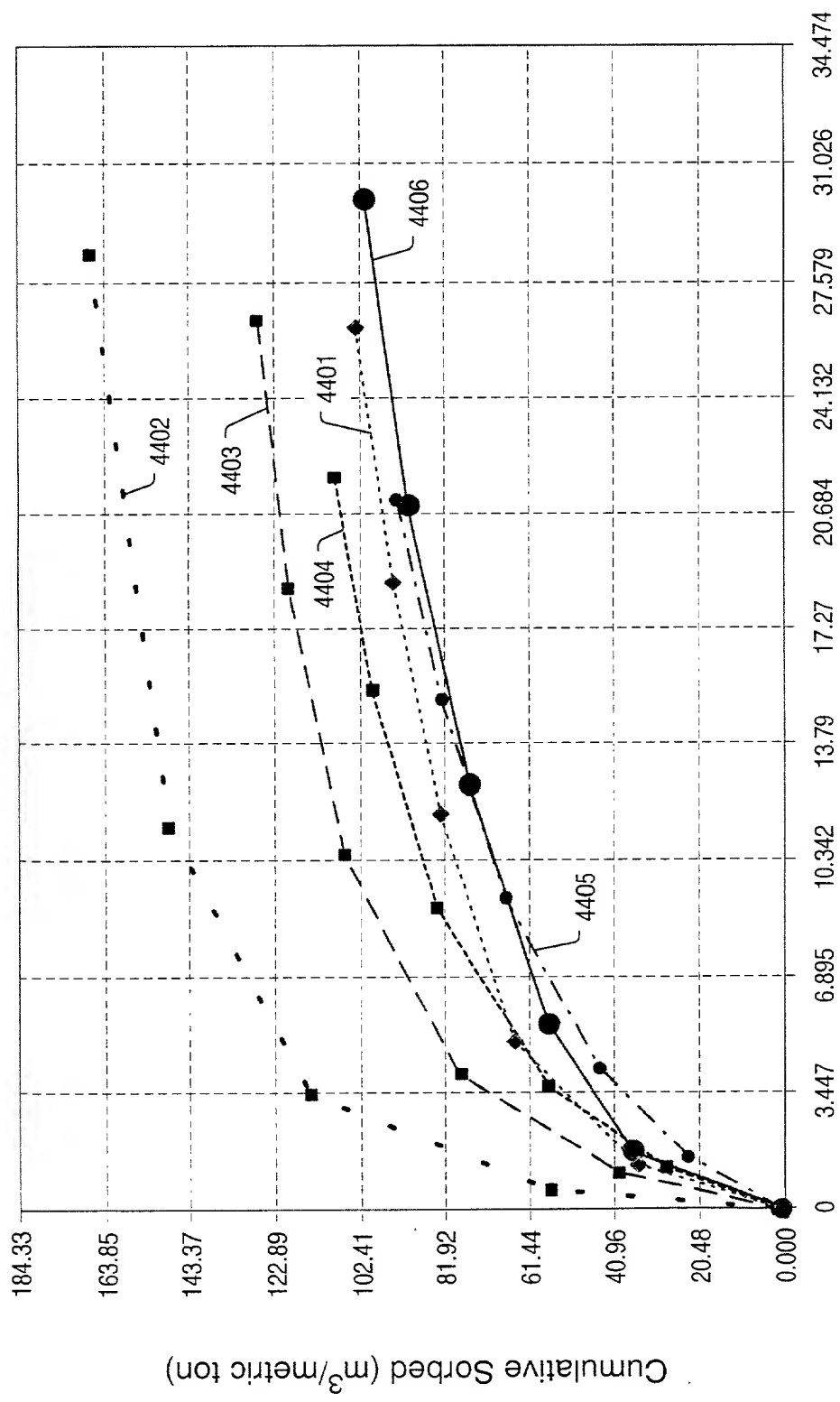


FIG. 165

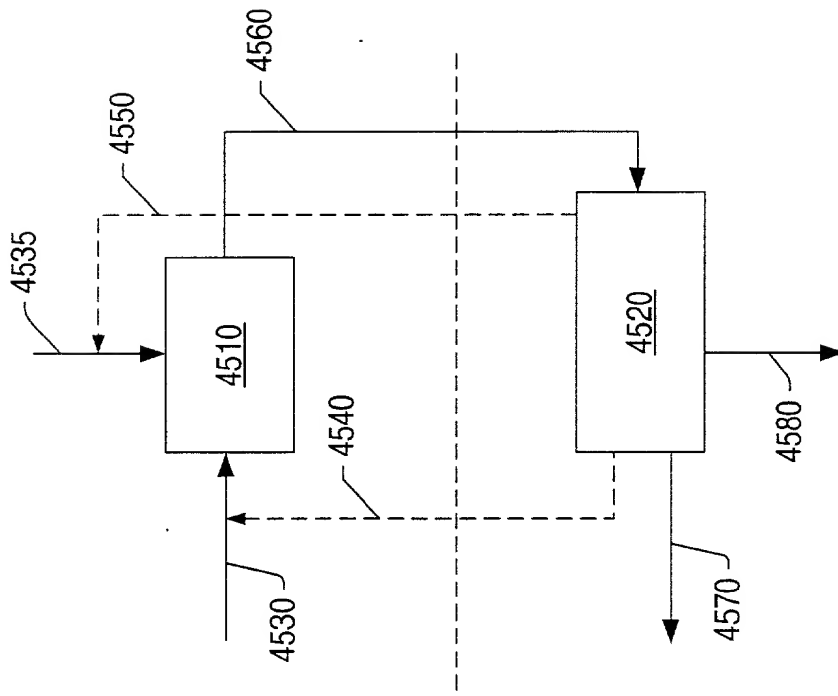


FIG. 166

upper and lower limits of the component fraction of the component in the sample

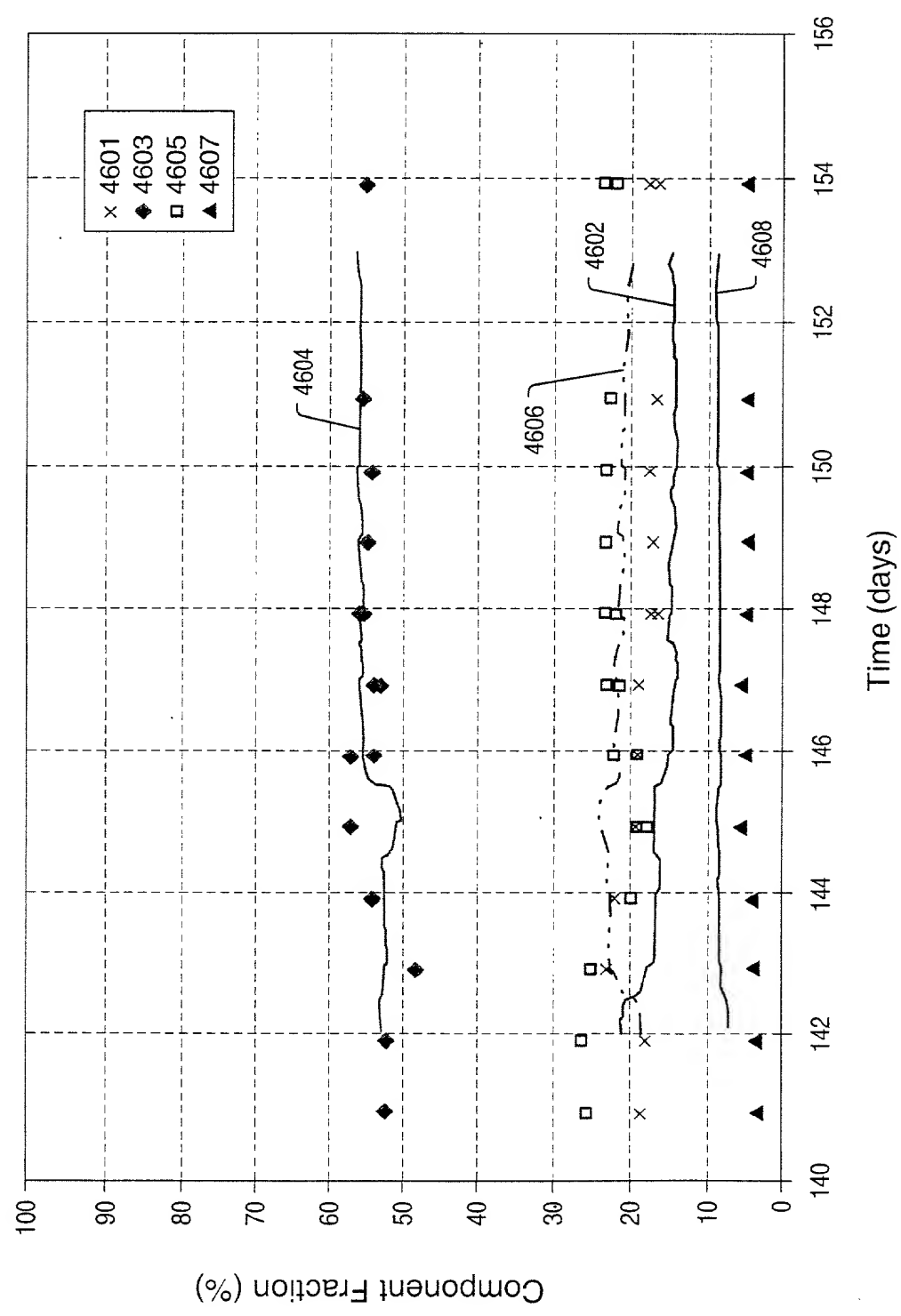


FIG. 167

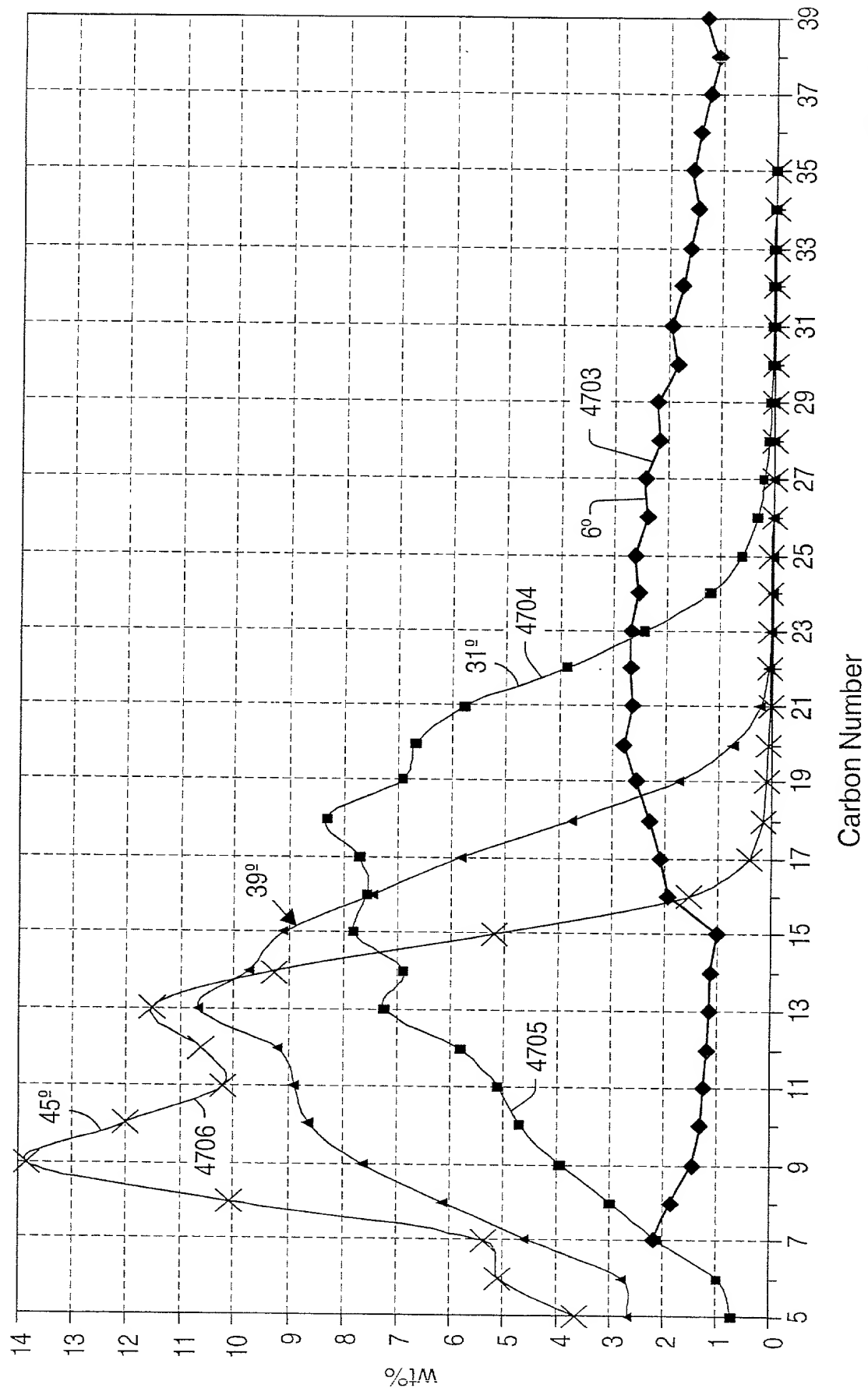


FIG. 168

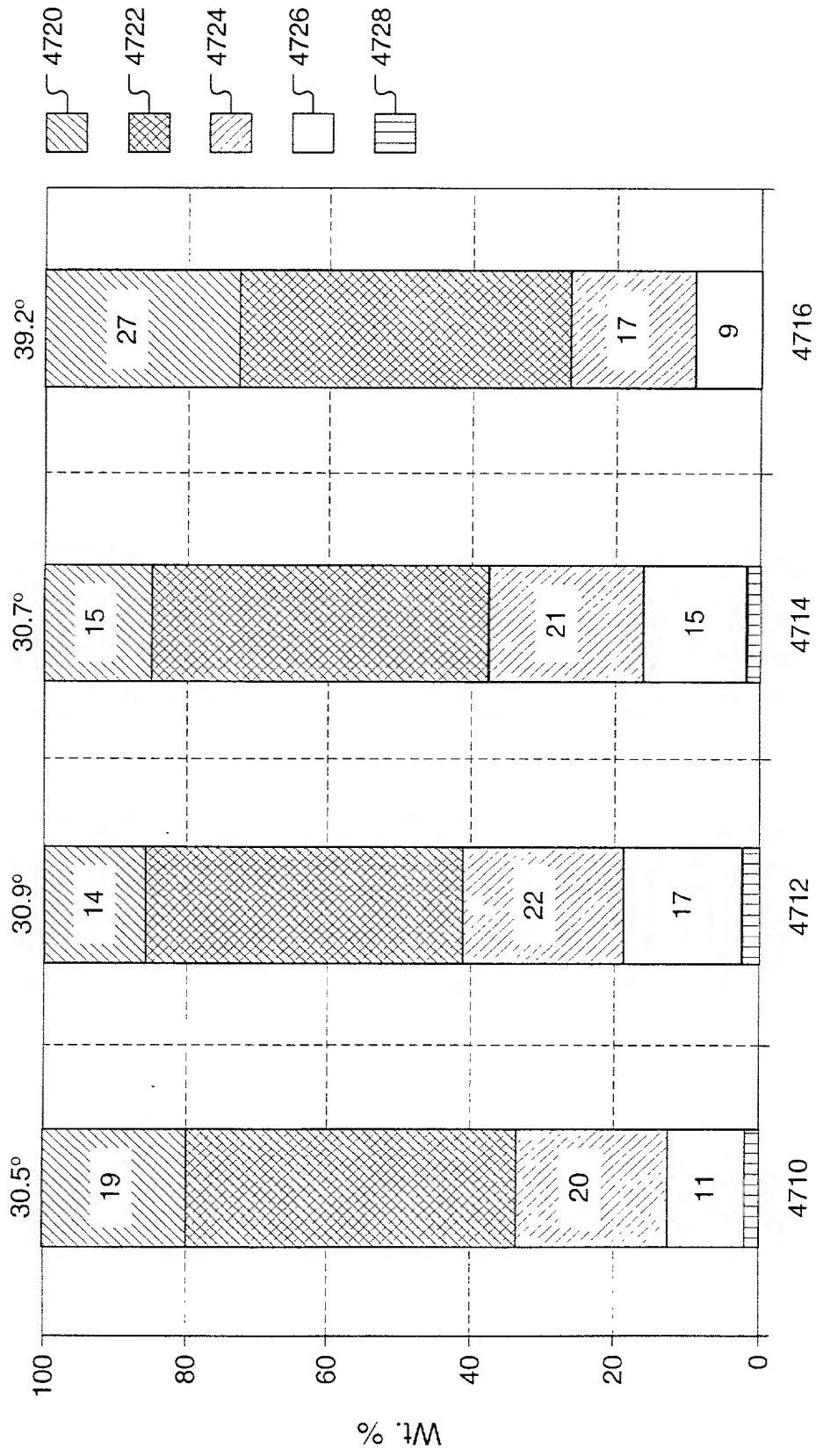


FIG. 169

FIG. 170

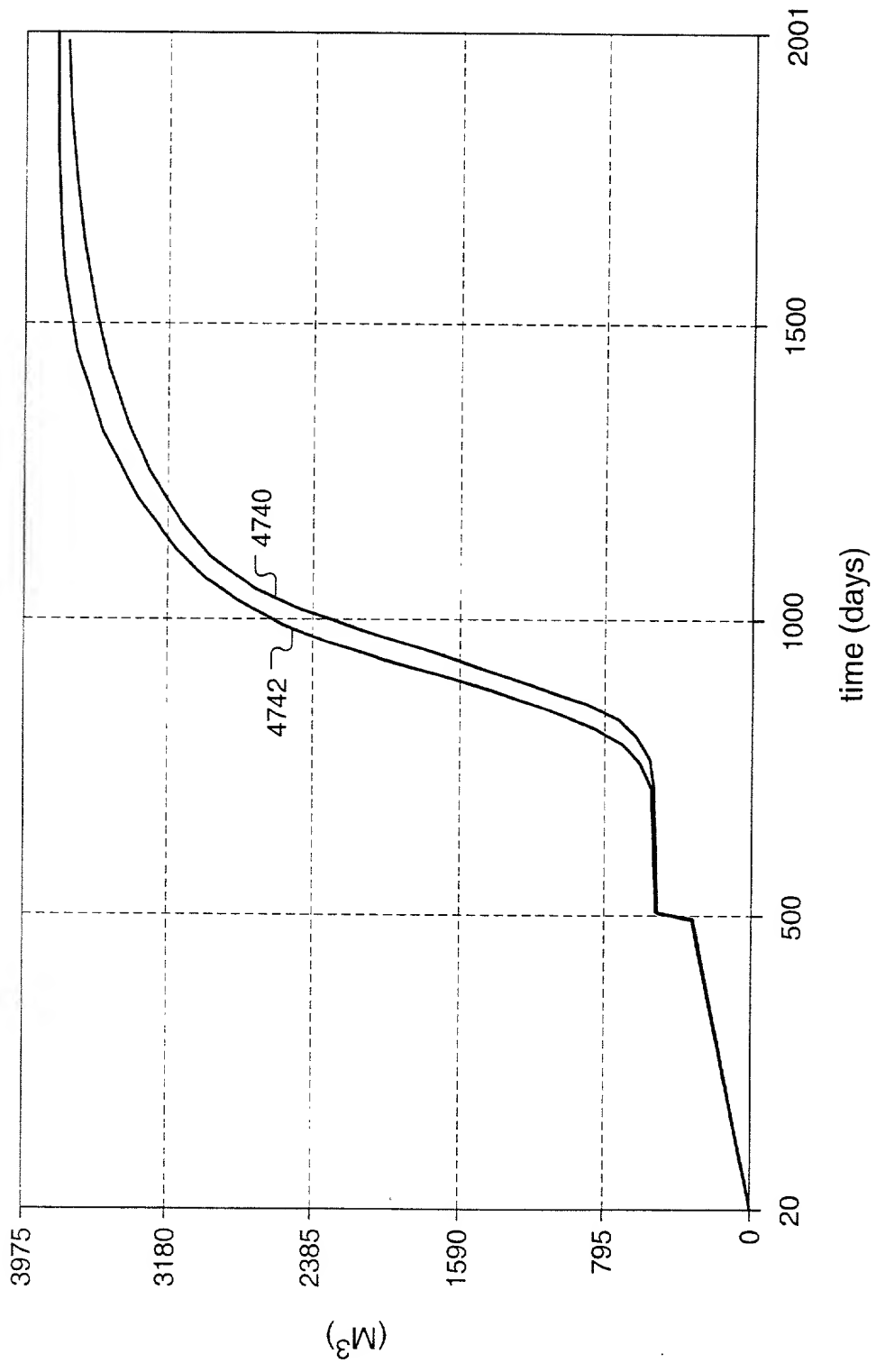


FIG. 170

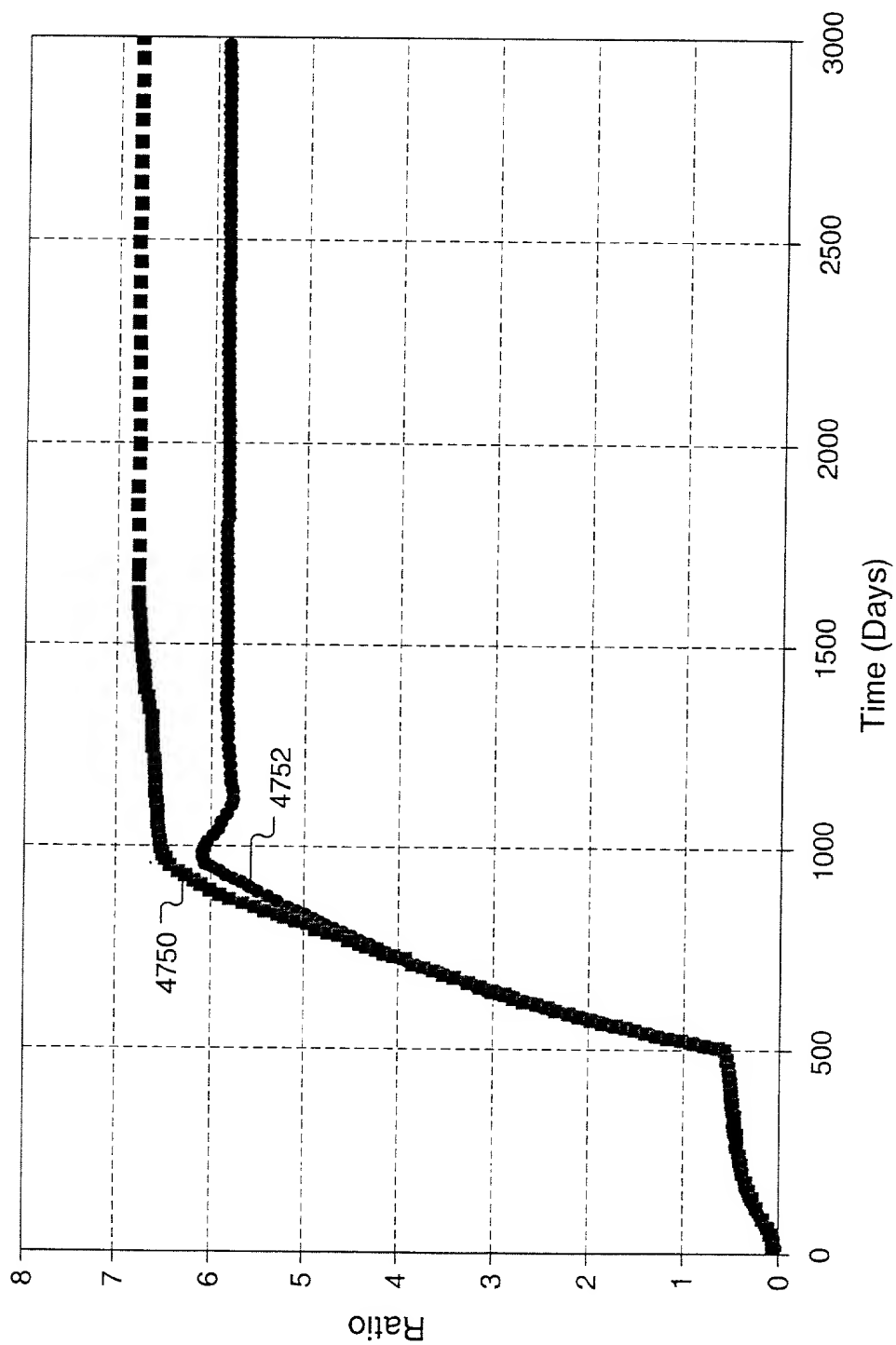


FIG. 171



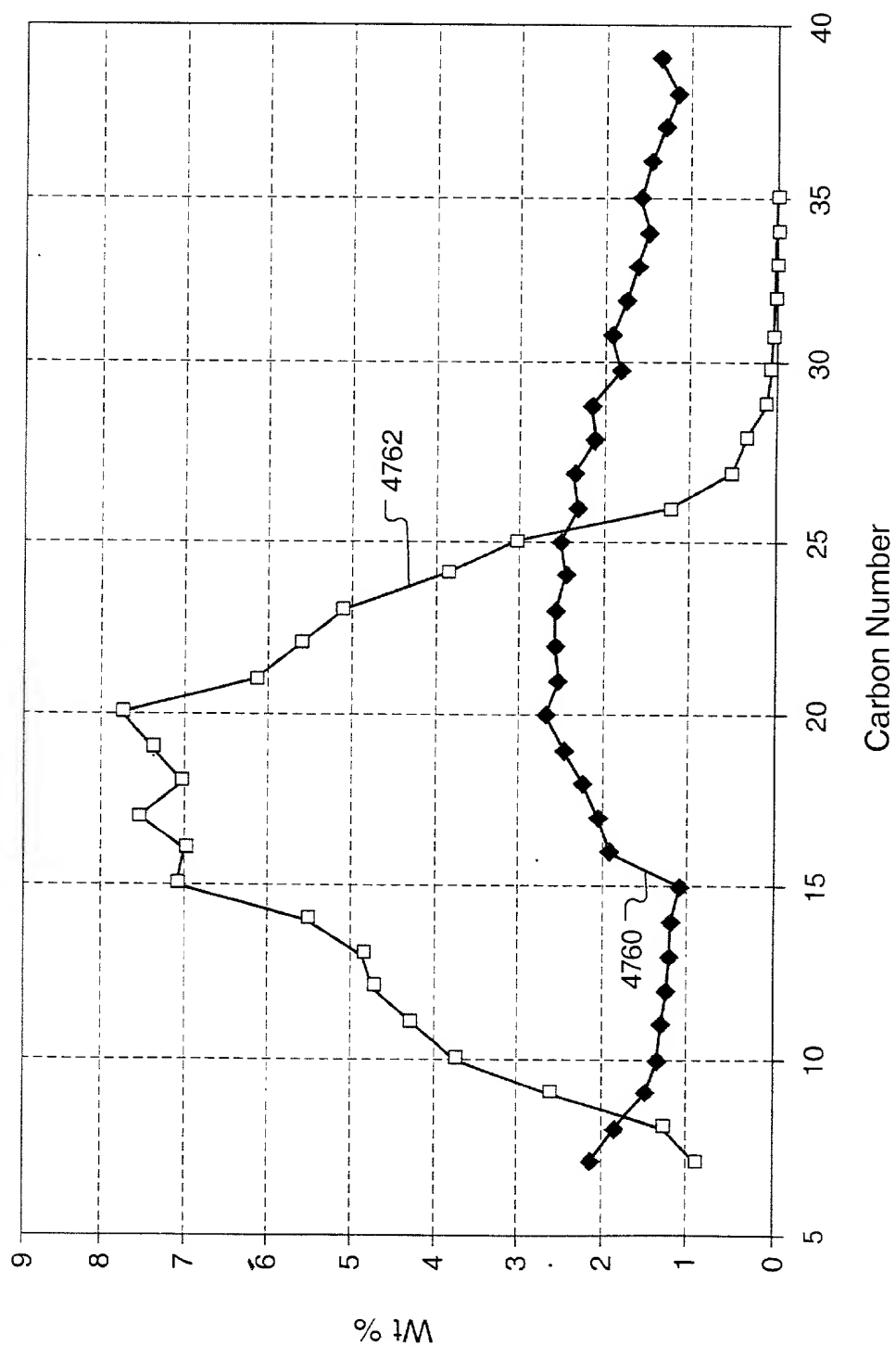


FIG. 172



$\eta_{sp}/c$  vs  $T$  for  $\text{H}_2\text{O}$  and  $\text{D}_2\text{O}$  at  $\text{pH} = 7.0$  and  $\text{pH} = 8.0$ . The data points are shown for  $\text{H}_2\text{O}$  (open squares) and  $\text{D}_2\text{O}$  (open circles). The curves represent the theoretical predictions for the two cases.

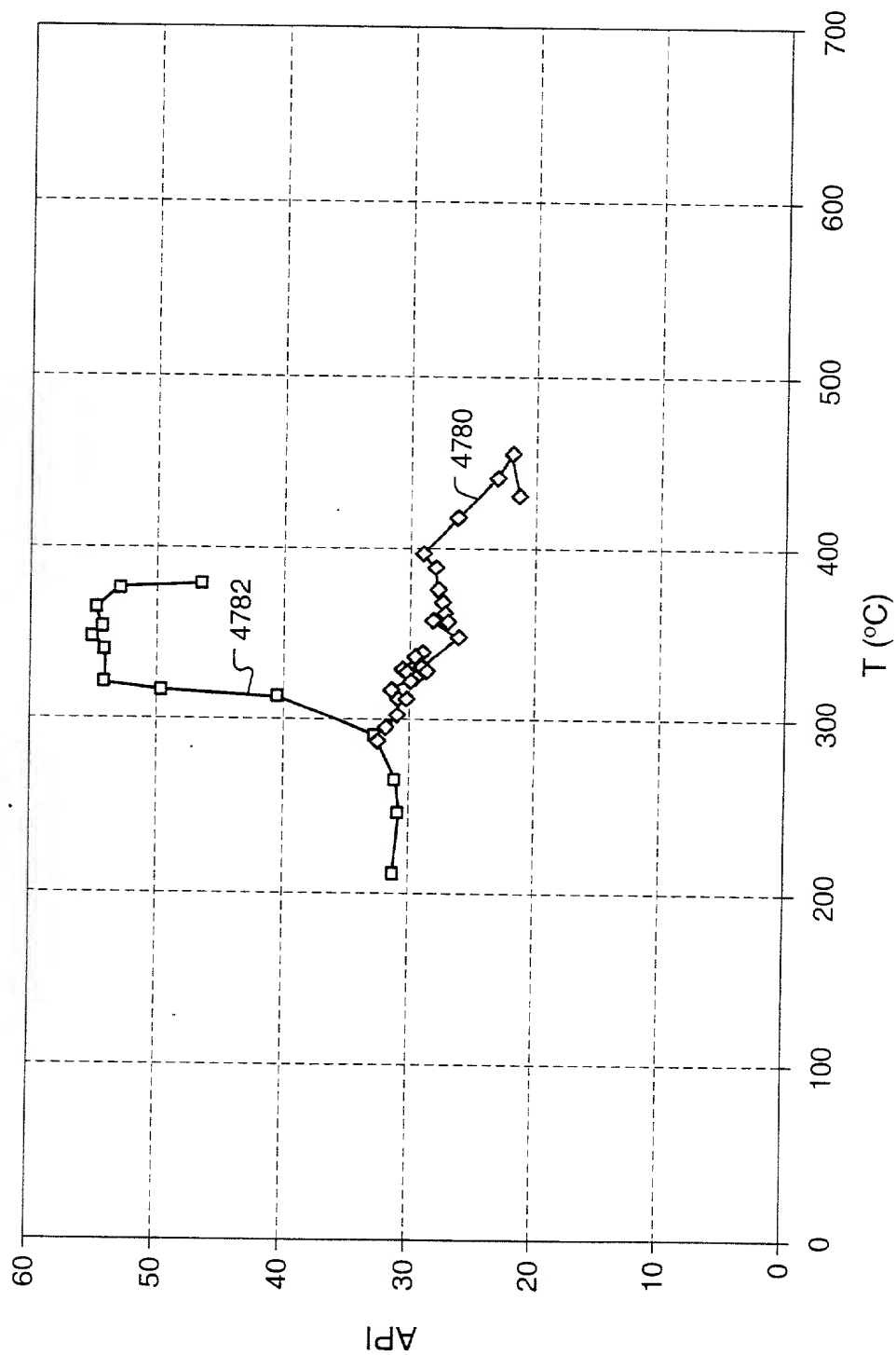
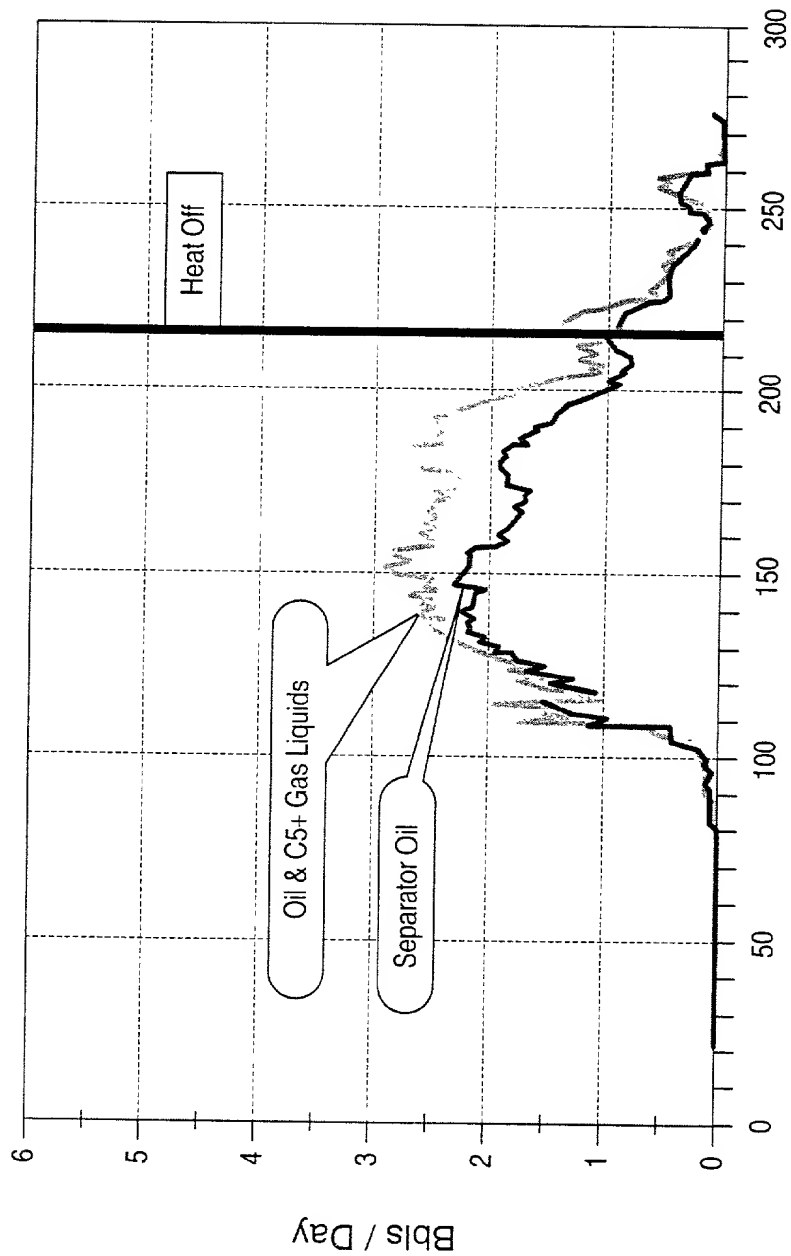


FIG. 174

Copyright 2000 by the American Petroleum Institute, Washington, D.C. All rights reserved. No part of this document may be reproduced without the written permission of the American Petroleum Institute.



Days From Start of Heat Injection

FIG. 175

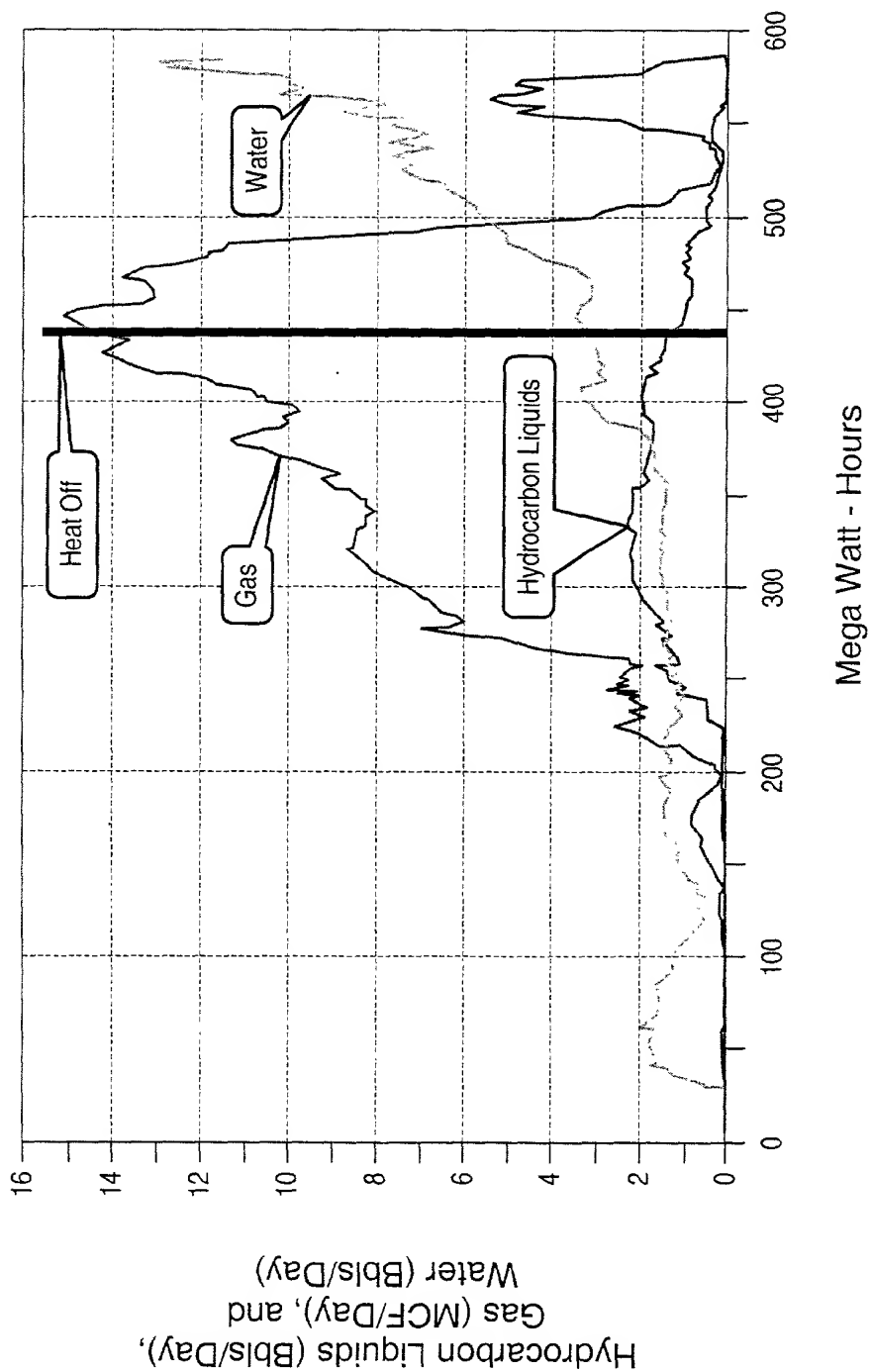
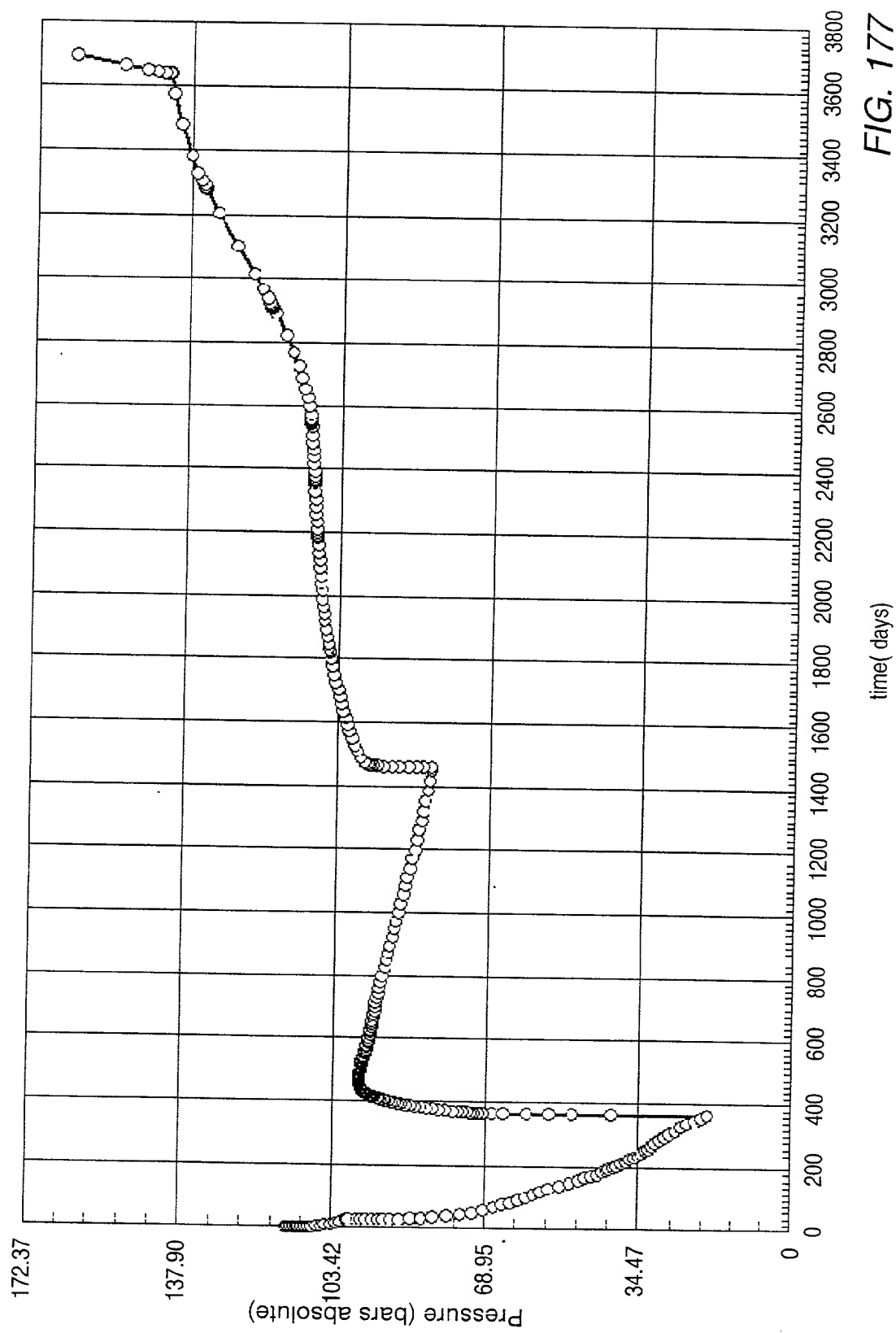


FIG. 176



Flow rate (Mm<sup>3</sup>/day) vs. time (days)

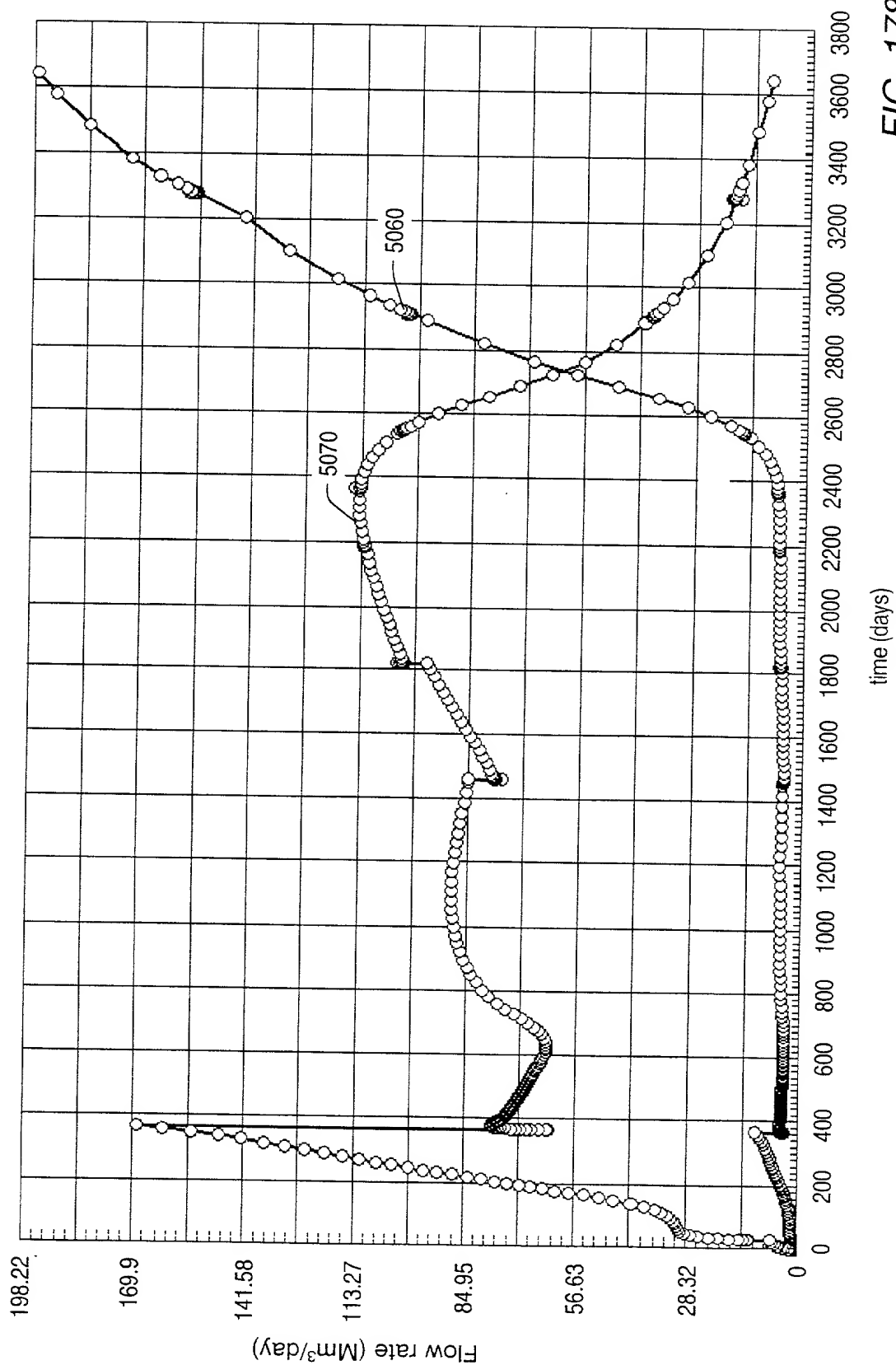


FIG. 178

$\frac{d^2 u}{dt^2} = \frac{1}{\rho} \frac{d}{dt} \left( \frac{1}{r} \frac{d}{dr} \left( r \frac{du}{dr} \right) \right)$   
 $\frac{d^2 u}{dt^2} = \frac{1}{\rho} \frac{d}{dt} \left( \frac{1}{r} \frac{d}{dr} \left( r \frac{du}{dr} \right) \right)$

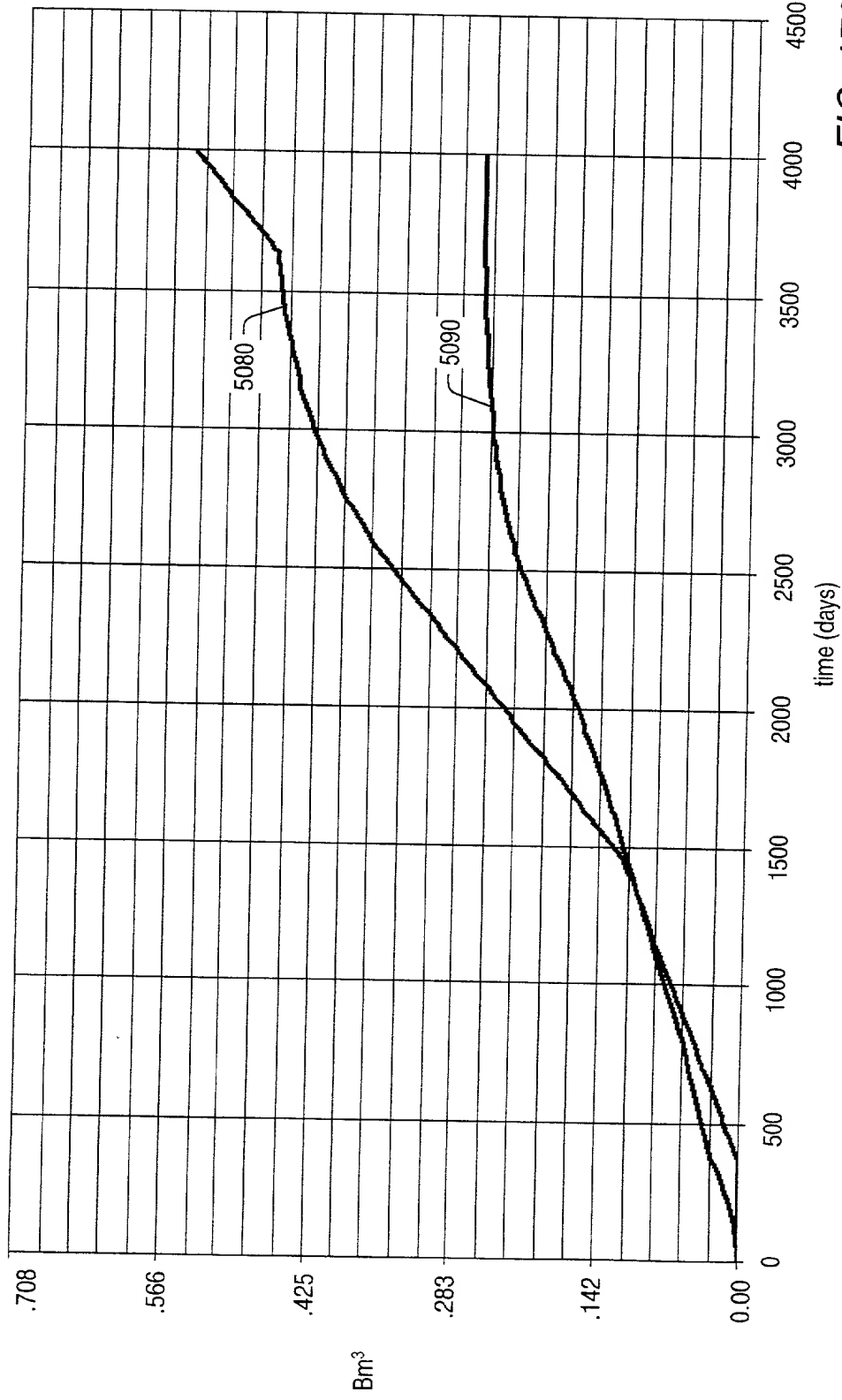


FIG. 179





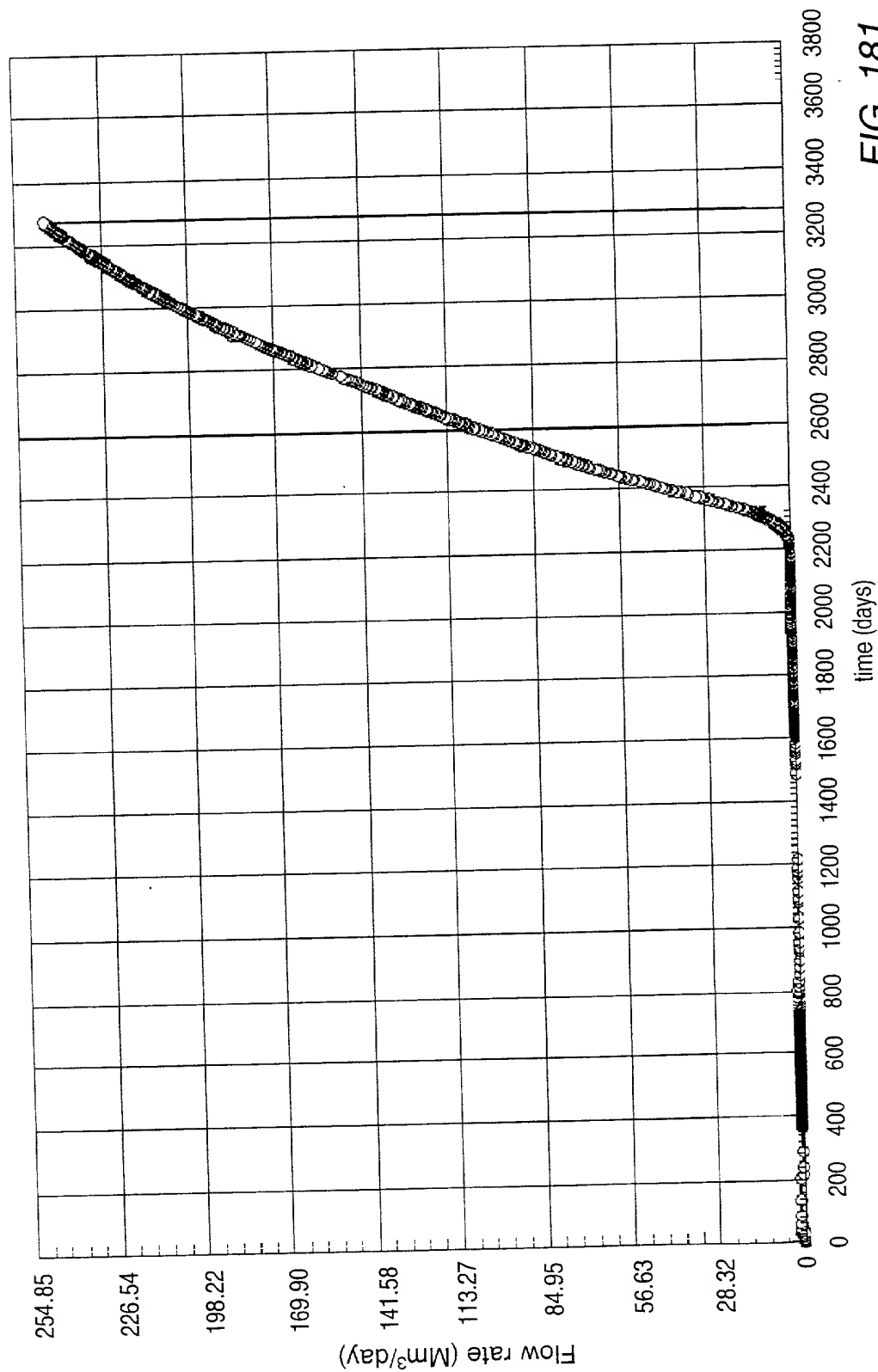


FIG. 181

